

UMCES

UNIVERSITY OF MARYLAND CENTER for ENVIRONMENTAL SCIENCE

CHESAPEAKE BAY

WATER QUALITY MONITORING PROGRAM

ECOSYSTEM PROCESSES COMPONENT (EPC)

LEVEL ONE REPORT #25 (INTERPRETIVE)

A Program Supported by the Department of Natural Resources
State of Maryland

September 2008

Maryland Department of Natural Resources

MARYLAND CHESAPEAKE BAY WATER QUALITY MONITORING PROGRAM

ECOSYSTEMS PROCESSES COMPONENT (EPC)

LEVEL ONE REPORT No. 25
INTERPRETIVE REPORT
(July 1984 – December 2007)

PREPARED FOR:

Maryland Department of Natural Resources
Tidewater Ecosystems Assessment
580 Taylor Avenue, D-2
Annapolis, MD 20401

September, 2008

Editors: E.M. Bailey, M.A.C. Ceballos, and W.R. Boynton

Contributing Authors:

CBL

W.R. Boynton	Principal Investigator, Professor
E.M. Bailey	Faculty Research Assistant
L.A. Wainger	Research Associate Professor
M.A.C. Ceballos	Laboratory Research Technician
K.V. Wood	Faculty Research Assistant

HPL

W.M. Kemp	Principal Investigator, Professor
J.M. Testa	Faculty Research Assistant
M.T. Brooks	Faculty Research Assistant
J.C. Cornwell	Principal Investigator, Research Associate Professor
M.S. Owens	Faculty Research Assistant
C. Palinkas	Principal Investigator, Assistant Professor

University of Maryland Center for Environmental Science

Chesapeake Biological Laboratory (CBL)
1 Williams Street
Solomons, MD 20688

Horn Point Laboratory (HPL)
2020 Horns Point Road
Cambridge, MD 21613

Consulting

E.S. Perry, PhD.	Statistician	2000 Kings Landing Road Huntingtown, MD 20639
T.A. Wisner	Artist/Musician	Prince Frederick, MD

Table of Contents

	Page No.
List of Figures	ii
List of Tables	v
Executive Summary	E-1
Introduction	1-1
Spatially Intensive Shallow Water Quality Monitoring of the Potomac River	2-1
Targeted Watershed Measurement Program and Key Process Evaluation. <i>YEAR 2: Metabolism in the Corsica River Estuary</i>	3-1
Targeted Watershed Measurement Program and Key Process Evaluation. <i>YEAR 2: Box-Modeling Analysis of the Corsica River Estuarine System</i>	4-1
Targeted Watershed Measurement Program and Key Process Evaluation. <i>YEAR 2: Analyses of Water Quality in the Corsica River Estuarine System: Nutrient Limitation and Factors Affecting Light Attenuation</i>	5-1
Targeted Watershed Measurement Program and Key Process Evaluation. <i>YEAR 2: Nutrient Balance in Corsica River Sediments: Improved Estimates of Nutrient Burial and Denitrification</i>	6-1
Estuarine Community Metabolism at Potomac River Estuary ConMon Sites (Maryland and Virginia – 2007)	7-1
Estuarine Community Metabolism Web Page Addition	8-1

Table of Contents

List of Figures

	Page No.
1-1 Degradation and restoration trajectories of an estuarine ecosystem.	1-5
2-1 Schematic diagram of DATAFLOW illustrating the path of water through the instrument.	2-2
2-2 Typical DATAFLOW cruise track for the Upper (tidal fresh) Potomac River.	2-4
2-3 Typical DATAFLOW cruise track for the Lower (mesohaline) Potomac River.	2-4
2-4 DATAFLOW calibration stations on the Upper Potomac, 2007.	2-5
2-5 DATAFLOW calibration stations on the Lower Potomac, 2007.	2-5
2-6 Average surface water dissolved inorganic nitrogen (grey bars) and dissolved inorganic phosphorus (red bars) for Potomac River Dataflow calibration stations in 2007 (units are mg L ⁻¹).	2-8
2-7 Average surface water DIN (top panel) and DIP (lower panel) for long term sampling stations in the Potomac River.	2-9
2-8 Average surface water total chlorophyll-a (µg L ⁻¹) for Potomac River Dataflow calibration stations in 2007.	2-10
2-9 Average surface water total suspended solids (mg L ⁻¹) for Potomac River Dataflow calibration stations in 2007.	2-11
2-10 Box plot (top panel) and average (lower panel) light attenuation calculated using light meter (LiCor®) measurements for Potomac River Dataflow calibration stations in 2007.	2-12
2-11 Figure 2-11. Bar graph of average Kd for 2007 Potomac River Dataflow calibration stations using three methods: LiCor (calculated light meter measurements), Elgin (from Perry 2006 and 2007, Romano 2008 and Tango 2007) and Secchi Depth (conversion of Secchi depth to Kd using: Kd = 1.45/Secchi depth).	2-13
2-12 Scatter plot of Kd calculated using light meter measurements versus Kd calculated from Perry (2005) and Tango (2007) from April-October 2007 at Dataflow calibration stations on the Potomac River.	2-14
2-13 Cumulative Frequency Diagram for the Upper Potomac.	2-17
2-14 Cumulative Frequency Diagram for the Lower Potomac.	2-17
2-15 Total potential SAV habitat (depth < 2 meters) and area in meeting all SAV habitat criteria (by cruise month).	2-18
2-16 SAV habitat hotspots – Tidal Fresh Potomac.	2-19
2-17 SAV habitat hotspots – Mesohaline Potomac.	2-20
2-18 Area of April non-compliance with SAV habitat criterion for Percent Light in Water (PLW) in the Tidal Fresh Potomac.	2-21
2-19a Minimum acreage meeting SAV habitat criteria in 2007 – Tidal Fresh Potomac	2-22
2-19b Maximum acreage meeting SAV habitat criteria in 2007 – Tidal Fresh Potomac.	2-22
2-20a Minimum acreage meeting SAV habitat criteria in 2007 – Mesohaline Potomac.	2-22
2-20b Maximum acreage meeting SAV habitat criteria in 2007 – Mesohaline Potomac.	2-22
2-21 Comparison of total suspended solids (TSS) and optical turbidity (NTU) measured at DATAFLOW calibration stations in 2007.	2-23

Table of Contents

3-1	Map of the Corsica River estuary showing location of the Sycamore Point ConMon site.	3-2
3-2	Screen shot showing the requisite input format needed by Metabolism.xls for calculation of metabolism variables.	3-5
3-3	A scatter plot of summer Pg^* versus nitrogen loading rate scaled for water residence time in the Patuxent River estuary in the vicinity of Benedict, MD.	3-6
3-4	Corsica River metabolism at Sycamore Point from April 2005 to December 2006.	3-8
3-5	Corsica River metabolism at Cedar-Possum Point from April 2005 to December 2006.	3-9
3-6	Monthly rates of production (Pg^*) and respiration (R_n) computed from data collected at Sycamore Point in the upper portion of the Corsica River estuary for the period 2005-2007.	3-11
3-7	Plot of production vs. respiration for Sycamore Point on the Corsica River for the period 2005-2007.	3-12
3-8	Lag plots (1 to 4 days) of R_n for Sycamore Point data.	3-13
3-9	Lag plots (1 to 4 days) of Pg^* for Sycamore Point data.	3-14
3-10	Box and whisker plots of monthly R_n and Pg^* data collected at Sycamore Point in the Corsica River.	3-15
3-11	Time series plots of the data with a loess regression curve superimposed to illustrate the trend of the data.	3-16
3-12	Graphic display of the autocorrelation function and partial autocorrelation function of the residuals from a year x season fit to each of Pg^* and R_n .	3-17
3-13	Mean monthly (Apr-Dec) values of Pg^* collected at Sycamore Point in the Corsica River estuary during 2005, 2006 and 2007.	3-21
3-14	Mean monthly (Apr-Dec) values of R_n collected at Sycamore Point in the Corsica River estuary during 2005, 2006 and 2007.	3-24
4-1	Map of Corsica River estuary, including box model boundaries, the Centreville wastewater treatments plant (WWTP), water quality monitoring stations from DNR (red circles) and UMCES SONE cruises (yellow circles), and nutrient sampling at stream gauges (brown circles).	4-2
4-2	Box and arrow diagram of transports coefficients calculated by the 1-box-model for the Corsica River estuary.	4-5
4-3	Box and arrow diagram of transports exchange coefficients calculated by the 2-box-model for the Corsica River estuary, and the calculated physical transport during the period of May to October in 2006.	4-6
4-4	Seasonal changes in DIN loads to the estuary from the watershed and from the Chester river at the Corsica estuary mouth.	4-7
4-5	Net production rates of DIN and DIP calculated monthly from May to October for the entire Corsica River estuary in 2006.	4-8
4-6	Net production rates of DIN and DIP calculated monthly from May to October for Box 1 and Box 2 in the Corsica River estuary in 2006.	4-9
4-7	Net production rates of TON in Box 1 and Box 2 (shaded bars) calculated monthly from May to October for the Corsica River estuary in 2006 and corresponding measured chlorophyll-a concentrations (circles).	4-9

Table of Contents

4-8	Map of the Chester River estuary, including box model boundaries and water quality monitoring stations for 2006.	4-11
4-9	Annual net production rates of DIN and DIP calculated for 3 boxes in the Chester River estuary in 2006.	4-11
5-1	Map of Corsica River estuary, including box model boundaries, the Centreville wastewater treatments plant (WWTP), water quality monitoring stations for 1997 (red circles) and 2006 (yellow circles)	5-2
5-2	Seasonal variation in the DIN:DIP ratio in the upper and lower Corsica estuary during 2006.	5-3
5-3	Axial distribution of particulate and dissolved inorganic forms of nitrogen (top lanel) and phosphorus (bottom panel).	5-3
5-4	Correlations between Secchi depth and Chl-a (top panel) and TSS (bottom panel) for all stations and sampling dates in the Corsica estuary, 2006.	5-4
5-5	Seasonal variation in TSS and $Cd_{w_{\text{phyt}}}$ in the upper (top panel) and lower (bottom panel) Corsica estuary for 2006.	5-4
5-6	Axial distributions of the mean depth of the Corsica estuary (filled circles) and the depth of 1% light ($Z_{1\%}$) for two months in 2006.	5-5
5-7	Plots of the % of the surface area below a given depth for the Corsica River (top panel), the upper region of the Corsica (middle panel), and the lower region (bottom panel).	5-5
6-1	Corsica River marsh sampling locations.	6-5
6-2	Photographs of the 4 sampling sites.	6-6
6-3	Sediment-water exchange of oxygen.	6-7
6-4	Sediment-water exchange of N_2-N .	6-7
6-5	Histogram of estuary and marsh denitrification rates.	6-8
6-6	Sediment-water exchange of NH_4^+ .	6-9
6-7	Sediment-water exchange of NO_{2+3}^- .	6-9
6-8	Sediment-water exchange of SRP.	6-10
6-9	Plots of sediment-water exchange of oxygen versus exchange of ammonium, di-nitrogen (denitrification), nitrate, ΣN ($NH_4^+ + NO_3^- + N_2-N$) and SRP.	6-11
6-10	Map of the 2007 core locations in the Corsica River.	6-14
6-11	A) ^{234}Th and B) ^7Be profiles for CR9.	6-15
6-12	^7Be and ^{234}Th activity profiles for CR10, CR11, and CR12.	6-16
6-13	Figure 6-13. Areas and data used in annual (^7Be) and decadal (^{210}Pb) sediment budgets.	6-19
6-14	^{210}Pb , ^{137}Cs , and grain-size profiles for CR9 and CR12.	6-21
6-15	^{210}Pb and ^{137}Cs profiles for CR10.	6-22
7-1	General locations and place names of ConMon sites in Maryland and Virginia portions of the Potomac River estuary.	7-4
7-2	Screen shot showing the requisite input format needed by Metabolism.xls for calculation of metabolism variables.	7-7

Table of Contents

7-3	Monthly box and whisker plots of gross primary production (Pg^*) and nighttime respiration at 14 shallow water ($z < 1.6$ m) sites in the Potomac River estuary and tributary rivers.	7-10 to 7-13
7-4	A contour plot of average monthly rates of gross primary production (Pg^*) at all 14 ConMon sites in the Potomac River estuary and tributary rivers.	7-15
8-1	A preliminary and crude sketch showing several important inputs to large-scale corn production and relating the magnitude of production to fertilization rates.	8-6
8-2	A preliminary and crude sketch showing the estuarine equivalent of the farmer's field.	8-6
8-3	A more formal depiction of the processes captured in Fig. 8-1. This cartoon was drawn by Tom Wisner (www.Chestory.org).	8-7
8-4	A more formal depiction of the processes captured in Fig. 8-2. This cartoon was drawn by Tom Wisner (www.Chestory.org).	8-8
8-5	Two preliminary and crude sketches of a “cause – effect chain” wherein nutrients from the land eventually cause eutrophic conditions (top sketch) and a first effort at developing a graphic based on ConMon data and resultant metabolism computations.	8-9
8-6	A preliminary and crude sketch of the output of metabolism computations based on data from a ConMon site.	8-9
8-7	A simple “cartoon figure” of what a web page summary of community metabolism might look like.	8-10

List of Tables

2-1	DATAFLOW cruise dates in 2007.	2-4
2-2	Location of DATAFLOW calibration stations (NAD83).	2-4
2-3	2007 DATAFLOW calibration station nutrient concentrations.	2-7
2-4	Habitat criteria applied to 2007 data.	2-15
2-5	Area of estuary meeting habitat criteria by cruise.	2-18
3-1	ConMon Station Code, Locations and Mean Depth (m) from 2007.	3-3
3-2	Analysis of variance for Pg^* based on a generalized least squares analysis with auto-regressive lag 1 error structure.	3-18
3-3	Model Means of Pg^* by Month	3-18
3-4	Comparison of Model Means between sequential months for Pg^*	3-19
3-5	Model Means of Pg^* by year	3-19
3-6	3-6. Comparison of Model Means between sequential years for Pg^*	3-19
3-7	Comparison of Model Means between sequential years within month for Pg^*	3-20
3-8	Analysis of variance for Rn based on a least squares analysis of with independent error structure.	3-21
3-9	Model Means of Rn by Month	3-22
3-10	Comparison of Model Means between sequential months for Rn	3-22
3-11	Model Means of Rn by year	3-23
3-12	Comparison of Model Means between sequential years for Rn	3-23
3-13	Comparison of Model Means between sequential years within month for Rn	3-23

Table of Contents

3-14	Minimum Significant Difference for Rn and Pg*	3-25
4-1	Summary of rates of net ecosystem metabolism and net denitrification in all boxes of the Corsica and Chester River estuaries.	4-10
6-1	Corsica River marsh station codes and grid locations (NAD 83).	6-4
6-2	Sediment-water exchange rates for Corsica marsh environments.	6-4
6-3	Deposition rates calculated from ⁷ Be inventories at all core locations.	6-17
6-4	A) Observed trends in deposition rates, mixing coefficients, and the ⁷ Be/ ²³⁴ Th ratio calculated from inventories. B) Expected trends in ⁷ Be and ²³⁴ Th based on assumed sources of material.	6-18
7-1	ConMon Station Names, Locations, Orientations and Mean Depth at Maryland and Virginia sites.	7-3
7-2	A summary of average monthly rates of gross primary production (Pg*) at a variety of Chesapeake Bay locations and for all 14 ConMon sites in the Potomac River estuary and tributary rivers.	7-14
8-1	A simple description of ConMon data and a cause-effect chain relating nutrient inputs to water quality problems (e.g., hypoxia and anoxia).	8-2

Executive Summary 2007

Background: Objectives of the Water Quality Monitoring Program

The EPC has undergone multiple and significant program modification since its inception in 1984 but its overall objectives have remained consistent with those of other Monitoring Program Components. The objectives of the 2007 EPC program were as follows:

1. Evaluate the variation in spatial and temporal scales of water quality in both **near-shore and off-shore areas of the Potomac River** estuary using the DATAFLOW mapping system. During 2006, 2007 and 2008 (active at present) we were responsible for mapping the most seaward and the most landward portions of the Potomac River estuary.
2. During 2007 we continued to analyze data previously and currently being collected in the **Corsica River** estuary in support of estuarine restoration of this system. Specifically, Dr. Mike Kemp's research team (from UMD-CES-HPL) continued to analyze results from **box-model computations** and to analyze results from water quality and dataflow mapping activities in the Corsica conducted by MD-DNR and MD-MDE. Dr. Jeff Cornwell and Dr. Cindy Palinkas (from UMD-CES-HPL) made additional field measurements of **denitrification and nutrient burial** in the tidal freshwater and marsh portions of the Corsica River estuary for use in developing a nutrient budget for this system. In addition, we continued to utilize Continuous Monitoring (ConMon) data for computing rates of **community production and respiration** in this system. These rates are closely linked to rates of nutrient inputs and reduction of nutrient inputs is the focal point of management actions. We computed these rates for the site in the Corsica (Sycamore Point) where there is a three year data record. We collaborated with Dr. Elgin Perry (research statistician) to explore this data set for trends and for establishing minimum significant difference guidelines.
3. During 2006 and continuing in 2007 were able to enlist the **assistance of several GIS analysts** with far more experience than our Ecosystems Processes Component (EPC) group has in these sorts of analyses. They utilized several DATAFLOW data sets to explore the pros and cons of various GIS approaches, to reach some conclusions regarding most efficient methods of data analysis, and to examine the database regarding areas of the Potomac River estuary where water quality conditions were adequate for SAV recolonization. Dr. Lisa Wainger, an associate research professor at UMD-CES-CBL is now a co-PI of the EPC of the MD Biomonitoring Program.
4. We have also utilized ConMon data from 14 of the 16 ConMon sites active in the Potomac River estuary to compute rates of **community production and respiration** for 2007. This is an un-funded activity but one that shows great potential as an additional tool for detecting change in estuarine systems. Almost a million observations were included in this analysis and results were highly interpretable.
5. We also initiated an effort (also un-funded) to translate the metabolism work supported by ConMon data to a **web page** that could be useful in public education of Bay restoration. At this point we have developed a series of possible cartoons and other sketches explaining the

Executive Summary

importance of community metabolism and how it is expected to change with changes in nutrient additions to Bay waters.

6. **Integrate the information** collected in this program with other elements of the monitoring program to gain a better understanding of the processes affecting water quality of the Chesapeake Bay and its tributaries and the maintenance and restoration of living resources. We have completed and published nutrient budgets (N and P) for the Patuxent River basin. We have retained in this management summary a few of the key findings of this effort. EPC have also developed and published an extensive review of nitrogen dynamics in estuarine systems and this work will appear in 2008.

Spatially Intensive Shallow Water Quality Monitoring of the Potomac River

1. Monitoring was successfully completed in the most seaward and most landward of the Potomac River sectors represented in the second year of a three year sequence of dataflow measurements.
2. There were very large differences in water clarity between the upper and lower Potomac River sectors with the upper being quite turbid, as expected.
3. Cumulative frequency diagrams indicated that relatively small areas were out of compliance in both the upper and lower sectors of the Potomac estuary. However, during spring 40-50% of the tidal fresh area meet SAV criteria but virtually none of the mesohaline area meet all of the criteria. Habitat criteria were more often met during the summer and fall periods.
4. In the tidal freshwater portion of the Potomac, both PLW and chlorophyll-*a* were factors limiting compliance during spring. In the mesohaline region, DIN was the critical factor limiting compliance.
5. There remain several issues of concern and the program needs to consider these. It appears that NTU sensors are at the lower limit of effectiveness in the range of importance for SAV habitat criteria (overall range = 0-1000 NTUs). However, the critical range for SAV work is in the 0-20 range, a very small fraction of the overall range of the sensor. We need to work with YSI to resolve this issue. Second, it appears that there is a bias in computing K_d for the tidal freshwater portion of the system that leads to an underestimate of the area meeting SAV criteria. Further testing of the regression model is warranted. Finally, nutrient concentrations are of central importance is SAV habitat considerations. However, nutrients are sampled only at calibration stations. On a typical cruise Dataflow records on the order of 5000 observations of each variable but we have 5-7 nutrient observations. This situation warrants additional attention.

Corsica River Community Metabolism

1. The Corsica River effort is part of a multi-pronged program that includes both landscape and in-estuary activities. Since 2005 Maryland DNR conducted continuous monitoring in the Corsica River estuary using the ConMon approach. One of our roles has been to compute rates of some key processes underlying the observed conditions in the estuary.

Executive Summary

2. Rates of primary production (P_g^*) and community respiration (R_n) are fundamental characteristics of aquatic ecosystems. However, these characteristics of estuarine systems have been less well studied or monitored than in some coastal waters and lakes. Since it is well-established that these rates are sensitive to nutrient loading rates, reliable estimates of these rates would serve both as an index of system performance as well as an indicator of system response to nutrient load reductions. During the last few decades, several things have changed in the monitoring/research world that have made it feasible and affordable to consider using open water community metabolism measurements as components of monitoring programs in estuarine systems. First, several generations of in-situ devices have come into common use, each providing more reliable measurements of DO, temperature, salinity, pH and more recently chlorophyll-a and turbidity. These devices now have the capability of making these measurements in a reliable fashion for periods of one to two weeks in nutrient-enriched estuarine ecosystems. The addition of wiper blades and other self-cleaning devices have further enhanced the reliability of these devices. These in-situ sondes are capable of making repeated measurements thus ensuring that a fine-scale record of diel changes in concentrations is captured. Computational capacity and associated software have also improved greatly. It is now possible to readily store and manipulate the large data files associated with a group of continuously recording sondes. It is also possible to develop programs to compute metabolism variables, thus largely removing the time consuming nature of these analyses.
3. We summarize here the main management-related points derived from the metabolism computations made for this report for the Corsica River estuary.
 - ConMon data from one site (Sycamore Point) in the Corsica River estuary were used for community production (P) and respiration (R) calculations covering three years of measurement (2005-2007). Both production and respiration rates were very large, again indicative of a very enriched system.
 - Seasonal patterns of P and R indicated summer maxima with much lower values during the cooler periods of the record. There were no statistically significant differences among years at this site, suggesting only small changes in nutrient loading rates.
 - Additional statistical analysis indicated that with sample size of about 20 metabolism measurements per month (commonly attained), a change of about 2.4 units for primary production and about 0.8 units for community respiration would be needed to find significant differences. With peak rates of about 17 units for production, a change of 2.4 units is relatively small, suggesting a sensitive management tool.
 - We recommend using these indices of ecosystem performance as they relate directly to the prime management focus which is nutrient load reduction. We expect that if loads decrease then the magnitude of P and R will decrease. In addition, we expect that the seasonal pattern will also change with lower maximum rates occurring in late spring rather than in summer as is now the case. These rates can be readily computed and there is an abundance of ConMon data available for a variety of sub-estuarine systems in the Chesapeake complex of estuaries.

Corsica River Box-Modeling Analysis

1. **The upper Corsica estuary appears to be a large sink of inorganic nitrogen and phosphorus.** Box-model-computed rates of inorganic N and P loss in the upper Corsica

Executive Summary

estuary during 2006 were quite large and appear to be driven by assimilation by highly-productive phytoplankton communities in the region, as well as denitrification. As a result, seaward transport of inorganic N and P out of the upper Corsica estuary was greatly reduced relative to watershed inputs.

2. **Watershed N inputs dominate in the upper Corsica.** A budget of nutrient transport and loading rates for the upper Corsica estuary indicated that watershed nutrient inputs dominated this region of the estuary during 2006, thus reductions in watershed N and P load will likely improve water quality.
3. **Lower Corsica fueled by watershed N inputs and N inputs from the Chester River.** Nitrogen budgets for the lower Corsica estuary indicated that watershed N inputs and N inputs from the Chester River contributed similarly to the total N load during 2006. Although total watershed N loads exceeded loads from the Chester River from May to October 2006, N loads from the Chester were the dominant N source in certain months of 2006.

Corsica River Denitrification and Long-Term Burial Analyses

1. During early fall of 2007 additional measurements of denitrification and nutrient burial were conducted in the tidal marsh region in the headwaters of the Corsica River estuary. These sites were selected because box-model results and water quality measurements suggested a large nitrogen sink in this region of the estuary.
2. Denitrification rates were very high ($264 \mu\text{mol N}_2\text{-N m}^{-2} \text{ hr}^{-1}$), about 3 times the average estuarine rate. Thus, use of previous information (box-model and water quality sampling) has led to a focus on a nitrogen sink “hotspot” in the landscape. On an areal basis these rates are equivalent to about $32 \text{ g N m}^{-2} \text{ year}^{-1}$ (285 pounds per acre per year). Thus, this small area appears to be a very important N sink.
3. Sediment deposition rate (via Pb-210) was about $2300 \text{ g dry sediment m}^{-2} \text{ yr}^{-1}$ in the Corsica River estuary, a value comparable to other sediment rich areas of the Bay.
4. There is an order of magnitude difference between annual and decadal-scale deposition rates, a typical situation in these environments.
5. The sources of sediment in the upper estuary were mainly fluvial, from shoreline erosion in the mid-estuary and from the Chester river estuary in the outer portion of the Corsica. Once again, the inter-connections between landscape and adjacent estuarine systems is clear and needs to be considered in restoration planning.

Potomac River Estuary Community Metabolism

1. During 2007 MD-DNR and VA-DEQ established a total of 16 ConMon sites along the shoreline and in tributary rivers and creeks of the Potomac River estuary. These sites collected data needed for a variety of assessments including community production and respiration measurements.

Executive Summary

2. At 14 of the 16 sites we computed rates of daily production (P_g^*) and respiration (R_n) for the period Mar (or April) through October.
3. Rates of production (P_g^*) ranged from modest to very large. There was a clear indication that rates at both mainstem and tributary sites were much higher in the upper than lower estuary. Rates at all locations were low in the spring and late fall. Two distinct seasonal patterns were evident wherein at the most enriched sites P_g^* was well correlated with water temperature and at less enriched sites P_g^* reached maximum rates in late spring or early summer.
4. If some of these sites remain as sentinel sites a longer time series could be developed and used as a sensitive index of either restoration or further degradation trends in this very large estuary.
5. The ConMon data set for the Potomac may well be the most intensive set of measurements available for computation of rate processes. Such a density of process data is, to our knowledge, unprecedented in the monitoring community. We should take advantage of this opportunity.

Community Metabolism Web Site: A Potential Addition to “Eyes on the Bay”

1. For several years we have discussed the possibility of adding another aspect of monitoring to the “Eyes on the Bay” web page. The ConMon program produces a huge number of observations each year at each site and these can be readily observed on the web page. We suggest that more can be done with these data to make the functioning of the Bay come alive for web page users.
2. We have made a sufficient number of community metabolism computations to get a good feel for the magnitude and pattern of these rates. Rates are almost an order of magnitude higher at very enriched sites than at much less impacted sites....so, the signal range is large and this is an advantage.
3. We have started the process towards a web page with the development of a series of cartoons that could, with refinements and additions, lead the user to an understanding of why these rates are important and how they will likely change if restoration is successful.
4. It appears that some serious web page code writing would be needed to implement this web page addition. However, it could serve as a useful tool for “getting the message” out to a broad range of folks interested in Bay issues.

1.0 Introduction

Walter R. Boynton and Eva M. Bailey

1.1	Background	1-1
1.2	Conceptual Model of Water Quality Processes in Chesapeake Bay	1-3
1.3	Objectives of the Water Quality Monitoring Program	1-4
1.4	References	1-6

1.1 Background

Over two decades ago an important agreement led to the establishment of the Chesapeake Bay Partnership whose mandate was to protect and restore the Chesapeake Bay ecosystem. The year 2000 saw the signing of *Chesapeake 2000*, a document that incorporated specific goals addressing submerged aquatic vegetation (SAV) restoration and protection and improvement and maintenance of water quality in Chesapeake Bay and tributaries rivers.

The first phase of the Chesapeake Bay Program was undertaken during a period of four years (1984 through 1987) and had as its goal the characterization of the existing state of the bay, including spatial and seasonal variation, which were keys to the identification of problem areas. During this phase of the program the Ecosystems Processes Component (EPC) measured sediment-water oxygen and nutrient exchange rates and determined the rates at which organic and inorganic particulate materials reached deep waters and bay sediments. Sediment-water exchanges and depositional processes are major features of estuarine nutrient cycles and play an important role in determining water quality and habitat conditions. The results of EPC monitoring have been summarized in a series of interpretive reports (Boynton *et al.* 1985, 1986, 1987, 1988, 1989, 1990, 1991, 1992, 1993, 1994, 1995, 1996, 1997, 1998, 1999, 2000, 2001, 2002, 2003, 2004, 2005 and 2006). The results of this characterization effort have confirmed the importance of deposition and sediment processes in determining water quality and habitat conditions. Furthermore, it is also now clear that these processes are responsive to changes in nutrient loading rates (Boynton and Kemp 2007).

The second phase of the program effort, completed during 1988 through 1990, identified interrelationships and trends in key processes monitored during the initial phase of the program. The EPC was able to identify trends in sediment-water exchanges and deposition rates. Important factors regulating these processes have also been identified and related to water quality conditions (Kemp and Boynton, 1992; Boynton *et al.* 1991).

In 1991 the program entered its third phase. During this phase the long-term 40% nutrient reduction strategy for the bay was reevaluated. In this phase of the process, the monitoring program was used to assess the appropriateness of targeted nutrient load reductions as well as provide indications of water quality patterns that will result from such management actions. The preliminary reevaluation report (Progress Report of the Baywide Nutrient Reduction Reevaluation, 1992) included the following conclusions: nonpoint sources of nutrients contributed approximately 77% of the nitrogen and 66% of the phosphorus entering the bay; agricultural sources were dominant followed by forest and urban sources; the "controllable" fraction of nutrient loads was

about 47% for nitrogen and 70% for phosphorus; point source reductions were ahead of schedule and diffuse source reductions were close to projected reductions; further efforts were needed to reduce diffuse sources; significant reductions in phosphorus concentrations and slight increases in nitrogen concentrations have been observed in some areas of the bay; areas of low dissolved oxygen have been quantified and living resource water quality goals established; simulation model projections indicated significant reductions in low dissolved oxygen conditions associated with a 40% reduction of controllable nutrient loads.

During the latter part of 1997 the Chesapeake Bay Program entered another phase of re-evaluation. Since the last evaluation, programs had collected and analyzed additional information, nutrient reduction strategies had been implemented and, in some areas, habitat improvements have been accomplished. The overall goal of the 1997 re-evaluation was the assessment of the progress of the program and the implementation of necessary modifications to the difficult process of restoring water quality, habitats and living resources in Chesapeake Bay. During this portion of the program, EPC has been further modified to include 1) development of intensive spatial water quality mapping and 2) intensive examination of SAV habitat conditions in major regions of the Chesapeake Bay.

Chesapeake 2000 involved the commitment of the participants “to achieve and maintain the water quality necessary to support aquatic living resources of the Bay and its tributaries and to protect human health.” More specifically, this Agreement focuses on: 1) living resource protection and restoration; 2) vital habitat protection and restoration; 3) water quality restoration and protection; 4) sound land use and; 5) stewardship and community engagement. The current EPC program has activities that are aligned with the habitat and water quality goals described in this agreement.

The Chesapeake Bay Water Quality Monitoring Program was initiated to provide guidelines for restoration, protection and future use of the mainstem estuary and its tributaries and to provide evaluations of implemented management actions directed towards alleviating some critical pollution problems. A description of the complete monitoring program is provided in the following documents:

Magnien *et al.* (1987),

Chesapeake Bay program web page <http://www.chesapeakebay.net/monprgms.htm>

DNR web page <http://www.dnr.state.md.us/bay/monitoring/eco/index.html>

In addition to the EPC program portion, the monitoring program also has components that measure:

1. Freshwater, nutrient and other pollutant input rates.
2. Chemical, biological and physical properties of the water column.
3. Phytoplankton community characteristics (abundances, biomass and primary production rates).
4. Benthic community characteristics (abundances and biomass).

1.2 Conceptual Model of Water Quality Processes in Chesapeake Bay

During the past three decades much has been learned about the effects of both natural and anthropogenic nutrient inputs (*e.g.*, nitrogen, phosphorus, silica) on such important estuarine features as phytoplankton production, algal biomass, seagrass abundance and distribution and oxygen conditions in deep waters (Nixon, 1981, 1988; Boynton *et al.* 1982; Kemp *et al.* 1983; D'Elia *et al.* 1983; Garber *et al.* 1989; Malone, 1992; Kemp and Boynton, 1992; Boynton and Kemp 2007). While our understanding is not complete, important pathways regulating these processes have been identified and related to water quality issues. Of particular importance here, it has been determined that (1) algal primary production and biomass levels in many estuaries (including Chesapeake Bay) are responsive to nutrient loading rates, (2) high rates of algal production and algal blooms are sustained through summer and fall periods by recycling of essential nutrients that enter the system during the high flow periods of the year, (3) the “nutrient memory” of estuarine systems is relatively short (one to several years) and (4) submerged aquatic vegetation (SAV) communities are responsive to water quality conditions, especially light availability, that is modulated both by water column turbidity regimes and epiphytic fouling on SAV leaf surfaces.

Nutrients and organic matter enter the bay from a variety of sources, including sewage treatment plant effluents, fluvial inputs, local non-point drainage and direct rainfall on bay waters. Dissolved nutrients are rapidly incorporated into particulate matter via biological, chemical and physical mechanisms. A portion of this newly produced organic matter sinks to the bottom, decomposes and thereby contributes to the development of hypoxic or anoxic conditions and loss of habitat for important infaunal, shellfish and demersal fish communities. Eutrophic (nutrient enriched) conditions favor the growth of a diverse assemblage of estuarine bacteria who play a major role in consuming dissolved oxygen and the development of hypoxic and anoxic conditions. The regenerative and large short-term nutrient storage capacities of estuarine sediments ensure a large return flux of nutrients from sediments to the water column that can sustain continued high rates of phytoplanktonic growth and biomass accumulation. Continued growth and accumulation supports high rates of deposition of organics to deep waters, creating and sustaining hypoxic and anoxic conditions typically associated with eutrophication of estuarine systems. To a considerable extent, it is the magnitude of these processes that determines water quality conditions in many zones of the bay. Ultimately, these processes are driven by inputs of organic matter and nutrients from both natural and anthropogenic sources. If water quality management programs are instituted and loadings of organic matter and nutrients decrease, changes in the magnitude of these processes are expected and will serve as a guide in determining the effectiveness of strategies aimed at improving bay water quality and habitat conditions. The schematic diagram in Figure 1-1 summarizes this conceptual eutrophication model where increased nitrogen (N) and phosphorus (P) loads result in a water quality degradation trajectory and reduced N and P loads lead to a restoration trajectory. There is ample empirical evidence for the importance of N and P load variation. For example, water quality and habitat conditions change dramatically between wet and dry years, with the former having degradation trajectory characteristics and the latter, restoration trajectory characteristics (Boynton and Kemp, 2000; Hagy *et al.* 2004; Kemp *et al.* 2005). However, the exact temporal sequence of restoration may range from simple and rapid reversals to complex and lengthy processes (Kemp and Goldman 2008).

Within the context of this model a monitoring component focused on SAV and other near-shore habitat and water quality conditions has been developed and was fully operational in the Potomac River estuary during 2006, 2007 and is continuing during 2008.

Specifically, this program involved monthly (April - October), detailed surface water quality mapping using the DATAFLOW system. In these monitoring activities the working hypothesis is if anthropogenic nutrient and organic matter loadings decrease, the cycle of high organic deposition rates to sediments, sediment oxygen demand, release of sediment nutrients, continued high algal production, and high water column turbidity will also decrease. As a result, the potential for SAV re-colonization will increase and the status of deep-water habitats will improve.

1.3 Objectives of the Water Quality Monitoring Program

The EPC has undergone program modification since its inception in 1984 but its overall objectives have remained consistent with those of other Monitoring Program Components. The objectives of the 2007 EPC program were as follows:

1. Conduct Dataflow monitoring of near shore and off shore environments in the Potomac River Estuary. In the Potomac the EPC component conducted Dataflow monitoring in the most downstream and most upstream portions of the estuary. A total of seven cruises were conducted in the Potomac. The goal of these investigations was to quantify habitat conditions relative to SAV water quality criteria.
2. Continue to explore GIS applications for interpretation of Dataflow results. Issues of proper and efficient mapping techniques and GIS modeling of results have been initiated and progress from earlier efforts.
3. The results of the second year of investigations and analyses of the Corsica River estuary have been completed. These analyses focused on the following, including:
 - a. A detailed review of community production and respiration during 2005 – 2007
 - b. Additional measurements of denitrification and nutrient burial in the tidal headwater area of the Corsica
 - c. Further development of the Corsica River estuary box model

Summary of Nutrient-Related Feedbacks in Bay Ecosystem

- Positive & negative feedbacks control paths of ecosystem change with Bay degradation
- Among other mechanisms, input of nutrients affects hypoxia & light
- Hypoxia leads to more nutrients, more algae, & more hypoxia
- Turbidity leads to less SAV causing more turbidity, less SAV
- Oysters & marshes tend to reinforce these feedbacks
- Processes reverse w/ restoration, thus reinforcing trends

From Kemp et al. 2005

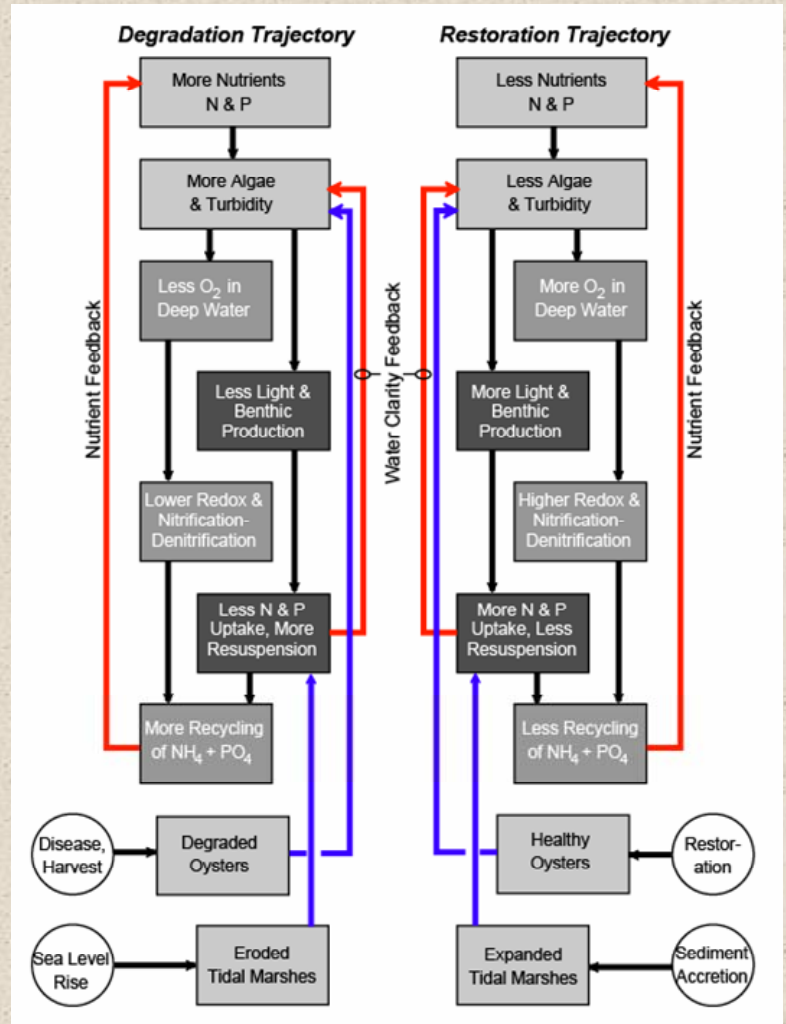


Figure 1-1. A simplified schematic diagram indicating degradation and restoration trajectories of an estuarine ecosystem. Lightly shaded boxes in the diagram indicate past and present components of the EPC program in the Patuxent River and Tangier Sound. (Adapted from Kemp *et al.* 2005)

1.4 References

Boynton et al. 1985 – 2007 EPC Interpretive Reports:

- Boynton, W.R., W.M. Kemp and J.M. Barnes.** 1985. Ecosystem Processes Component Level I Data Report No. 2. Chesapeake Biological Laboratory (CBL), University of Maryland System, Solomons, MD 20688-0038. Ref. No.[UMCEES]CBL 85-121.
- Boynton, W.R., W.M. Kemp, J.H. Garber and J.M. Barnes.** 1986. Ecosystem Processes Component Level 1 Interpretive Report No. 3. Chesapeake Biological Laboratory (CBL), University of Maryland System, Solomons, MD 20688-0038. Ref. No.[UMCEES]CBL 86-56b.
- Boynton, W.R., W.M. Kemp, J.H. Garber, J.M. Barnes, L.L. Robertson and J.L. Watts.** 1987. Ecosystem Processes Component Level 1 Interpretive Report No. 4. Chesapeake Biological Laboratory (CBL), University of Maryland System, Solomons, MD 20688-0038. Ref. No.[UMCEES]CBL 88-06.
- Boynton, W.R., W.M. Kemp, J.H. Garber, J.M. Barnes, L.L. Robertson and J.L. Watts.** 1988. Ecosystem Processes Component Level 1 Interpretive Report No. 5. Chesapeake Biological Laboratory (CBL), University of Maryland System, Solomons, MD 20688-0038. Ref. No.[UMCEES]CBL 88-69.
- Boynton, W.R., J.H. Garber, W.M. Kemp, J.M. Barnes, J.L. Watts, S. Stammerjohn and L.L. Matteson.** 1989. Ecosystem Processes Component Level 1 Interpretive Report No. 6. Chesapeake Biological Laboratory (CBL), University of Maryland System, Solomons, MD 20688-0038. Ref. No.[UMCEES]CBL 89-080.
- Boynton, W.R., J.H. Garber, W.M. Kemp, J.M. Barnes, L.L. Matteson, J.L. Watts, S. Stammerjohn and F.M. Rohland.** 1990. Ecosystem Processes Component Level 1 Interpretive Report No. 7. Chesapeake Biological Laboratory (CBL), University of Maryland System, Solomons, MD 20688-0038. Ref. No.[UMCEES]CBL 90-062.
- Boynton, W.R., W.M. Kemp, J.M. Barnes, L.L. Matteson, J.L. Watts, S. Stammerjohn, D.A. Jasinski and F.M. Rohland.** 1991. Ecosystem Processes Component Level 1 Interpretive Report No. 8. Chesapeake Biological Laboratory (CBL), University of Maryland System, Solomons, MD 20688-0038. Ref. No.[UMCEES]CBL 91-110.
- Boynton, W.R., W.M. Kemp, J.M. Barnes, L.L. Matteson, J.L. Watts, S. Stammerjohn, D.A. Jasinski and F.M. Rohland.** 1992. Ecosystem Processes Component Level 1 Interpretive Report No. 9. Chesapeake Biological Laboratory (CBL), University of Maryland System, Solomons, MD 20688-0038. Ref. No.[UMCEES]CBL 92-042.
- Boynton, W.R., W.M. Kemp, J.M. Barnes, L.L. Matteson, F.M. Rohland, D.A. Jasinski and H.L. Kimble.** 1993. Ecosystem Processes Component Level 1 Interpretive Report No. 10.

Chesapeake Biological Laboratory (CBL), University of Maryland System, Solomons, MD 20688-0038. Ref. No.[UMCEES]CBL 93-030a.

Boynton, W.R., W.M. Kemp, J.M. Barnes, L.L. Matteson, F.M. Rohland, D.A. Jasinski and H.L. Kimble. 1994. Ecosystem Processes Component Level 1 Interpretive Report No. 11. Chesapeake Biological Laboratory (CBL), University of Maryland System, Solomons, MD 20688-0038. Ref. No.[UMCEES]CBL 94-031a.

Boynton, W.R., W.M. Kemp, J.M. Barnes, L.L. Matteson, F.M. Rohland, L.L. Magdeburger and B.J. Weaver. 1995. Ecosystem Processes Component Level 1 Interpretive Report No 12. Chesapeake Biological Laboratory (CBL), University of Maryland System, Solomons, MD 20688-0038. Ref. No.[UMCEES]CBL 95-039.

Boynton, W.R., W.M. Kemp, J.M. Barnes, L.L. Matteson, F.M. Rohland, D.A. Jasinski, J.D. Hagy III, L.L. Magdeburger and B.J. Weaver. 1996. Ecosystem Processes Component Level 1 Interpretive Report No. 13. Chesapeake Biological Laboratory (CBL), University of Maryland System, Solomons, MD 20688-0038. Ref. No. [UMCEES]CBL 96-040a.

Boynton, W.R., J.M. Barnes, F.M. Rohland, L.L. Matteson, L.L. Magdeburger, J.D. Hagy III, J.M. Frank, B.F. Sweeney, M.M. Weir and R.M. Stankelis. 1997. Ecosystem Processes Component Level 1 Interpretive Report No. 14. Chesapeake Biological Laboratory (CBL), University of Maryland System, Solomons, MD 20688-0038. Ref. No. [UMCEES]CBL 97-009a.

Boynton, W.R., R.M. Stankelis, E.H. Burger, F.M. Rohland, J.D. Hagy III, J.M. Frank, L.L. Matteson and M.M. Weir. 1998. Ecosystem Processes Component Level 1 Interpretive Report No. 15. Chesapeake Biological Laboratory (CBL), University of Maryland System, Solomons, MD 20688-0038. Ref. No. [UMCES]CBL 98-073a.

Boynton, W.R., R.M. Stankelis, J.D. Hagy III, F.M. Rohland, and J.M. Frank. 1999. Ecosystem Processes Component Level 1 Interpretive Report No. 16. Chesapeake Biological Laboratory (CBL), University of Maryland System, Solomons, MD 20688-0038. Ref. No. [UMCES]CBL 99-0070a.

Boynton, W.R., R.M. Stankelis, J.D. Hagy, F.M. Rohland, and J.M. Frank. 2000. Ecosystem Processes Component Level 1 Interpretive Report No. 17. Chesapeake Biological Laboratory (CBL), University of Maryland System, Solomons, MD 20688-0038. Ref. No. [UMCES]CBL 00-0174.

Boynton, W.R., R.M. Stankelis, F.M. Rohland, J.M. Frank and J.M. Lawrence. 2001. Ecosystem Processes Component Level 1 Interpretive Report No. 18. Chesapeake Biological Laboratory (CBL), University of Maryland System, Solomons, MD 20688-0038. Ref. No. [UMCES]CBL 01-0088.

Boynton, W.R., R.M. Stankelis, F.M. Rohland, J.M. Frank, J.M. Lawrence and B.W. Bean. 2002. Ecosystem Processes Component Level 1 Interpretive Report No. 19. Chesapeake

Biological Laboratory (CBL), University of Maryland System, Solomons, MD 20688-0038.
Ref. No. [UMCES]CBL 02-0125a.

Boynton, W.R. and F.M. Rohland (eds.); R.M. Stankelis, E.K. Machelor Bailey, P.W. Smail and M.A.C. Ceballos. 2003. Ecosystem Processes Component (EPC). Level 1 Interpretive Report No. 20. Chesapeake Biological Laboratory (CBL), Univ. of Maryland Center for Environmental Science, Solomons, MD 20688-0038. Ref. No. [UMCES]CBL 03-303. [UMCES Technical Series No. TS-419-03-CBL].

Boynton, W.R., R.M. Stankelis, P.W. Smail and E.K. Bailey. 2004. Ecosystem Processes Component (EPC). Maryland Chesapeake Bay Water Quality Monitoring Program, Level 1 report No. 21. Jul. 1984 - Dec. 2003. Ref. No. [UMCES] CBL 04-086. [UMCES Technical Series No. TS-447-04-CBL].

Boynton, W.R., R.M. Stankelis, P.W. Smail, E.K. Bailey and H.L. Soulen. 2005. Ecosystem Processes Component (EPC). Maryland Chesapeake Bay Water Quality Monitoring Program, Level 1 report No. 22. Jul. 1984 - Dec. 2004. Ref. No. [UMCES] CBL 05-067. [UMCES Technical Series No. TS-492-05-CBL].

Boynton, W.R., P.W. Smail, E.M. Bailey and S.M. Moesel. 2006. Ecosystem Processes Component (EPC). Maryland Chesapeake Bay Water Quality Monitoring Program, Level 1 report No. 22. Jul. 1984 - Dec. 2005. Ref. No. [UMCES] CBL 06-108. [UMCES Technical Series No. TS-253-06-CBL].

Boynton, W.R., E.M. Bailey, S.M. Moesel, L.A. Moore, J.K. Rayburn, L.A. Wainger and K.V. Wood. 2007. Ecosystem Processes Component (EPC). Maryland Chesapeake Bay Water Quality Monitoring Program, Level 1 report No. 22. Jul. 1984 - Dec. 2006. Ref. No. [UMCES] CBL 07-112. [UMCES Technical Series No. TS-536-07-CBL].

Chapter 1 Text References:

Boynton, W.R. and W.M. Kemp. 2000. Influence of River Flow and Nutrient Loads on Selected Ecosystem Processes: A Synthesis of Chesapeake Bay Data, p. 269-298. In: J.E. Hobbie, [Ed.], *Estuarine Science: A Synthetic Approach to Research and Practice*, Island Press, Washington, D.C.

Boynton, W.R. and W.M. Kemp. 2007. Nitrogen in Estuaries in Capone, D.G., Bronk, D.A., Mulholland, M.R., Carpenter, E.J., 2007. Nitrogen in the Marine Environment, in press.

Boynton, W.R., W.M. Kemp and C.W. Keefe. 1982. A comparative analysis of nutrients and other factors influencing estuarine phytoplankton production, p. 69-90. In: V.S. Kennedy, [Ed.], *Estuarine Comparisons*, Academic Press, NY.

D'Elia, C.F., D.M. Nelson, and W.R. Boynton. 1983. Chesapeake Bay nutrient and plankton dynamics: III. The annual cycle of dissolved silicon. *Geochim. Cosmochim. Acta* 14:1945-1955.

- Garber, J.H., W.R. Boynton, J.M. Barnes., L.L. Matteson., L.L. Robertson., A.D. Ward and J.L. Watts.** 1989. Ecosystem Processes Component and Benthic Exchange and Sediment Transformations. Final Data Report. Maryland Department of the Environment. Maryland Chesapeake Bay Water Quality Monitoring Program. Chesapeake Biological Laboratory (CBL), University of Maryland System, Solomons, MD 20688-0038. Ref. No.[UMCEES]CBL 89-075.
- Hagy, J.D., W.R. Boynton, C.W. Keefe, and K.V. Wood.** 2004. Hypoxia in Chesapeake Bay, 1950-2001: Long-term Change in Relation to Nutrient Loading and River Flow. *Estuaries* 27(4):634-658.
- Kemp, W.M. and W.R. Boynton.** 1992. Benthic-Pelagic Interactions: Nutrient and Oxygen Dynamics. In: D.E. Smith, M. Leffler and G. Mackiernan [Eds.], *Oxygen Dynamics in the Chesapeake Bay: A synthesis of Recent Research*. Maryland Sea Grant Book, College Park, MD, p. 149-221.
- Kemp, W.M and Goldman.** 2008. Thresholds in the Recovery of Eutrophic Ecosystems. A Synthesis of Research and Implications for Management. A Workshop Report Sponsored by: Chesapeake Bay Program Scientific and Technical Advisory Committee and Maryland Sea Grant, Belmont Conference Center, Elkridge, MD. February 14-15, 2007.
- Kemp, W.M., W.R. Boynton, J.C. Stevenson, R.W. Twilley and J.C. Means.** 1983. The decline of submerged vascular plants in Chesapeake Bay: summary of results concerning possible causes. *Mar. Tech. Soc. J.* 17(2):78-89.
- Kemp, W. M., W. R. Boynton, J. E. Adolf, D. F. Boesch, W. C. Boicourt, G. Brush, J. C. Cornwell, T. R. Fisher, P. M. Glibert, J. D. Hagy, L. W. Harding, E. D. Houde, D. G. Kimmel, W. D. Miller, R. I. E. Newell, M. R. Roman, E. M. Smith, and J. C. Stevenson.** 2005. Eutrophication of Chesapeake Bay: Historical trends and ecological interactions. *Mar Ecol Prog Ser* 303: 1-29.
- Magnien R.E. et al.** 1987. Monitoring for management actions. First Biennial Report. The Maryland Office of Environmental Programs, Chesapeake Bay, Water Quality Monitoring Program, Baltimore, MD.
- Malone, T.C.** 1992. Effects of Water Column Processes on Dissolved Oxygen Nutrients, Phytoplankton and Zooplankton. In: D.E. Smith, M. Leffler and G. Mackiernan [Eds.], *Oxygen Dynamics in the Chesapeake Bay: A synthesis of Recent Research*. Maryland Sea Grant Book, College Park, MD, p. 149-221.
- Nixon, S.W.** 1981. Remineralization and nutrient cycling in coastal marine ecosystems, p. 111-138. In: B.J. Neilson and L.E. Cronin [Eds.], *Estuaries and Nutrients*. Humana Press, Clifton, NJ.
- Nixon, S.W.** 1988. Physical energy inputs and comparative ecology of lake and marine ecosystems. *Limnol. Oceanogr.* 33 (4, part 2), 1005-1025.

Progress Report of the Baywide Nutrient Reduction Reevaluation, Chesapeake Bay Program.
1992. U.S. Environmental Protection Agency for the Chesapeake Bay Program
[CSC.LR18.12/91

2.0 Spatially Intensive Shallow Water Quality Monitoring of the Potomac River

Lisa A. Wainger, Maria A.C. Ceballos, Eva M. Bailey and Walter R. Boynton

2.1	Introduction	2-1
2.2	Methods, Locations and Sampling Frequency	2-1
2.3	Calibration Station Results	2-7
2.4	Evaluating Potential SAV Habitat	2-14
2.5	Results of comparing water quality data with SAV habitat criteria	2-16
2.6	Discussion	2-23
2.7	References	2-25

2.1 Introduction

During 2007 we evaluated patterns in surface water quality using the DATAFLOW© mapping system (first designed by Madden and Day 1992) in the Potomac River. Our Potomac effort was part of a multi-team monitoring design intended to sample the entire Potomac within the shortest practicable timeframe. We sampled the mesohaline (extreme lower) and tidal fresh portions of the river. DATAFLOW© was deployed from a small research vessel and provided high-resolution spatial mapping of surface water quality variables. Our cruise tracks included both shallow (<2.0 m) and deeper waters, and sampling was weighted towards the littoral zone that represents habitat critical to Submerged Aquatic Vegetation (SAV) and associated organisms.

Traditional water quality monitoring in the Chesapeake Bay, and in tributary estuaries such as the Potomac, has been conducted almost exclusively in deeper channel waters, and conditions in these areas do not adequately represent water quality conditions in shallow zones. Thus, it was important to collect water quality data in both shallow water and deeper off-shore habitats and to determine the extent of gradients in water quality parameters between these areas of the estuary. The DATAFLOW© cruise track covered as much area as possible, in both shallow and deeper portions of the system. The vessel traveled at approximately 20 knots, or 10 meters per second and collected data at 3 second intervals which amounts to about one observation made every 30 meters.

2.2 Methods, Locations and Sampling Frequency

2.2.1 DATAFLOW©

DATAFLOW© is a compact, self-contained surface water quality mapping system, suitable for use in a small boat operating at speeds of up to 20 knots. A schematic of this system is shown in Figure 2-1. Our newer version differs from older models through the addition of a wireless display and miniature, ruggedized PC data-logger, which eliminates the need for separate depth and YSI data-loggers. Surface water (approximately 0.5 m deep depending on vessel speed and angle of plane) is collected through a pipe (“ram”) secured to the transom of the vessel. Assisted by a high-speed pump, water is passed through a hose to a flow meter and then to an inverted flow-through cell to ensure that no air bubbles interfere with sampling or data sonde performance. An array of water quality sensors are positioned within the flow-through cell.

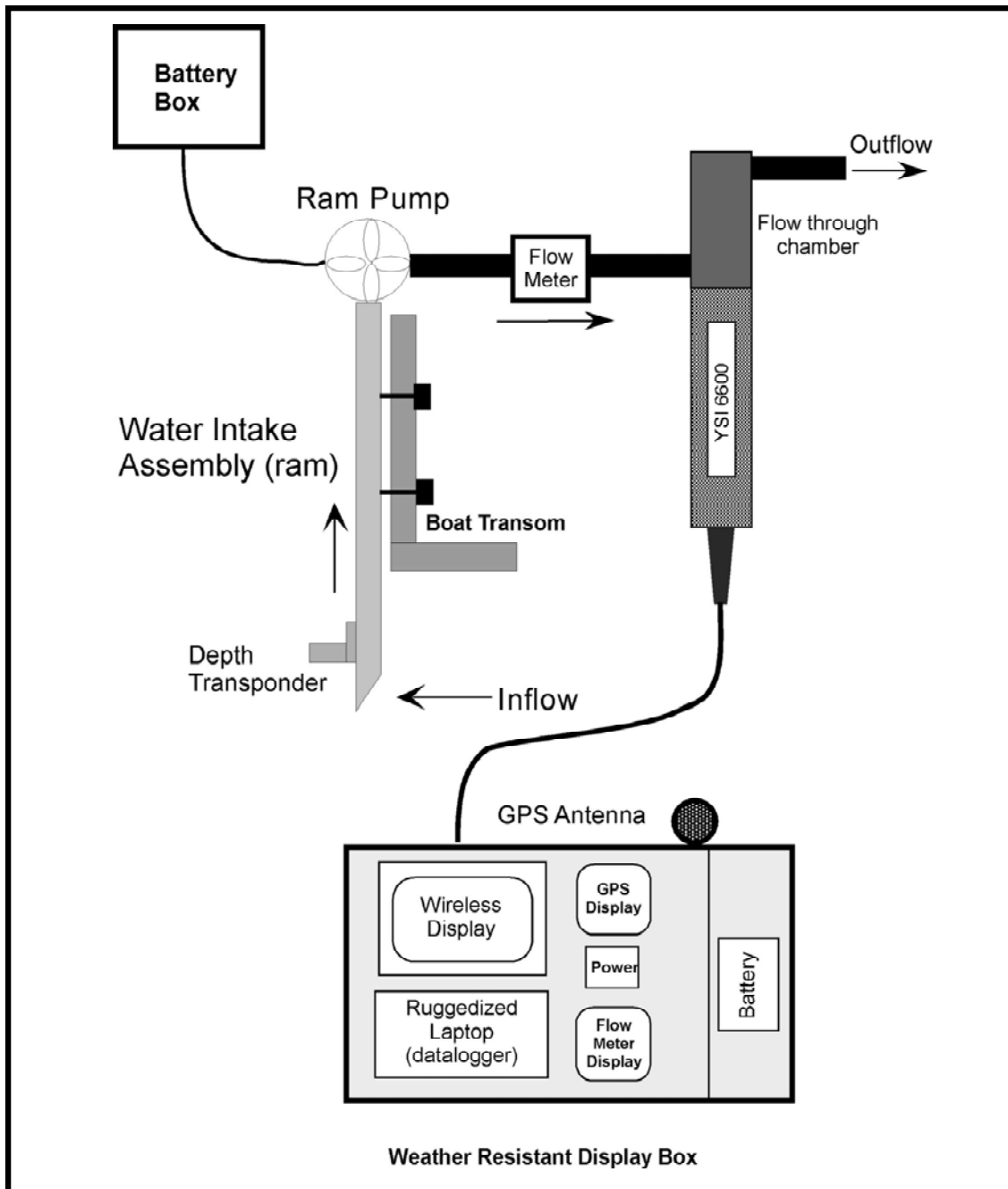


Figure 2-1. Schematic diagram of DATAFLOW© illustrating the path of water through the instrument.

Seawater is drawn up through the ram behind the transom of the research vessel. A centrifugal pump mounted on the ram (ram pump) boosts the flow. The water flows through a paddle-wheel type flow meter that triggers a horn if the flow rate falls below 3 L min^{-1} , and then to an inverted flow-through chamber where it is sampled by the YSI 6600 datasonde sensors. The inverted mount is used in order to evacuate any air bubbles in the system. After sampling, the water is discharged overboard. The displays for the instruments, including the wireless display for the ruggedized laptop, Garmin 168 GPS/depthsounder, and flow meter are located on the instrument platform.

DATAFLOW© surveys were conducted from a CBL vessel and typically involved two field technicians to perform sampling operations and safe navigation. The DATAFLOW© package consists of a water circulation system that is sampled at a prescribed rate by a Yellow Springs, Inc. 6600 DataSonde sensor combined with a ruggedized minicomputer running data-logging software. This sensor system provides data on dissolved oxygen, temperature, conductivity, salinity, turbidity and fluorescence (from which is derived chlorophyll-*a* concentration). The computer also records latitude and longitude and depth output from a Garmin 168 GPS/Depthsounder unit utilizing an NMEA 0183 v. 2.0 data format. Data files were output in a comma and space delimited format. Although the flow rate does not affect any of the sensor readings, decreased flow is an indication of either a partial blockage or an interruption of water flow to the instrument and affects the water turnover rate of the system. An inline flow meter wired to a low-flow alarm alerts the operators of potential problems. The low-flow alarm is set to 3.0 liters per minute. A single 1100 gallon per hour “Rule Pro Series” pump provides approximately 20-25 liters per minute of flow to the system on station at idle and 35-40 liters per minute of flow while underway at 20 knots due to additional flow created by the ram effect.

During the course of a cruise, the vessel stopped at established calibration stations located along the cruise track. While anchored, whole water samples were taken from the water circulation system. The Nutrient Analytical Services Laboratory (NASL) at Chesapeake Biological Laboratory (CBL) analyzed those water samples for dissolved nutrient content, concentrations of total suspended and volatile solids, and chlorophyll-*a*. Samples were also taken and analyzed for chlorophyll-*a* by the Maryland Department of Health and Mental Hygiene (MD DHMH), and these data were transmitted directly from MD DHMH to Maryland DNR. The crew also measured turbidity using a Secchi disk, and determined the flux of Photosynthetically Active Radiation (PAR) in the water column using Li-Cor quantum (Q) and underwater quantum (UNQ) sensors. These calibration stations provide additional enhancement of the high-resolution description of a tributary, and provide laboratory values to verify instrument parameter values obtained in the field. The data that were collected substantially improved characterization of water quality conditions in the near shore habitats as well as system-wide water quality.

2.2.2 Sampling locations and frequency

DATAFLOW cruises were performed on a monthly basis in 2007 from April to October on both the lower (mesohaline) portion and the upper (tidal fresh) portion of the Potomac River estuary, for a total of fourteen cruises. The cruise dates are listed in Table 2-1. Every effort was made to coordinate with the other monitoring teams so as to simultaneously sample adjacent portions of the river whenever feasible. Cruise tracks were chosen to provide a reasonable coverage of each water body while sampling both near-shore and mid-river waters. Sample cruise tracks are shown Figures 2-2 and 2-3. Target shallow water sampling depth was < 2 meters. However this was not always possible due to bottom contour, fishing equipment, vessel traffic or debris in the water. The selection of calibration station locations was made to sample the greatest possible range of water quality conditions found during each cruise and to sample a broad spatial area. Every effort was made to maintain the same location of calibration stations between cruises. The coordinates for those stations are listed in Table 2-2. On every Upper Potomac cruise, an extra water chemistry sample was taken at station XFB0500 (CBL 355) as an analytical duplicate (bottle code 666).

Table 2-1. DATAFLOW cruise dates in 2007.

Region	Spring	Summer	Fall
Upper Potomac River	4/18, 5/17, 6/12	7/17, 8/14	9/11, 10/02
Lower Potomac River	4/20, 5/14, 6/11	7/16, 8/13	9/10, 10/01

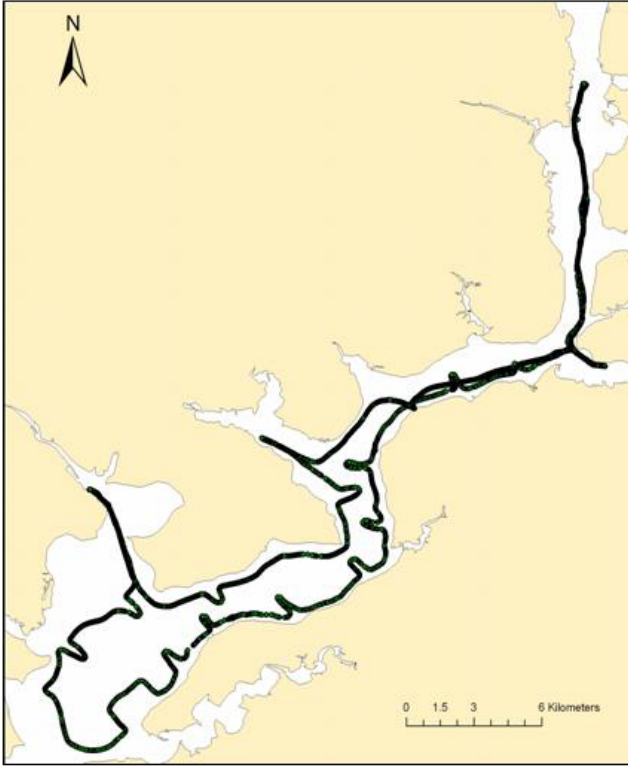


Figure 2-2. Typical DATAFLOW cruise track for the Upper (tidal fresh) Potomac River.

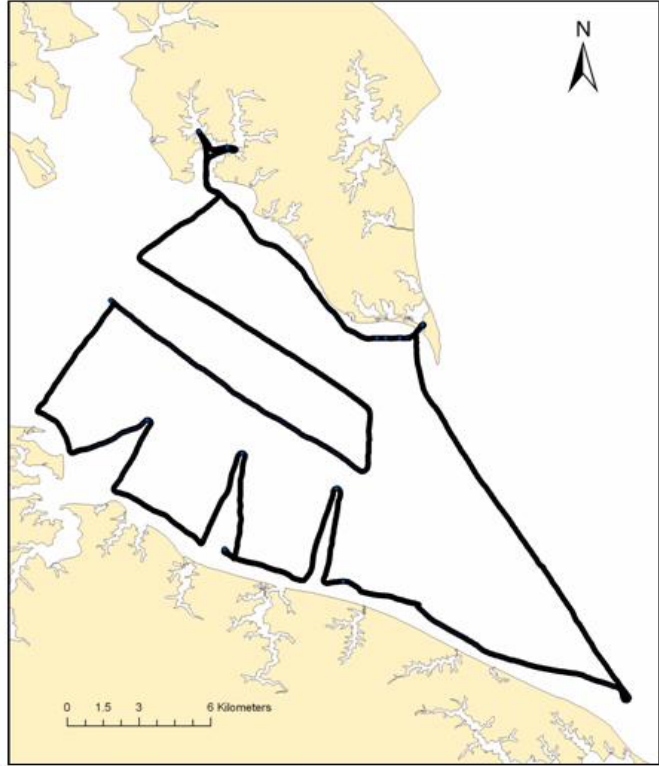


Figure 2-3. Typical DATAFLOW cruise track for the Lower (mesohaline) Potomac River.

Table 2-2. Location of DATAFLOW calibration stations (NAD83).

Region	Station	CBL Bottle #	Latitude	Longitude
Upper Potomac	XFB0500	355	38.6758	-77.1663
	XFB8408	357	38.8079	-77.0321
	XFB0231	358	38.6699	-77.1151
	XFB2184	359	38.7016	-77.0259
	TF2.3	360	38.6081	-77.1739
	XEA8467	361	38.6600	-77.2300
Lower Potomac	XBF0956 (XBF7254)*	349	38.1205	-76.4101
	LE2.3	350	38.0215	-76.3477
	XBF3534	351	38.0595	-76.4440
	XBG2601	352	38.0443	-76.3334
	XBF6903	354	37.9483	-76.3283

*XBF0956 changed to XBF7254 in 2008

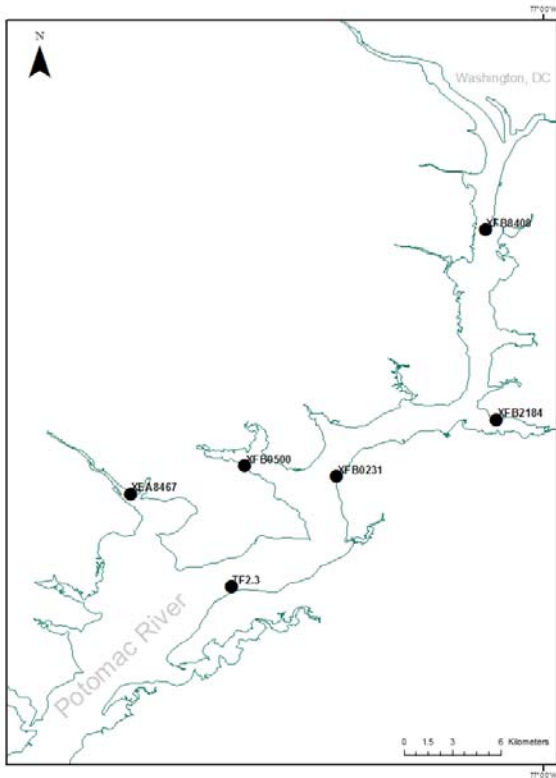


Figure 2-4. DATAFLOW calibration stations on the Upper Potomac, 2007

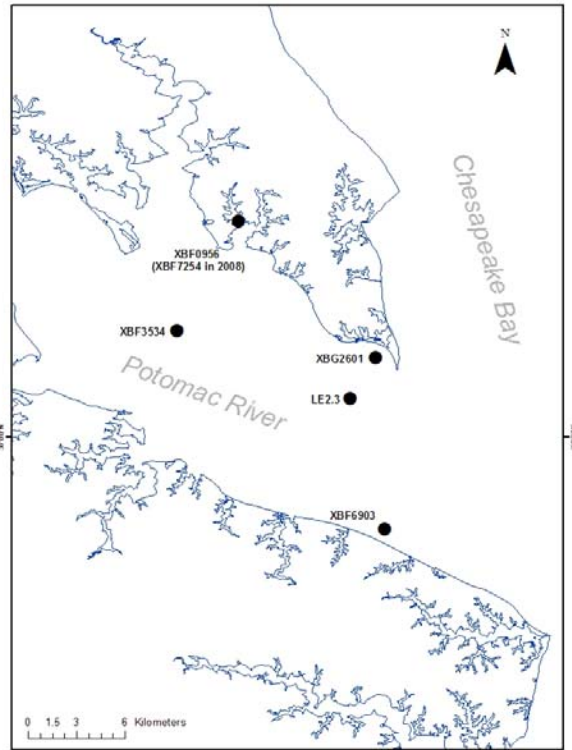


Figure 2-5. DATAFLOW calibration stations on the Lower Potomac, 2007.

2.2.3 Calibration Station Sampling

At each calibration station, a series of measurements were made and whole water samples collected. Locations of the calibration stations are shown in Figures 2-4 and 2-5. Secchi depths were recorded and Li-Cor quanta sensors were used to determine the amount of photosynthetically active radiation (PAR) in the water column. These data were used to determine the water-column light attenuation coefficient (K_d). YSI datasonde turbidity sensor output (NTU) was individually regressed against Secchi depth and K_d values. Whole water samples were taken and sent for analysis to Nutrient Analytical Services Lab (NASL) at CBL for both total and active chlorophyll-*a*, total suspended solids (TSS) and total volatile solids (TVS). These chlorophyll-*a* values were compared against chlorophyll sensor output. Water samples were also analyzed by NASL to determine concentrations of dissolved nutrients. These nutrients included dissolved inorganic nitrogen (DIN; summation of ammonium $[\text{NH}_4^+]$, nitrite $[\text{NO}_2^-]$, nitrate $[\text{NO}_3^-]$) and dissolved inorganic phosphorus (DIP). Other nutrients analyzed included Dissolved Organic Carbon (DOC), Particulate Carbon (PC), Particulate Phosphorus (PP), Particulate Inorganic Phosphorus (PIP), Total Dissolved Nitrogen (TDN), Total Dissolved Phosphorus (TDP), and Silicate (SiO_2). A detailed explanation of all field and laboratory procedures is given in the annual CBL QAPP documentation (Boynton *et al.* 2007).

2.2.4 Data QA/QC Procedures

The data gathered with DATAFLOW underwent QA/QC processes approved by managers and researchers from Maryland and Virginia through Chesapeake Bay Program Tidal Monitoring and

Analysis Workgroup meetings (Smail *et al.* 2005). Data files were formatted and checked for erroneous values using a macro developed by Maryland DNR for Microsoft Excel. The QA/QC process ensures that extreme values resulting from data concatenation error (a function of how the instrument data are logged) or turbidity spikes resulting from operating a vessel in shoal areas can be flagged in the proofed dataset. Data are also visually inspected using ArcGIS where specific values can be compared with calibration data and the cruise log in order to eliminate obvious erroneous values as described above. Combined datasets from the entire sampling season were also plotted in order to reveal extreme values or other temporal patterns.

2.2.5 Spatial Interpolation

Two types of interpolation were used to estimate spatial distribution of water quality conditions from the points sampled by DATAFLOW. Inverse Distance Weighting (IDW) is a spatial interpolation method that uses a weighted average of observed data points to estimate values for unsampled locations. The inverse of the square (or other power function) of the distance between an observation and the point being estimated is used to weight observations when estimating unsampled areas. In effect, this means that unsampled points are estimated primarily from the closest points and distant points are barely considered.

Kriging is a more sophisticated interpolation method than IDW because it uses a statistical model to establish the weights on observed points when estimating unsampled areas. Patterns of spatial covariance in the data are evaluated to fit a statistical model that describes how the data vary in space and to establish weights on observation points to minimize estimation variance. The weights create unbiased estimates, meaning there is no systematic under- or over-estimation. Similar to IDW, the closest observations are given the largest weights when estimating unsampled points. Kriging is also sufficiently flexible that anisotropic variance can be considered. If, for example, points are more closely correlated latitudinally than longitudinally, this data structure can be considered during estimation.

For this analysis, we applied both IDW and ordinary kriging to interpolate the collected data. IDW was used when data were sparse (e.g., for nutrient data that are only available from calibration stations) or when the data collection transect was linear over large areas. Kriging is either impossible or unadvisable under these data conditions because the underlying statistical model cannot be estimated or cannot be estimated with confidence. For the majority of the data collected, ordinary kriging was used to conduct interpolations.

During kriging, we used the land margins of the estuary as barriers to data interpolation. Barriers are used within the kriging algorithm (ArcInfo Workstation 9.2 software) to prevent interpolation that disregards peninsulas or land structures that affect water flow and water quality. This technique differs from the default algorithm behavior within ArcMap 9.2 Extensions (Spatial Analyst or Geostatistical Analyst) and ArcInfo Workstation 9.2 in which the algorithm weights points using a straight line distance, as if peninsulas or other features of the shoreline were not present. When the barrier option is used in ArcInfo Workstation, the algorithm only uses points for interpolation that are on the same side of the barrier. The use of the barriers option greatly increases processing time of the data but appears to provide more realistic interpretations around peninsulas and generally smoother interpolation overall, with some exceptions.

2.3 Calibration Station Results

2.3.1 Fixed Calibration Station Nutrient Concentrations

Average surface water nutrient concentrations at fixed calibration stations (April-October, 2007) were generally higher in the upper compared to the lower Potomac estuary (Table 2-3 and Figure 2-6). Dissolved inorganic nitrogen ranged from 0.06 to 1.26 mg L⁻¹ and dissolved inorganic phosphorus ranged from 0.003 to 0.016 mg L⁻¹. These DIN concentrations are always well above nutrient half-saturation concentrations ($K_s = 0.5 - 2.5 \mu\text{M}$; 0.007 – 0.035 mg L⁻¹) for estuarine phytoplankton. However, PO₄ concentrations were much closer to K_s values (0.05 – 0.2 μM ; 0.0015 – 0.006 mg L⁻¹) suggesting possible P-limitation of phytoplankton growth.

Table 2-3. 2007 DATAFLOW calibration station nutrient concentrations.

Surface water DIN (dissolved inorganic nitrogen) (mg L⁻¹).

Area	Station	Bottle Code	Mean	N	Standard Deviation	Min	Max
Upper Potomac	XFB8408	357	1.26	7	0.22	0.87	1.45
	XFB0231	358	0.71	7	0.44	0.27	1.45
	TF2.3	360	0.74	7	0.36	0.38	1.20
	XFB2184	359	0.94	7	0.35	0.21	1.27
	XFB0500	355	0.79	7	0.45	0.18	1.33
	XEA8467	361	0.15	7	0.22	0.01	0.54
Lower Potomac	XBF3534	351	0.12	7	0.18	0.01	0.44
	LE2.3	350	0.12	7	0.20	0.01	0.52
	XBG2601	352	0.10	7	0.15	0.01	0.35
	XBF6903	354	0.14	7	0.23	0.01	0.62
	XBF0956	349	0.06	7	0.08	0.01	0.20

Surface water DIP (dissolved inorganic phosphorus) (mg L⁻¹).

Area	Station	Bottle Code	Mean	N	Standard Deviation	Min	Max
Upper Potomac	XFB8408	357	0.016	7	0.008	0.005	0.026
	XFB0231	358	0.008	7	0.003	0.002	0.011
	TF2.3	360	0.014	7	0.010	0.002	0.027
	XFB2184	359	0.014	7	0.008	0.001	0.024
	XFB0500	355	0.003	7	0.003	0.002	0.011
	XEA8467	361	0.003	7	0.002	0.001	0.008
Lower Potomac	XBF3534	351	0.004	7	0.002	0.001	0.008
	LE2.3	350	0.003	7	0.001	0.002	0.004
	XBG2601	352	0.003	7	0.001	0.001	0.005
	XBF6903	354	0.003	7	0.001	0.002	0.005
	XBF0956	349	0.003	7	0.002	0.002	0.007

Potomac River Dataflow Calibration Station Nutrients 2007

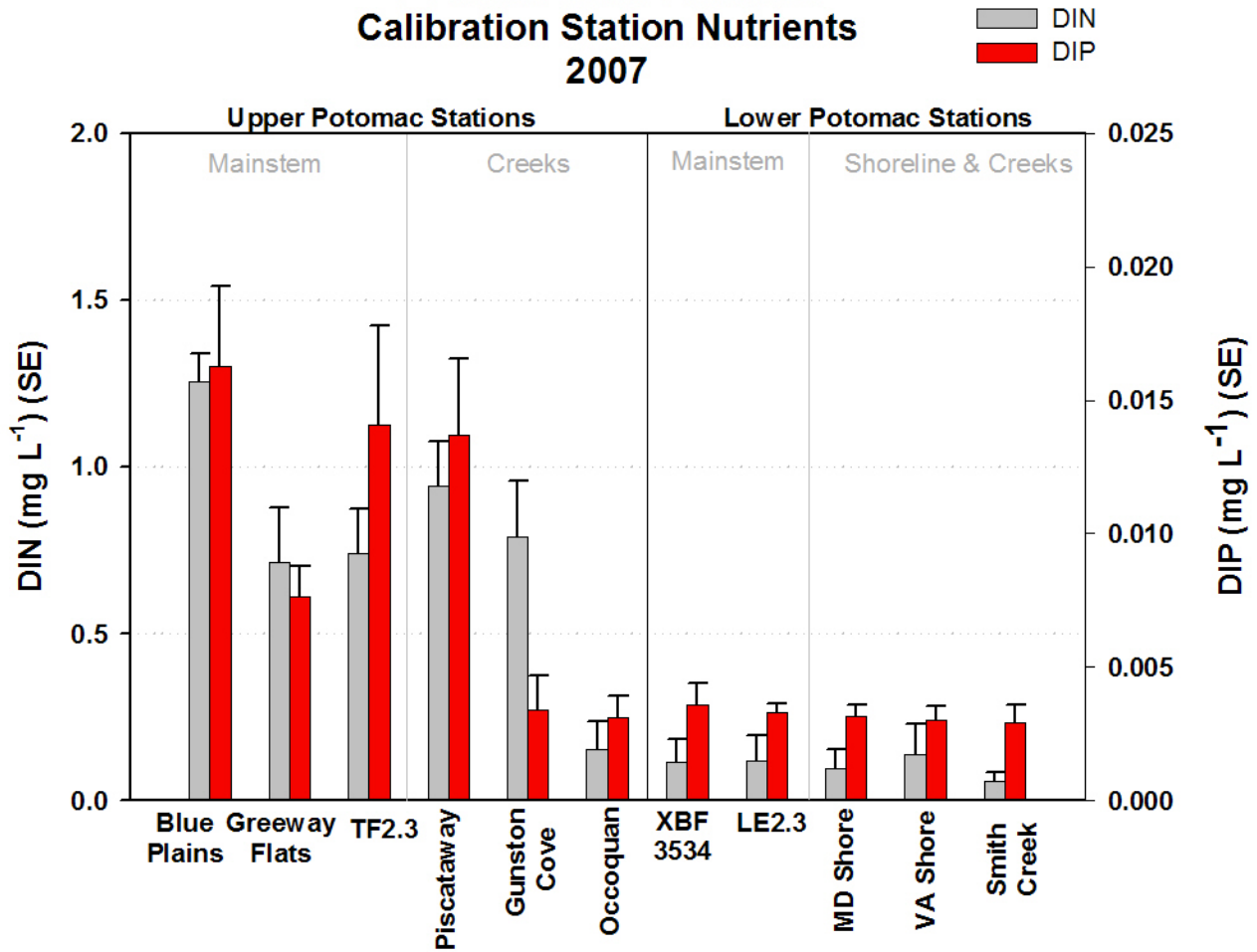


Figure 2-6. Average surface water dissolved inorganic nitrogen (grey bars) and dissolved inorganic phosphorus (red bars) for Potomac River Dataflow calibration stations in 2007 (units are mg L⁻¹). N= 7 cruises per station and error bars are standard error. Stations arranged in relative position from upstream (left) to downstream (right) in the main river and creeks.

Concentrations of DIN and DIP (Figure 2-7) at station TF2.3 (upper Potomac) were lower in 2007 when compared to long term averages for the same months (April-October). In the lower Potomac (station LE2.3) dissolved nutrients were similar to long term averages.

Potomac River Surface Water Nutrients April - October Averages

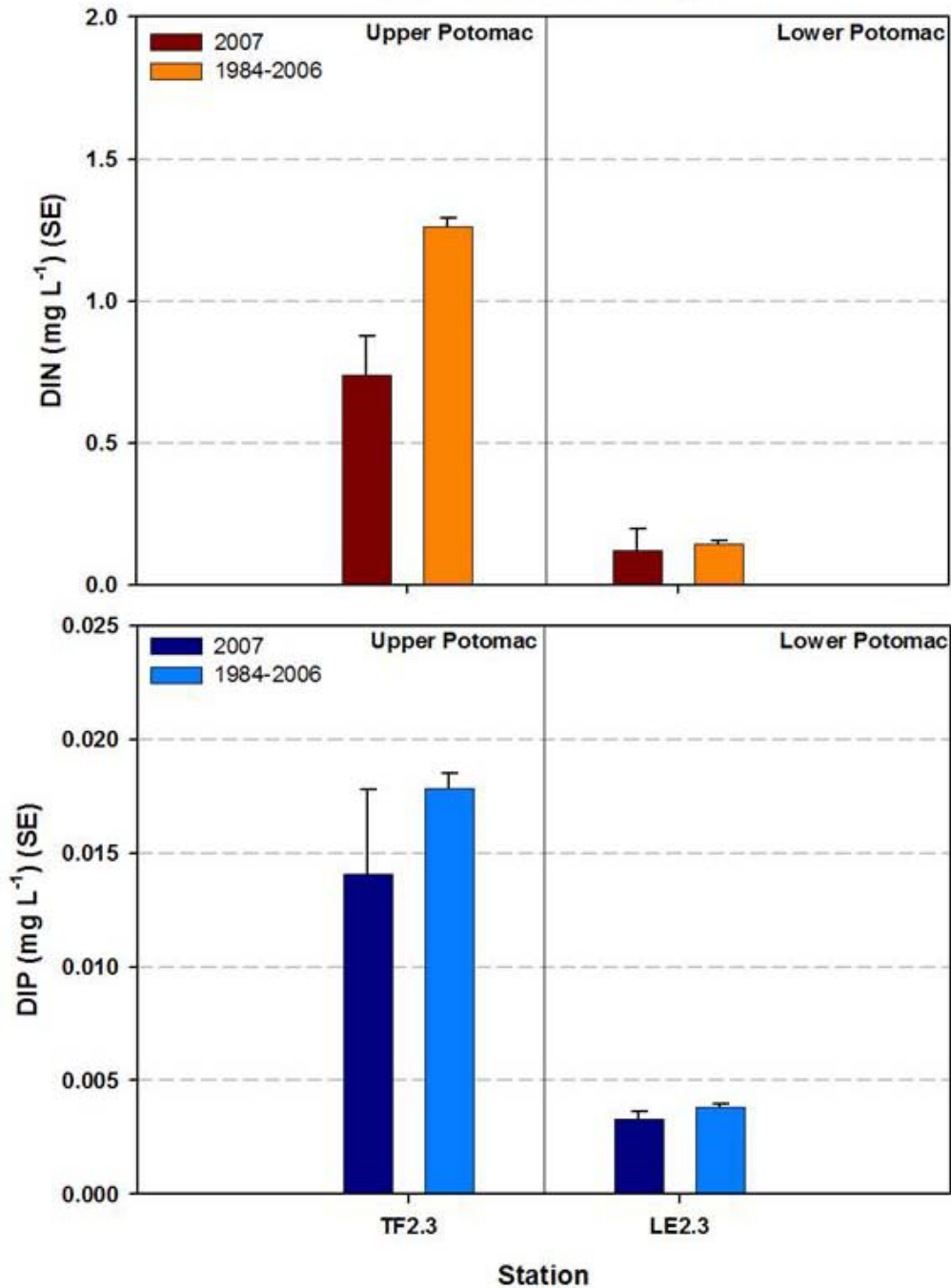


Figure 2-7. Average surface water DIN (top panel) and DIP (lower panel) for long term sampling stations in the Potomac River. The 2007 data from Dataflow calibration stations (N=7) and 1984-2006 data taken from Chesapeake Bay Program water quality monitoring program database (N~300).

2.3.2 Fixed Calibration Station Selected Water Quality Conditions

Multiple water quality parameters were collected at each DATAFLOW calibration station as described previously. Water column chlorophyll, turbidity and light attenuation conditions (Figures 2-8 to 2-10) are important indicators of habitat suitability for SAV growth. Average surface water

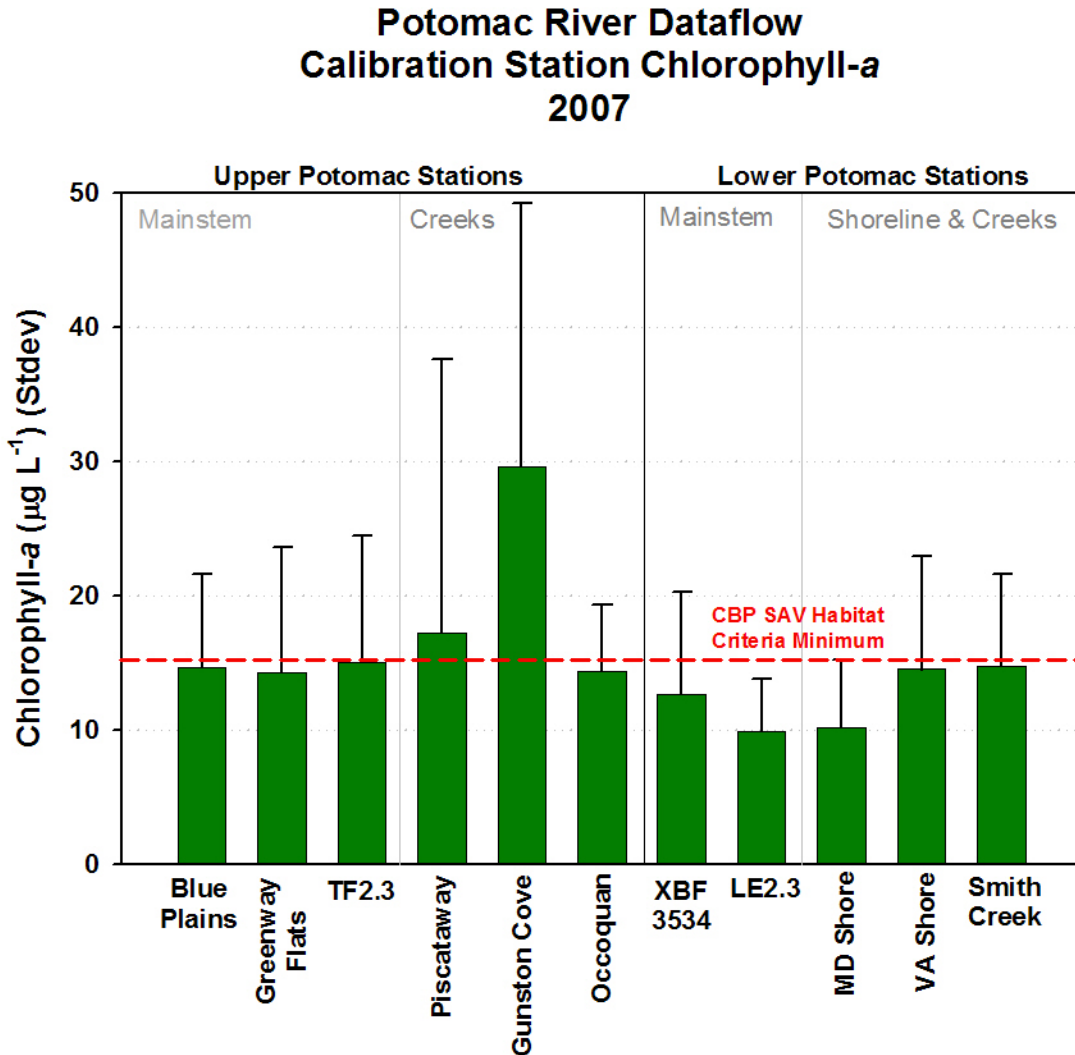


Figure 2-8. Average surface water total chlorophyll-a ($\mu\text{g L}^{-1}$) for Potomac River Dataflow calibration stations in 2007. N= 7 cruises per station and error bars are standard deviations. Stations arranged in relative position from upstream (left) to downstream (right) in the main river and creeks. The red dashed line indicates the Chesapeake Bay Program's SAV habitat criteria minimum of $15 \mu\text{g L}^{-1}$.

chlorophyll-a concentrations ranged from around 10 to $30 \mu\text{g L}^{-1}$ with the highest values occurring in upper Potomac River creeks. In the lower Potomac, the highest values were measured close to the Virginia shore and in Smith Creek (MD). In most months, chlorophyll-a concentrations were close to the Chesapeake Bay Program's SAV habitat criteria minimum of $15 \mu\text{g L}^{-1}$ with some stations like Gunston Cove exceeding this limit almost every month during the sampling period.

Potomac River Dataflow Calibration Station TSS 2007

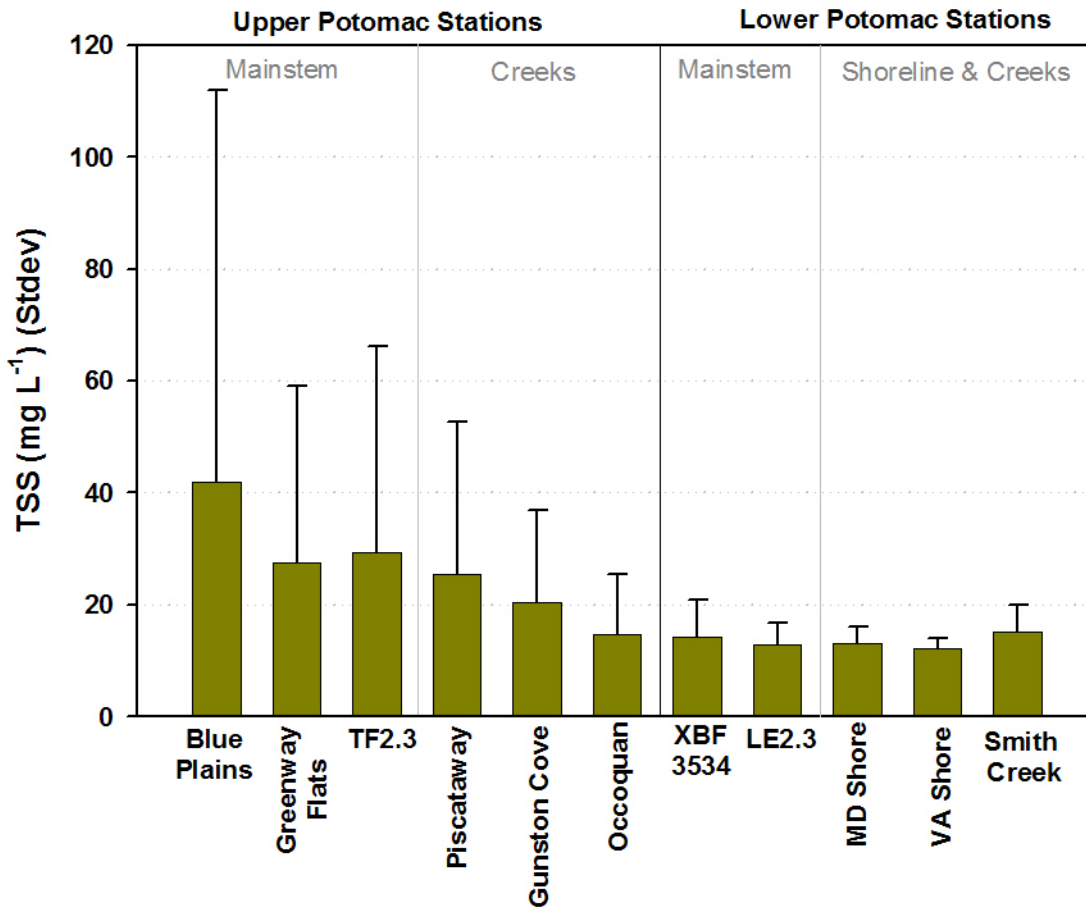


Figure 2-9. Average surface water total suspended solids (mg L^{-1}) for Potomac River Dataflow calibration stations in 2007. $N=7$ (except Occoquan where $n=6$) cruises per station and error bars are standard deviations. Stations arranged in relative position from upstream (left) to downstream (right) in the main river and creeks.

Average surface water total suspended solids decreased from upstream to downstream (Figure 2-9) with a large amount of month to month variability in the upper Potomac stations. Of note is the extreme range of concentrations measured at the Blue Plains station (XFB8408). Total suspended solids at this station ranged from around 10 to over 200 mg L^{-1} .

As we would expect, water column light attenuation (K_d) was higher in the upper Potomac compared to sites in the vicinity of the mouth (Figure 2-10 lower panel). At most of the lower Potomac stations K_d values were < 1 with the highest value (1.85) occurring at a shallow station close to the Virginia shore. Using the SAV habitat K_d criteria of 1.5 for the mesohaline Potomac River (Landwehr et al. 1999) the lower Potomac River Dataflow calibration stations appear to meet this criteria during most of the SAV growing season. The upper Potomac River stations had much higher K_d values (Figure 2-10) and varied greatly (e.g., factor of ~ 2) at almost all stations. K_d values in this region ranged from close to 1 up to a value of over 11 at the Blue Plains station.

Potomac River Dataflow 2007
 Calibration Station Light Attenuation

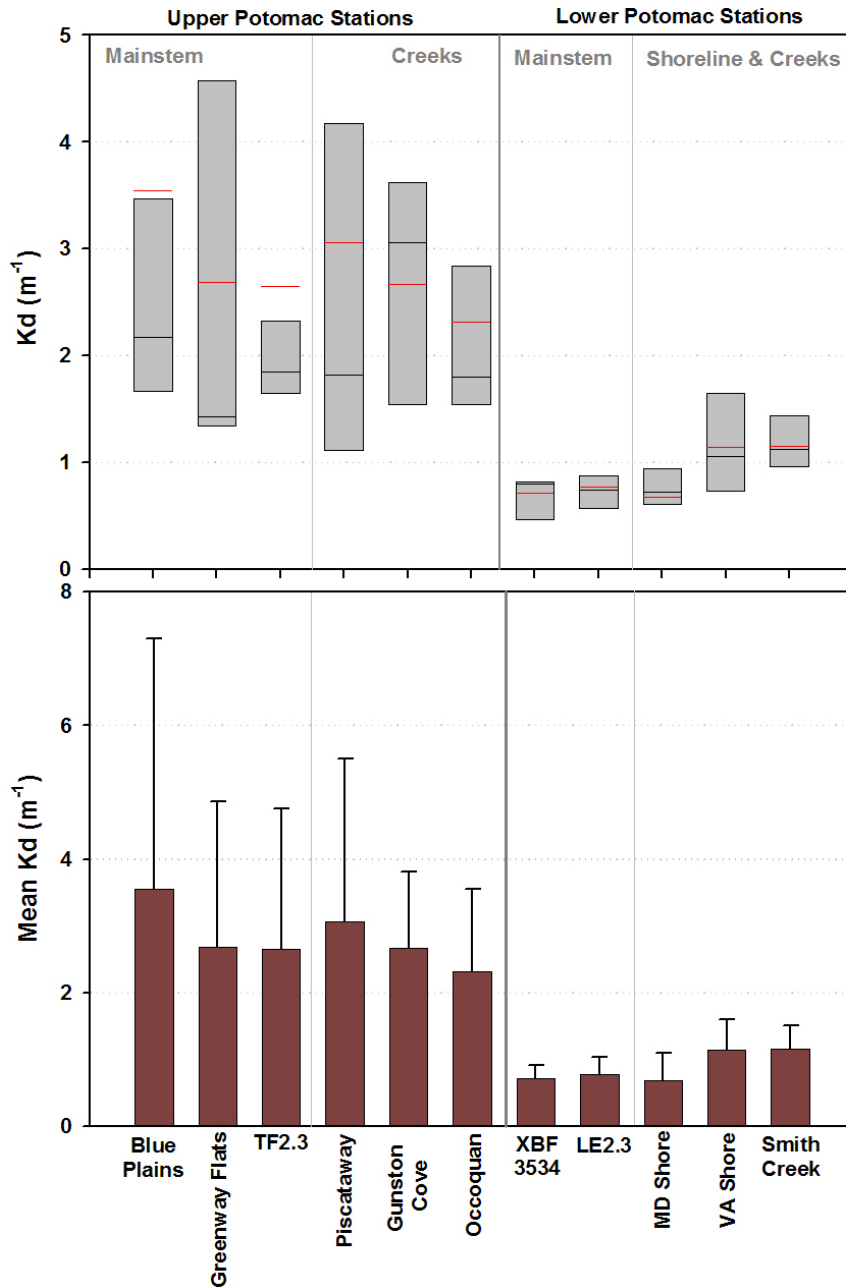


Figure 2-10. Box plot (top panel) and average (lower panel) light attenuation calculated using light meter (LiCor®) measurements for Potomac River Dataflow calibration stations in 2007. Error bars (lower panel) are standard deviation and stations are arranged in relative position from upstream (left) to downstream (right) in the main river and creeks.

**Potomac River Dataflow
Calibration Station Light Attenuation
2007**

LiCor Kd
 Elgin Kd
 Secchi Kd

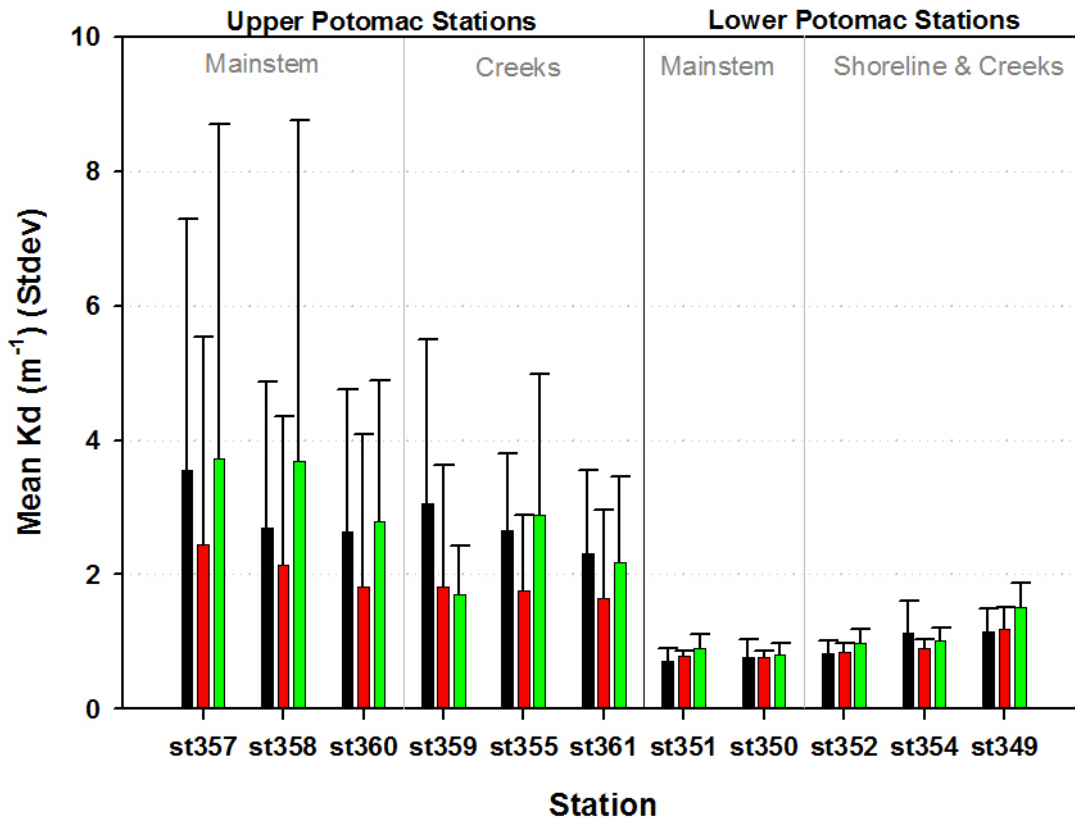


Figure 2-11. Bar graph of average Kd for 2007 Potomac River Dataflow calibration stations using three methods: LiCor (calculated light meter measurements), Elgin (from Perry 2006 and 2007, Romano 2008 and Tango 2007) and Secchi Depth (conversion of Secchi depth to Kd using: $Kd = 1.45/\text{Secchi depth}$). Stations are arranged in relative position from upstream (left) to downstream (right) in the main river and creeks.

We chose to calculate light attenuation (Kd) using three different methods and compare this data with the Potomac River Dataflow calibration stations (Figure 2-11). The first method (LiCor) calculates Kd using water column profiles of light measurements, the second (Elgin; from Elgin Perry, research statistician; Perry 2008) combines turbidity (as NTU), chlorophyll-a and salinity in a regression model and the third (Secchi) bases the Kd value on the measured Secchi depth ($Kd = 1.45/\text{Secchi depth}$). There was very good agreement amongst the three methods at calibration stations in the lower Potomac River (Figure 2-11). At upper Potomac River stations, the within method variation appeared similar for each station. At most stations the Secchi method indicated a higher degree of light attenuation than the other. A comparison of the LiCor and Elgin methods showed a strong and statistically significant relationship (Figure 2-12) with a slope of 0.74 (assuming perfect correspondence would have a slope of 1.0). We suggest that a more robust analysis could be performed on the larger, whole Potomac River dataset in order to understand

better the variability in the Elgin method used in generating Kd values for the spatial Dataflow data.

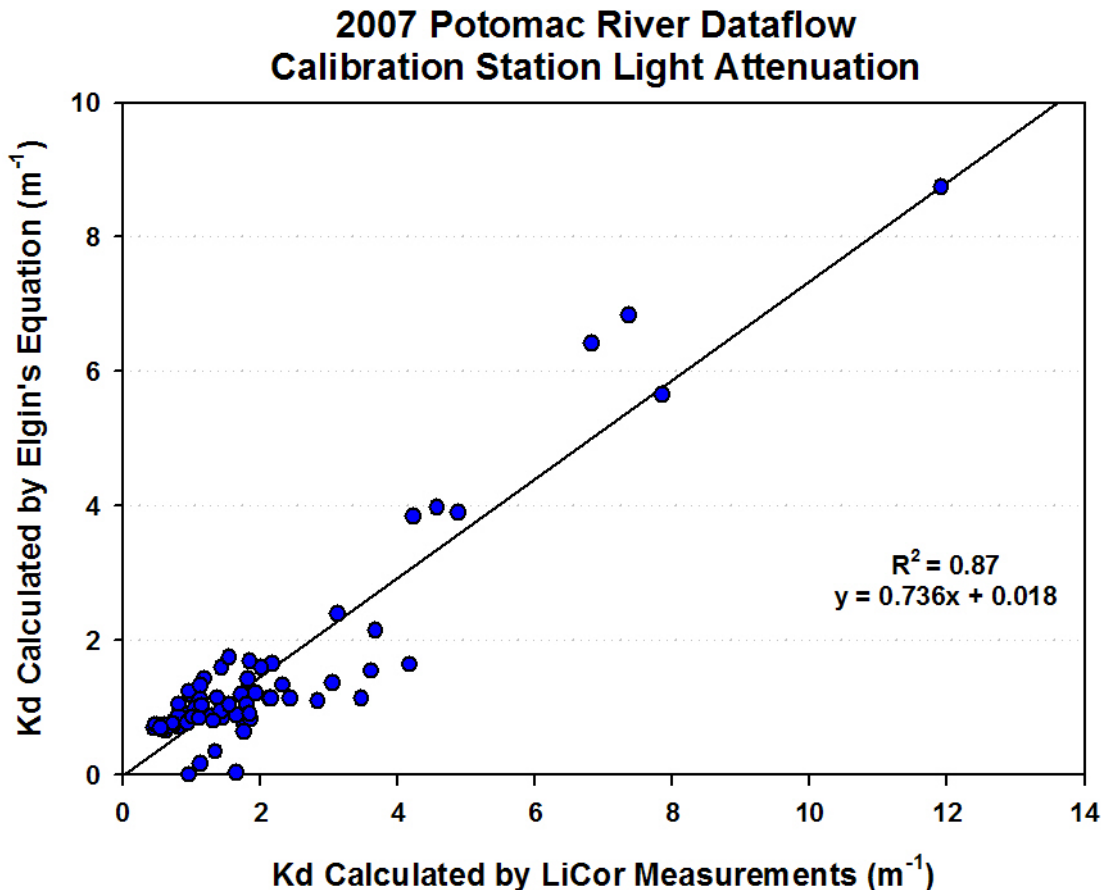


Figure 2-12. Scatter plot of Kd calculated using light meter measurements versus Kd calculated from Perry (2005) and Tango (2007) from April-October 2007 at Dataflow calibration stations on the Potomac River.

2.4 Evaluating Potential SAV Habitat

A goal of the spatial interpolation analysis was to evaluate the water quality conditions for submerged aquatic vegetation (SAV) within the sampled areas of the Potomac Estuary. To achieve that goal, we developed GIS maps of water quality conditions by interpolating the DATAFLOW data and data collected (during DATAFLOW cruises) at the calibration stations. We then compared those data to established SAV habitat criteria to determine which areas of the estuary experienced conditions promoting SAV growth and persistence.

2.4.1 Habitat Criteria

Water quality criteria have been developed by the US EPA Chesapeake Bay Program (CBP, 2000) to evaluate the conditions likely to support SAV health and survival. Table 2-4 shows the criteria used in our analysis and these generally respond to the “secondary criteria” developed by CBP with two exceptions. The first exception was that the level of total suspended solids (TSS) was not

evaluated, because of some concerns about the performance of the criterion. The second exception was that the Tidal Fresh criterion for dissolved inorganic phosphorus (DIP) criterion was omitted because the criterion appears to be too conservative based on previous data analyses of SAV distribution. In other words, the criterion suggests that SAV should be unable to thrive in areas where it is commonly seen to be growing in our field areas.

Table 2-4. Habitat criteria applied to 2007 data

Salinity Regime	Water Quality Criteria for SAV Habitat				Depth (Z)
	Water Column Light Requirement (PLW)	Chlorophyll a (CHLA)	Dissolved Inorganic Phosphorus (DIP)	Dissolved Inorganic Nitrogen (DIN)	
Tidal Fresh	>13%	<15 µg/L	none*	none	< 2 meters
Mesohaline	>22%	<15 µg/L	<0.01 mg/L	<0.15 mg/L	< 2 meters

*Criteria were derived from US EPA CBP 2000, with the exception that we omitted the DIP criterion for the Tidal Fresh of <0.02 mg/L because seagrass have been observed to withstand these levels in the Potomac and Patuxent tidal fresh estuaries.

The Water Column Light Requirement (PLW) is a derived value calculated from several other variables. PLW is considered a secondary habitat criterion but may be substituted for the primary criterion of percent light at leaf (PLL) when data are not available to calculate PLW (Chapter VII in EPA 2000). As envisioned by the criteria developers, “The attainment of the water-column light requirements at a particular site can be tested with the new ‘percent light through water’ parameter (PLW), which is calculated from Kd and water column depth and can be adjusted for both tidal range and varying restoration depths...” (US EPA 2000). The equation used for developing PLW from Kd is:

$$PLW = 100 * e^{(-Kd*Z)} \quad (Eqn. 1)$$

where

Kd = water-column light attenuation coefficient and

Z = depth (measured as a positive value)

The water-column light attenuation coefficient (Kd) is calculated from a combination of variables measured with DATAFLOW. The primary driver of Kd is turbidity which is measured by the DATAFLOW sensor as nephelometric turbidity units (NTU). The relationship between NTU and Kd has been developed as a fitted regression based on previous years’ DATAFLOW data and includes the variables of chlorophyll a and salinity (E. Perry, pers. comm. 2007). Regression equations have been developed for distinct groupings of estuaries in Maryland and Virginia tributaries and Maryland tributaries were divided into six groups. The Potomac Tidal Fresh and Mesohaline reaches fell into Group 2 and are estimated with the equation:

$$Kd = -0.1247 + 0.2820(\sqrt[1.5]{Turb}) + 0.0207(Chla) + 0.0515(Salinity) \quad (Eqn. 2)$$

where all variables *Turb*, *Chla* and *Salinity* are in the units measured within the DATAFLOW instruments. (P. Tango, pers. comm. 2007 and confirmed for current use by B. Romano, pers. comm. 2008). This derived Kd is used to calculate PLW using equation 1.

2.5 Results of comparing water quality data with SAV habitat criteria

Using the interpolation methods described, spatial data interpolations (GIS maps) were created for all water quality parameters used in SAV habitat assessment or intermediate calculations of criteria (chl_a, DIN, DIP, salinity, turbidity) and for each monthly cruise. These maps were evaluated and combined to evaluate habitat quality spatially and temporally. The Tidal Fresh (Upper Potomac) and the Mesohaline (Lower Potomac) sections were evaluated separately using the habitat criteria specific to those estuaries (Table 2-4).

2.5.1 Temporal and spatial patterns of potential SAV habitat

The overall picture for SAV habitat potential in 2007 was that substantial portions of the tidal fresh and mesohaline areas we sampled met the habitat criteria, the majority of the time. As shown in the Cumulative Frequency Diagrams (CFDs, Figures 2-13 – 2-14), the area out of “compliance” with SAV habitat criteria was generally low as indicated by the generally convex shape of the curves. The CFDs do not show a reference curve for this estuary but generally, the closer the curve is to the axes, the greater the level of compliance with water quality criteria. Each point on the curve represents the percent of time that the spatial extent of noncompliance meets or exceeds the percent area value. So the value of (16%, 50%) on the tidal fresh Potomac CFD (Figure 2-13) means that the spatial extent of noncompliance equals or exceeds 50% of the area about 16% of the time.

Despite the overall good level of habitat quality, the spring was marked by substantial areas of the tidal fresh and mesohaline estuary that did not meet the SAV habitat criteria. In the spring, 40-50% of the tidal fresh area of potential habitat met all criteria, but virtually none of the mesohaline Potomac met all criteria (Figure 2-15, Table 2-5). Later in the year, the pattern changed. Although the mesohaline section had less area of potential habitat compared to the tidal fresh reach (defined as areas less than 2 m deep), a higher proportion of that potential habitat met the criteria for any given month in the summer and fall.

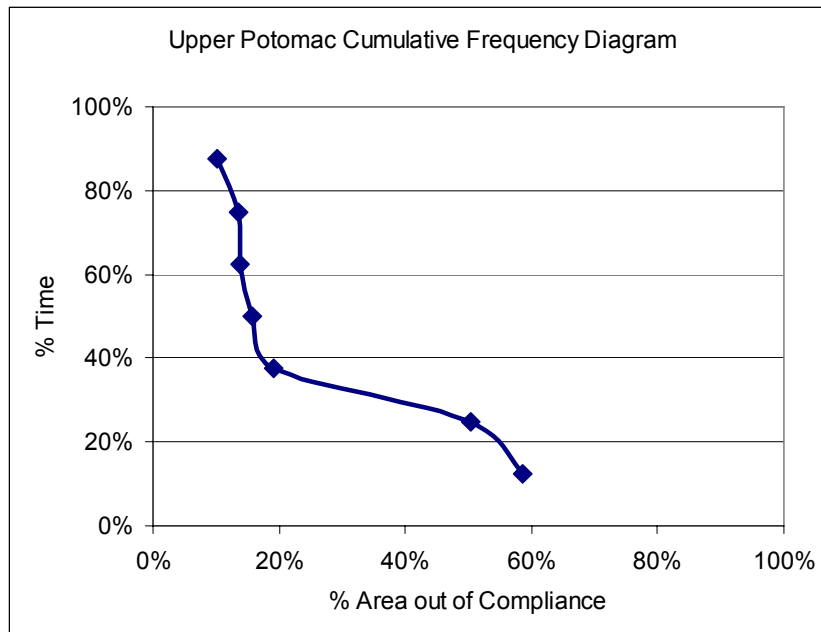


Figure 2-13. Cumulative Frequency Diagram for the Upper Potomac.

Each point on the curve represents the percent of time that the spatial extent of noncompliance meets or exceeds the percent area value. The closer the curve is to the axes, the higher the level of compliance.

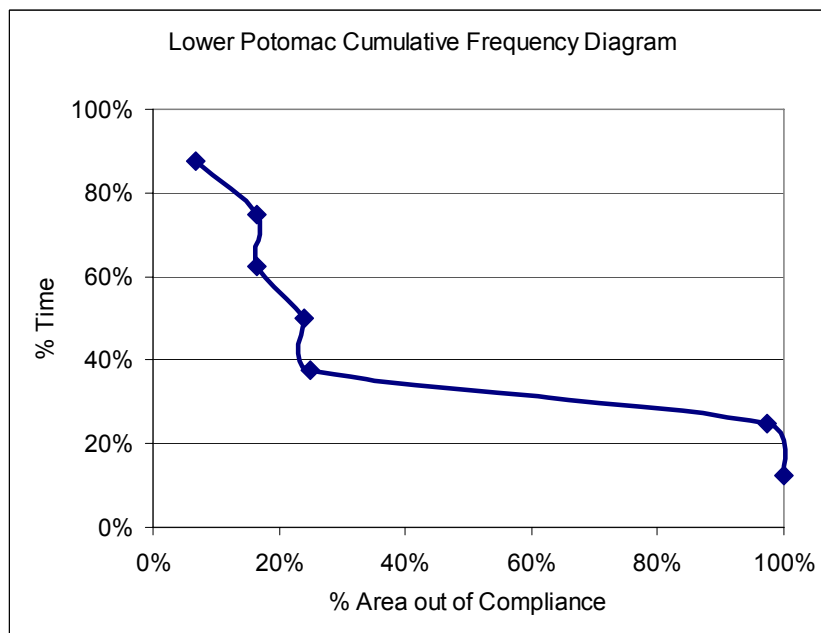


Figure 2-14. Cumulative Frequency Diagram for the Lower Potomac.

Each point on the curve represents the percent of time that the spatial extent of noncompliance meets or exceeds the percent area value. The closer the curve is to the axes, the higher the level of compliance.

2007 Potomac River DATAFLOW Cruises

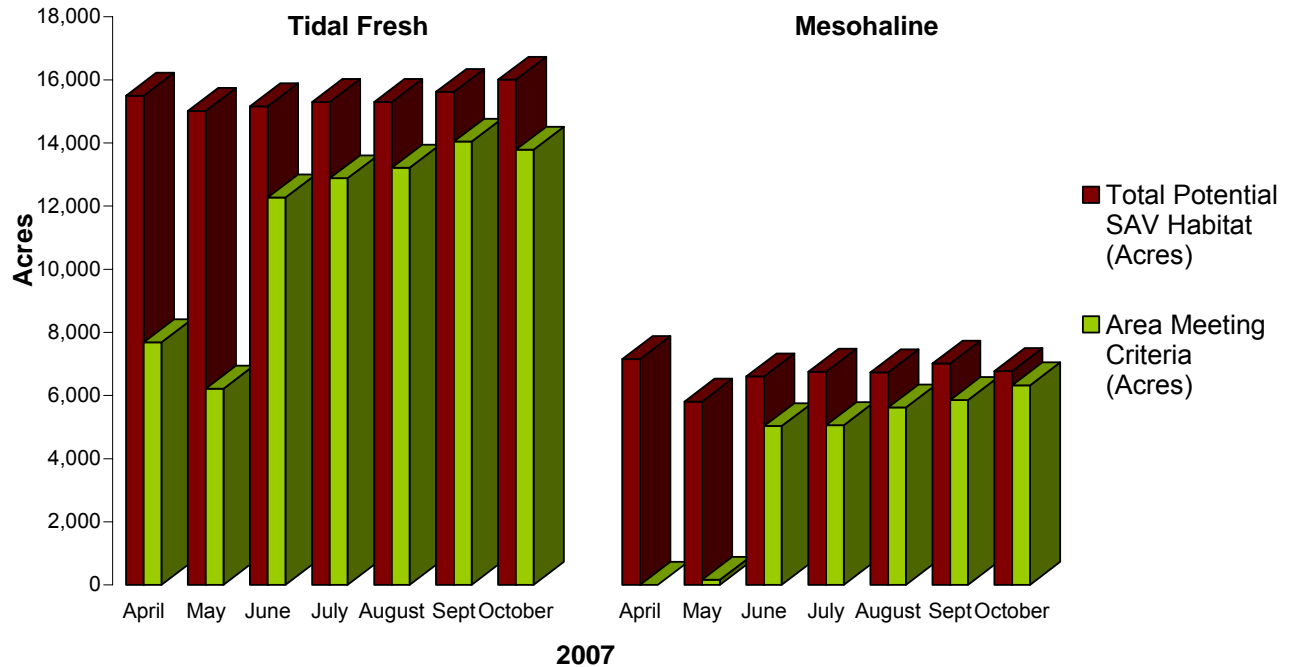


Figure 2-15. Total potential SAV habitat (depth < 2 meters) and area in meeting all SAV habitat criteria (by cruise month).

Table 2-5. Area of estuary meeting habitat criteria by cruise.

	Month	Cruise Date	Area Meeting Criteria (Acres)	Total Potential SAV Habitat (Acres)	% Potential Habitat Meeting Criteria
Tidal Fresh Potomac	April	18-Apr-07	7,687	15,495	50%
	May	17-May-07	6,216	15,018	41%
	June	12-Jun-07	12,275	15,163	81%
	July	17-Jul-07	12,883	15,298	84%
	August	14-Aug-07	13,216	15,298	86%
	Sept	11-Sep-07	14,042	15,618	90%
	October	2-Oct-07	13,788	16,005	86%
Mesohaline Potomac	April	20-Apr-07	0	7,157	0%
	May	14-May-07	159	5,807	3%
	June	11-Jun-07	5,029	6,605	76%
	July	16-Jul-07	5,061	6,752	75%
	August	13-Aug-07	5,619	6,730	83%
	Sept	10-Sep-07	5,855	7,012	84%
	October	1-Oct-07	6,323	6,776	93%

The spatial distribution of the areas meeting habitat criteria is shown in Figures 2-16 – 2-17. These figures demonstrate the frequency in time during which any given pixel in the map met all SAV habitat criteria. Since cruises were conducted monthly, the frequency can either be considered the monthly frequency or the observation frequency, where an observation equals a cruise. Only pixels with a depth of 2 meters or less are considered potential habitat and the area of evaluation is limited by the available bathymetry data and the cruise track. The area shown represents the intersection of the spatial extent covered by the bathymetry data and the 7 cruises in 2007.

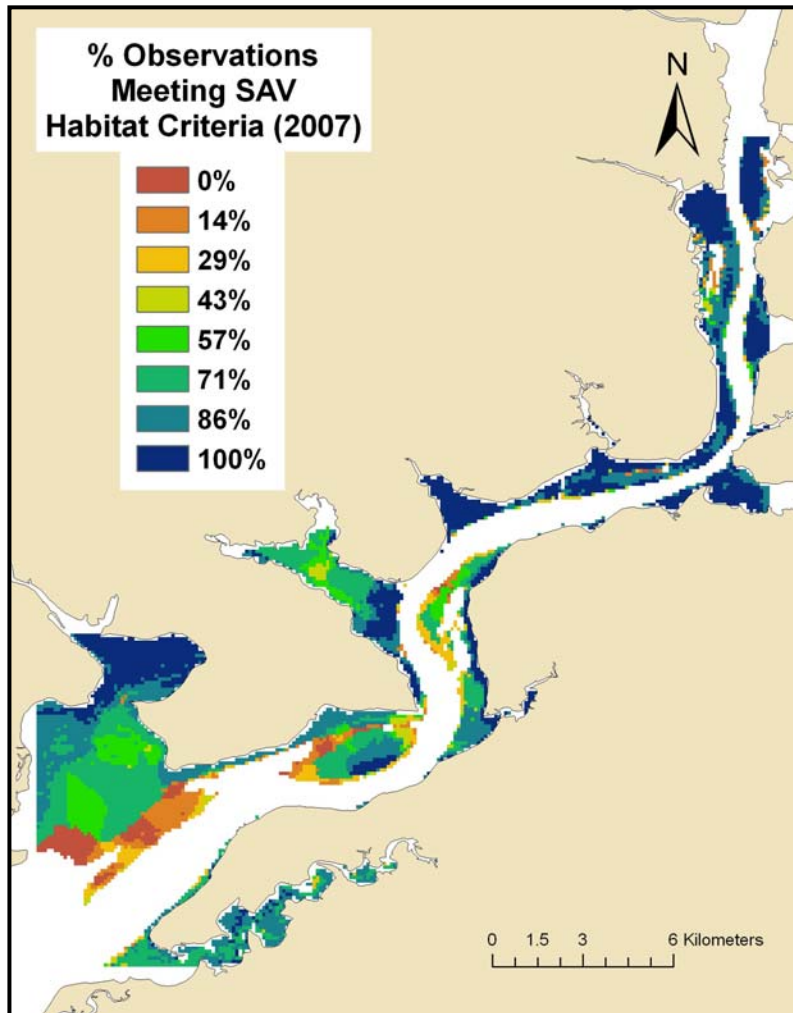


Figure 2-16. SAV habitat hotspots – Tidal Fresh Potomac.

Percent of monthly observations in which water quality for a given map pixel met all SAV habitat criteria in the Tidal Fresh Potomac. Since cruises were conducted monthly, the frequency of compliance with water quality criteria can either be considered the monthly frequency over the growing season or the observation frequency, where an observation equals a cruise.

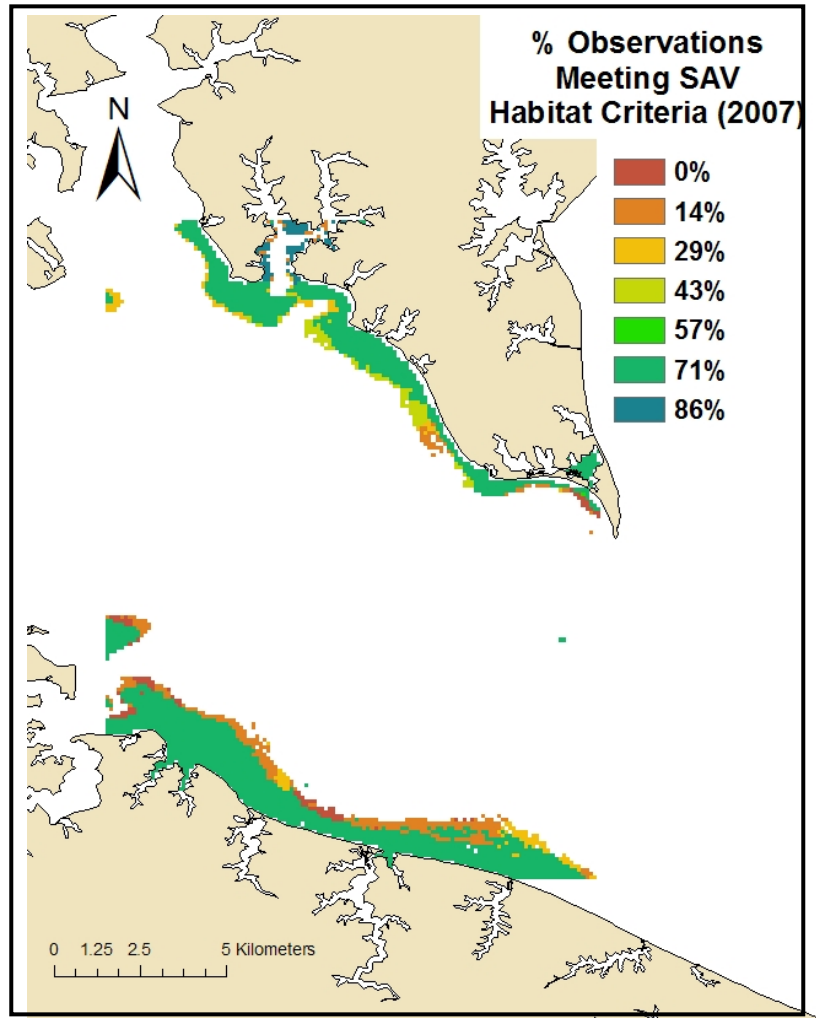


Figure 2-17. SAV habitat hotspots – Mesohaline Potomac.

Percent of monthly observations in which water quality for a given map pixel met all SAV habitat criteria in the Mesohaline Potomac. Since cruises were conducted monthly, the frequency of compliance with water quality criteria can either be considered the monthly frequency over the growing season or the observation frequency, where an observation equals a cruise.

2.5.2 Factors limiting compliance with SAV water quality criteria

The general temporal pattern of habitat quality is evident from the data. The proportion of area meeting water quality parameters was lowest in the spring and increased throughout the summer and early fall (Figure 2-15) for both the tidal fresh and mesohaline reaches sampled. In the tidal fresh Potomac both PLW and chlorophyll a (chl_a) were limiting factors in the spring. The areas in non-compliance in the spring tend to be in deeper areas (Figure 2-18). The tidal fresh cruise with the minimum acreage meeting criteria (May 17, 2007) still showed substantial acreage in compliance with all criteria (Figure 2-19a, Table 2-5). For the cruise with the maximum area meeting all habitat criteria (September 11, 2007), 90% of the area of 2 m depth or less was in compliance (Figure 2-19b, Table 2-5).

In the lower Potomac, DIN was the factor preventing sites from meeting water quality criteria in the spring. It should be noted that nutrient data (DIN and DIP) were not collected as part of DATAFLOW but only collected at calibration stations. Therefore, the spatial resolution of DIN was dramatically lower than that of the other water quality parameters, preventing a comparison of all habitat criteria at an equivalent spatial scale.

In the lower Potomac, the April cruise revealed that no acreage met all the habitat criteria and in May only 3% of potential habitat met all criteria (Figure 2-20a, Table 2-5). The cruise with the maximum acreage meeting habitat criteria was conducted on October 1, 2007 and showed 93% of potential acreage met all criteria (Figure 2-20b, Table 2-5).

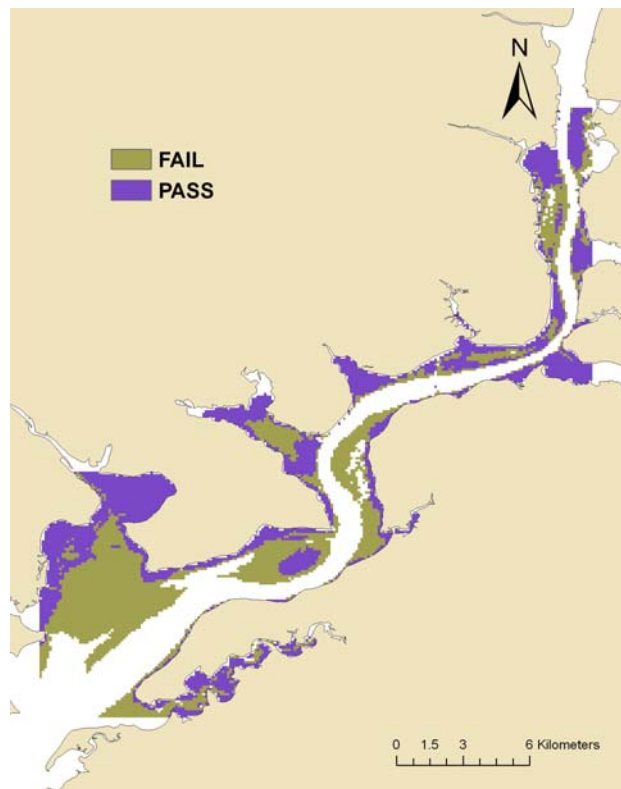


Figure 2-18. Area of April non-compliance with SAV habitat criterion for Percent Light in Water (PLW) in the Tidal Fresh Potomac. This April cruise is typical of early spring cruises that tend to show the greatest percentage of area failing to meet the water quality criteria. Both PLW and chlorophyll a standards were exceeded over substantial portions of the Tidal Fresh potential habitat in Spring 2007.



Figure 2-19a. Minimum acreage meeting SAV habitat criteria in 2007 – Tidal Fresh Potomac.

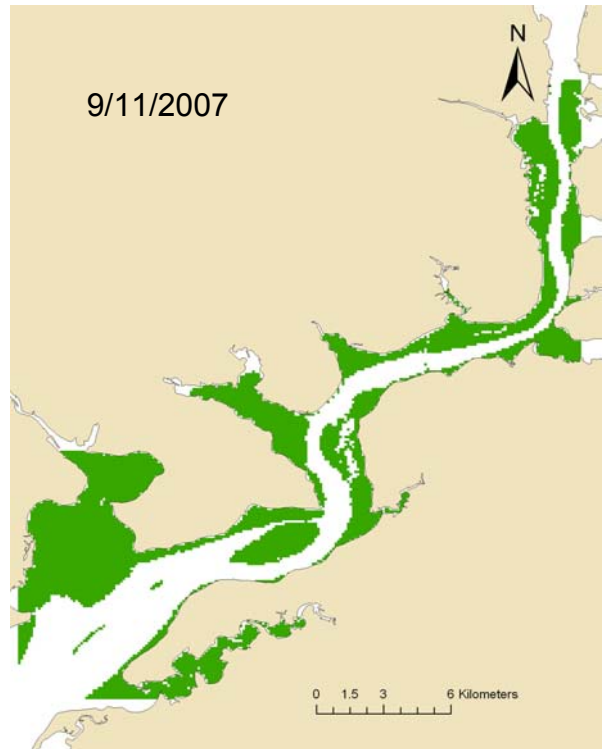


Figure 2-19b. Maximum acreage meeting SAV habitat criteria in 2007 – Tidal Fresh Potomac.

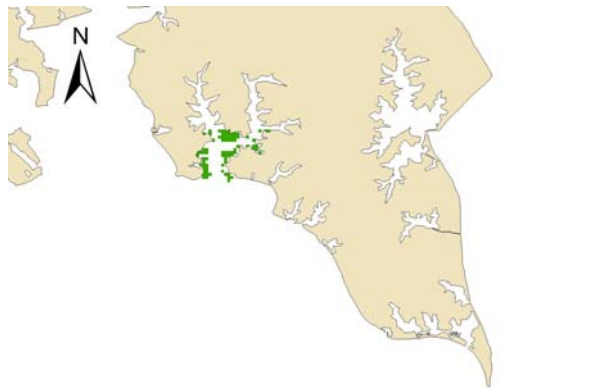


Figure 2-20a. Minimum acreage meeting SAV habitat criteria in 2007 – Mesohaline Potomac.



Figure 2-20b. Maximum acreage meeting SAV habitat criteria in 2007 – Mesohaline Potomac.

2.6 Discussion

The sampling and interpretation of DATAFLOW data provides a highly informative picture of the water quality conditions in 2007. We continue to refine our methods but found no major problems with either sampling or analysis techniques. Several minor issues or points of discussion include:

1) Sensors have limited ability to detect fine differences in turbidity at the low end of range

We use the YSI 6136 turbidity sensor on both the DATAFLOW system and calibration station profile instruments. YSI gives the following specifications for these sensors (www.ysi.com):

Range: 0 to 1000 NTU

Resolution: 0.1 NTU

Accuracy: $\pm 2\%$ of reading or 0.3 NTU (whichever is greater)

Standards: YSI AMCO-AEPA Polymer Standards

The standard calibration for these sensors uses a two point calibration in DI water (zero) and a standard solution of 123 NTU. After noticing that many values below 10 NTU varied quite a bit when compared to total suspended solids (Figure 2-21) we have been working with YSI to develop better resolution at the lower end of the sensor's range. Our next step will be to evaluate the use of an intermediate standard (~ 50 NTU) or use of two turbidity probes (one specifically calibrated for the lower NTU range) in areas of lower turbidity.

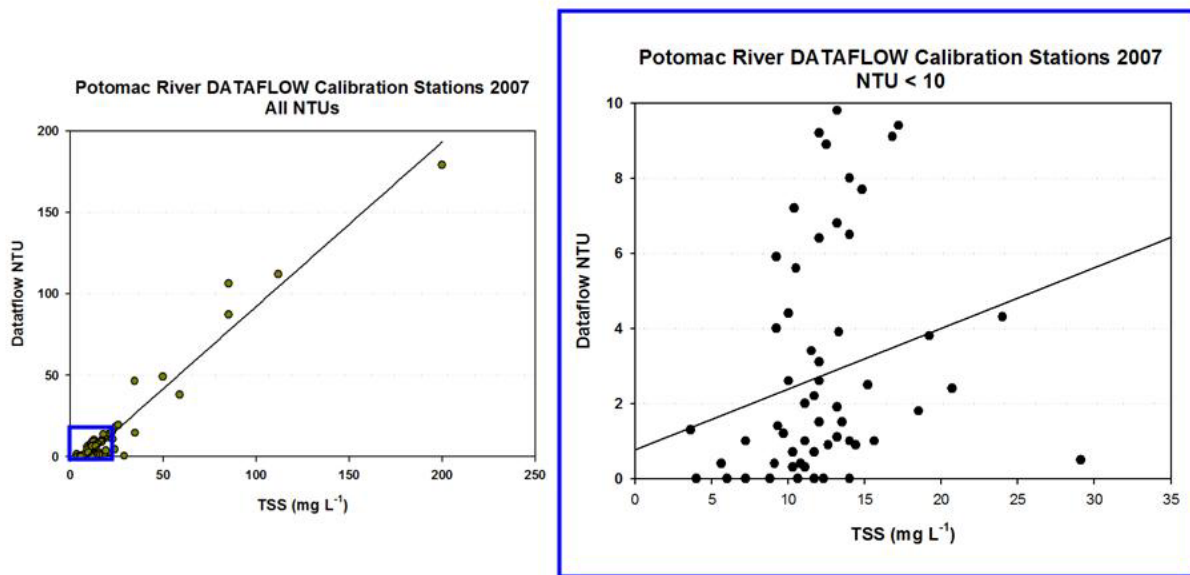


Figure 2-21. Comparison of total suspended solids (TSS) and optical turbidity (NTU) measured at DATAFLOW calibration stations in 2007. The right panel shows all NTU measurements under 10.

2) Habitat criteria used in 2007 differed from previous years

This is the first year we used the PLW criterion for SAV habitat because we were able to translate NTU into K_d using the regression equations developed by Elgin Perry (P. Tango, pers comm. 2007), which allowed us to calculate PLW. The values for PLW produced with the regression equation appeared to be in the correct range. However, these calculations are relatively untested and further evaluation of this method is warranted.

3) PLW performs well for mesohaline; may be biased downward for tidal fresh

Our initial tests suggest the regression equation to calculate K_d works well, however, it appears there may be a consistent downward bias in K_d for the tidal fresh reach of the Potomac (Section 2.3.2). However, no such bias is evident in the mesohaline section and we have high confidence in calculations for that region.

If PLW is being underestimated for the tidal fresh portion, that bias would tend to underestimate the acreage meeting SAV habitat criteria when PLW is the limiting factor. We found that both PLW and chl_a were limiting factors in the spring, not only PLW, so this may be a minor concern. However, if the same K_d regression equation is going to be used for analysis in the future, further testing will be needed to determine how a bias could affect future results and whether the regression should be re-fit for this region.

4) Spatial resolution of nutrient criteria a concern

A source of continuing concern is the non-parallel comparison of some habitat criteria at a fine spatial scale and other criteria at a coarse spatial scale. This is particularly troubling since the nutrient criterion for DIN was the limiting factor on habitat compliance in the mesohaline reach in the spring. Yet, we do not know how well the calibration stations represent conditions throughout the shallow areas of the estuary. We are planning to evaluate a greater number of nutrient samples in 2008 in the hope that this will improve understanding of the representativeness of the calibration station data for predicting spatial distribution of nutrient levels.

2.7 References

- Boynton, W.R., E.M. Bailey, S.M. Moesel and L.A. Moore.** 2007. Maryland Chesapeake Bay Water Quality Monitoring Program. Ecosystem Processes Component (EPC). Work/Quality Assurance Project Plan for Water Quality Monitoring in Chesapeake Bay for FY2007. Chesapeake Biological Laboratory (CBL), University of Maryland System, Solomons, MD 20688-0038. Ref. No. [UMCES] CBL 07-068.
- Landwehr, J.M., J.T. Reel, N.B. Rybicki, H.A. Ruhl, V. Carter.** 1999. Chesapeake Bay Habitat Criteria Scores and the Distribution of Submerged Aquatic Vegetation in the Tidal Potomac River and Potomac Estuary, 1983-1997. U.S. Geological Survey Open-File Report 99-219. Reston, VA.
- Madden, C.J. and J.W. Day Jr.** 1992. An instrument system for high-speed mapping of chlorophyll an and physico-chemical variables in surface waters. *Estuaries* 15(3): 421-427.
- Perry, E.** 2006. Personal communication, December 27, 2006.
- Perry, E.** 2007. Personal communication, March 27, 2008.
- Romano, Bill.** 2008. Personal communication, email of March 31, 2008.
- Smail, P.W., R.M. Stankelis, W.R. Boynton and E.M. Bailey.** 2005. Maryland Chesapeake Bay Water Quality Monitoring Program. Ecosystem Processes Component (EPC). Work/Quality Assurance Project Plan for Water Quality Monitoring in Chesapeake Bay for FY2006. Chesapeake Biological Laboratory (CBL), University of Maryland System, Solomons, MD 20688-0038. Ref. No. [UMCES] CBL 05-066.
- Smail, P.W., W.R. Boynton and E.M. Bailey.** 2006. Maryland Chesapeake Bay Water Quality Monitoring Program. Ecosystem Processes Component (EPC). Work/Quality Assurance Project Plan for Water Quality Monitoring in Chesapeake Bay for FY2006. Chesapeake Biological Laboratory (CBL), University of Maryland System, Solomons, MD 20688-0038. Ref. No. [UMCES] CBL 06-068.
- Tango, Peter.** 2007. Personal communication, Report on the Lumping vs. Splitting for MDDNR dataflow Kd vs. Turbidity calibration (by Elgin Perry, 2006). In. *Technical Support Documentation for CAP of Chesapeake Bay Tidewaters*. (Draft Version 6/18/07 PT).
- US EPA Chesapeake Bay Program.** 2000. Chesapeake Bay Submerged Aquatic Vegetation Water Quality and Habitat-Based Requirements and Restoration Targets: A Second Technical Synthesis. Annapolis Maryland. Report available at: <http://www.chesapeakebay.net/pubs/sav/index.html>

3.0 Corsica River Estuary Community Metabolism

Walter R. Boynton, Kathryn V. Wood, and Elgin Perry

3.1	Introduction and Objectives	3-1
3.2	Station Location	3-2
3.3	Community Metabolism: Production and Respiration Rates in the Corsica River using Continuous Monitoring Data	3-3
3.4	Results	3-6
3.5	Statistical Analyses of Corsica River Estuary Metabolism Data (2005 - 2007)	3-12
3.6	References	3-26

3.1 Introduction and Objectives

The condition of Maryland's watersheds were assessed, categorized and classified according to designated levels of water quality enforced by the United Watershed Assessment (UWA.) Multiple watersheds in Maryland are considered "impaired" and in need of restoration. The Corsica River was selected to be the first targeted watershed in Maryland to undergo Watershed Restoration. The project goal is to attain the new state water quality standards in the Corsica River, remove it from the Impaired Waters List (303(d) list) and use the watershed as a template for selection and restoration of subsequent watersheds. The initial focus of the Targeted Watershed Restoration program is on nutrient and sediments but planning and further assessment will also address other impairments.

This effort (included in our portion of the EPC) is part of a multi-pronged program that includes both landscape and in-estuary activities. Since 2005 Maryland DNR has conducted surface water quality mapping and continuous monitoring in the Corsica River estuary. Our role has been to measure some of the key processes underlying the observed conditions in the estuary. To that end our measurement program was designed to evaluate key processes by:

- a. Estimating land and atmospheric loads of N (nitrogen) and P (phosphorus)
- b. Measuring the fluxes of N and P between the Chester and Corsica River
- c. Computing community rates of production and respiration using continuous monitoring data sets (ConMon data)
- d. Measuring the consumption of O₂ (dissolved oxygen) by sediments
- e. Measuring the release of N and P by sediments
- f. Measuring the terminal in-system losses of N and P by denitrification (for N) and long-term burial for both N and P

Items (d) and (e) were fully reported in previous reports. Items (b) and (f) were also reported in previous reports and more recent analyses are included as separate chapters in this report. We have recently received the information needed to complete item (a) and will submit a separate report later in 2008 addressing that issue. In this Chapter we address item (c) for a three year period using ConMon data collected at Sycamore Point in the Corsica River estuary. Additionally, statistical analyses have been performed on these data to find if any seasonal or inter-annual scale trends have

emerged and to estimate the magnitude of change in community metabolism needed to detect statistically significant trends.

3.2 Station Location

Station location is shown in Figure 3-1 and more specific information is provided in Table 3-1. Sycamore Point was selected for these analyses for several reasons, including: 1) it is the site in the Corsica River estuary with the longest and most complete data set; 2) it is the site closest to landside nutrient inputs and therefore likely most effected by these nutrient loads; 3) it is a ConMon site whose location has not been modified during the measurement period.

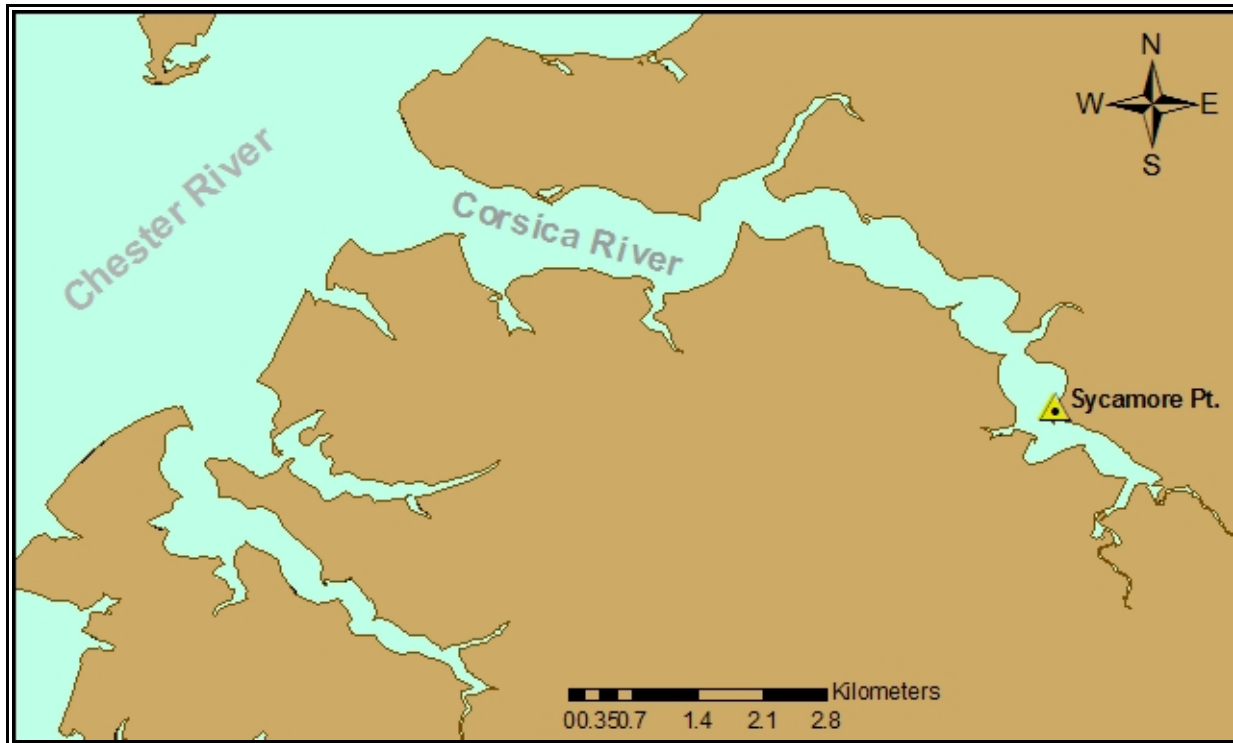


Figure 3-1. Map of the Corsica River estuary showing location of the Sycamore Point ConMon site. More specific station information is provided in Table 3-1.

Table 3-1. ConMon Station Code, Locations and Mean Depth (m) from 2007.
 Latitude and longitude values are expressed as decimal degrees (Datum NAD 83).

Station	Tributary	Latitude Decimal Degrees	Longitude Decimal Degrees	Mean Depth (m)
Sycamore Point	Corsica River	39.0628	-76.0816	1.0

3.3 Community Metabolism: Production and Respiration Rates in the Corsica River using Continuous Monitoring Data

Community production and respiration have repeatedly been shown to be responsive to nutrient enrichment in lakes (e.g., Vollenweider 1976 and many others), estuaries and coastal waters (Boynton et al 1982; Boynton and Kemp 2008). In the case of the Corsica River estuary, nutrient enrichment was cited as one of the reasons for listing this waterway as being impaired and in need of restoration. In many instances measurements of such fundamental features of ecosystem function as production and respiration are too expensive or simply too difficult to undertake. However, in the Corsica the State of Maryland DNR has established several water-quality monitors making measurements of water quality variables needed to make these estimates. In this chapter we report on the methods and results of community production and respiration computations for a key site in the Corsica River estuary.

3.3.1 Methods

The basic concept and method for computing community production and respiration was developed by H.T. Odum and C.M. Hoskin (1959) and, with numerous modifications, has been used since for measuring these rate processes in streams, rivers, lakes, estuaries and the open ocean. The technique is based on following the oxygen concentration in a body of water for at least a 24 hour period. During hours of daylight, oxygen increases in the water due to the release of O₂ as a by-product of photosynthesis. During hours of darkness, O₂ declines due to O₂ consumption by both primary producers and all other heterotrophs. The rate processes (gross photosynthesis, Pg; nighttime respiration, Rn) are estimated by computing the rate of change in O₂ concentrations during day and night periods. This rate of change is then corrected for O₂ diffusion across the air-water interface and the result is an estimate of Pg and Rn. ConMon data are exactly the type of data needed for these computations in that all the needed variables are measured (dissolve oxygen, temperature and salinity), the measurement frequency is high (15 minute intervals) and the measurement period is for 9 or more months. It is very rare when a rate process can be measured with such temporal intensity.

Based on earlier work by Burger and Hagy (1998) for calculating water column metabolism from near-continuous monitoring data, an automated Excel spreadsheet (Metabolism.xls) was developed by Mr. David Jasinski (Personal Communication). The worksheet was automated using Microsoft's Visual Basic for Applications (VBA) programming language. Briefly, the steps the spreadsheet undertakes are as follows:

1. An excel file, containing the continuous monitoring data configured by the user in a requisite format (Fig.3-2) is read into the spreadsheet.
2. Dates and times are reformatted into a continuous time variable or serial number.
3. Sunrise and Sunset times for each date are calculated based on the latitude and longitude of the station.
4. Rows are inserted into the dataset to create an observation at sunrise and sunset on each day.
5. Each observation in the dataset is assigned a daypart – Sunrise, Day, Sunset, or Night
6. Each observation is assigned to a “Metabolic Day”. Each metabolic day begins at sunrise on the current day and continues to the observation immediately before sunrise on the following day.
7. For sunrise/sunset observations created in Step 4, values for water temperature, salinity, dissolved oxygen and dissolved oxygen saturation are calculated by taking the mean of the observations immediately before and after sunrise and sunset.
8. The change in DO, time, air/sea exchange and oxygen flux is calculated between each consecutive observation.
9. The minimum and maximum DO values are calculated between sunrise and sunset on each day and these values are labeled “metabolic dawn” and “metabolic dusk”.
10. Sums of the changes in DO, time, air/sea exchange and DO flux (step 8) are calculated for each metabolic day for the periods between sunrise and metabolic dawn, metabolic dawn and metabolic dusk, metabolic dusk and sunset, and sunset and the following sunrise.
11. From these sums, 6 metabolic variables are calculated and these include: Rn, Rnhourly, pa, pa_star, pg, Pg*.

These variables are defined as follows:

Rn = Nighttime (sunset to following sunrise) summed rates of DO flux corrected for air/water diffusion.

Rnhourly = Rn divided by the number of nighttime hours

pa = The sum (both positive and negative) of oxygen flux (corrected for air-water diffusion) for the dawn, day and dusk periods.

pa_star = summed oxygen flux (corrected for air-water diffusion) for the day period

pg = pa + daytime respiration. Daytime respiration = Rnhourly * (number of hours of daytime+dawntime+dusktime).

Pg* = pa_star + daytime respiration as defined above.

Air-water diffusion of oxygen is considered in these computations and the diffusion correction is based on the difference between observed DO percent saturation and 100% saturation multiplied by a constant diffusion coefficient. For these computations a diffusion coefficient of $0.5 \text{ g O}_2 \text{ m}^{-2} \text{ hr}^{-1}$

was selected as generally representative of conditions frequently encountered in estuarine tributary situations (Caffrey 2004).

One of the primary assumptions of this method is that temporal changes in DO measured by the continuous monitors are due solely to metabolism (i.e., oxygen production from photosynthesis and oxygen loss from respiration) occurring at the station and not due to advection of water masses with different oxygen conditions moving past the instrument. Because Chesapeake Bay is a tidal system, this may not always be the case. Depending on the hydrodynamics of a given station, this assumption may be more or less realistic and may also be variable from date to date. One way of censoring dates where DO is affected by advection is to preview the data graphically prior to metabolism calculations and determine if there is a relationship between salinity and DO. Large changes in salinity suggest moving water masses and therefore, advection. These dates could then be flagged and reviewed before metabolism variables are calculated.

	A	B	C	D	E	F	G	H	I	J	K
1	Date	Time	WTEMP	SALIN	DOSAT	DO	Lat	Long	timezone	daylightsavings	
2	6/20/1997	11:45:00	25.42	1.1	114.4	9.3	38.49068	-76.6641	-5	1	
3	6/20/1997	12:00:00	25.44	1.1	117.4	9.55	38.49068	-76.6641	-5	1	
4	6/20/1997	12:15:00	25.45	1.1	117.1	9.52	38.49068	-76.6641	-5	1	
5	6/20/1997	12:30:00	25.38	1.1	112.9	9.19	38.49068	-76.6641	-5	1	
6	6/20/1997	12:45:00	25.45	1.1	115.2	9.37	38.49068	-76.6641	-5	1	
7	6/20/1997	13:00:00	26.07	1.1	127	10.21	38.49068	-76.6641	-5	1	
8	6/20/1997	13:15:00	27.02	1	155.3	12.29	38.49068	-76.6641	-5	1	
9	6/20/1997	13:30:00	27.41	1	173.7	13.65	38.49068	-76.6641	-5	1	
10	6/20/1997	13:45:00	27.48	1	177.8	13.95	38.49068	-76.6641	-5	1	
11	6/20/1997	14:00:00	27.62	1	182.6	14.29	38.49068	-76.6641	-5	1	
12	6/20/1997	14:15:00	27.7	0.9	181.5	14.19	38.49068	-76.6641	-5	1	
13	6/20/1997	14:30:00	27.66	0.9	181.4	14.2	38.49068	-76.6641	-5	1	
14	6/20/1997	14:45:00	27.74	0.9	181.1	14.15	38.49068	-76.6641	-5	1	
15	6/20/1997	15:00:00	27.93	0.9	185.5	14.44	38.49068	-76.6641	-5	1	
16	6/20/1997	15:15:00	28.38	0.9	194.7	15.04	38.49068	-76.6641	-5	1	
17	6/20/1997	15:30:00	28.46	0.8	201.9	15.58	38.49068	-76.6641	-5	1	
18	6/20/1997	15:45:00	28.24	0.8	200.8	15.57	38.49068	-76.6641	-5	1	
19	6/20/1997	16:00:00	28.09	0.7	194.7	15.14	38.49068	-76.6641	-5	1	

Figure 3-2. Screen shot showing the requisite input format needed by Metabolism.xls for calculation of metabolism variables.

Another way of dealing with advection is to incorporate in the code a method of detecting changes in DO associated with changes in salinity. It might then be possible to apply a site specific correction factor to remove the advection affect on DO. These possibilities could be investigated further in the future. At the present time we examine data from each site graphically and if there are erratic patterns in dissolved oxygen or salinity we do not attempt calculations for that site. In

addition, the algorithm indicates when a site has unusual dissolved oxygen patterns (e.g., increases in dissolved oxygen during hours of darkness) and these computations are excluded.

3.4 Results

3.4.1 Previous Metabolism Results from the Bay and Elsewhere

The longest time-series record of data suited for metabolism calculations that we are aware of in Chesapeake Bay was initially collected by Cory working for the USGS at a bridge site in the Patuxent River estuary (MD Rt. 231 Bridge at Benedict, MD). Cory started making measurements in 1963 and his record continued until 1969. Cory used an arrangement of pumps, manifolds, early YSI probes and strip-chart recorders to develop the data set. Fortunately, Cory was very attentive to calibration concerns and he devoted considerable effort to ensuring good quality data. This data set was then used by Sweeney (1995) to compute metabolism for the 1963-1969 period and he also deployed a more modern instrument at the same location during 1992. We later deployed instruments during the late-1990's, again at the same location. Data were also available for this area of the Patuxent for 1978 but these data were not collected at the Rt. 231 bridge site.

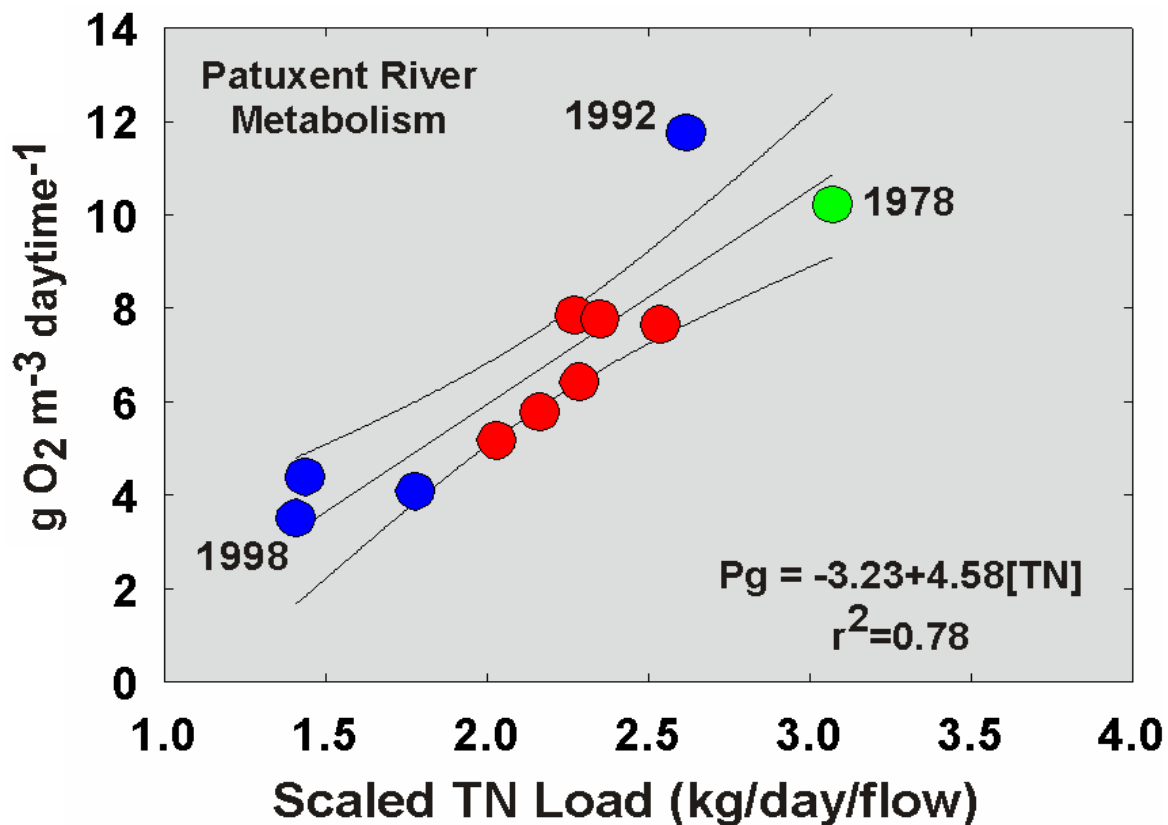


Figure 3-3. A scatter plot of summer P_g^* versus nitrogen loading rate scaled for water residence time in the Patuxent River estuary in the vicinity of Benedict, MD. Red dots represent years between 1963 and 1969 and blue dots are observations from the 1990's. Data for 1978 were collected at a site near Benedict, MD. Data are from Sweeney (1995).

We have summarized much of these data in a scatter plot (Figure 3-3) where average daily summer metabolism was plotted as a function of nitrogen loading rate corrected for water residence time. The results suggest that this site in the Patuxent is sensitive to changes in nutrient loading rate and that the response is quite large. Note that metabolism rates were considerably lower in recent years following the institution of Biological Nitrogen Removal (BNR) at sewage treatment plants in the upper basin (after 1992). In addition, the red dots represent data collected during the 1960's and there is a clear indication of increasing metabolism through that decade as sewage treatment plants began discharging and land-use changes became large-scale leading to increased diffuse source nutrient inputs to the estuary.

In addition to the system metabolism work done in the Patuxent, this technique has been gaining much broader applications in estuarine and near-coastal areas. Perhaps the best single example of this was reported by Caffrey (2004). Caffrey assembled high frequency DO, temperature and salinity data from 42 sites located within 22 National Estuarine Research Reserves between 1995 and 2000. She computed the same sort of metabolism estimates described here and found the following: 1) highest production and respiration rates occurred in the SE USA during summer periods; 2) temperature and nutrient concentrations were the most important factors explaining variation in rates within sites; 3) freshwater sites were more heterotrophic than more saline sites; 4) nutrient loading rates explained a large fraction of the variance among sites and; 5) metabolic rates from small, shallow, near-shore sites were generally much larger than in adjacent, but larger, deeper off-shore sites. The fact that nutrient loading rates and concentrations were strong predictors of rates is especially relevant to efforts being made in Chesapeake Bay tributaries. Finally, Danish investigators have been using this technique in a variety of shallow Danish systems and they have, quite importantly, started to use four different approaches for estimating the metabolic parameters of interest here (Gazeau et al. 2005), including the open water DO approach. Significantly, their evaluations suggest that all techniques produce the same estimates with regard to magnitude and direction (production or respiration). A convergence of estimates, using different techniques, suggests a robust set of variables and that is consistent with the needs of a monitoring program.

3.4.2 Earlier Results for Corsica River Estuary (2005 and 2006)

We have previously summarized a portion of the community production and respiration measurements potentially available for the Corsica River estuary (Figs. 3-4 and 3-5). It is interesting to note that each panel in these figures summarizes about 65,000 observations; these are robust patterns and show both pattern and variability, not something that is often associated with monitoring programs.

Primary production (P_g^* ; gross primary production) and respiration (R_n ; respiration during hours of darkness) values were large, indicating substantial nutrient-based eutrophication, and exhibited very strong seasonal patterns with highest values of both P_g^* and R_n during summer and lower values during winter. Additionally, rates were slightly higher during 2005 than during 2006 although the difference may not be statistically significant. There was also a consistent shift in the seasonal pattern of production and respiration wherein during 2005 rates increased sharply to July and then decreased sharply into the fall. During 2006 rates increased more slowly through September and then declined rapidly. Finally, rates at the head of the estuary were only slightly higher than those at the down-estuary site. This may be a reflection that nutrients are supplied to

this estuary both from the adjacent drainage basin and, at least at times, from the Chester River estuary.

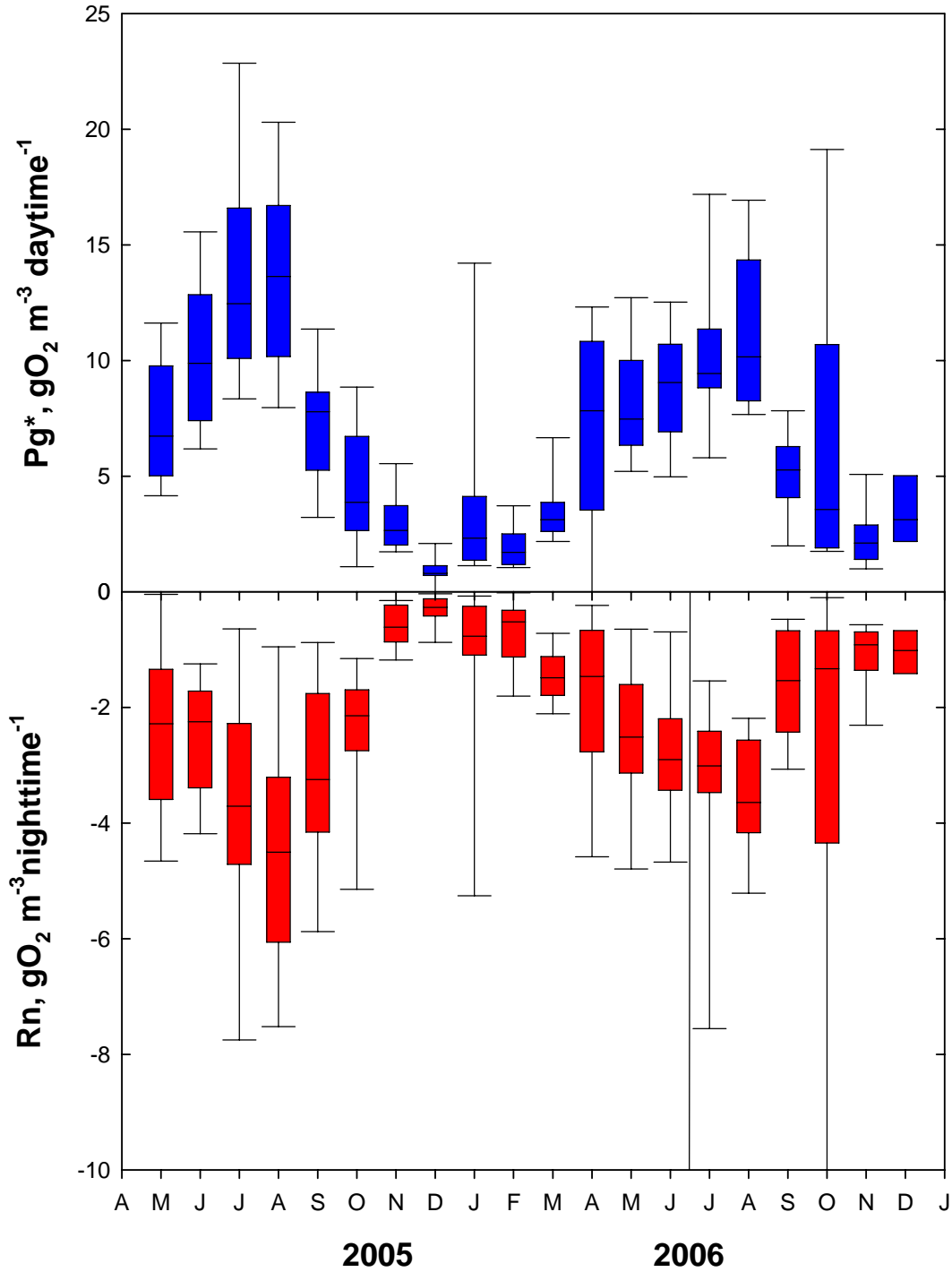


Figure 3-4. Corsica River metabolism at Sycamore Point from April 2005 to December 2006.

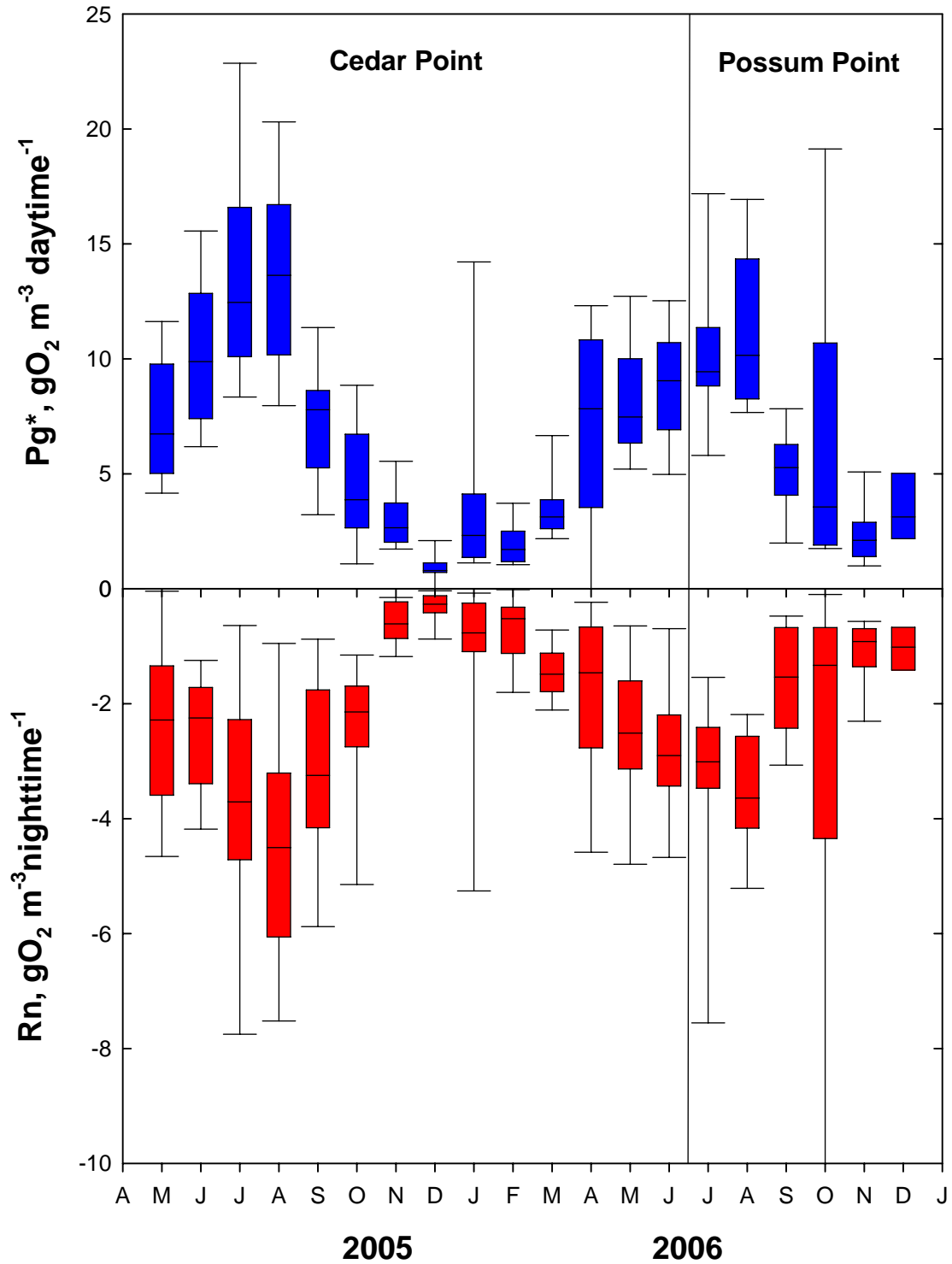


Figure 3-5. Corsica River metabolism at Cedar-Possum Point from April 2005 to December 2006.

We have reported earlier on metabolism rates (e.g., Pg^* and Rn) from a variety of Chesapeake Bay tributaries. Rates measured in the Corsica River are among the highest, being comparable to those

measured in the Back River, a highly eutrophic tributary adjacent to Baltimore, MD. If nutrient reductions in the Corsica are successful we would predict that rates of Pg* and Rn would generally decrease and that the seasonal pattern would change to one where maximum rates would occur during late spring and be much lower than present during the summer. Thus, both magnitude and pattern would change with nutrient input reductions.

3.4.3 Current Results for Corsica River Estuary (2005 - 2007)

When the full record is examined (2005-2007) there appear to be some inter-annual differences in both the magnitude and pattern of production (Figure 3-6). As indicated earlier, Pg* reached very high rates ($\sim 17 \text{ gO}_2 \text{ m}^{-3} \text{ day}^{-1}$) during July 2005 but declined on either side of this date. Average rates were less than $7 \text{ gO}_2 \text{ m}^{-3} \text{ day}^{-1}$ for all other months of 2005. During 2006 Pg* increased steadily from January through August reaching rates of about $13 \text{ gO}_2 \text{ m}^{-3} \text{ day}^{-1}$ in August a full month later than in the previous year. Peak rates were lower during 2006 than during the previous year although relatively high rates ($> 8 \text{ g O}_2 \text{ m}^{-3} \text{ day}^{-1}$) were maintained for 7 months. A third pattern was evident during 2007 wherein very high rates ($> 13 \text{ gO}_2 \text{ m}^{-3} \text{ day}^{-1}$) were maintained from April through July and then declined sharply for the remainder of the summer and fall. Rates above $10 \text{ g O}_2 \text{ m}^{-3} \text{ day}^{-1}$ were maintained for 5 months during 2007. There were not such extreme qualitative inter-annual differences in respiration. Peak rates during all years tended to be about $6\text{-}8 \text{ g O}_2 \text{ m}^{-3} \text{ night}^{-1}$. However, the temporal pattern of respiration was very similar to Pg* for all three years.

We have yet to fully develop nutrient loading rates for the Corsica River estuary although significant progress has been made in this direction (see Chapter 4 by Kemp et al.). We have argued that production is a function (possibly a complex function) of nutrient loading rates. We have yet to explore these data for such relationships but intend to do so when the appropriate data become available. It is possible that the differences in production magnitude and seasonal patterns described above are related to patterns and magnitude of nutrient loads.

We have completed metabolism computations for a variety of tributary sites where ConMon data are available. Thus, it is possible to make some qualitative comparisons between the data collected at Sycamore Point in the Corsica River estuary with other sites in the Chesapeake Bay system (see Summary Table in Chapter 7-2 of this report). By any standard, Pg* and Rn in the upper reaches of the Corsica River estuary are very, very high. Rates are comparable to several other super-enriched sites like the Back River, MD that receives sewage discharge from the City of Baltimore and the dead-end canals of the upper St. Martins River on Maryland's eastern shore. Our conceptual model of nutrient effects in estuarine systems indicates that should nutrient loads change (either increase or decrease) both Pg* and Rn should also respond and that the response should be reasonably rapid (weeks to seasons) rather than slow (years to decades).

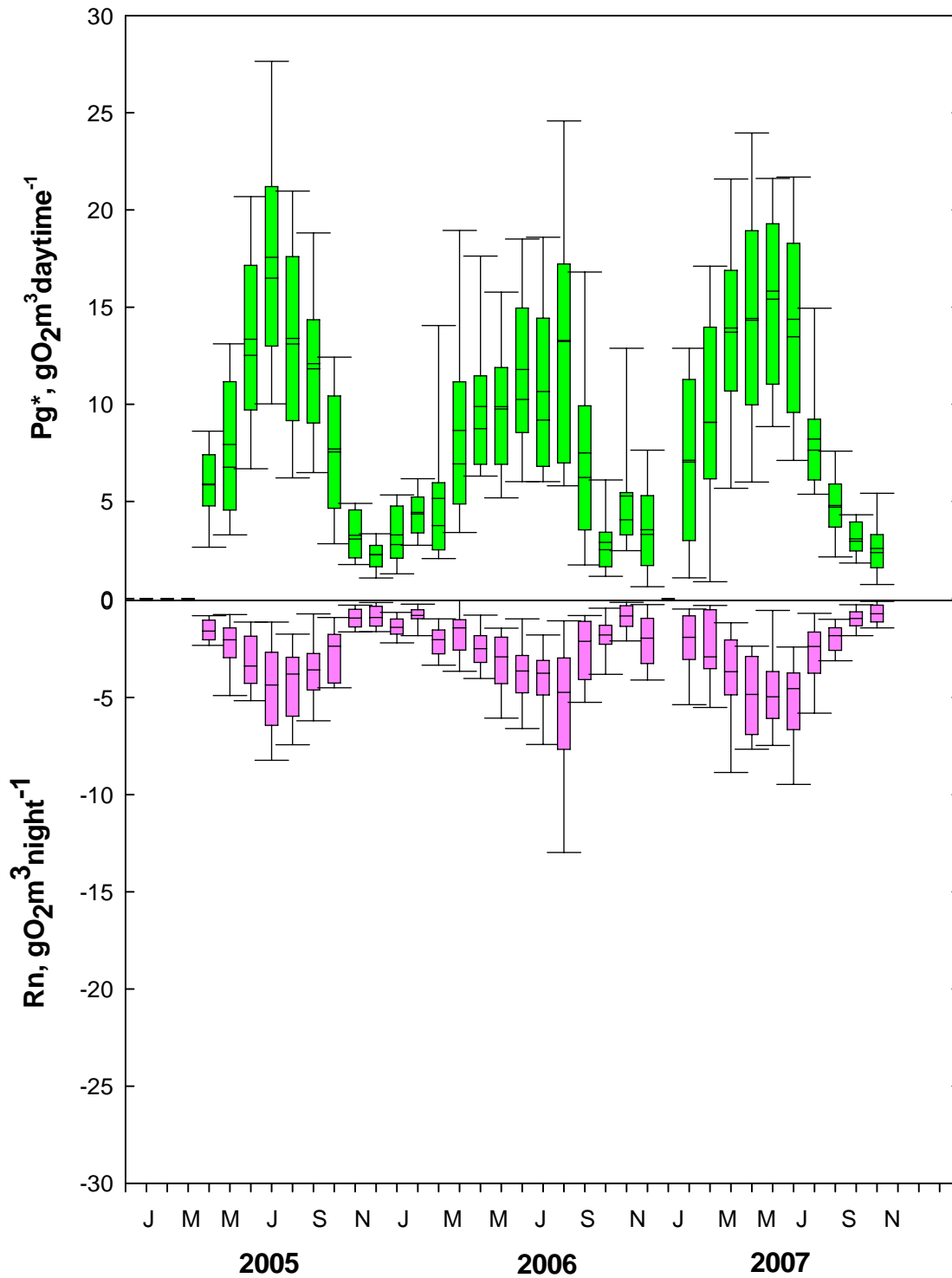


Figure 3-6. Monthly rates of production (Pg^*) and respiration (Rn) computed from data collected at Sycamore Point in the upper portion of the Corsica River estuary for the period 2005-2007. Data are displayed as box and whisker plots

3.5 Statistical Analyses of Corsica River Estuary Metabolism Data (2005 - 2007)

3.5.1 Statistical Methods

The objective of these analyses is to determine the seasonal and interannual trends in the production (Pg^*) and respiration (Rn) observations collected via ConMon at Sycamore Point on the Corsica River. The seasonal and annual patterns were estimated by fitting a linear model with year and month categorical terms. In addition to the primary analysis, preliminary graphical and descriptive analyses were used to assess the stochastic properties of the data (Figure 3-7). These preliminary analyses revealed that after adjusting for seasonal and annual trends, Pg^* , exhibits autocorrelation, but Rn does not. Thus the linear model for Rn was estimated using ordinary least

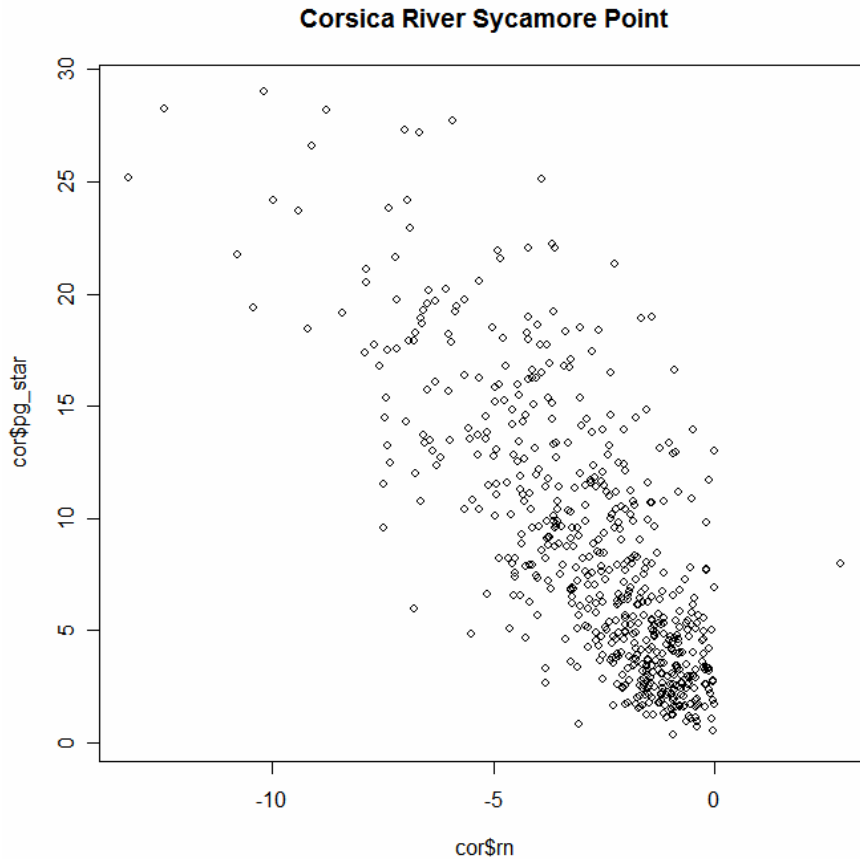


Figure 3-7. Plot of production vs. respiration for Sycamore Point on the Corsica River for the period 2005-2007.

squares as assuming independent and identically distributed normal random errors. The linear model for Pg^* was estimated using generalized least squares and assumes the errors have an autoregressive lag 1 dependence. The least squares analysis was done using the `lm()` function and the generalized least squares analysis was done using the `gls()` function where both functions are part of the r-statistical programming language (R Development Core Team, 2007). Where p-values are reported, those denoted by “#” are judged not-significant ($p > 0.05$), those denoted by “*” are significant ($0.01 < p \leq 0.05$) and those denoted by “**” are highly significant ($p \leq 0.01$).

3.5.2 Preliminary Analysis Results

The raw Pearson correlation for Rn and Pg* is Spearman's rank correlation $\rho = -0.76$ with a p-value $<0.0001^{**}$ which indicates a highly significant association between the two variables when there is no adjustment for seasonal effects. This could be a spurious correlation due to each variable having a seasonal pattern. However, a partial correlation analysis which adjusts for seasonal and annual effects finds a partial Pearson Correlation of $\rho = -0.597187$ with a p-value $<0.0001^{**}$ which shows that while some of the association shown in Figure 3-7 is due to both variables having seasonal trends, there is also a day to day negative correlation between the two. This result makes intuitive sense, as well. Pg* is basically a rate measurement quantifying the amount of labile organic matter being produced while Rn is a measure of the amount of this material being consumed. Thus, the potential exists for higher or lower values of Rn in relation to higher or lower values of Pg*.

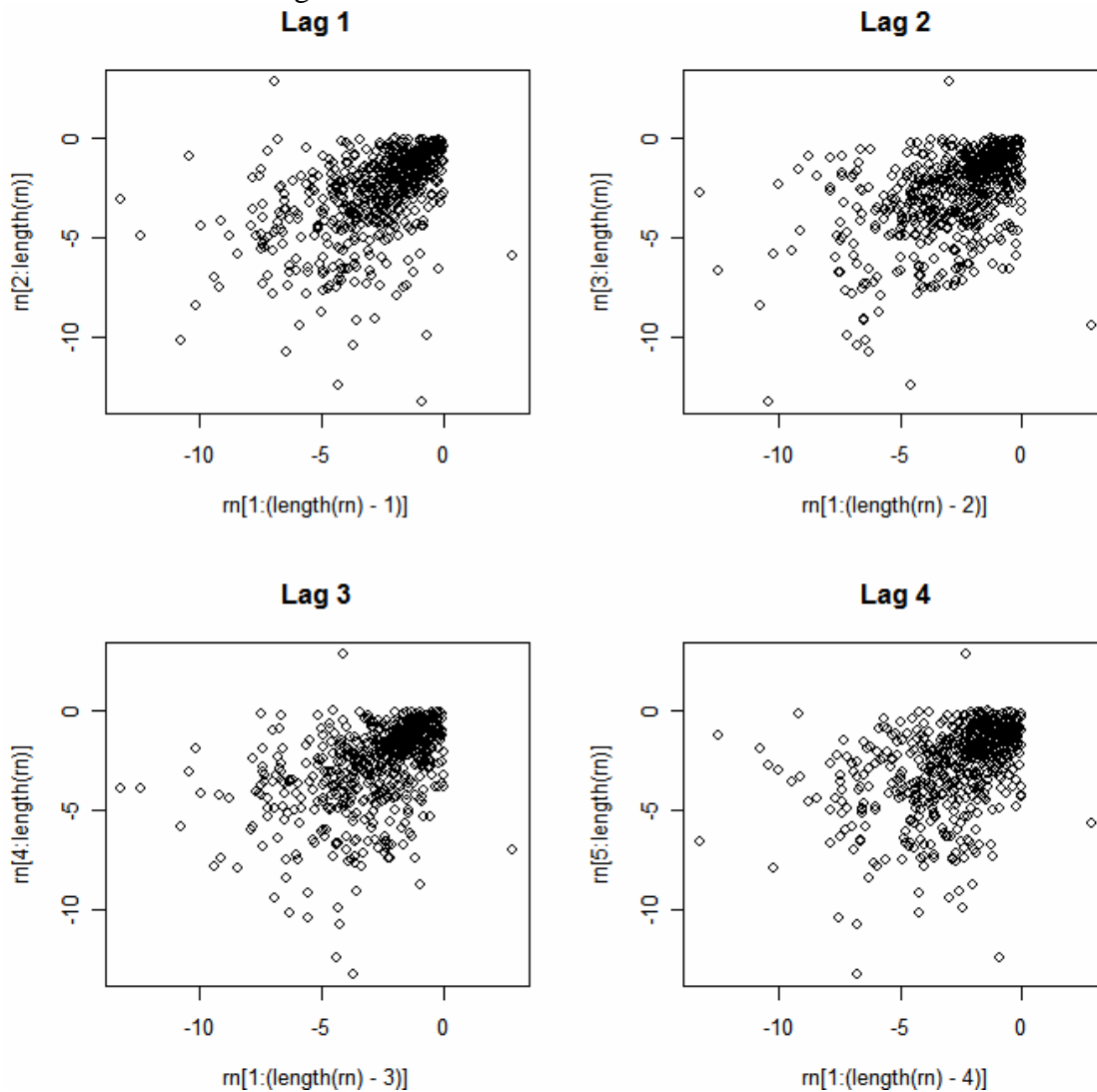


Figure 3-8. Lag plots (1 to 4 days) of Rn for Sycamore Point data.

Lag-plots (Figures 3-8 and 3-9) are a visual tool to examine data for auto-correlation. Lag-plots are prepared by ordering the data by sampling date and for a lag of 1 to show the (i+1)th observation paired with the ith observation. For a lag of 2, it is the (i+2)nd paired with the ith, and so on. In these data, most sequential observations are one day apart so the lag is roughly in units of days. A linear pattern in the plot suggests sequential points in the data tend to be large followed by large or small followed by small, a pattern which suggests autocorrelation. However, keep in mind that this pattern might be driven by an underlying seasonal trend and thus additional testing will appear below that examines autocorrelation after the seasonal and annual trends have been removed.

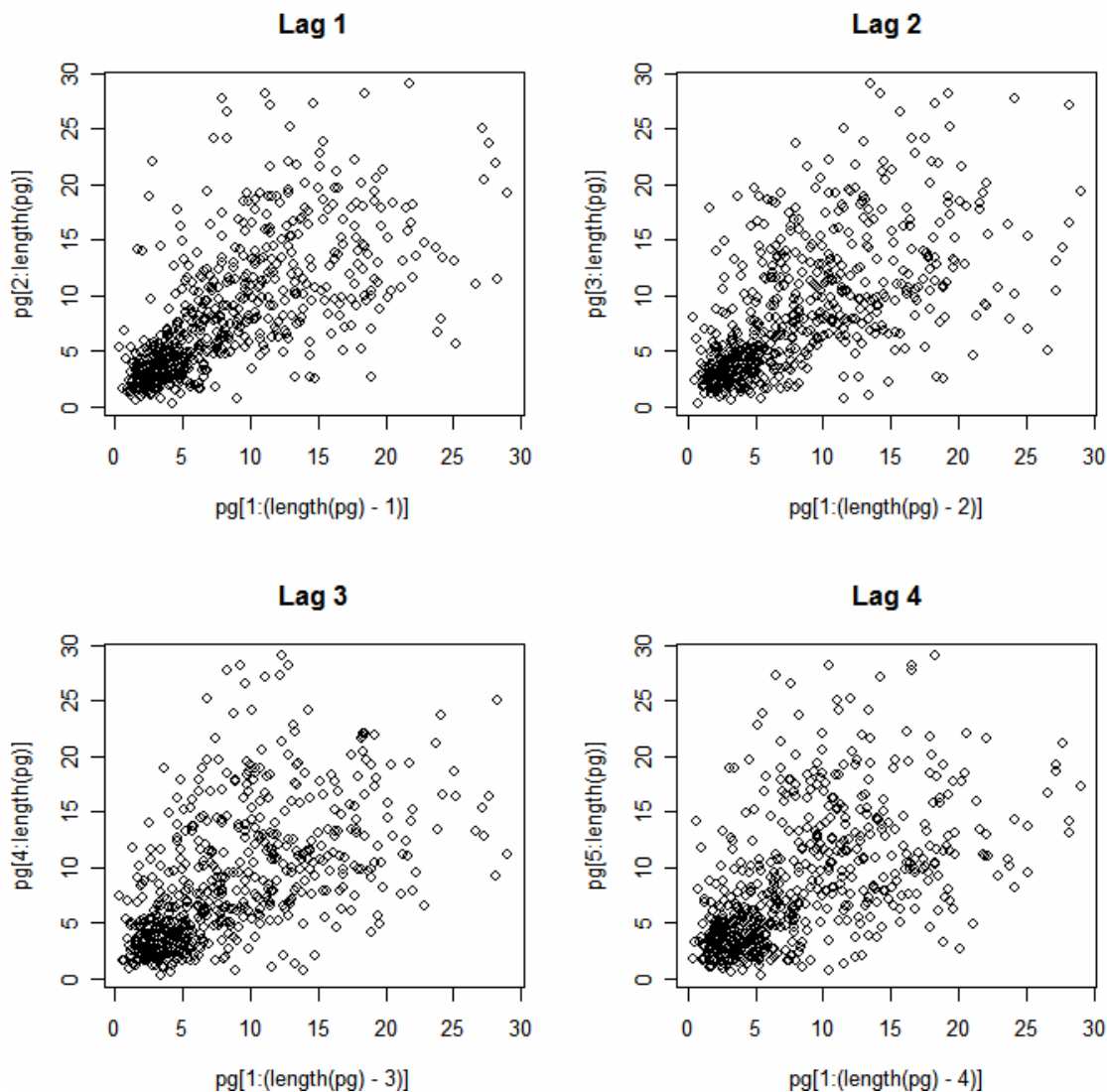


Figure 3-9. Lag plots (1 to 4 days) of Pg* for Sycamore Point data. Lag-plots for Pg* show evidence of autocorrelation. The lag plots for Pg* show stronger evidence of autocorrelation than those for Rn.

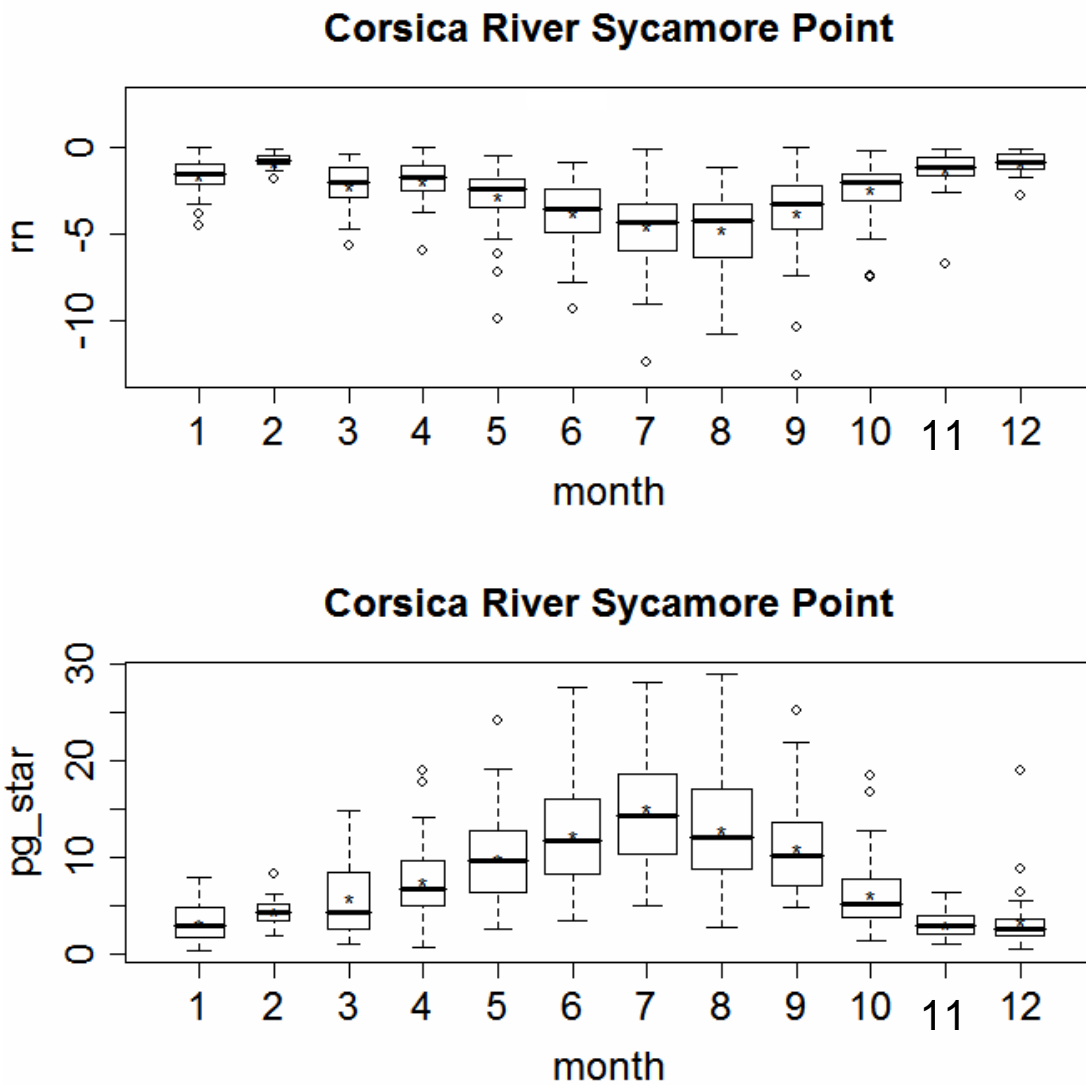


Figure 3-10. Box and whisker plots of monthly Rn and Pg* data collected at Sycamore Point in the Corsica River. Data for 2005-2007 were included in this plot.

Box plots (Figure 3-10) show a clear seasonal pattern in both parameters. The seasonal pattern is quite smooth which suggests there are two options for modeling this effect. One is to use month as a class variable which models each dependent variable as a step-function of month. Another approach would be to use a generalized additive model (gam) and fit the seasonal pattern as a smooth function of day of year. A decision was made to proceed with option 1.

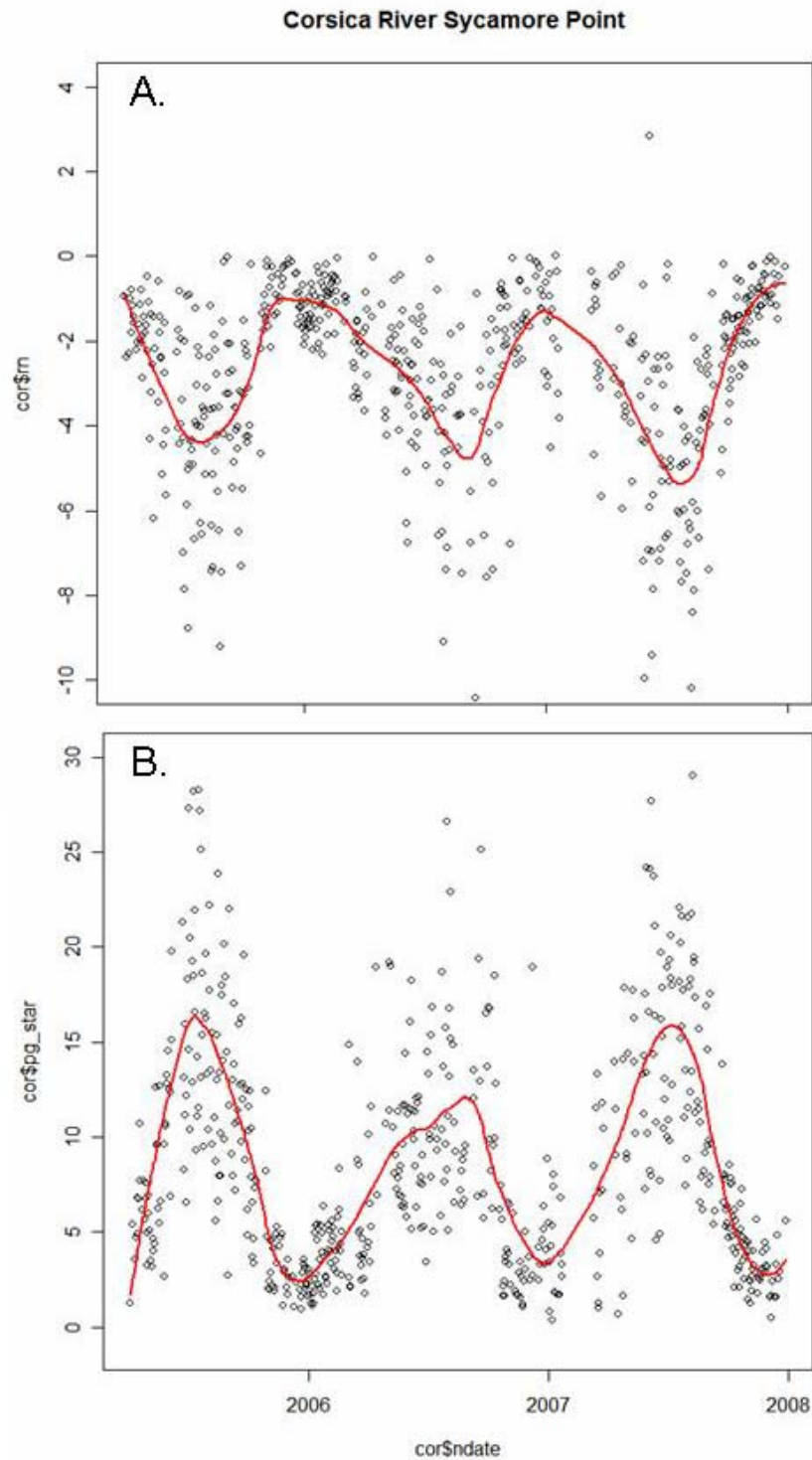


Figure 3-11A and 3-11B. Time series plots of the data with a loess regression curve superimposed to illustrate the trend of the data.

The smoothness of the loess curve (Figure 3-11A and B) also supports the idea that the seasonal component might have been a smooth function of day of year or perhaps with water temperature as a covariate.

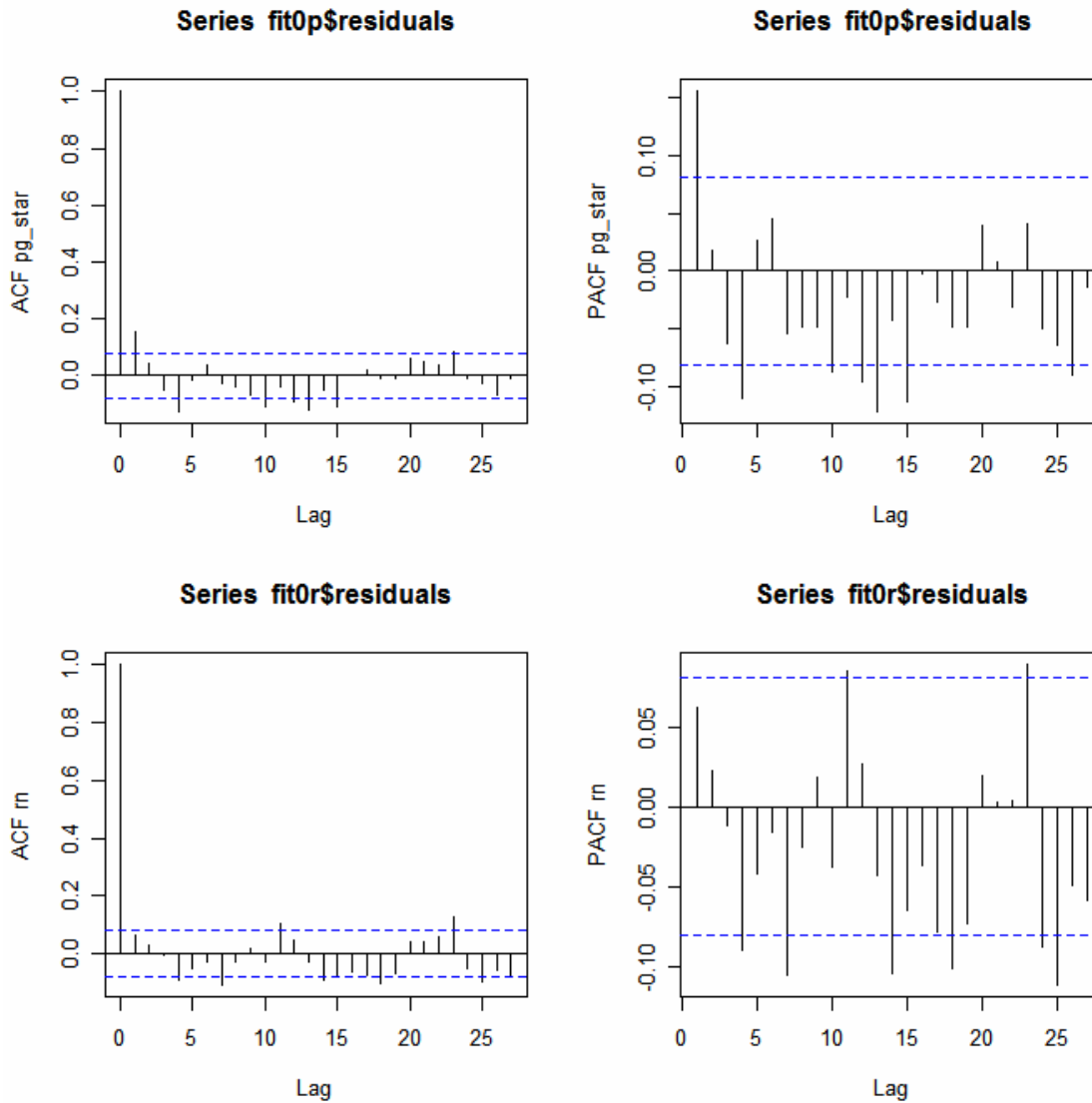


Figure 3-12. Graphic display of the autocorrelation function and partial autocorrelation function of the residuals from a year x season fit to each of Pg* and Rn.

Figure 3-12 shows the autocorrelation function and partial autocorrelation function of the residuals from a year x season fit to each of Pg* and Rn. For Pg* at lag 1 the line for the ACF extends above the blue line which suggests we should use an ar(1) model for these data. The Box-Pierce test for auto-correlation suggests the same. These two indicators for Rn suggest that an independent errors model is acceptable. These results suggest that Pg* has a little more “memory” than Rn. That is, Rn seems to be subject to greater stochastic dynamics so that deviations present in the last observation are erased by the time the next measurement is acquired. In the variable Pg*, there is some persistence of deviations from the mean from one observation to the next.

Box-Pierce test for Pg*
 X-squared = 14.1611, df = 1, p-value = 0.0001678 **
 Box-Pierce test for Rn

X-squared = 2.305, df = 1, p-value = 0.1290 #

3.5.3 Hypothesis Testing Results

What remains to be done is tabulate the results of running ANOVA's on each variable along with month to month comparisons and year to year comparisons. In order to get clean comparisons over months, data were sub-setted to only those months that are represented in all years (Apr-Dec). In later comparisons that examine means by year and month, all data are included.

Table 3-2. Analysis of variance for Pg* based on a generalized least squares analysis with auto-regressive lag 1 error structure.

Effect	Numerator DF	F-value	p-value
intercept	1	1725.31	<0.0001**
month	8	41.1	<0.0001**
year	2	1.27	0.2824#
month by year	16	3.64	<0.0001**

In Table 3-2, we confirm that for Pg*, the seasonal trend is significant ($p < 0.0001$) and there is also evidence that the seasonal trend was not consistent in each year ($p = < 0.0001$). When averaging over months, it appears that Pg* is fairly consistent from year to year.

Table 3-3. Model Means of Pg* by Month

Month	Mean	Std Err	t-stat	p-value
4	7.79	0.8205	9.5	<0.0001**
5	10.57	0.6569	16.09	<0.0001**
6	12.51	0.6572	19.03	<0.0001**
7	14.86	0.6069	24.49	<0.0001**
8	12.65	0.6137	20.61	<0.0001**
9	11.2	0.7288	15.36	<0.0001**
10	6.64	0.6168	10.76	<0.0001**
11	3.14	0.6293	4.99	<0.0001**
12	3.37	0.7445	4.53	<0.0001**

Table 3-3 shows the pattern of monthly means from April to December. Note that the model means are the predicted value for each month (averaging over years) from the model. These will be slightly different from simple arithmetic means of the data by month. The t-statistic and p-value of this table show that the means are significantly different from zero, which is of little interest.

Table 3-4. Comparison of Model Means between sequential months for Pg*

Month pair	Mean difference	Std Err	t-stat	p-value
5 - 4	2.78	1.0441	2.66	0.0082**
6 - 5	1.94	0.9244	2.1	0.0370*
7 - 6	2.35	0.8902	2.64	0.0086**
8 - 7	-2.21	0.859	-2.58	0.0104*
9 - 8	-1.45	0.9472	-1.53	0.1264#
9 - 10	-4.56	0.9497	-4.8	<0.0001**
10 - 11	-3.5	0.8769	-3.99	<0.0001**
11 - 12	0.23	0.9692	0.24	0.8087#

In Table 3-4 we see that as the season progresses, in general the mean Pg* for each month differs significantly ($p < 0.05$) from the previous month with August-September and November-December as exceptions.

Table 3-5. Model Means of Pg* by year

year	Mean	Std Err	t-stat	p-value
2005	9.22	0.3752	24.57	<0.0001**
2006	8.83	0.415	21.27	<0.0001**
2007	9.53	0.3951	24.12	<0.0001**

The average Pg* for each year shows a pattern of decreasing between 2005 and 2006 (Table 3-5) and then increasing between 2006 and 2007 but this effect is not statistically significant. From a management point of view this is an important result. It suggests that nutrient load changes have been insufficient to reduce the magnitude of Pg*.

Table 3-6. Comparison of Model Means between sequential years for Pg*

Year pair	Mean difference	Std Err	t-stat	p-value
2006 - 2005	-0.39	0.5594	-0.7	0.4857#
2007 - 2006	0.7	0.573	1.23	0.2214#

Because the Anova results (Table 3-6) shows non-significant year effect, we should not spend time on these year comparisons.

Table 3-7. Comparison of Model Means between sequential years within month for Pg*

month	mean 2005	mean 2006	mean 2007	p-value 05 v 06	p-value 06 v 07
1	NA	3.27	3.55	NA	0.8536#
2	NA	4.33	NA	NA	NA
3	NA	5.3	6.99	NA	0.3262#
4	5.82	8.41	9.08	0.1777	0.7461#
5	8	9.95	13.79	0.1640	0.0183*
6	13.35	9.8	14.38	0.0304	0.0012**
7	17.48	11.81	15.28	<0.0001	0.0201*
8	12.94	10.57	14.41	0.1118	0.0115*
9	12.21	13.12	8.26	0.6049	0.0094**
10	7.62	7.51	4.79	0.9484	0.0401*
11	3.31	3.01	3.12	0.8465	0.9423#
12	2.25	5.25	2.61	0.0687	0.1508#

Table 3-7 is based on a refit of the model to data including all months. The mean for the year of each month are shown in columns 2-4 and the p-values for comparing sequential years are in columns 5 and 6. The month by year interaction is best discerned in the figure below. In spring months (Apr-May), Pg* is highest in 2007. In summer months (Jun-Aug), 2006 is considerably below 2005 and 2007. In the Fall, 2007 falls below 2005 and 2006.

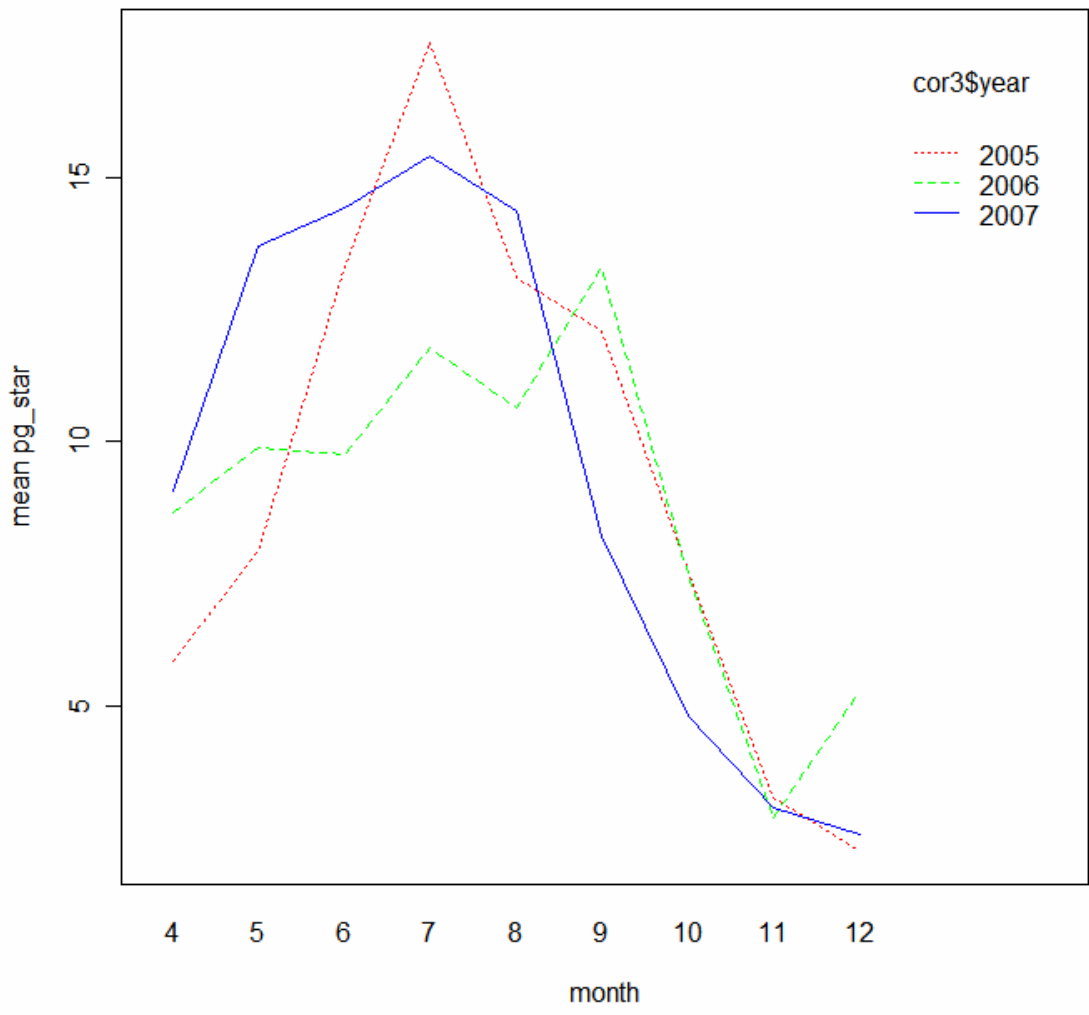


Figure 3-13. Mean monthly (Apr-Dec) values of Pg* collected at Sycamore Point in the Corsica River estuary during 2005, 2006 and 2007.

Table 3-8. Analysis of variance for Rn based on a least squares analysis of with independent error structure.

Effect	Numerator DF	F-value	p-value
month	8	36.27	<0.0001**
year	2	1.53	0.2181#
month by year	16	3.5	<0.0001**
residual	468	NA	NA

The important effects in Rn are similar to Pg* (Figure 3.13 and Table 3-8). The seasonal trend is significant on average and the seasonal trend is not consistent among years. On average over months, means for years do not differ significantly. Rn reaches it largest magnitude in July-August (Table 3-9).

Table 3-9. Model Means of Rn by Month

Month	Mean	Std Err	t-stat	p-value
4	-1.93	0.2939	-6.56	<0.0001**
5	-2.93	0.2341	-12.5	<0.0001**
6	-3.76	0.2356	-15.98	<0.0001**
7	-4.47	0.2158	-20.71	<0.0001**
8	-4.64	0.2183	-21.26	<0.0001**
9	-4.04	0.2606	-15.49	<0.0001**
10	-2.53	0.2179	-11.6	<0.0001**
11	-1.28	0.224	-5.73	<0.0001**
12	-0.83	0.2658	-3.13	0.0018**

Table 3-10. Comparison of Model Means between sequential months for Rn

Month pair	Mean difference	Std Err	t-stat	p-value
5 - 4	-1	0.3758	-2.65	0.0083**
6 - 5	-0.84	0.3322	-2.53	0.0119*
7 - 6	-0.71	0.3195	-2.21	0.0277*
8 - 7	-0.17	0.307	-0.56	0.5776#
9 - 8	0.61	0.34	1.78	0.0756#
9 - 10	1.51	0.3397	4.44	<0.0001**
10 - 11	1.25	0.3125	3.98	<0.0001**
11 - 12	0.45	0.3476	1.29	0.1963#

In general, the means Rn for sequential months differ significantly. The exceptions being July-August and the winter months November-December (Table 3-10).

Table 3-11. Model Means of Rn by year

year	Mean	Std Err	t-stat	p-value
2005	-2.72	0.1324	-20.53	<0.0001**
2006	-2.99	0.1465	-20.39	<0.0001**
2007	-3.1	0.1399	-22.14	<0.0001**

Table 3-12. Comparison of Model Means between sequential years for Rn

Year pair	Mean difference	Std Err	t-stat	p-value
2006 - 2005	-0.27	0.1975	-1.35	0.1775#
2007 - 2006	-0.11	0.2026	-0.55	0.5795#

Because the Anova table shows non-significant year effect, we should not spend time on these year comparisons (Tables 3-11 and 3-12).

Table 3-13. Comparison of Model Means between sequential years within month for Rn

month	mean 2005	mean 2006	mean 2007	05 v 06	06 v 07
1	NA	-1.36	-2.09	NA	0.1543#
2	NA	-0.8	NA	NA	NA
3	NA	-2.1	-2.23	NA	0.8277#
4	-1.57	-1.69	-2.53	0.8641	0.2449#
5	-2.36	-2.48	-3.94	0.8031	0.0102*
6	-3.17	-3.18	-4.94	0.974	0.0004**
7	-4.74	-3.89	-4.79	0.0806	0.0827#
8	-4.41	-4.22	-5.3	0.7194	0.0419*
9	-3.66	-5.68	-2.77	0.0011	<0.0001**
10	-2.77	-2.86	-1.95	0.8659	0.0444*
11	-0.93	-1.94	-0.98	0.0615	0.0686#
12	-0.87	-0.93	-0.69	0.912	0.7086#

Table 3-13 is based on a refit of the model to data including all months. The mean for the year of each month are shown in columns 2-4 and the p-values for comparing sequential years are in columns 5 and 6. The month by year interaction is best discerned in the Figure 3-14). In spring and summer months (Apr-Jul), Rn has greatest magnitude in 2007. After the summer the magnitude of Rn is less than 2005 - 2006.

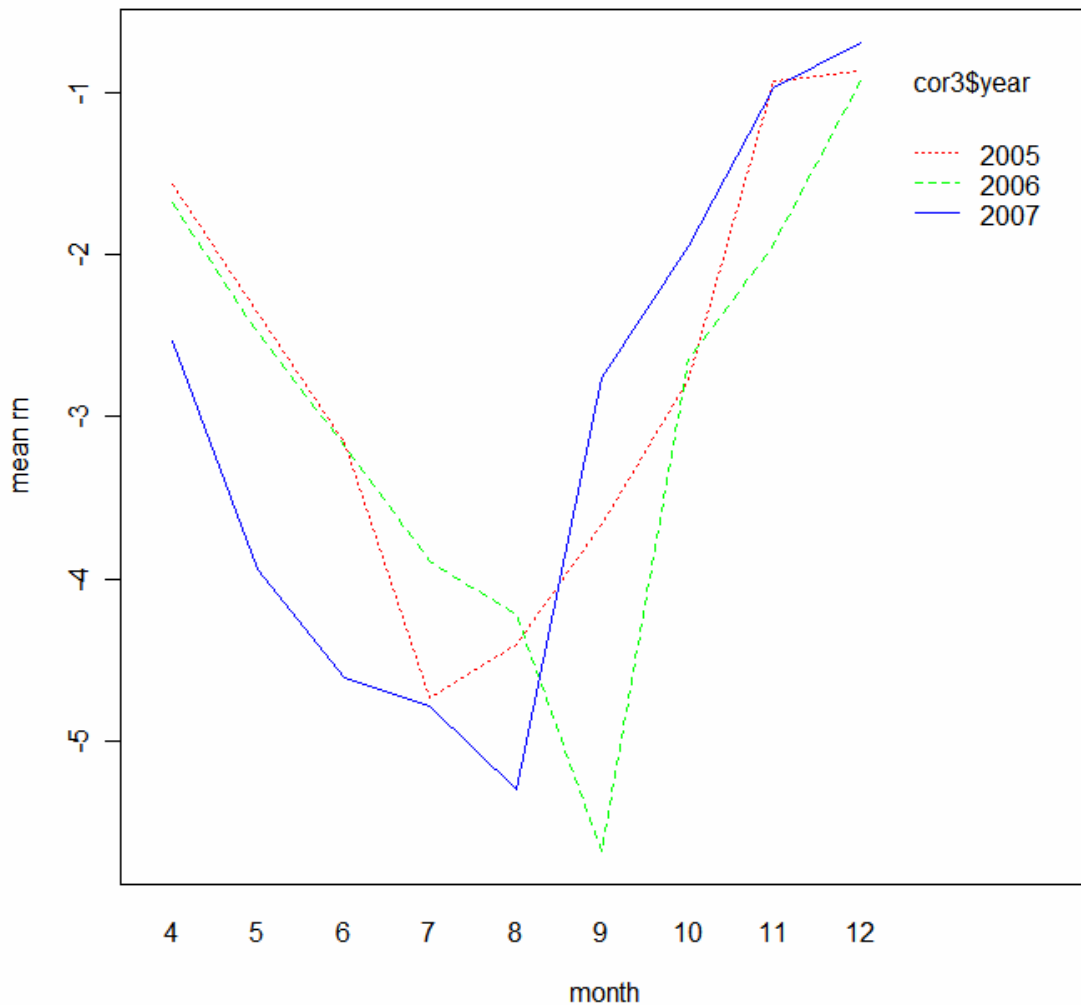


Figure 3-14. Mean monthly (Apr-Dec) values of Rn collected at Sycamore Point in the Corsica River estuary during 2005, 2006 and 2007. Note that maximum rates of Rn were larger when they occurred later in the summer period.

Computing a general minimum significant difference (MSD) for these parameters is a little problematic because the MSD is sample size dependent and there is an issue of auto-correlation for Pg*. Results shown in Table 3-14 are based on the rule of thumb that if the difference exceeds two standard errors it is significant. For pg-star, I inflated the factor to 2.5 standard errors to allow for auto-correlation. The table shows how this would change as sample size increases. The sample size was increased up to 30 to make comparisons among months when there is data for each day of the month. In most months, at least 20 days had ConMon data available for Pg* and Rn computations. Thus, differences between months of different years are about 2.4 for Pg* and 0.8 for Rn then significant change is likely to have occurred. This finding provides us with a measure of change that will be useful.

Table 3-14. Minimum Significant Difference for Rn and Pg*

sample size	Pg* MSD	Rn MSD
5	4.7	1.53
10	3.33	1.08
15	2.72	0.89
20	2.35	0.77
25	2.1	0.69
30	1.92	0.63

3.6 References

- Boynton, W.R., Kemp, W.M.,** Nitrogen in Estuaries in Capone, D.G., Bronk, D.A., Mulholland, M.R., Carpenter, E.J., 2008. Nitrogen in the Marine Environment, in press.
- Boynton, W.R., W.M. Kemp and C.W. Keefe.** 1982. A comparative analysis of nutrients and other factors influencing estuarine phytoplankton production, p. 69-90. In: V.S. Kennedy, [Ed.], Estuarine Comparisons, Academic Press, NY.
- Burger, N. H. and J. D. Hagy.** 1998. Patuxent River high frequency monitoring, p. 153-183. In: W. R. Boynton and F. M. Rohland (eds.). Ecosystem Processes Component Interpretive Report No. 15. Ref. No. [UMCES]CBL 98-073a. Solomons, MD.
- Caffrey, J.** 2004. Factors controlling net ecosystem metabolism in U. S. Estuaries. *Estuaries* 27 (1): 90-101.
- Gazeau, F. et al.** 2005. Net ecosystem metabolism in a micro-tidal estuary (Randers Fjord, Denmark): evaluation of methods. *Mar Ecol Prog Ser* 301: 23-41.
- R Development Core Team** (2007). R: A language and environment for statistical computing. R Foundation for Statistical Computing, Vienna, Austria. ISBN 3-900051-07-0, URL <http://www.R-project.org>.
- Sweeney, B. F. 1995.** Community metabolism in the Patuxent River estuary: 1963-1969 and 1992. Masters Thesis. University of Maryland, College Park, MD. 83p.
- Vollenweider, R. A.** 1976. Advances in defining critical loading levels for phosphorus in lake eutrophication. *Mem. Ist. Ital. Idrobiol.* 33: 53-8.

4.0 Box-Modeling Analysis of the Corsica River Estuarine System

W. Michael Kemp, Jeremy M. Testa, and Maureen T. Brooks

4.1	Introduction and Implications for Management	4-1
4.2	Methods	4-1
4.3	Results	4-7
4.4	Summary and Implications for Management	4-12
4.5	References	4-13

4.1 Introduction and Implications for Management

Box-modeling analysis provides a relatively straight-forward method for integrating water quality monitoring data and developing empirical calculations of nutrient cycling, nutrient transport (and exchange), and net nutrient assimilation by the integrated estuarine system. These analyses are useful to managers, as they reveal how nutrient input reductions in the watershed affect water quality, nutrient transport and nutrient processing in the estuarine system. Net nutrient exchange rates between the Chester and Corsica Rivers also reveal the Chester River as an important DIN source to the Corsica, a fact which must be considered when planning regional scale nutrient reduction strategies. Results of this analysis, which reveal high rates of DIN and DIP uptake in the upper Corsica River, suggest that management actions should carefully consider the role of high rates of marsh denitrification and should gear to reduce algal growth and turbidity via nutrient input reduction from diffuse sources.

Here, we describe a box-modeling analysis of nutrient cycling and transport in the Corsica River estuarine system and the adjacent, connected Chester River estuarine system. We have developed two different box-model configurations for the Corsica system with varying degrees of spatial resolution, where the estuarine system is analyzed as (1) a single integrated system and (2) as a 2-region system. The Corsica system is analyzed at monthly and annual scales for 2006. The Chester River system is analyzed as a 3-region system at an annual scale for an idealized year.

4.2 Methods

1. Data for Box-Model Development and Analysis. Data requirements for developing this box-model analysis in the Corsica and Chester River estuarine systems include water volumes and areas, watershed areas, freshwater (river flow, precipitation, etc.) input data, and nutrient concentrations in inflowing freshwater and within the estuary. We gathered these data from multiple sources to support box-model computations for the spring, summer, and fall of 2006 for the Corsica River and an idealized May-October season for the Chester River.

Corsica River estuary

(a) Hypsographic Data. We have obtained water area and volume data for the three regions of the Corsica River estuary from the 2000 TMDL report (MDE 2000b). Box 1 in our model includes the boxes 1-7 from the TMDL report and Box 2 in our model includes boxes 8-16 from the TMDL

report (see MDE 2000a,b and Fig.4-1). These data compared favorably with bathymetric data (<http://estuarinebathymetry.noaa.gov/>).

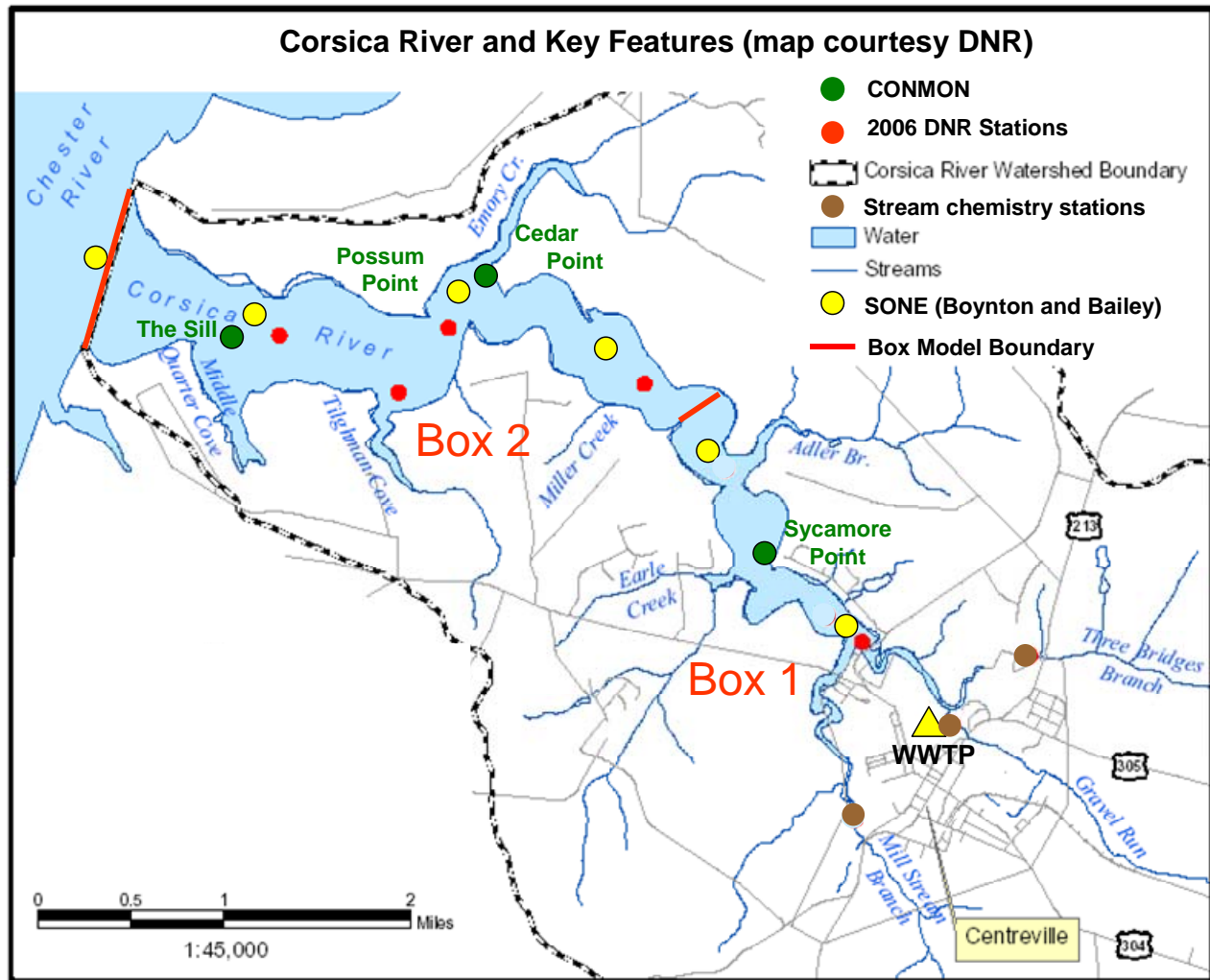


Figure 4-1: Map of Corsica River estuary, including box model boundaries, the Centreville wastewater treatments plant (WWTP), water quality monitoring stations from DNR (red circles) and UMCES SONE cruises (yellow circles), and nutrient sampling at stream gauges (brown circles).

(b) Freshwater Inputs. We estimated the total freshwater entering the estuary from stream flow and from precipitation. Monthly evaporation rates were obtained from 10-year mean rates from the annual NOAA climate summary for Maryland and Delaware (<http://www7.ncdc.noaa.gov/IPS/CDPubs?action=getstate>). Monthly precipitation rates were obtained from the National Atmospheric Deposition Program (NADP) station at Wye Mills, Maryland (<http://nadp.sws.uiuc.edu/sites/siteinfo.asp?net=NTN&id=MD13>). Freshwater inputs in stream flow for 2006 were estimated from stream gauges at Three Bridges Branch (TBB), Gravel Run (GR), and Mill Stream Branch (MSB) in the Corsica River, and nearby Tuckahoe Creek (<http://md.water.usgs.gov/>). Although it would be preferable to use Corsica River stream gauge data to directly compute freshwater inputs, we estimated freshwater inputs for two reasons: 1)

stream monitoring in the Corsica watershed did not begin until July 13, 2006, and 2) the stream gauges in the Corsica only measure flow from 64% of the watershed.

(c) Estuarine Water Quality and Salinity Concentrations. We obtained existing, in-estuary water quality and salinity data from several stations during April to October, 2006, including data collected during COMMON and DATAFLOW field efforts (MD DNR) and as part of the Corsica River SONE experiments (Fig. 4-1). Water quality data included dissolved inorganic nitrogen ($\text{DIN} = \text{NO}_2^- + \text{NO}_3^- + \text{NH}_4^+$), (2) dissolved inorganic phosphorus ($\text{DIP} = \text{PO}_4^{3-}$), total nitrogen (TN), and total phosphorus (TP).

(d) Nutrient Inputs. We obtained N and P inputs from the Centreville wastewater facility for 2006, but these inputs were not included in box-model computations because sewage water is tertiary treated and then sprayed onto adjacent fields (P. Papali, personal communication). DIN concentrations in precipitation were obtained from the National Atmospheric Deposition Program station at Wye Mills, MD (<http://nadp.sws.uiuc.edu/sites/siteinfo.asp?net=NTN&id=MD13>). DIP concentrations in precipitation were assumed to be zero. TN and TP concentrations in stream flow entering the Corsica River were obtained from weekly composite samples obtained at stream gauging stations from Three Bridges Branch, Gravel Run, and Mill Stream Branch from May 2006 to October 2006. The composite samples, which collect and mix stream water samples collected periodically over a week-long period, were analyzed for TN and TP, while in-stream grab samples species were collected and analyzed for inorganic N and P concentrations each time the composite samples sites were visited. Because the composite samples provide a more integrated view of nutrient concentrations in inflowing stream water, we used the TN and TP in these samples to compute DIN and DIP concentrations in stream water. Parallel measurements of TN, DIN, TP, and DIP were made in Three Bridges Branch, and correlations of TN and DIN in data collected between July 2005 and September 2007 were highly significant ($r^2=0.83$, $p<0.01$), as were TP and DIP ($r^2=0.67$, $p<0.01$). Thus, we estimated DIN and DIP in TBB, GR, and MSB based on the TN and TP concentrations in each sub-watersheds composite samples and equations of the linear fit between TN/DIN and TP/DIP for TBB. Nutrient loads for each sub-watershed were then computed by multiplying the nutrient concentration by the estimated stream flow for each sub-watershed. The GR concentrations of TN and TP were used for the portion of the sub-watershed containing Centreville, while the TN and TP concentrations from TBB were used for the non-gauged portion of the watershed outside of Centreville.

Chester River estuary

(a) Hypsographic Data. Water area and volume data for the Chester River estuary were obtained using GIS 3-D surface analysis of NOAA bathymetric data (<http://estuarinebathymetry.noaa.gov/>). The 3 boxes of the model were defined in a manner consistent with the depth distribution of the estuary.

(b) Freshwater Inputs. Stream flow was obtained from 6 USGS gauging stations in the Chester River watershed (<http://md.water.usgs.gov/>). Data from 2000 through 2005 was used to create May-Oct average flow into the 3 boxes of the Chester River model. May-Oct average evaporation rates were obtained from 10-year mean rates from the annual NOAA climate summary for Maryland and Delaware (<http://www7.ncdc.noaa.gov/IPS/CDPubs?action=getstate>). Daily mean precipitation rates were obtained from the National Atmospheric Deposition Program (NADP)

station at Wye Mills, Maryland and aggregated into monthly and seasonal (May-Oct.) values (<http://nadp.sws.uiuc.edu/sites/siteinfo.asp?net=NTN&id=MD13>).

(c) Estuarine Water Quality and Salinity Concentrations. As with the Corsica River box models, water quality and salinity were obtained from existing stations including data collected during CONMON and DATAFLOW field efforts (MD DNR). In addition, several long-term monitoring stations (MD DNR) with data from 1984 – 2007 were available in the Chester River estuary. These data included salinity, dissolved inorganic nitrogen ($DIN = NO_2^- + NO_3^- + NH_4^+$), dissolved inorganic phosphorus ($DIP = PO_4^{3-}$), total nitrogen (TN), and total phosphorus (TP). Averages from May-Oct were used to ensure consistent levels of data availability for all 3 boxes of the model.

(d) Nutrient Inputs. N and P inputs to the Chester River were calculated using 10-year average values from the Chesapeake Bay Watershed Model (CBWM). Data from CBWM were reported for a watershed segment (segment 380) which encompasses an area greater than the Chester River watershed. The watershed areas were determined to be 286.4, 103, and 96.6 km² for boxes 1, 2 and 3 respectively. The loads for each box of the Chester River model were obtained by scaling the segment data by watershed area and weighted by land-use-type (MD DNR). Point-source N and P inputs were obtained from sewage treatment plant data as May-Oct averages using data from 1985-2005.

2. Box-Model Computation. Box-models compute the time-dependent mean circulation in estuarine systems where salinity distribution and input of freshwater is known. Thus, the box modeling approach computes advective and diffusive exchanges of water and salt between adjacent control volumes and across end-member boundaries using the solution to non-steady state equations balancing salt and water inputs, outputs, and storage changes (Pritchard 1969, Officer 1980, Hagy et al. 2000). The control volumes, hereafter referred to as “boxes”, are assumed to be well mixed. Boundaries separating adjacent boxes were chosen based upon several factors: (1) data availability; (2) maintaining uniform bathymetry in each box; and (3) relatively uniform salinity gradients and water volumes among boxes (Figs. 4-1, 4-3).

Corsica River and Chester River estuaries

Independent box models were created for the Corsica and Chester Rivers. The Corsica River box model used in this analysis calculates advection and mixing for 2 scenarios; (a) the estuary is considered one integrated system (1 Box) and (b) the estuary is divided into 2 interacting boxes. The Chester River box model was used to examine only one scenario, in which the estuary is divided into 3 boxes. The models compute horizontal advective transport (Q) and horizontal diffusive exchanges in two directions (E) and freshwater input (Q_r , Q_{ww} , Q_f). Thus, the salt balance for a box “m” in the 1-box scheme is described below (Fig. 4-2)

$$V_m \frac{ds_m}{dt} = Q_r s_r + Q_{ww} s_{ww} + Q_f s_f - Q_m s_m + E_{m,m+1} (s_{m+1} - s_m) \quad (1)$$

which simplifies to

$$V_m \frac{ds_m}{dt} = Q_m s_m + E_{m,m+1} (s_{m+1} - s_m) \quad (2)$$

and the water balance is

$$\frac{dV_m}{dt} = 0 = Q_m - (Q_r + Q_{ww} + Q_f) \quad (3)$$

Alternatively, the salt balance for a box “m” in the 2-box or 3-box scheme is as below (Fig. 4-3a)

$$V_m \frac{ds_m}{dt} = Q_{m-1}s_{m-1} + Q_r s_r + Q_{ww} s_{ww} + Q_f s_f + E_{m-1,m}(s_{m-1} - s_m) + E_{m,m+1}(s_{m+1} - s_m) - Q_m s_m \quad (4)$$

and the water balance is

$$\frac{dV_m}{dt} = 0 = Q_m - (Q_{m-1} + Q_r + Q_{ww} + Q_f) \quad (5)$$

where Q_{m-1} and $E_{m-1,m} = 0$ for Box 1 and $Q_{ww} = 0$ for Box 2 and Box 3. V_m is the volume of the box, Q_m is the advective transport to the seaward box, Q_{m-1} is the advective transport from the landward box, Q_f is the freshwater input from precipitation-evaporation, Q_r is the freshwater input from streamflow and runoff, $E_{m-1,m}$ is the diffusive exchange with the landward box, $E_{m,m+1}$ is the diffusive exchange with the seaward box, s_m is the salinity in the box, s_{m-1} is the salinity in the landward box, and s_{m+1} is the salinity in the seaward box. The left hand side of Eq. 1 is computed as the monthly salinity change (salinity distribution assumed to be uniform in each box), while the left hand side of Eq. 2 is assumed to be zero at monthly time scales.

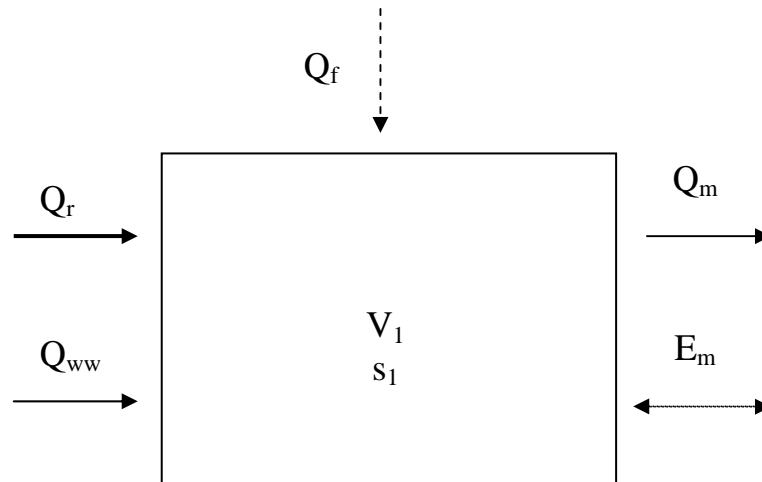


Figure 4-2: Box and arrow diagram of transports coefficients calculated by the 1-box-model for the Corsica River estuary.

In this analysis, we also calculated transport and net production rates for non-conservative variables, including dissolved inorganic nitrogen ($DIN = NO_2^- + NO_3^- + NH_4^+$), dissolved inorganic phosphorus ($DIP = PO_4^{3-}$), total nitrogen (TN), total phosphorus (TP), and total organic nitrogen ($TON = \text{particulate} + \text{dissolved organic nitrogen}$). Physical transport rates for these non-conservative variables were computed by multiplying the solute concentration by the advective and non-advective fluxes (Q 's and E 's, respectively) for each box. Monthly mean values of N and P species were computed for each box (and upstream and downstream boundaries) using water

quality data from 2006 for the Corsica River (Fig. 4-1) and water quality data from 1985-2005 for the Chester River.

Mass balance equation(s) (Eq. 6 and 7) of the resulting nutrient transports into and out of each box, combined with the volume-weighted concentration change of the variable, yield a residual term (P_m) that represents the non-conservative net production rate (production – consumption) of nutrients. For any Box m in the 2-box or 3-box scheme, the mass balance equation is

$$V_m \frac{dc_m}{dt} = Q_{m-1}c_{m-1} + Q_r c_r + Q_{ww}c_{ww} + Q_f c_f + E_{m+1,m}(c_{m+1}-c_m) - E_{m,m-1}(c_m-c_{m-1}) - Q_m c_m + P_m \quad (6)$$

which can be rearranged to calculate P_m

$$P_m = V_m \frac{dc_m}{dt} - Q_{m-1}c_{m-1} - Q_r c_r - Q_{ww}c_{ww} - Q_f c_f - E_{m+1,m}(c_{m+1}-c_m) + E_{m,m-1}(c_m-c_{m-1}) + Q_m c_m \quad (7)$$

where c is the nutrient concentration in each box and P_m is the net production (or consumption) rate (calculated in units of mass per time within the box volume (mmol d^{-1}) and mass flux per unit area or volume using geometry data for each box.

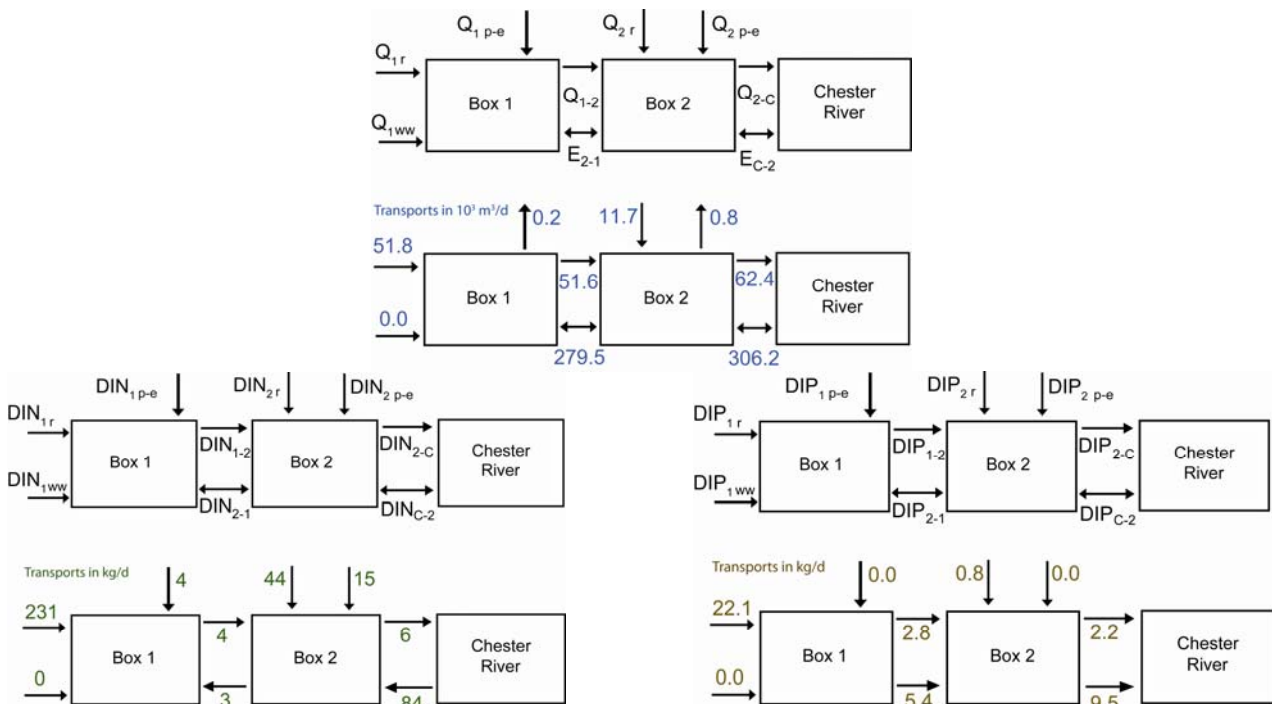


Figure 4-3: Box and arrow diagram for the Corsica River estuary of (top) transport and exchange coefficients calculated by the 2-box-model for the Corsica River estuary, and the calculated physical transport during the period of May to October in 2006, (left) DIN transport from May-October 2006 (units = 10^3 kg d^{-1}). Box 1 is the most upstream region of the system and receives the largest fraction the total watershed DIN load. Box 2 is connected to the Chester River, from which it receives a large fraction of its DIN load, and (right) DIP transport from May-October 2006 (units = kg d^{-1}). Box 1 receives the largest fraction the total watershed DIP load. Box 2 exports a large fraction of its DIP load to the Chester River.

4.3 Results

Box-Modeling Analysis. This analysis provided quantitative, well-constrained estimates of net hydrodynamic transport and net biogeochemical transformation of DIN and DIP averaged over distinct time and space scales.

Corsica River estuary

(1) *Net hydrodynamic exchanges of nutrients.* An important special case of this calculation is the estimate of net nutrient exchanges at the estuary mouth. Previous box-modeling and nutrient budget studies for tributary systems within the Bay have demonstrated that many of the middle and upper Bay tributaries have a net import of nutrients from the Bay through the tributary mouth. Box-modeling analyses in the Corsica River suggest that the Corsica generally imports DIN from the adjacent Chester, but exports DIP (Fig. 4-3b, 4-3c). From May-October 2006, the magnitude of the DIN input is roughly 10% of total watershed DIN inputs to the Corsica, but ~50% of total DIN inputs to the seaward region (Box 2) of the Corsica system in some months. We conclude for 2006 that although the Corsica River can import large quantities of DIN in certain months (Fig. 4-4), the watershed contributes most of the total N to this system. Consequently, it is anticipated that continued reductions in N loading from the Corsica watershed will help to improve water quality in the estuary. Further box-model analyses for 2007 will provide some indication of the inter-annual variability in Corsica-Chester nutrient exchanges.

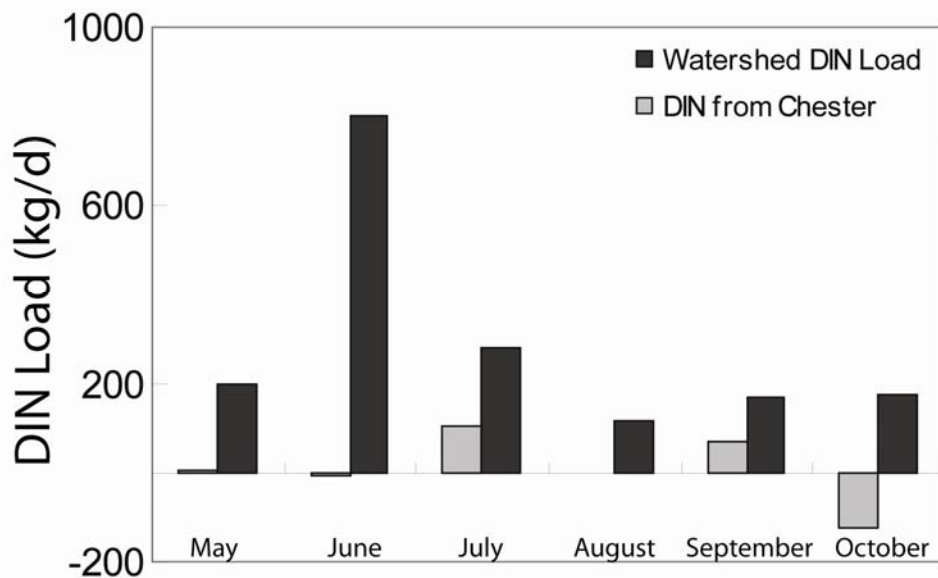


Figure 4-4: Seasonal changes in DIN loads to the estuary from the watershed and from the Chester river at the Corsica estuary mouth. Watershed DIN inputs dominate the total load to the Corsica in all months, but DIN inputs from the Chester River are largest (~50 % of watershed loads) in July and September.

(2) *The box-model analysis also computes rates of net biogeochemical fluxes of nutrients.* Thus, box-model calculations of net nutrient recycling fluxes for specific estuarine regions also provide a basis for placing individual sediment oxygen-nutrient exchanges, primary production, and

denitrification measurements into a system-wide context. The two main results of this analysis are that (a) **80%** of the DIN and **70%** of the DIP entering the upper Corsica River is removed from the water column and sequestered in this region, as evident in the computed net DIN uptake rate of $572 \mu\text{mol m}^{-2} \text{h}^{-1}$. A significant fraction of this uptake occurred in June (Fig. 4-5, 4-6), and is associated with seasonal peaks in total organic nitrogen production (Fig. 4-7).

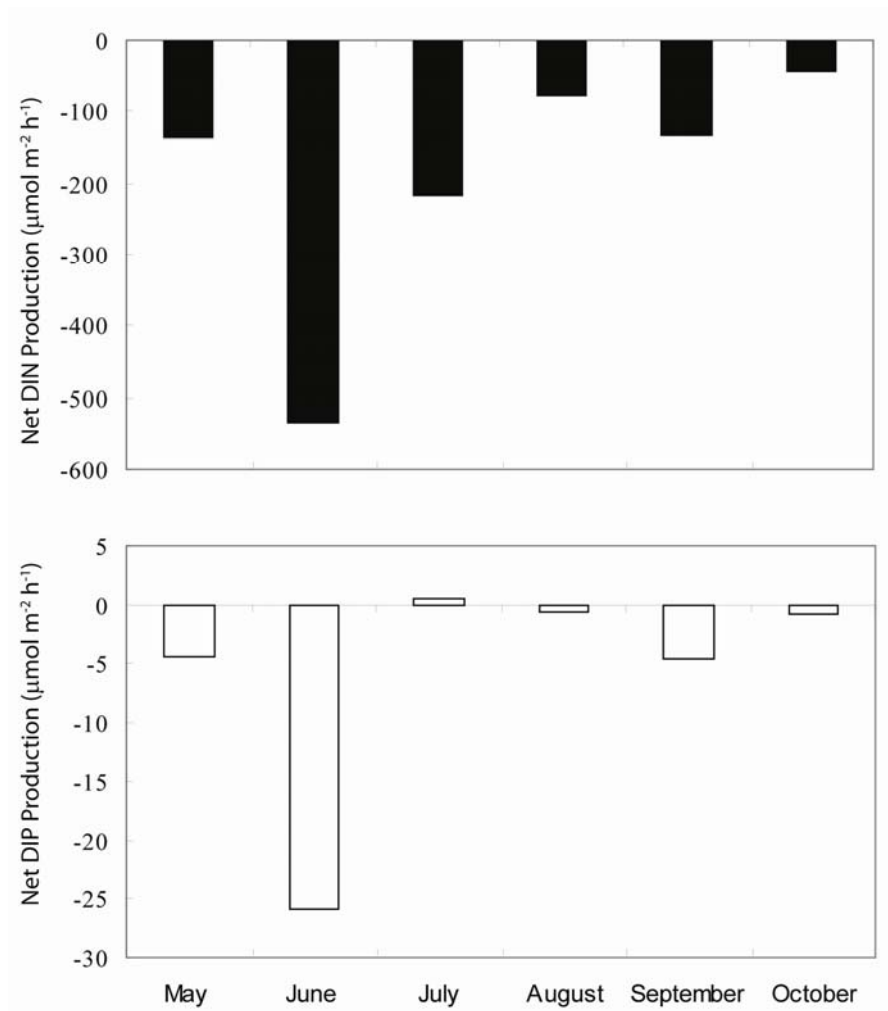


Figure 4-5: Net production rates of DIN and DIP calculated monthly from May to October for the entire Corsica River estuary in 2006. The Corsica estuary consumed DIN in all months from May to October, with peak consumption in June, while the estuary produced DIP in all months except September. The coupled nature of net DIN and DIP uptake suggest that similar processes are driving their consumption and are likely related to algal growth within the estuary.

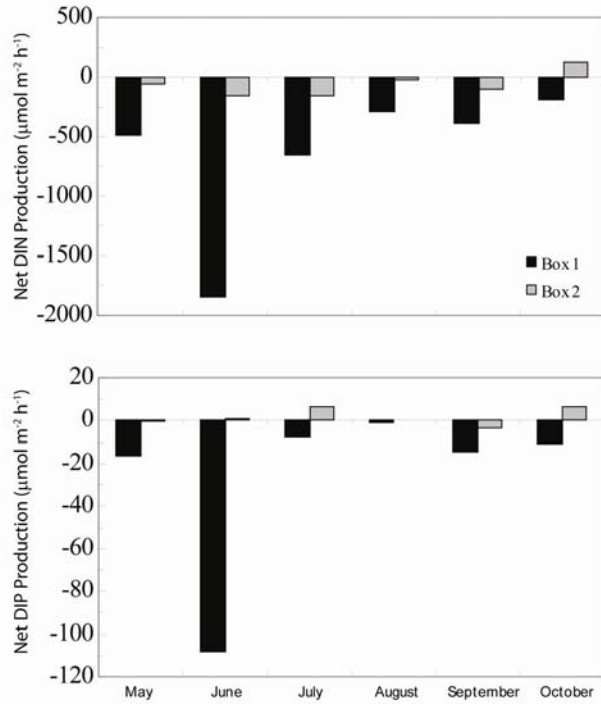


Figure 4-6: Net production rates of DIN and DIP calculated monthly from May to October for Box 1 and Box 2 in the Corsica River estuary in 2006. These data suggest that Box 1 is the dominant region of nutrient loss in the system, where algal biomass and denitrification are highest.

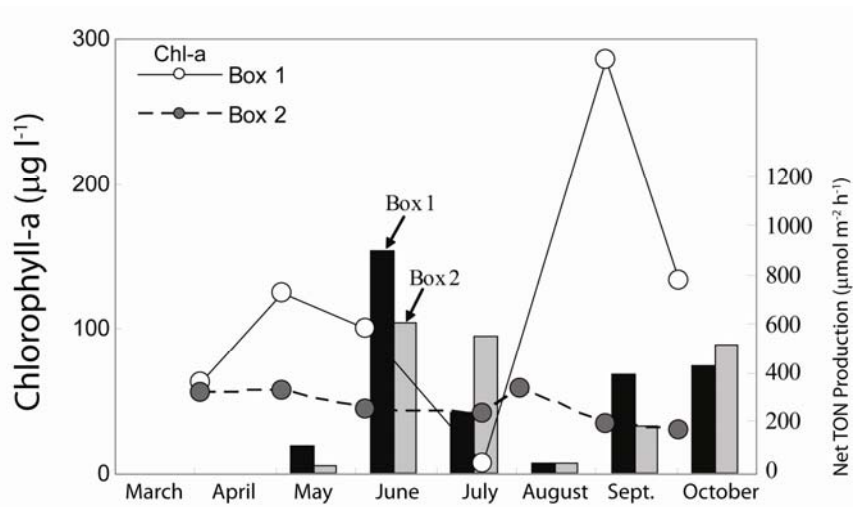


Figure 4-7: Net production rates of TON in Box 1 and Box 2 (shaded bars) calculated monthly from May to October for the Corsica River estuary in 2006 and corresponding measured chlorophyll-a concentrations (circles). The Corsica estuary produced TON in all months from May to October, with peak consumption in June, which indicates the conversion of DIN to organic nitrogen in these months.

Estimates of net ecosystem production computed from the box models exhibited consistent net autotrophic ($P > R$) and highest rates at the landward ends of the estuaries (Table 4-1). Rates in the upper region of the Corsica were extremely high, reflecting high rates of phytoplankton production and export. The location and timing of these high rates of nutrient uptake and organic matter production correspond to seasonal and regional peaks in net primary production (Boynton et al. Chapter 3), net ecosystem metabolism (Table 4-1) and high denitrification rates (200 to $>300 \mu\text{mol m}^{-2} \text{h}^{-1}$) in fringing marshes around Box 1 (Cornwell et al., Chapter 6, Table 6-2).

Table 4-1: Summary of rates of net ecosystem metabolism and net denitrification in all boxes of the Corsica and Chester River estuaries. Rates are for the May-October period for both systems.*

System	Box	Net ecosystem production ($\text{g C m}^{-2} \text{d}^{-1}$)	Net denitrification ($\mu\text{mol N m}^{-2} \text{h}^{-1}$)
Corsica River	1	0.76	215
	2	0.17	84
Chester River	1	0.18	22
	2	0.07	18
	3	0.02	7

*Note: Net ecosystem production (NEP) is equivalent to total ecosystem primary production minus community respiration, which is the net production of organic carbon in the system. NEP is computed by converting the box-model-computed net DIP consumption rate into carbon units assuming Redfield stoichiometry (C:P = 106). This computation assumes that DIP changes are driven primarily by photosynthesis and respiration and that physical/chemical processes have a minimal effect on the net DIP production rates (e.g., Gordon et al. 1996). Net denitrification is computed as the difference between net DIP (converted to equivalent N units, again assuming Redfield stoichiometry, N:P = 16) and net DIN consumption, where DIN consumption in excess of that expected from NEP is assumed to be associated with net flux of N_2 associated with denitrification minus nitrogen fixation.

Chester River estuary

The Chester River estuary consumed DIN and DIP in all 3 Boxes over the annual average (Fig. 4-8). Net nutrient consumption in the Chester River decreases toward the mouth of the estuary. Further analysis will clarify any seasonal trends which we expect will be similar to those in the Corsica River estuary. In the Chester River, over 90% of the DIN and over 85% of the DIP entering the estuary is sequestered there, with the majority of these processes taking place in Box 1. Box 3, which could directly influence the mouth of the Corsica River showed the lowest uptake of DIN and DIP. Comparisons of net DIN uptake in Box 3 of the Chester River with net DIN exchange between Chester Box 3 and Corsica Box 2 indicate that 15-20% of net DIN loss in Chester Box 3 is due to export to the Corsica. Future analysis of monthly rates is necessary to confirm seasonal export from the Chester River to the Corsica River.

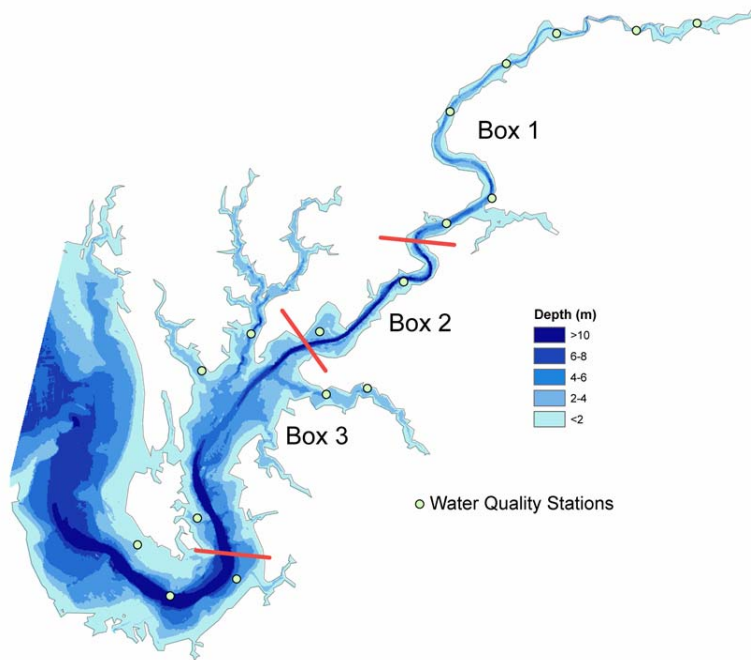


Figure 4-8: Map of the Chester River estuary, including box model boundaries and water quality monitoring stations for 2006.

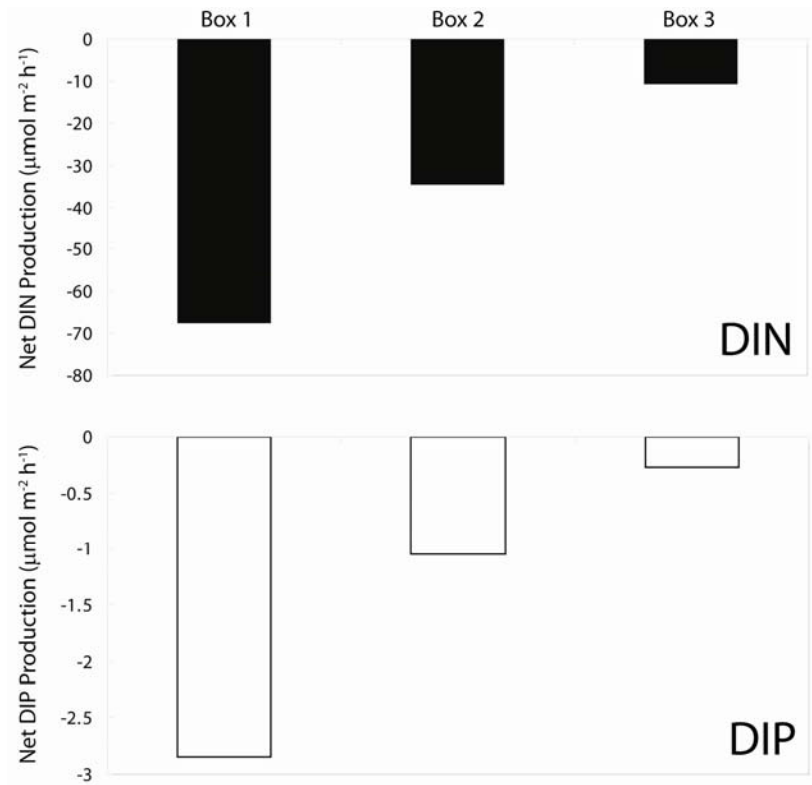


Figure 4-9: Annual net production rates of DIN and DIP calculated for 3 boxes in the Chester River estuary in 2006. The coupled nature of net DIN and DIP uptake suggest that similar processes are driving their consumption and are related to algal growth within the estuary.

4.4 Summary and Implications for Management

The box-modeling analysis provides a relatively straight-forward method for integrating water quality monitoring data and developing empirical calculations of nutrient cycling, nutrient transport (and exchange), and nutrient assimilation by the integrated estuarine system. These data will help reveal how nutrient input reductions in the watershed translate into nutrient transport reductions within the estuary.

Net nutrient exchange rates between the Chester River and Corsica also reveal the Chester River as an important DIN source to the lower Corsica River in certain months of 2006, a fact which must be considered when planning regional scale nutrient reduction strategies (Figure 4-9). The predominance of watershed N inputs indicates that reducing these loads, which are primarily from diffuse sources and enter the Corsica in stream flow and runoff, should be a high priority. High rates of DIN and DIP loss in the upper Corsica River suggest that phytoplankton productivity and denitrification in this region (on an aerial basis) are substantial in comparison to other Chesapeake Bay tributaries. It appears that the combination of high nutrient loading rates, moderate flushing, and a high degree of sediment-water column interaction promote such high productivity. Modest increases in light availability may permit a feedback cycle that allows accelerated water quality improvements.

4.5 References

- Gordon, D.C., Jr, Boudreau, P.R., Mann, K.H., Ong, J.-E., Silvert, W.L., Smith, S.V., Wattayakorn, G., Wulff, F., Yanagi, T.** 1996. LOICZ biogeochemical modeling guidelines. LOICZ Reports and Studies, LOICZ, Texel, The Netherlands, No.5.
- Hagy, J.D., Sanford, L.P., Boynton, W.R.** 2000. Estimation of net physical transport and hydraulic residence times for a coastal plain estuary using box models. *Estuaries* 23:328-340.
- Maryland Department of the Environment.** 2000a. Total maximum daily loads of nitrogen and phosphorus for Corsica River. p.1-24.
- Maryland Department of the Environment.** 2000b. Total maximum daily loads of nitrogen and phosphorus for Corsica River. Appendix A. p.A1-A37.
- Maryland Department of Natural Resources.** 2003. Report on nutrient synoptic surveys in the Corsica River watershed, Queen Annes County, Maryland, April 2003 as part of the Watershed Restoration Action Strategy. MD DNR Watershed Services. p.1-17.
- Officer, C.B.** 1980. Box models revisited. In: Hamilton P, Macdonald RB (eds) *Estuarine and wetland processes*. Plenum Press, New York, p 65-114.
- Pritchard, D.W.** 1969. Dispersion and flushing of pollutants in estuaries. *American Society of Civil Engineers Journal of Hydraulics Division* 95(HYI):115-124.

5.0 Analyses of Water Quality in the Corsica River Estuarine System: Nutrient Limitation and Factors Affecting Light Attenuation

W. Michael Kemp, Jeremy M. Testa and Maureen Brooks

5.1	Introduction and Implications for Management	5-1
5.2	Methods	5-1
5.3	Results, Discussion and Implications	5-2

5.1 Introduction and Implications for Management

Water quality conditions, including turbidity, phytoplankton abundance and dissolved O₂, are among the primary interests motivating watershed management in the Chesapeake Bay and its tributaries (e.g., Corsica River). Although water quality is a broad term that encompasses diverse aspects of estuarine ecology and biogeochemistry, we focus this analysis of the Corsica River on nutrient limitation and light attenuation. Understanding nutrient limitation is essential for identifying which nutrient(s) (e.g., nitrogen, phosphorus) should be the focus of watershed load reduction strategies. Understanding the factors affecting light attenuation in the Corsica will allow us to (1) determine if reducing a specific variable (TSS, chlorophyll) will greatly increase water clarity and (2) to quantify how improvements in water clarity will promote feedbacks that enhance benthic primary productivity and nutrient retention in sediments.

5.2 Methods

Estuarine Water Quality Data. We obtained existing, in-estuary water quality data from several stations during April to October, 2006, including data collected during CONMON and DATAFLOW field efforts (MD DNR) (Fig. 5-1). Water quality data included dissolved inorganic nitrogen (DIN = NO₂⁻ + NO₃⁻ + NH₄⁺), dissolved inorganic phosphorus (DIP = PO₄³⁻), total nitrogen (TN), total phosphorus (TP), total organic nitrogen (TON = TN-DIN), chlorophyll-*a* (Chl-*a*), Secchi depth (Z_{sd}), and total suspended solids (TSS).

Light Attenuation Analyses. We estimated several additional variables relevant to light conditions. (1) The light attenuation coefficient (k_d) was computed via the following equation: $k_d = 1.6/Z_{sd}$ (2) The depth of 1% of surface light (Z_{1%} = maximum depth where phytoplankton can achieve net growth) was computed via a derivation of an expression to compute light availability as a function of depth and light attenuation:

$$I_z = I_0 e^{-k_d Z}$$

where I_z is the light available at each depth (Z) and I₀ is the light available at the waters surface. The following rearrangements of this equation yield a formulation to convert the light attenuation coefficient (k_d) into Z_{1%}.

(a) $I_z/I_0 = e^{-k_d Z}$

(b) $\ln(I_z/I_0) = -k_d Z$

(c) $\ln(0.01) = -k_d Z$ (1% surface light)

(d) $-4.6 = -k_d Z$

(e) $Z_{1\%} = 4.6/k_d$

Lastly, chlorophyll-*a* concentrations were converted into concentrations of phytoplankton-carbon (for quantitative comparison with TSS concentrations) using the following equations:

(a) $\text{Chl-a} * C:\text{Chl-a} = C_{\text{phyt}}$

(b) $\text{Cdw}_{\text{phyt}} = C_{\text{phyt}} * 2$

Where C:Chl-a is the carbon to chlorophyll-a ratio (50), C_{phyt} is phytoplankton carbon (mg l^{-1}) and Cdw_{phyt} is the dry weight of phytoplankton carbon (mg l^{-1}).

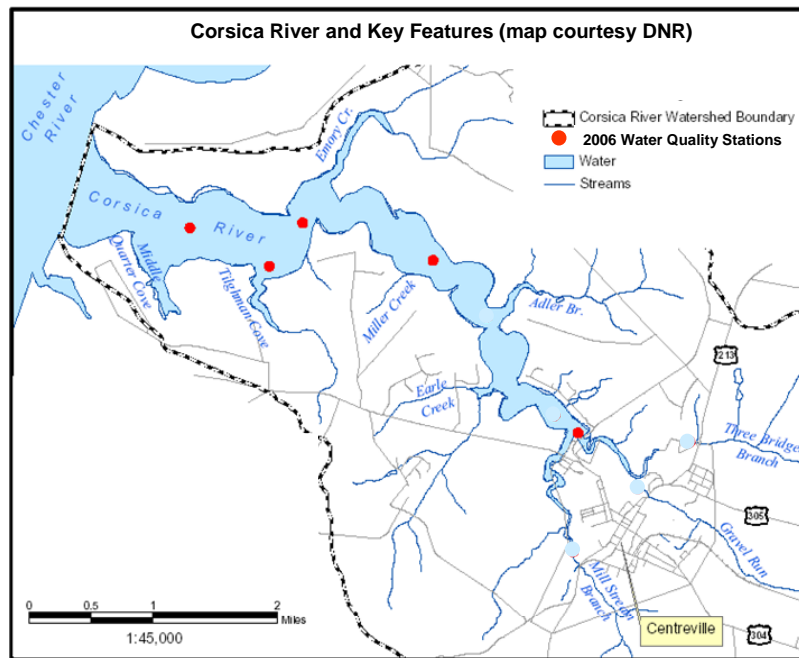


Figure 5-1: Map of Corsica River estuary, including box model boundaries, the Centreville wastewater treatments plant (WWTP), water quality monitoring stations for 1997 (red circles) and 2006 (yellow circles)

5.3 Results, Discussion and Implications

Corsica River estuary

(1) *Nutrient limitation.* Seasonal DIN and DIP concentrations in the upper and lower Corsica indicate that DIN was potentially more limiting for phytoplankton growth ($\text{DIN:DIP} < 16$) in the estuary from July to October, but that DIP was more limiting for growth in April to June in the upper estuary and in April in the lower estuary (Fig. 5-2). Both DIN and DIP concentrations were, however, sufficiently high that phytoplankton may have been more limited by light in many instances. The fact that Chl-*a* levels were relatively high both in “P-limited” spring months and “N-limited” summer months, both N and P should be targeted for watershed load reductions.

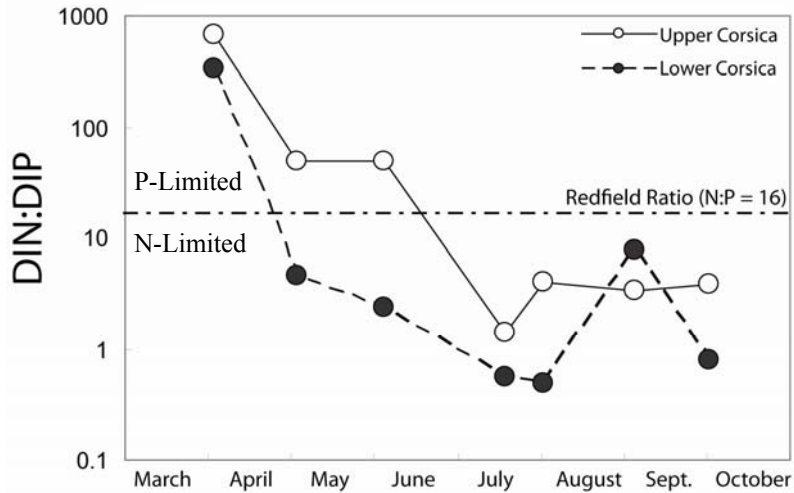
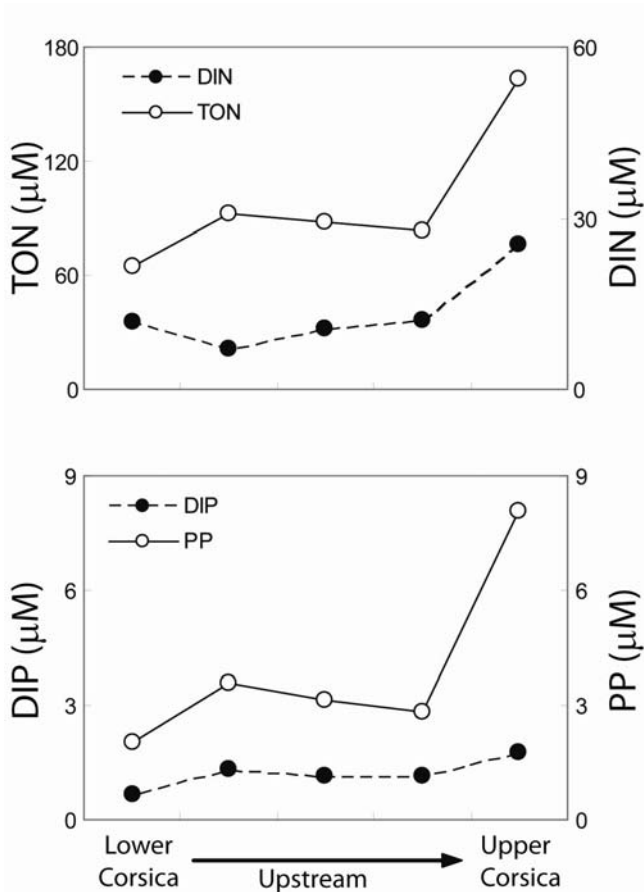


Figure 5-2: Seasonal variation in the DIN:DIP ratio in the upper and lower Corsica estuary during 2006. Note that the Y-axis is a log scale and that the Redfield Ratio of 16 indicates a switch from N-limited algal production (DIN:DIP <16) to P-limited production (DIN:DIP > 16).



(2) *Particulate-Dissolved Nutrient Interactions.* Axial distributions of inorganic and organic forms of N and P indicate that DIN interacts with the particulate organic pool differently than DIP. With the exception of the most upper reaches of the Corsica in 2006, DIN was inversely correlated with TON along the estuarine axis (Fig. 5-3), indicating a shift from DIN to TON that is consistent with DIN incorporation into organic N via algal growth. Conversely, DIP was positively correlated with PP (particulate phosphorus) along the estuarine axis (Fig. 5-3), suggesting that these forms of P have similar sources and sinks, or that DIP supply was regulated by sorption-desorption reactions on sediment or water-column particles.

Figure 5-3: Axial distribution of particulate and dissolved inorganic forms of nitrogen (top panel) and phosphorus (bottom panel). PP is particulate phosphorus (organic and inorganic forms) while TON is total organic nitrogen and is equivalent to particulate and dissolved organic nitrogen.

(3) *Factors Regulating light attenuation.* Correlations between Secchi depth and both Chl-a and TSS suggests that TSS dominates light attenuation in the Corsica river estuary, as TSS is negatively correlated with Secchi depth (Fig. 5-4). However, because Chl-a and TSS may interact when algal exudates flocculate inorganic materials together, TSS concentrations may represent the combined light attenuation of algal and inorganic particles. Thus, computations of phytoplankton carbon ($Cd_{w_{\text{phyt}}}$) provide a specific measure of phytoplankton contributions to TSS. Our calculations indicate that $Cd_{w_{\text{phyt}}}$ generally represents 10-30% of the TSS pool in the upper and lower Corsica, while in certain months (Sept. and Oct.) $Cd_{w_{\text{phyt}}}$ can be as much as 50% of TSS (Fig. 5-5). We therefore conclude that both phytoplankton and inorganic particles contribute significantly to light attenuation, and that reductions in Chl-a via nutrient load reductions should result in increased water clarity in the Corsica estuary.

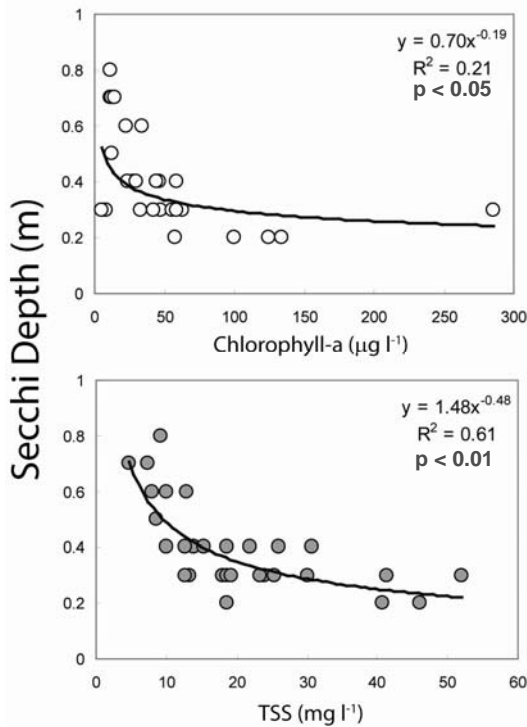


Figure 5-4: Correlations between Secchi depth and Chl-a (top panel) and TSS (bottom panel) for all stations and sampling dates in the Corsica estuary, 2006.

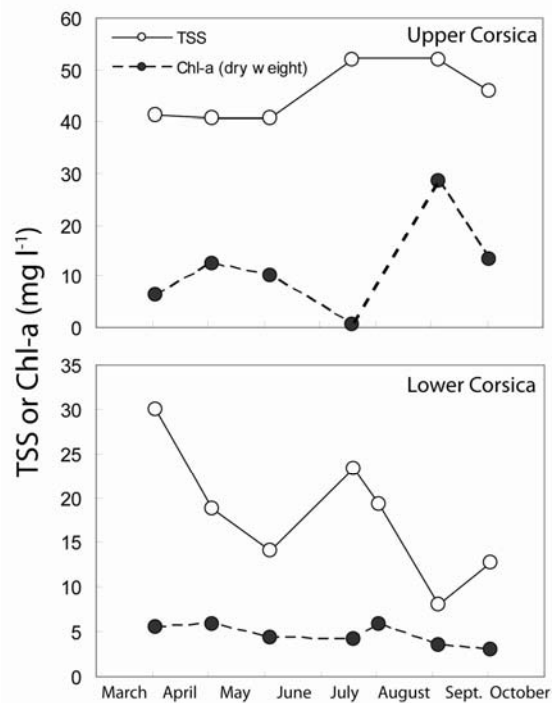


Figure 5-5: Seasonal variation in TSS and $Cd_{w_{\text{phyt}}}$ in the upper (top panel) and lower (bottom panel) Corsica estuary for 2006. Data indicate the relative contribution of phytoplankton mass to total suspended material in the estuary over a year.

(4) *Potential Benefits of Improved Water Clarity.* Axial distributions of mean water depth and depth of 1% surface light ($Z_{1\%}$) indicate that the far upper Corsica is the only region where light may reach estuarine sediments (Fig. 5-6). Because photic sediments support submerged aquatic vegetation and benthic algae, nutrient uptake by these benthic plants reduces nutrient availability for water column algae (who reduce water clarity). Sediment releases of N and P are also reduced in sediments colonized by plants, thus providing a sediment sink for nutrients that causes a feedback where increased light to the sediments increases sediment nutrient uptake, which reduces

nutrients available for water column algal growth and allows even more light available to sediments. A hypothetical increase in current Secchi depths by 0.3 m would allow light to reach 25% more of the sediment surface area in the upper Corsica and >50% of the total Corsica area (Fig. 5-7).

Figure 5-6: Axial distributions of the mean depth of the Corsica estuary (filled circles) and the depth of 1% light ($Z_{1\%}$) for two months in 2006. Note that there is sufficient light reaching the sediment surface to support benthic algal growth when mean $Z \leq Z_{1\%}$, and this occurred only in the most upper reaches of the estuary

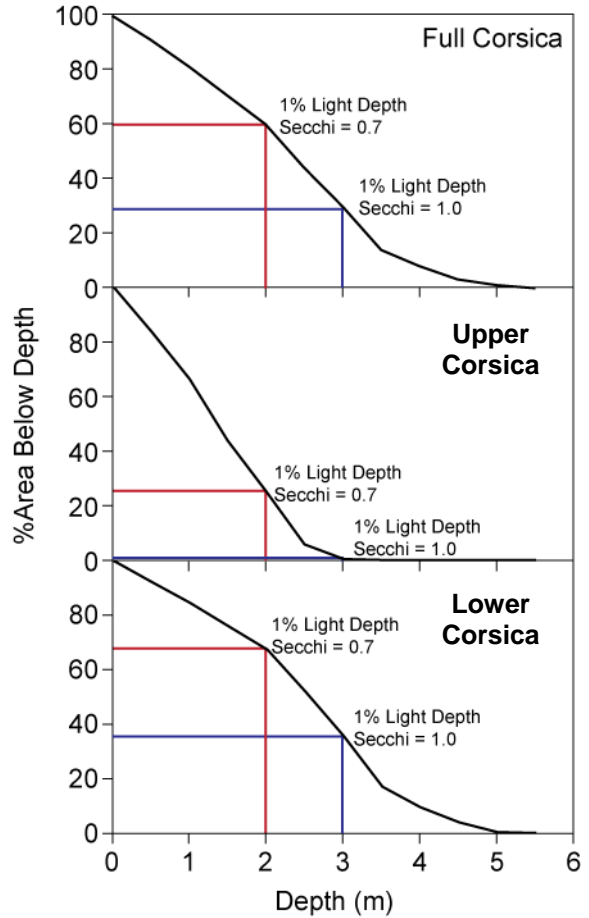
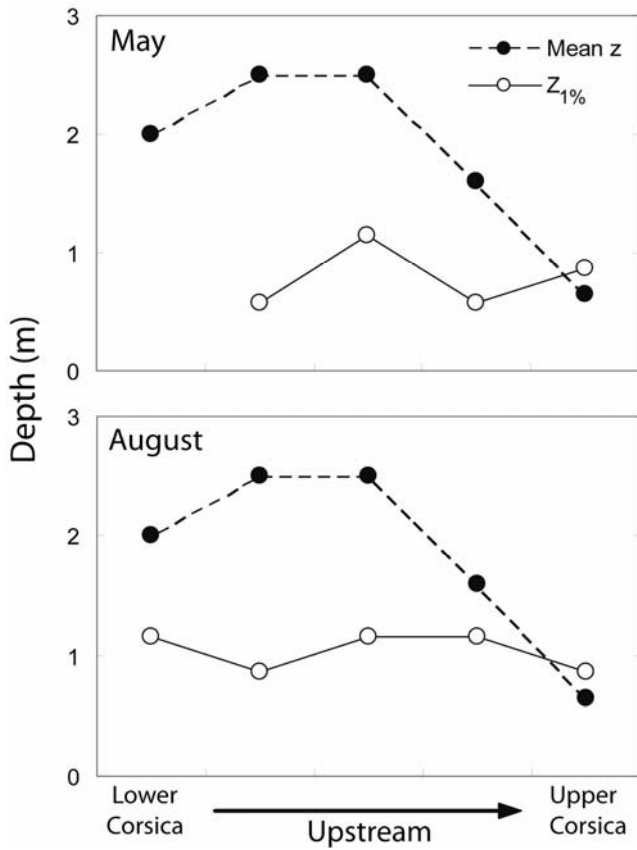


Figure 5-7: Plots of the % of the surface area below a given depth for the Corsica River (top panel), the upper region of the Corsica (middle panel), and the lower region (bottom panel). Cross lines indicate the percentage of the Corsica surface area that will have 1% of surface light available at the sediment surface at a given Secchi depth. Note that a large increase in the area of photic sediments (receiving >1% surface light) would result from a relatively small increase in water clarity as indicated by Secchi depth (increasing from 0.7 to 1.0 m).

6.0 Nutrient Balance in Corsica River Sediments: Improved Estimates of Nutrient Burial and Denitrification

Jeffery Cornwell, Cindy Palinkas and Mike Owens

6.1 Introduction	6-1
6.2 Denitrification	6-1
6.3 2007 Sedimentation Study	6-13

6.1 INTRODUCTION

The work described here is an extension of our 2006 studies (Boynton et al. 2007). In 2006 we measured denitrification on 6 occasions at 6 sites, two of which were shallow and illuminated. Based on our field observations and the modeling analysis of Michael Kemp and Jeremy Testa, there were two main questions that remain regarding “sinks” for nitrogen and phosphorus:

1. Is there an unmeasured, upstream sink for nitrogen? The model output suggested that the main N sink was at the head of the estuary. We observed little water column nitrate in the main part of the Corsica River, so most denitrification was driven by coupled nitrification-denitrification.
2. What are the rates of sediment and nutrient burial in the Corsica River? In 2006, Sea Grant REU intern Collette LeBeau carried out sediment dating on two cores with Cindy Palinkas; in addition, Rebecca Halvorson, a Sea Grant REU with Jeffrey Cornwell, carried out chemical analyses on these same cores. In the Chesapeake main stem, Boynton et al. (1995) have suggested that N burial rates are similar to denitrification rates. Thus, constraining the N budget requires sufficient N burial information.

6.2 DENITRIFICATION

6.2.1 Methods

We chose 4 sites in the marshes upstream of the Corsica “estuary” (Table 6-1, Figure 6-1, Figure 6-2). Because of the drought and consequent low flow conditions in the summer of 2007, we waited as long as possible in the year to collect the cores in the hope of having a largely low salinity marsh ecosystem. Nevertheless we ended up sampling during the drought and our sampling sites were chosen on the basis of low salinity. To accomplish this, we ran our small aluminum skiff upstream as far as we could go; to get up to sites 2007-3 and 2007-4, we had to haul the skiff over several obstructions. We used a combination of hand insertion of core liners and pole coring to sample sediments. At each “site”, we collected two marsh cores and two subtidal cores. The marsh cores had creek water added to them at the time of collection. We also collected 20 L carboys of water for replacement water for our experiments. Salinity, temperature and dissolved oxygen were measured in creek water at each site using a YSI model 85.

The general approach to measuring denitrification is detailed in Kana et al. (1998) and Kana et al. (2006). We used changes in the N₂:Ar ratio during incubation to estimate N₂ fluxes (Ar is inert).

Triplicate cores were incubated. Sediment was subsampled using 10 cm diameter x 30 cm tall acrylic cylinders. Approx. 15 cm of sediment was contained in each cylinder. Sediment cores were pre-incubated for 16 hours in a fully submersed condition within a donut-shaped bath with top caps off and with the bath water being gently bubbled. Bath water consisted of previously collected bottom water. Top caps were inserted at time 0. Stirring of the isolated headspace above each core was carried out by a suspended magnet with rotation by a magnetic turntable in the center of the bath housing. Subsamples were collected at 1.5-2h intervals for solute and dissolved gas measurements. Four time-points were collected during each incubation. Make-up water was automatically dispensed into the headspace. Samples for gas analysis were collected in 7mL ground glass stoppered tubes, forced by gravity flow from the ambient water. Mercuric chloride (0.1% v/v saturated solution) was added as a preservative and the sample tubes were stored underwater at ambient or subambient temperatures until measurement using a mass spectrometer. Nutrient samples were collected in 20mL syringes, filtered (0.2 μm), and frozen for subsequent analysis.

We measured the ratio of $\text{N}_2:\text{Ar}$ using a quadrupole mass spectrometer, following Kana and Weiss (2002). Typical precision of the gas ratio is $< 0.03\%$. We analyzed time courses for soluble reactive phosphorus (SRP or “orthophosphate”), ammonium and nitrate following Parsons et al. 1984. Sediment chlorophyll a was measured fluorimetrically.

6.2.2 Results

Overall, we had good agreement between the two replicate cores from each marsh and subtidal site. Table 6-2 presents all of the sediment-water exchange rates from the Corsica River marshes. In several cases for ammonium and nitrate, we had non-interpretable results from our time courses. The key features of the flux data are presented here:

- Marsh core rates of oxygen uptake were somewhat lower than the rates observed in estuarine sub-tidal sediments in our 2006 program (Figure 6-3). Replication was excellent and the overall means were well-constrained.
- Denitrification replication was better than we generally observe in most environments (Figure 6-4), with rates averaging a very high $264 \mu\text{mol N}_2\text{-N m}^{-2} \text{h}^{-1}$. These are exceedingly high rates driven by high concentrations of nitrate (Sites 1 and 2 had $197 \mu\text{mol L}^{-1}$ nitrate incubation water, sites 3 and 4 had $173 \mu\text{mol L}^{-1}$). Marsh denitrification rates were > 3 times higher than the 2006 estuarine rates, with relatively little overlap between individual measurements in each data set (Figure 6-5).
- Ammonium fluxes were generally above $100 \mu\text{mol m}^{-2} \text{h}^{-1}$ (Figure 6-6), with no systematic difference between marsh and subtidal cores at each site. Average flux rates in the marsh environments were $198 \mu\text{mol m}^{-2} \text{h}^{-1}$, about 60% of the average 2006 estuarine rate.
- Nitrate fluxes were mostly directed into the sediment (Figure 6-7), with an average uptake of $-205 \mu\text{mol m}^{-2} \text{h}^{-1}$. The sensitivity of the flux measurement is strongly affected by the high nitrate concentrations, with a lower signal to noise ratio. It is clear that a substantial proportion of the nitrate needed for denitrification is supplied by nitrate uptake.
- Although not a main emphasis of this study, the flux of soluble reactive phosphorus was measured at all sites. Rates were generally low and directed out of the sediment, averaging $4 \mu\text{mol m}^{-2} \text{h}^{-1}$, about 20% of the 2006 estuarine rates.

Overall, the 2007 marsh rates were well-constrained, with only a moderate amount of variability between sites and between marsh and subtidal environments.

6.2.3 Discussion

The key flux data for understanding nutrient sinks in the Corsica River marshes was the measurement of denitrification. From a measurement perspective, this program went better than expected, with excellent replication and similar numbers at most sites. The rates of denitrification were somewhat higher than observed in Potomac marshes (average = $147 \mu\text{mol m}^{-2} \text{h}^{-1}$; Hopfensperger et al. accepted) and our previous work in the Patuxent River (generally $< 60 \mu\text{mol m}^{-2} \text{h}^{-1}$; Merrill and Cornwell 2000).

We examined the flux data set for inter-relationships (Figure 6-9), emphasizing the influence of oxygen flux on N and P flux rates. The only relationship that was significant ($P < 0.05$) was that between oxygen and ammonium fluxes, a relationship often observed in fully aerobic estuarine sediments.

We believe that the general question about marsh denitrification has been addressed well, albeit with a limited temporal and spatial sampling. Estimating the overall importance of marshes to net nutrient balance requires consideration of:

- Water residence time. When we sampled during drought, we were at a base-flow condition, with nitrate-rich groundwater likely the main freshwater input to the creeks upstream of the marsh. Under these circumstances, N retention/denitrification would have a large proportional impact on N inputs.
- Seasonality. We sampled under relatively warm conditions when marsh macrophytes were long past their peak. We did not carry out dark/light experiments because of high turbidity and a presumed high shading by marsh plants. Benthic microalgae may have an important role in the cycling of N during some seasons.
- Spatial variability. We emphasized freshwater conditions, we have little knowledge of how changing salinity and upstream/downstream location may influence denitrification.
- To quantify the effects of temperature, salinity, water residence time, seasonally-varying nutrient inputs, more sample locations and times would be required. Currently there is little guidance from other Chesapeake Bay studies.

Despite the caveats, it is clear from this study that these marsh environments are poised to intercept dissolved nitrogen before it reaches the mid-estuary. Although not measured, sedimentation of N and P in the marsh may also be an important water quality benefit (Merrill and Cornwell 2000). In the Patuxent River, extensive tidal marshes play a key role in attenuating N inputs to the estuary (Boynton et al. accepted). In the Corsica River, tidal marshes likely play a similar role, and this study confirms the potential for a large N sink in the upper estuary.

The Corsica marshes were also a potential tertiary treatment for point sources in the past, with decades of effluent entering the marshes. Potential interesting studies for the future would include looking at the time course of N, P and metals retention in the marshes using dated cores, and a more thorough examination of marsh denitrification and nutrient burial. This would become particularly important if marsh restoration or creation was considered as a management option.

6.2.4 Denitrification Section Tables and Figures

Table 6-1. Corsica River marsh station codes and grid locations (NAD 83). Samples were collected October 10, 2007.

Station	Latitude N	Longitude W	Salinity	T (°C)	O ₂ mg L ⁻¹
2007-1	39.04341	-76.07432	0.2	22.5	2.50
2007-2	39.04662	-76.07464	1.3	23.0	1.57
2007-3	39.05367	-76.05955	0.2	21.6	1.48
2007-4	39.05225	-76.06253	3.1	24.8	3.08

Table 6-2. Sediment-water exchange rates for Corsica marsh environments. Cores were collected on October 10, 2007 and the flux experiments run on October 11, 2007 at a temperature of 22.1°C. We use n.s. to indicate a non-significant flux (i.e. a non-interpretable time course).

Site		O ₂	O ₂ ave	N ₂ -N	N ₂ -N ave	SRP	SRP ave	NH ₄ ⁺	NH ₄ ⁺ ave	NO ₃ ⁻	NO ₃ ⁻ ave
		$\mu\text{mol m}^{-2} \text{h}^{-1}$									
1 Subtidal	A	-1488	-1500	367	366	17.4	12.7	353	354	-390	-390
	B	-1512		365		8.0		355		n.s.	
1 Marsh	C	-681	-683	313	331	7.6	6.2	102	91	-177	98
	D	-685		349		4.9		81		374	
2 Subtidal	A	-694	-787	329	335	0.0	0.5	222	222	-626	-421
	B	-879		340		1.0		n.s.		-216	
2 Marsh	C	-946	-1009	278	295	1.4	1.9	306	306	-159	-159
	D	-1073		312		2.4		n.s.		n.s.	
3 Subtidal	A	-570	-700	193	184	-2.7	-1.2	184	160	-577	-320
	B	-830		175		0.3		136		-63	
3 Marsh	C	-754	-1016	171	230	-6.4	0.8	123	185	-169	-136
	D	-1277		289		8.0		248		-103	
4 Subtidal	A	-559	-672	208	209	8.5	9.4	101	173	-74	-99
	B	-785		209		10.3		245		-125	
4 Marsh	C	-772	-686	95	163	2.1	5.0	112	95	-256	-212
	D	-600		231		7.9		78		-168	

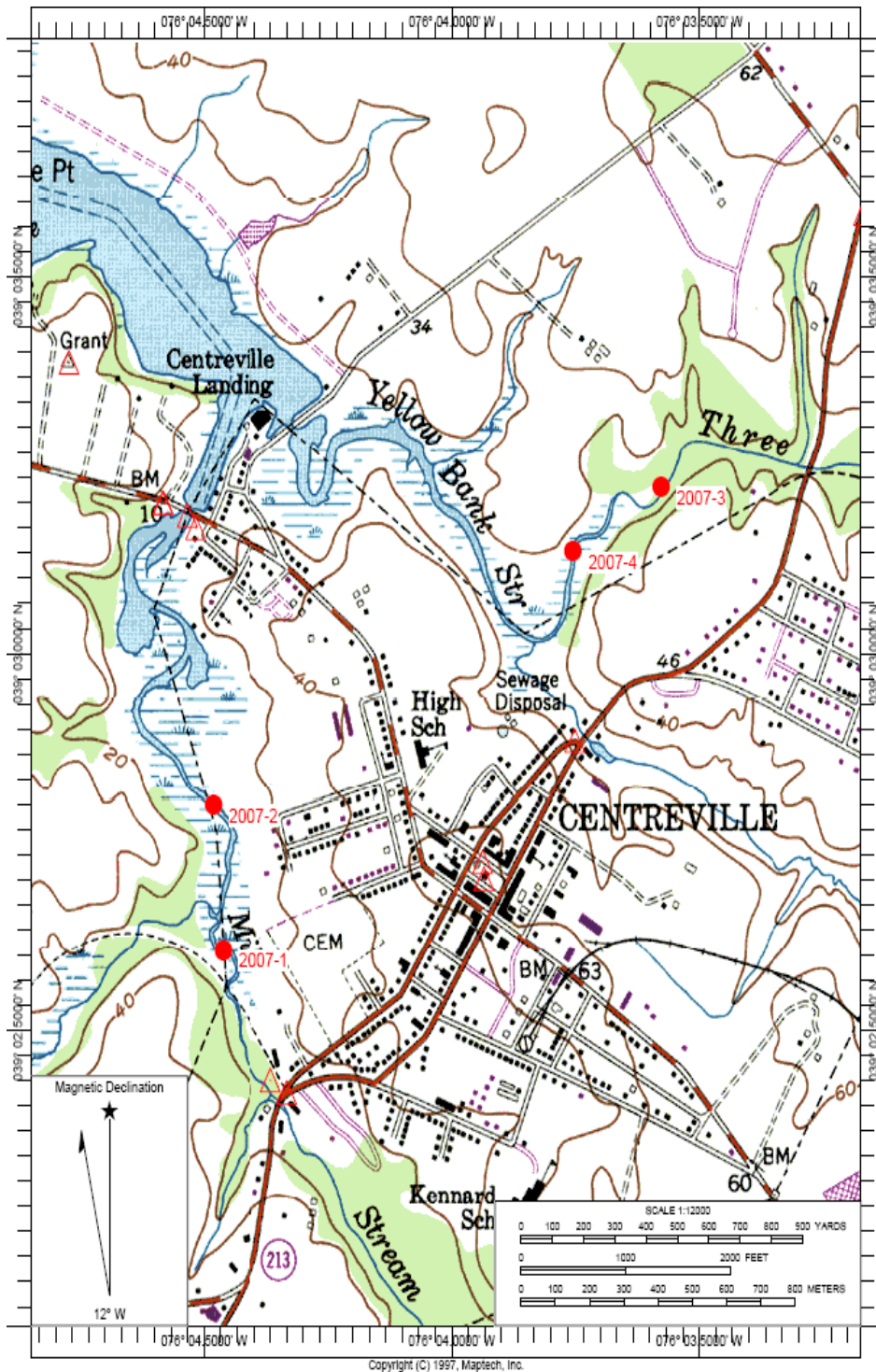


Figure 6-1. Corsica River marsh sampling locations. One pair of marsh cores and one pair of subtidal cores were collected at each of the 4 sites on October 10, 2007.



Figure 6-2. Photographs of the 4 sampling sites. All of the sites were tidal, with only 2007-3 having substantial tree growth adjacent to the marshland. The sample date was October 10, 2007.

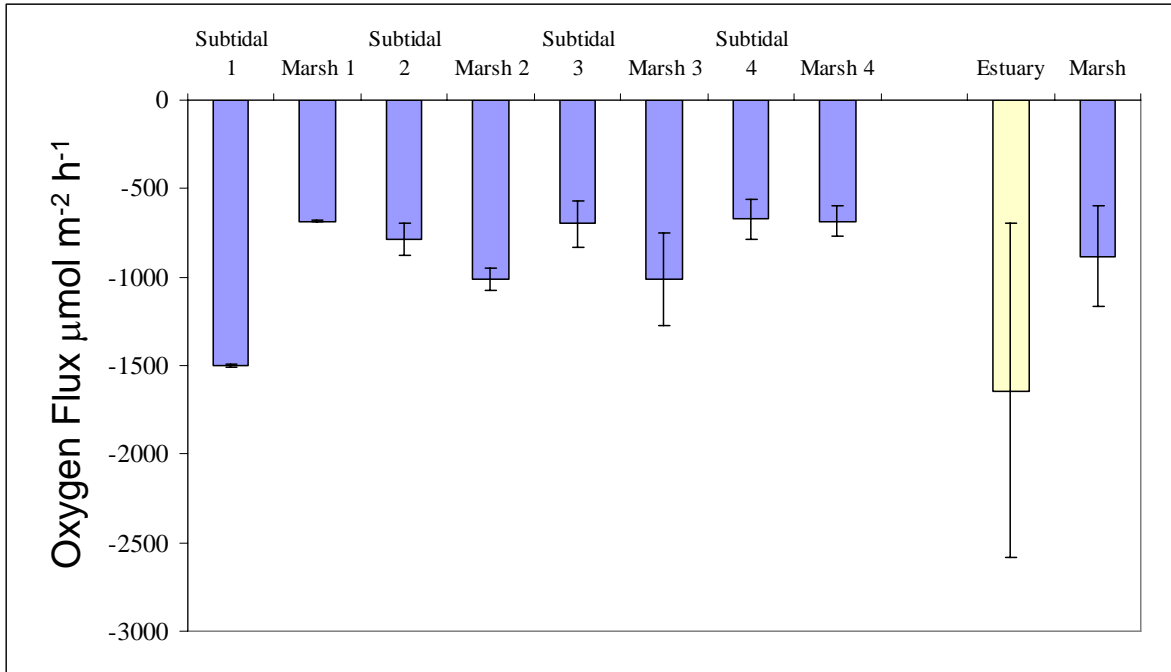


Figure 6-3. Sediment-water exchange of oxygen. Negative rates indicate flux of oxygen into the sediment. The error bars indicate the range of difference between duplicate cores. The bars on the right are the mean of the 2006 estuarine sediment flux data and the 2007 marsh flux data, error bars are one standard deviation.

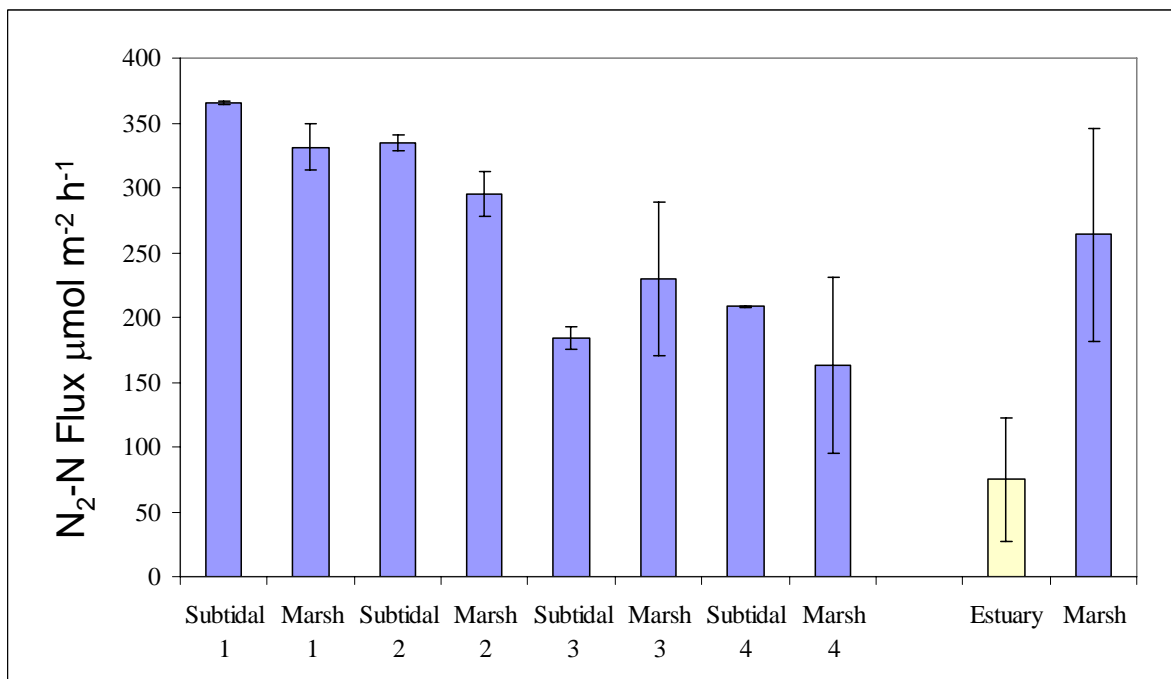


Figure 6-4. Sediment-water exchange of N₂-N. Positive rates indicate flux of N₂-N out of the sediment. The error bars indicate the range of difference between duplicate cores. The bars on the right are the mean of the 2006 estuarine sediment flux data and the 2007 marsh flux data, error bars are one standard deviation.

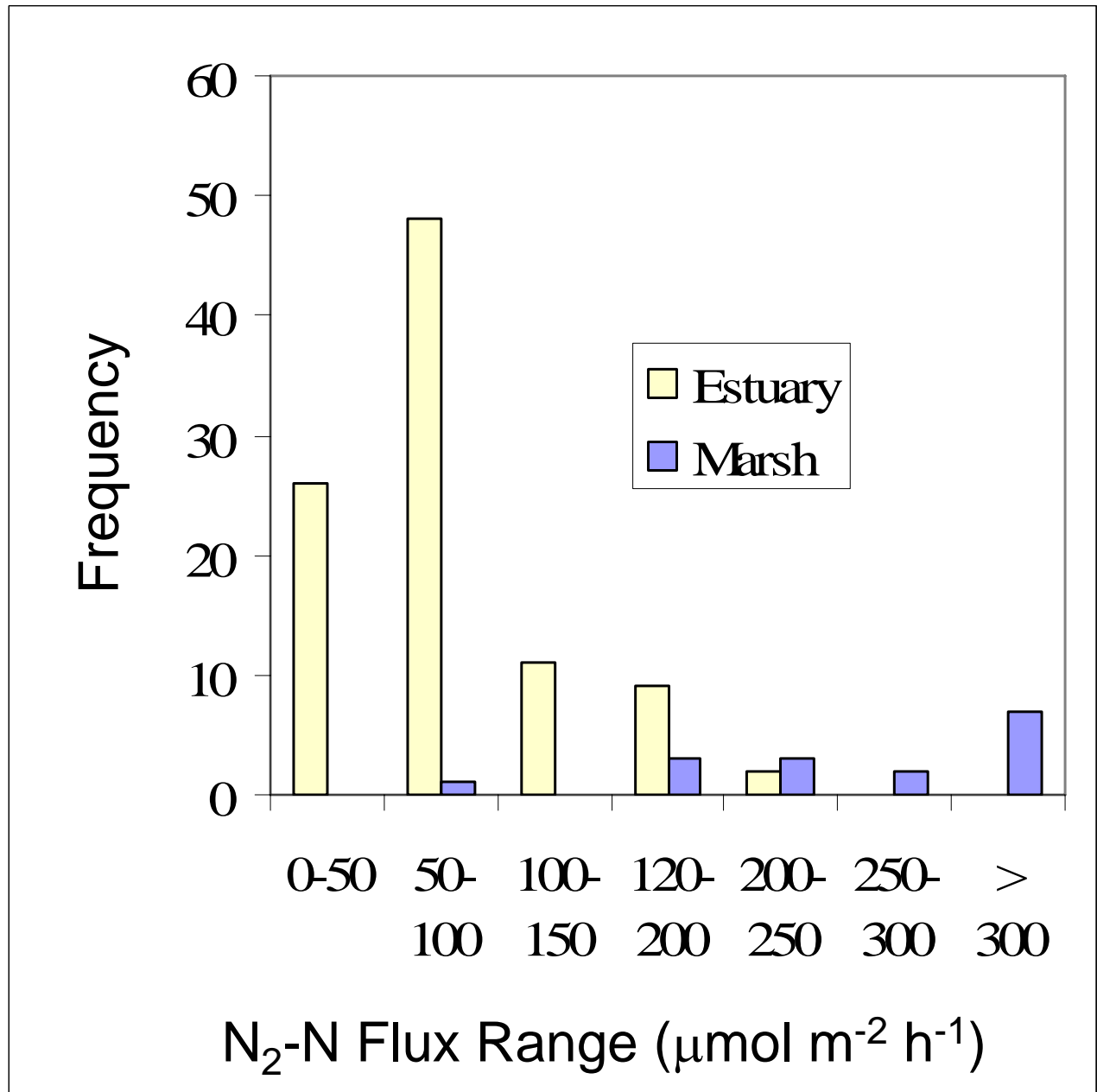


Figure 6-5. Histogram of estuary and marsh denitrification rates. Individual cores are used for the frequency (Site N = 2), with 6 sites in each environment.

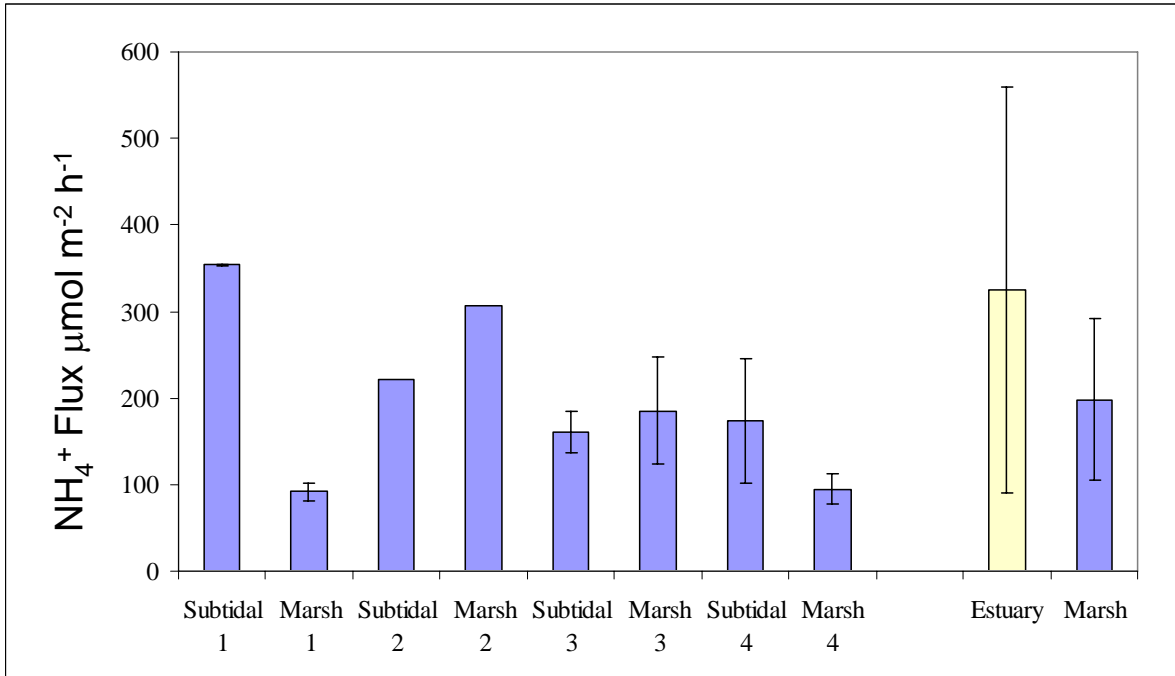


Figure 6-6. Sediment-water exchange of NH₄⁺. Positive rates indicate flux of ammonium out of the sediment. The error bars indicate the range of difference between duplicate cores. The bars on the right are the mean of the 2006 estuarine sediment flux data and the 2007 marsh flux data, error bars are one standard deviation.

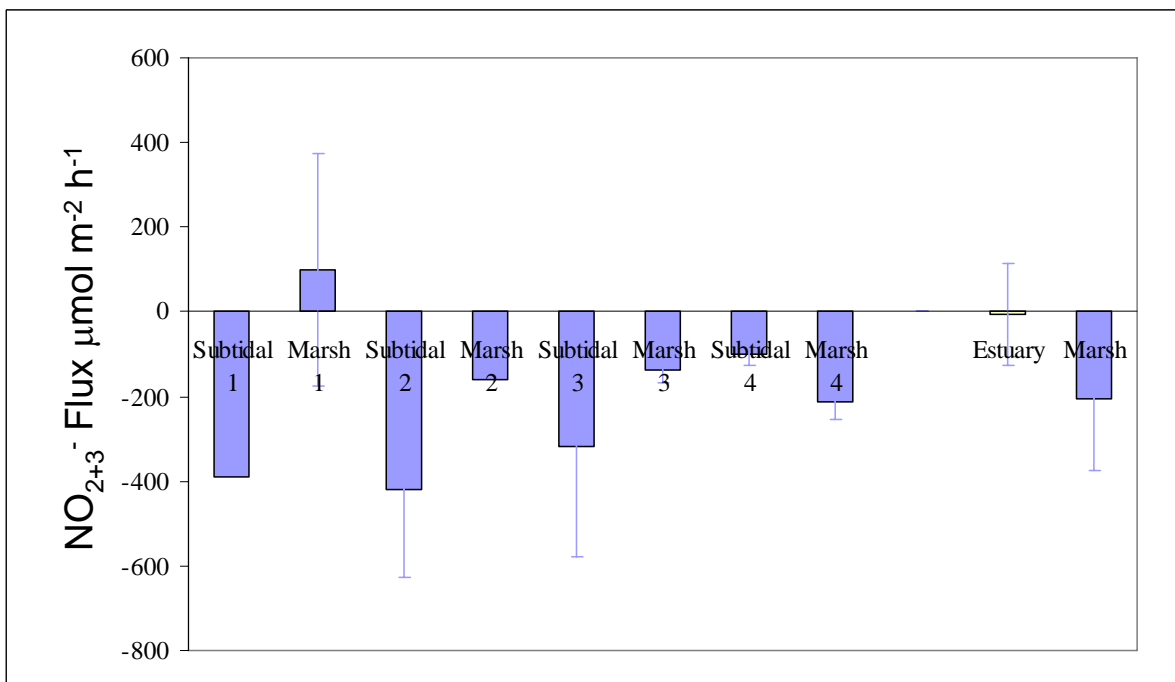


Figure 6-7. Sediment-water exchange of NO₂₊₃⁻. Positive rates indicate flux of oxygen out of the sediment, negative rates indicate flux into the sediment. The error bars indicate the range of difference between duplicate cores. The bars on the right are the mean of the 2006 estuarine sediment flux data and the 2007 marsh flux data, error bars are one standard deviation.

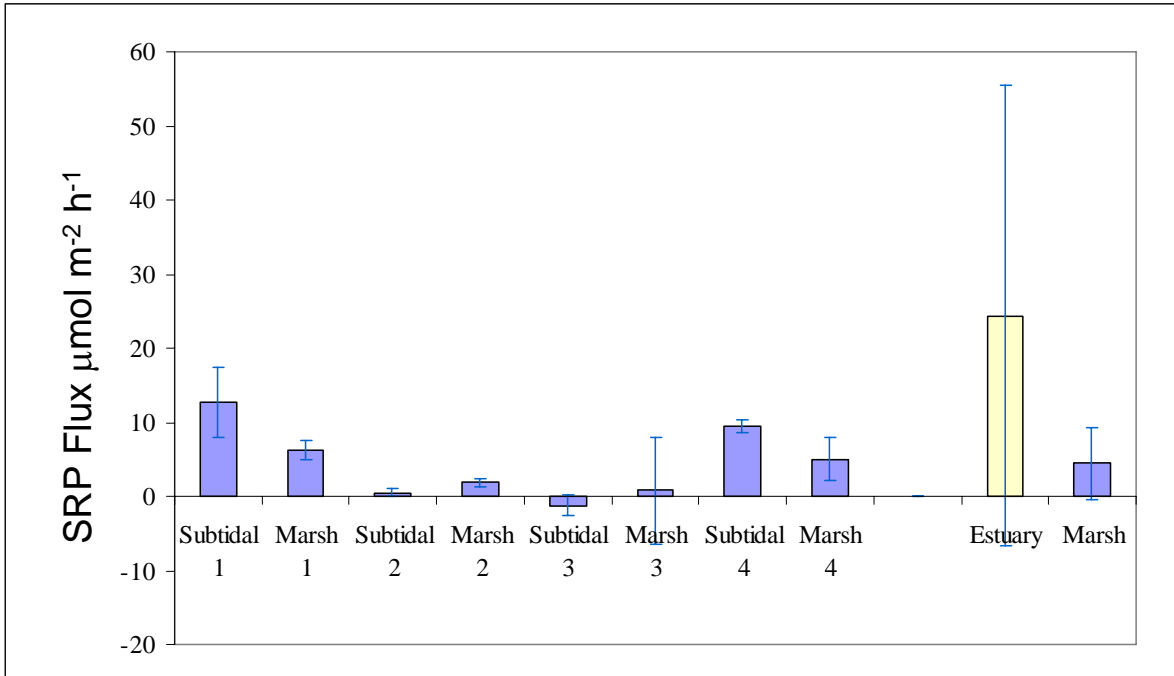
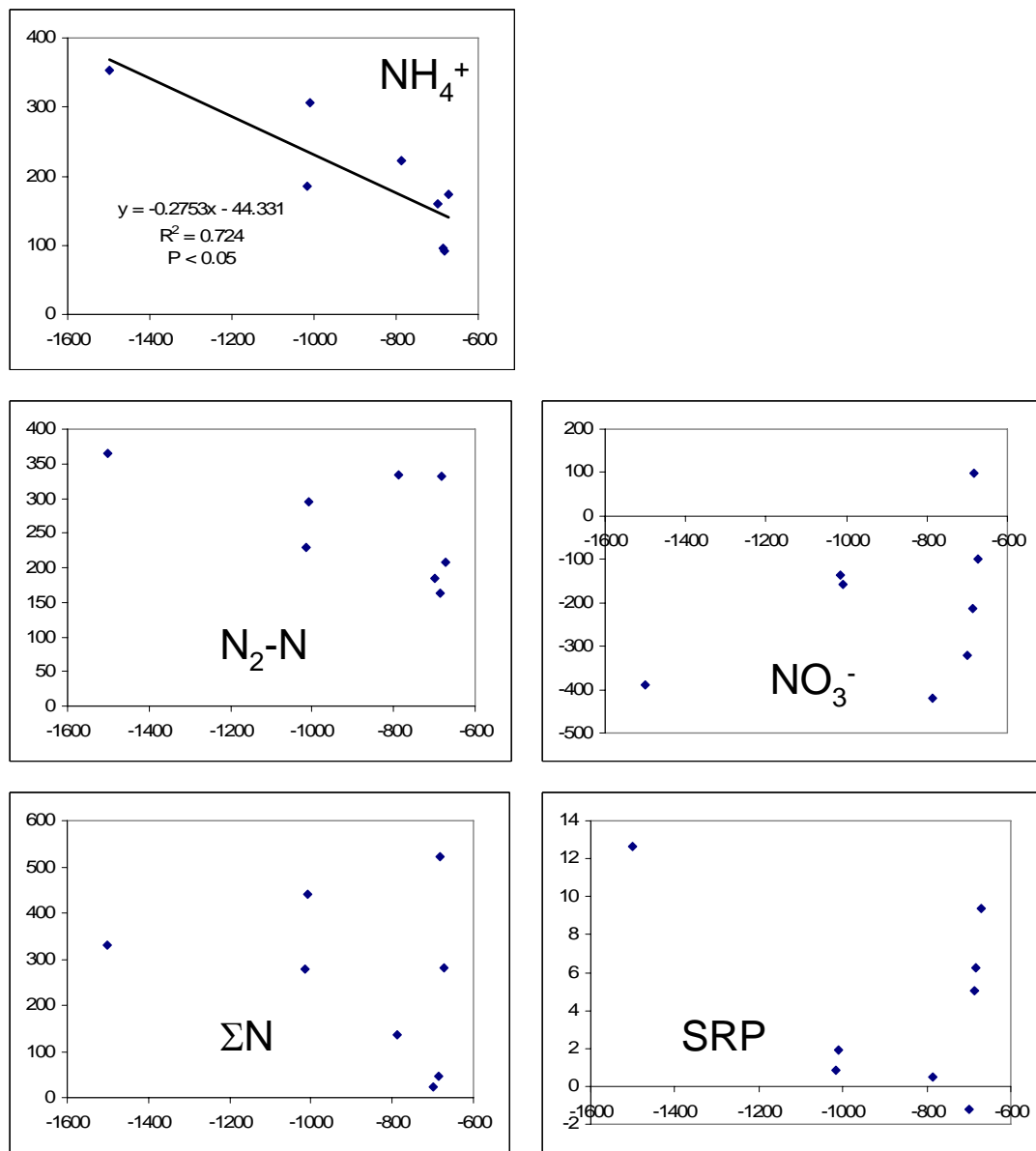


Figure 6-8. Sediment-water exchange of SRP. Positive rates indicate flux of oxygen out of the sediment. The error bars indicate the range of difference between duplicate cores. The bars on the right are the mean of the 2006 estuarine sediment flux data and the 2007 marsh flux data, error bars are one standard deviation.

N or P Flux $\mu\text{mol m}^{-2} \text{h}^{-1}$



Oxygen Flux $\mu\text{mol m}^{-2} \text{h}^{-1}$

Figure 6-9. Plots of sediment-water exchange of oxygen versus exchange of ammonium, di-nitrogen (denitrification), nitrate, ΣN ($\text{NH}_4^+ + \text{NO}_3^- + \text{N}_2\text{-N}$) and SRP. Mean rates from each site were used. Only the ammonium versus oxygen relationship was significant ($P < 0.05$).

6.2.5 Denitrification References

- Boynton, W. R., J.C. Cornwell, W.M. Kemp, C. Palinkas, J. Testa, E.M. Bailey, M.S. Owens, K.V. Wood, S. Moesel, L. Moore. 2007.** Targeted watershed measurement program and key process evaluation. Year 1: Corsica River Estuary. Data Report to Maryland DNR, TS-531-07-CBL. University of Maryland Center for Environmental Science.
- Boynton, W.R. , J. D. Hagy, J. C. Cornwell, W. M. Kemp, S. M. Greene, M. Owens, J. E. Baker, and R. K. Larsen. 2008.** Nutrient Budgets and Management Actions in the Patuxent River Estuary, Maryland. Accepted to *Estuaries and Coasts*. .
- Hopfensperger, K.N., S.S. Kaushal, S.E.G. Findlay, and J.C. Cornwell.** Influence of plant communities on denitrification in a tidal freshwater marsh of the Potomac River, U.S.A. *J. Environ. Research*, *accepted*.
- Kana, T. M., J. C. Cornwell, and L. J. Zhong.** 2006. Determination of denitrification in the Chesapeake Bay from measurements of N₂ accumulation in bottom water. *Estuaries and Coasts* **29**: 222-231.
- Kana, T. M., M. B. Sullivan, J. C. Cornwell, and K. Groszkowski.** 1998. Denitrification in estuarine sediments determined by membrane inlet mass spectrometry. *Limnol. Oceanogr.* **42**: 334-339.
- Kana, T. M., and D. L. Weiss.** 2004. Comment on "Comparison of isotope pairing and N₂ : Ar methods for measuring sediment denitrification" by B. D. Eyre, S. Rysgaard, T. Daisgaard, and P. Bondo Christensen. 2002. *Estuaries* **25** : 1077-1087. *Estuaries* **27**: 173-176.
- Merrill J.Z., and J.C. Cornwell.** 2000. The role of oligohaline marshes in estuarine nutrient cycling. p. 425–441. In M.P. Weinstein, and D.A. Kreeger (eds.) *Concepts and controversies in tidal marsh ecology*. Kluwer Academic Publishers, Dordrecht, The Netherlands.
- Parsons, T. R., Y. Maita, and C. M. Lalli.** 1984. *A Manual of Chemical and Biological Methods for Seawater Analysis*. Pergamon Press.

6.3 2007 SEDIMENTATION STUDY

6.3.1 Introduction

This report contains data from the sedimentation work in 2007, which was an extension of a preliminary study completed in 2006. Because nutrients, like most chemical constituents, adhere strongly to fine-grained (clay-sized) material, our observations provide valuable information for constraining nutrient burial and long-term storage within Corsica River bottom sediments. Our goals were to 1) determine short-term (i.e., seasonal to annual) deposition rates via ^7Be and ^{234}Th (half-lives 53.3 and 24.1 d, respectively), 2) compare these rates with longer-term (i.e., decadal) accumulation rates determined with ^{210}Pb (half-life 22.3 y), and 3) construct a preliminary sediment budget on both annual and decadal time scales.

6.3.2 Background - Calculating Sedimentation Rates and Mixing Coefficients

Rates of sedimentation and biological mixing coefficients are calculated via the advection-diffusion equation

$$D_b \frac{\partial^2 C}{\partial t^2} - A \frac{\partial C}{\partial z} - \lambda C = 0, \quad (\text{Eq. 1})$$

where D_b is the biological mixing coefficient, C is the activity of a radionuclide tracer, A is the sedimentation rate, and z is the depth in the seabed. This equation models sedimentation and mixing as advective and diffusive processes, respectively. The solution to the equation, assuming steady-state processes over the same time scale as the tracer (usually 4-5 times the half-life) is

$$A = \frac{\lambda z}{\ln \frac{C_o}{C_z}} - \frac{D_b}{z} \left(\ln \frac{C_o}{C_z} \right), \quad (\text{Eq. 2})$$

where C_o is the activity at a reference height, λ is the decay constant of the tracer, and C_z is the activity at depth z . ^7Be and ^{210}Pb are the tracers for deposition and accumulation, respectively. The mixing coefficient, D_b , is calculated from ^{234}Th using the equation

$$D_b = \lambda \left(\frac{z}{\ln \frac{C_o}{C_z}} \right)^2, \quad (\text{Eq. 3})$$

which assumes that sedimentation is negligible in the region of mixing over this short time scale (i.e., $A = 0$). Accumulation rates are calculated by assuming that mixing is negligible below this region (i.e., $D_b = 0$), and the equation reduces to

$$A = \frac{\lambda z}{\ln \frac{C_o}{C_z}}. \quad (\text{Eq. 4})$$

Because ^7Be is typically present in the upper portion of the seabed, coinciding with the surface mixed layer, the full equation given in Eq. 2 is used to calculate deposition rates. When radionuclide activities are plotted on a semi-log plot, the slope (m) of a best-fit linear regression is given by

$$m = \left(\frac{z}{\ln \frac{C_o}{C_z}} \right), \quad (\text{Eq. 5})$$

facilitating the calculation of these rates.

Accumulation rates determined via ^{137}Cs geochronology are calculated from the penetration depth of ^{137}Cs and the thickness of the mixed layer. The penetration depth minus the mixed layer thickness is divided by the number of years since 1954 (the date of first appearance).

6.3.3 Methodology

In this study, 4 cores were collected for radiochemical and textural analyses with a hand-deployed piston corer (Fig. 6-10). Cores were returned to the laboratory, where they were sectioned into 1- and 2-cm intervals prior to further analysis. Short-term (seasonal) deposition rates were determined for all sites using ^7Be and ^{234}Th . Longer-term (decadal) accumulation rates were determined for CR12 and CR9 with ^{210}Pb geochronology and verified with ^{137}Cs . Accumulation rates at CR10 and CR11 were determined previously by LeBeau (2006).

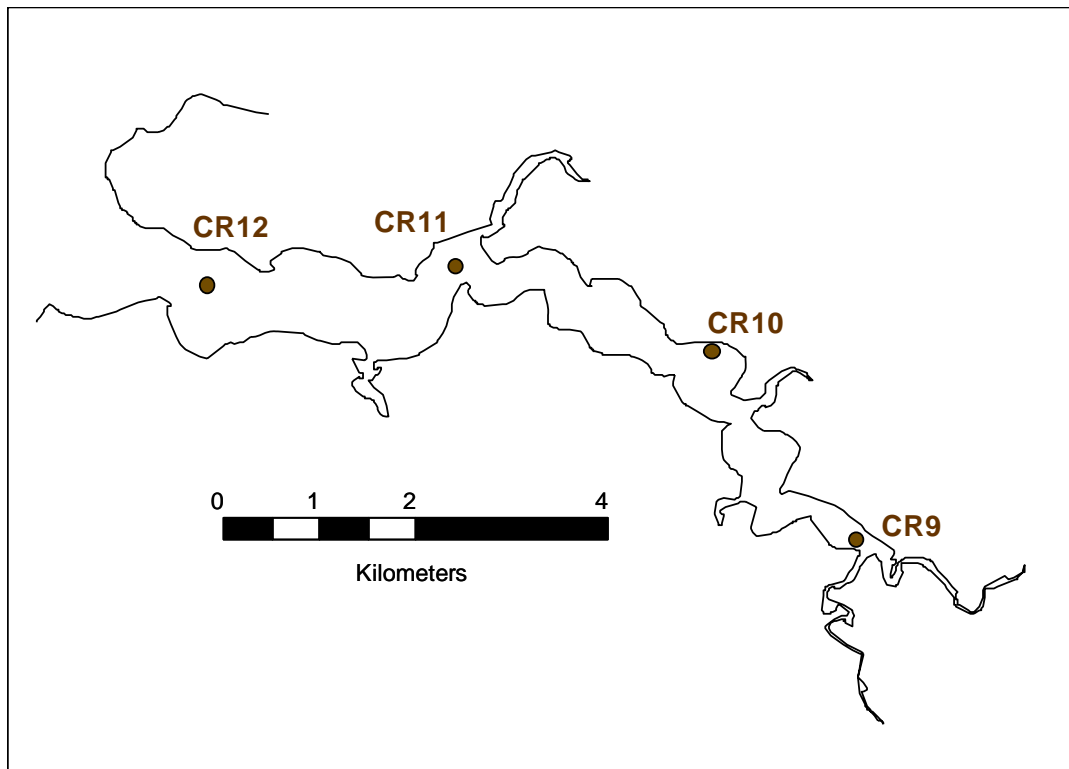


Figure 6-10. Map of the 2007 core locations in the Corsica River.

In the laboratory, ^7Be and ^{234}Th measurements were performed using gamma spectroscopy. Wet sediment from each sampling interval was dried, ground, and sealed in 60-mL plastic jars. Consistent counting geometry of samples was ensured by using identical counting jars filled to the same height. The gamma emissions from each sample were counted for approximately 24 h using

a calibrated germanium detector. Activities were normalized to the salt-corrected dry mass (expressed as dpm g⁻¹; disintegration per minute per gram dry sediment) and decay-corrected to the time of collection. ⁷Be and ²³⁴Th activities were measured from the 477.7 and 63.3 keV photopeaks, respectively, of the gamma spectrum. Samples were recounted several months after collection to determine the activity of ²³⁴Th supported by decay of its parent (²³⁸U) in the seabed.

Longer-term sediment accumulation rates were determined via measurement of ²¹⁰Pb activities by alpha spectroscopy, following the procedure of Palinkas and Nittrouer (2007). ²¹⁰Pb rates were verified by ¹³⁷Cs (half-life 30.7 y), a bomb-produced radionuclide that serves as an independent geochronometer. ¹³⁷Cs activities were measured via gamma spectroscopy of the 661.6 photopeak.

Grain-size analyses were conducted by wet-sieving samples (at 64 μm) to separate the mud and sand components. The mud fraction was then dispersed in sodium metaphosphate and placed in an ultrasonic bath before analysis with a Sedigraph III to determine the particle size distribution. These data were used to describe the textural characteristics of each site and to aid in the interpretation of radiochemical profiles.

6.3.4 Results

Deposition Rates and Mixing Coefficients via Short-Lived Radioisotopes

²³⁴Th and ⁷Be data for CR9 are shown in Fig. 6-11. The mixing coefficient for this site is 24.7 cm²/y, and the deposition rate is 4.89 cm/y (3.24 g/cm²/y). Because of our relatively coarse sampling intervals (1 cm), this site is the only one with enough resolution to calculate use linear

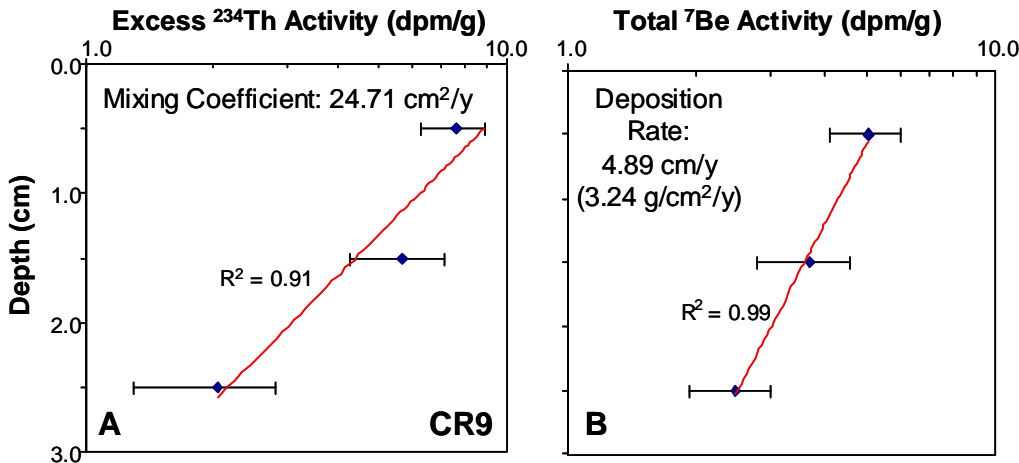


Figure 6-11. A) ²³⁴Th and B) ⁷Be profiles for CR9. The slope of the best-fit linear regression was used to determine the mixing coefficient and deposition rates via Eq. 3 and 2 in the text, respectively. Neither radionuclide was detected in samples below 3 cm.

regression fits to the data (Fig. 6-12), although estimates can be made at the other sites. Deposition rates can be estimated through the depth-integrated inventory of ⁷Be, which is unaffected by mixing, by dividing the inventory by the surficial dry bulk density (determined in the lab) and ⁷Be activity. This yields the depth of “new” sediment that is then divided by the detection time of ⁷Be (~200 d), yielding a minimum average deposition rate over this time period (Table 6-3). ⁷Be was not detected at CR10, which may be due either to negligible deposition, erosion, and/or intense

mixing that effectively dilutes the ^7Be signal below detection levels. Data from other measurements (see below) suggest that the latter scenario is the likeliest possibility. CR10 has the highest apparent mixing coefficient and the thickest mixed layer. The long-term accumulation rate is greatest at this site and the surficial grain size is the finest, suggesting that this site is relatively sheltered from erosional processes, relative to the other sites.

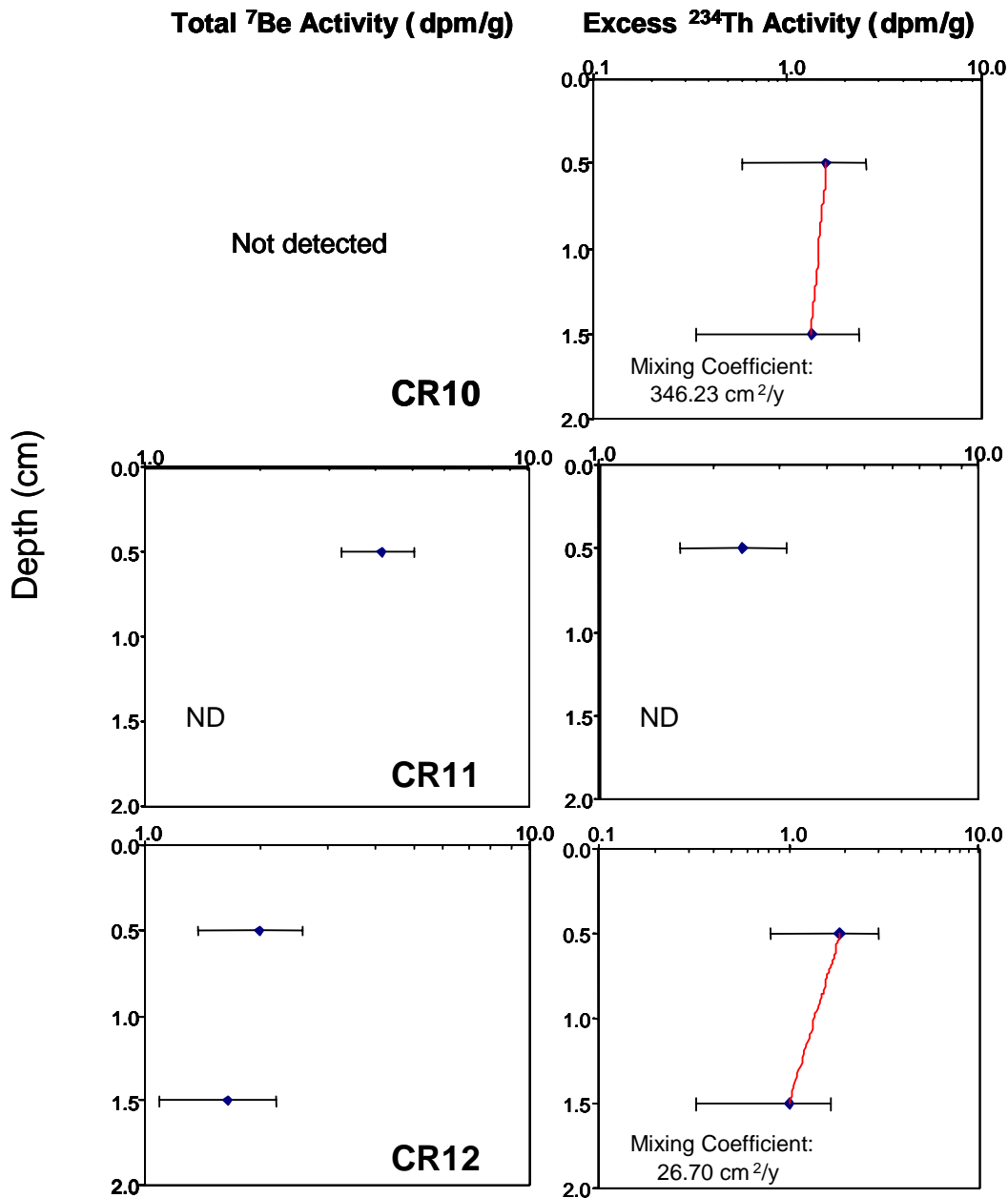


Figure 6-12. ^7Be and ^{234}Th activity profiles for CR10, CR11, and CR12. At CR10, ^7Be is not detected and the mixing coefficient is likely an overestimate. Both radioisotopes are present only in the surficial (0-1 cm) sample at CR11. At CR12, ^7Be activities are relatively uniform, reflecting the influence of mixing. The mixing coefficient for this site is reasonable, although based on few data.

Table 6-3. Deposition rates calculated from ⁷Be inventories at all core locations.

Core	Inventory (dpm/cm ²)	Bulk Density (g/cm ³)	Surficial Activity (dpm/g)	Depth of New Sed (cm)	Deposition Rate (cm/y)
CR9	2.91	0.26	5.04	2.22	3.04
CR10	ND	0.14	ND	NA	NA
CR11	0.88	0.21	4.14	1.01*	1.39
CR12	1.51	0.39	1.94	1.94	2.66

ND = not detected

* = ⁷Be present only in surficial (0-1 cm) layer

The mixing coefficient at CR10 and CR12 can be calculated from the ²³⁴Th profiles, although caution should be used due to the coarse sampling resolution (i.e., both profiles have 2 measurements, which is sufficient to fit a linear regression but not to assess its validity). At CR10, the mixing coefficient calculated from the profile is 346.23 cm²/y, which is much higher than the ~10-100 cm²/y typically observed (e.g., Fuller et al., 1999). The calculated mixing coefficient for CR12 is 26.70 cm²/y, which is similar to that observed at CR9. Whether these coefficients are reasonable can be ascertained by use of the dispersion equation,

$$h = (2D_b t)^{1/2} + At, \quad (\text{Eq. 6})$$

where h is the depth a particle reaches at time t with a mixing coefficient D_b and sedimentation rate A . Within the surface mixed layer, the appropriate time scale is the annual average and so 1 y is used for the purposes of this calculation. For CR9, using the ⁷Be- and ²¹⁰Pb-derived sedimentation rates, Eq. 6 gives a mixed layer of 11.93 and 7.53 cm, respectively. The observed mixed layer from the ²¹⁰Pb profile (see next section) is ~10 cm, indicating that the dispersion equation can give reasonable results. At CR12, this equation yields a mixed layer of 8-10 cm, which is of similar magnitude as the observed ~5-cm layer. This indicates that the apparent mixing coefficient is reasonable, although likely an overestimate. Using the calculated mixing coefficient at CR10 with its ²¹⁰Pb-derived sedimentation rate (no ⁷Be rate is available at this site) results in a 27.3-cm thick mixed layer, which is approximately what we observed in 2006 (~30 cm mixed layer). However, in 2007, we observe a 50-cm thick layer, which would require a mixing coefficient of 1200 cm²/y – an order of magnitude greater than typical values. One possibility for this discrepancy is deposition of a 20-cm thick flood layer from the heavy rains in summer 2006 (the 2006 core was collected prior to this event). However, this is unlikely as flood layers typically have uniform ⁷Be and low ²¹⁰Pb values (Palinkas et al., 2005), neither of which is observed. More likely is some type of physical disturbance; this would not be accounted for in Eq. 6, as this equation assumes that only diffusional (i.e., biological mixing) processes are active. At CR11, ²³⁴Th is present only at the surface, but we observed a 15-cm thick mixed layer in 2006. A mixing coefficient of ~100 cm²/y would yield a layer 14.5-15.5-cm thick and is probably a reasonable order-of-magnitude estimate for this site. The trends in these observations are shown in Table 6-4a. In general, higher deposition rates and lower mixing coefficients are observed at the up- and down-stream ends of the system (CR9 and CR12, respectively), and the reverse is true in the middle (CR11).

Table 6-4. A) Observed trends in deposition rates, mixing coefficients, and the $^7\text{Be}/^{234}\text{Th}$ ratio calculated from inventories. B) Expected trends in ^7Be and ^{234}Th based on assumed sources of material. Note the observed ratio for CR12 is higher than expected, likely due to the combined influence of material derived from the shoreline and the Chester River.

A)

	CR12	CR11	CR10	CR9
Deposition Rate (cm/y)	Medium (2.66)	Low (1.39)	NA	High (4.89)
Mixing Coefficient (cm ² /y)	Low (26.70)	High (~100)	High (346.23)	Low (24.71)
$^7\text{Be}/^{234}\text{Th}$ Ratio	Medium (1.34)	High (1.96)	NA	Low (0.96)

B)

	CR12	CR11	CR9
^7Be	Low (assume Chester source)	High (assume shoreline source)	Low (assume fluvial source)
^{234}Th	High	Medium-High	Low
Ratio	Low	High	Medium

The likely source of sediment (e.g., fluvial versus shoreline erosion) can be described by the $^7\text{Be}/^{234}\text{Th}$ ratio, which normalizes differences in the absolute activities due to focusing, changes in grain size, etc. The ratios reported in Table 6-2a are based on inventory values, although the same trends are seen in ratios calculated from the surficial activities. ^7Be and ^{234}Th have different source functions – ^7Be is a cosmogenic radioisotope deposited by precipitation and dry deposition onto terrestrial vegetation (Olsen et al. 1986), whereas ^{234}Th is produced directly from decay of its parent ^{238}U in the water column (Aller and Cochran 1976). The activity of ^{238}U , and therefore ^{234}Th varies nearly conservatively with salinity (Feng et al., 1999), which decreases with distance upstream in the Corsica River (MD-DNR monitoring data; not shown), resulting in the expected trend shown in Table 6-2b. The ^7Be trend is based on assumed sources of sediment. Sediment that has been stored on the riverbed (i.e., out of contact with the atmosphere) typically has reduced ^7Be due to radioactive decay. Thus, sediment that originates in the Corsica River channel or is imported from the Chester River should have a relatively low ^7Be signal, whereas “fresh” material delivered from shoreline erosion would be expected to have a high ^7Be signal. The ratios observed at CR9 and CR11 agree with expectations of material source. CR9 has a low ratio and is clearly the depocenter of upstream fluvial material – it has a high deposition rate, low ^7Be , and low ^{234}Th . CR11 has a high ratio, reflecting the influence of shoreline-derived material. In contrast, CR12 has a higher ratio than would be expected if the Chester River dominated the source of material. Rather, it has an intermediary value between CR9 and CR11, suggesting a mixed source of shoreline- and Chester-derived material. The dynamics at CR10 are difficult to ascertain, because of intense mixing and lack of ^7Be . There is no water-quality monitoring station located in the cove, but water-quality mapping from 2006-2007 by MD-DNR shows no evidence of different dynamics in the cove relative to the rest of the system. It should be noted that there is no data during winter months, when sediment is likely being actively redistributed throughout the system.

A preliminary sediment budget can be constructed from the ^7Be deposition rates, using the bulk density to convert linear rates (cm²/y) to mass deposition rates (g/cm²/y). The Corsica River

shoreline was obtained from the Maryland Geological Survey website (<http://www.mgs.md.gov/coastal/maps/shorevect.html>) and imported into ArcGIS, where areas were measured. To construct the budget, we assumed that the system can be represented by 4 boxes, each with an average deposition rate equal to that observed at a coring location (Fig. 6-13). We calculated the budget in three ways, assuming that CR10 has a deposition rate equal to: 1) 10 times its long-term average, 2) 3.5 times its long-term average, and 3) the average of CR11 and CR9. With these assumptions, the annual average mass deposition in the Corsica River is $7.69-10.12 \times 10^3$ t/y. Note that this is based on 2006-2007 end-of-summer conditions; the interannual variability in this estimate is unknown. This represents the “sink” term of the sediment budget, or the portion that deposits on the riverbed. The other terms in the budget –upstream input, shoreline erosion, and Chester River influences – are unknown. Future work on the seasonal/annual dynamics in the Corsica should focus on constraining these terms and examining the interannual variability in short-term sediment dynamics.

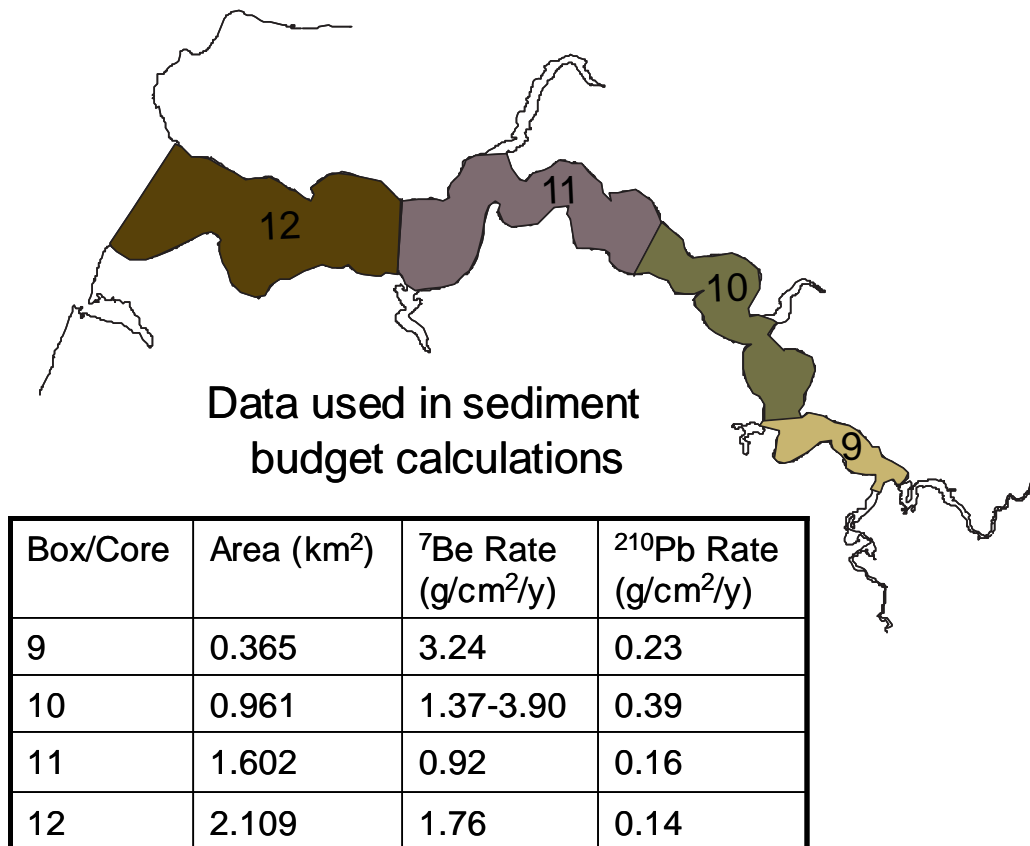


Figure 6-13. Areas and data used in annual (⁷Be) and decadal (²¹⁰Pb) sediment budgets.

100-y Average Accumulation Rates via ^{210}Pb and ^{137}Cs

Because accumulation rates at CR10 and CR11 have been established previously by the 2006 pilot study, our focus is first on determining long-term rates at CR9 and CR12. Radiochemical and textural (grain-size) data for these cores are shown in Fig. 6-14. The average rate at CR9 is 4.45 mm/y (0.23 g/cm²/y). Based on this rate, ^{137}Cs should penetrate to 34 cm, but it is found much deeper in the core (~50 cm). Looking closer at the ^{210}Pb profile, there is a change in slope that reflects a change in sedimentation rate. The slopes of the lower and upper portions of the profile yield rates of 3.17 and 15.86 mm/y, respectively. It should be noted that the upper portion of the profile is drawn with relatively few data points and therefore should be regarded as a preliminary estimate. Nevertheless, this suggests a recent increase in sedimentation, occurring at 25-37 cm deep in the core. Applying the faster sedimentation rate below the ~10-cm mixed layer yields a date for this shift – 10-17 y ago or the early to mid-1990s. Below 25-37 cm, the slower rate is used for the time between the shift and 1954 (the first appearance of ^{137}Cs) to determine a ^{137}Cs penetration depth of 39-49 cm, which agrees well with the ^{210}Pb data. The cause of this increase in sedimentation is unknown. This is the only site with an apparent change in sedimentation, and it is likely responding to a change upstream. Either the signal has not yet propagated to the downstream sites or it is progressively damped as it travels downstream and is lost after CR9. Additional cores upstream of CR9 would lend some insight into these possibilities. For purposes of the sediment budget, the average rate is used to be consistent with the other sites.

A more typical ^{210}Pb profile is observed at CR12; the accumulation rate is 2.70 mm/y (0.14 g/cm²/y). The ^{137}Cs data agree well with this rate – the expected and observed penetration depths are ~20 cm. The ^{210}Pb rates are approximately an order of magnitude larger than the ^7Be -derived deposition rates; this is common in fluvial systems and due to the incorporation of periods not captured in sampling that emphasizes depositional periods (McKee et al., 1983). Thus, efforts to monitor the response of the Corsica to restoration should focus on short-term deposition rates to ensure that observed changes are not affected by temporal artifacts.

In 2006, we verified the accumulation rate at CR11 with total Pb observations, but we did not verify the rate at CR10. Because the piston cores we collected for the short-term observations were ~ 1 m long, we could measure the ^{137}Cs activity with depth to verify the rate. Surprisingly, ^{137}Cs penetrated to the base of the core; we expected it to be ~90 cm deep based on the 2006 observations of mixed layer depth and accumulation rate. Because excess ^{210}Pb activities and the accumulation rates derived from them via alpha and gamma (46.5 keV photopeak) spectroscopy are similar (e.g., Zaborska et al., 2007), we compared the 2006 and 2007 profiles for CR10 (Fig. 6-15). The gamma-derived 2007 excess activities and sedimentation rate are somewhat higher than the 2006 alpha-derived values. However, the most significant difference between the profiles is the ~20-cm increase in mixed-layer thickness between 2006 and 2007. With a thicker mixed layer, we would expect the 2007 ^{137}Cs penetration to be at 102 cm, which is below the depth penetrated by our core. The change in mixed layer depth at CR10 highlights the potential interannual variability present in the Corsica River system. The long-term accumulation rate and profile under the mixed layer is relatively unchanged; the mixed layer is the region affected by short-term processes. A long-term sediment budget for the Corsica has been constructed using the same areas and logic as the short-term budget described above. The total mass accumulating on the Corsica riverbed is 1.01×10^3 t/y. This is 7-10 times less than the annual-scale budget based on the 2007 data. The difference is consistent with the notion that rates often decrease with increasing time scale.

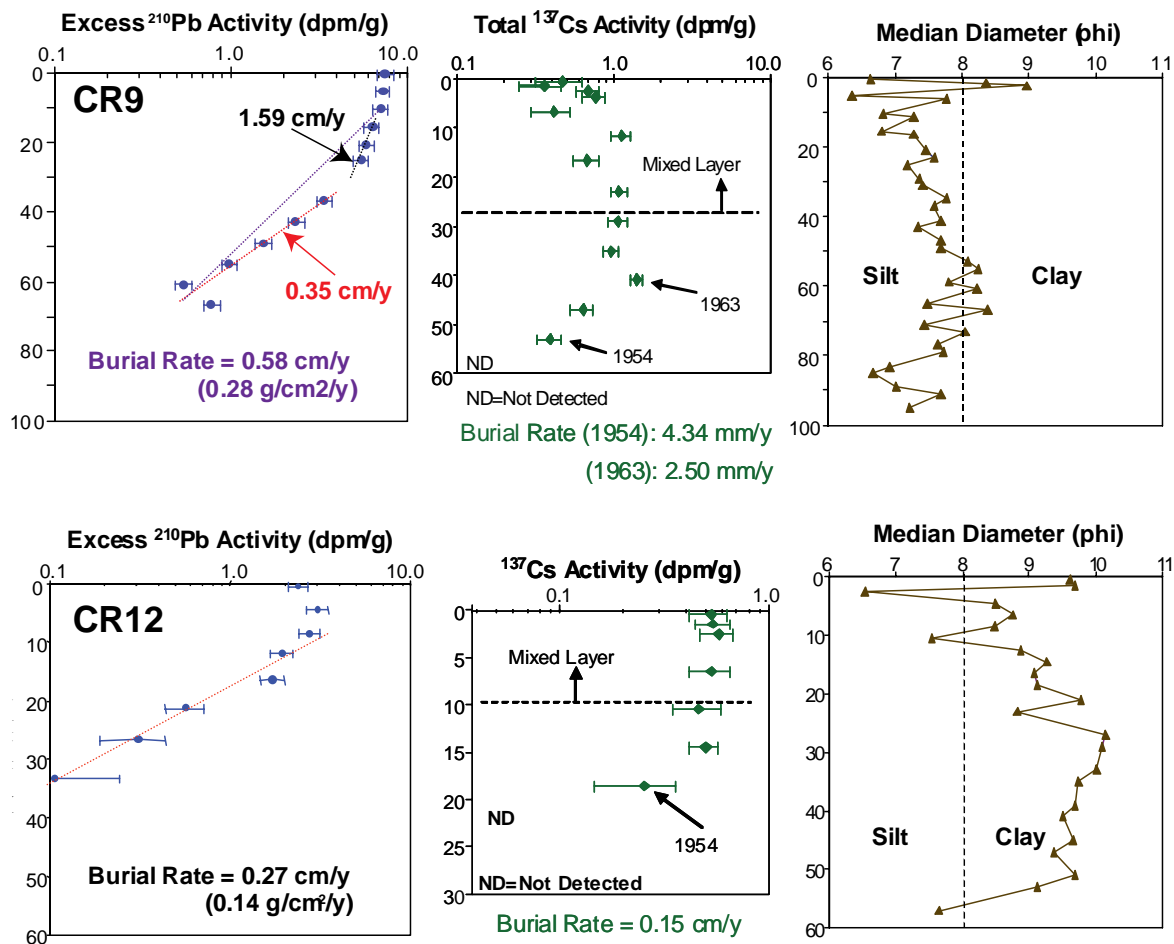


Figure 14. ^{210}Pb , ^{137}Cs , and grain-size profiles for CR9 and CR12. CR9 has an apparent recent increase in accumulation rate, although the upper portion of the ^{210}Pb profile is based on few data points. Both cores are composed of muddy material; however CR12 is finer-grained than CR9 ($\phi = \log_2(\text{particle diameter in mm})$).

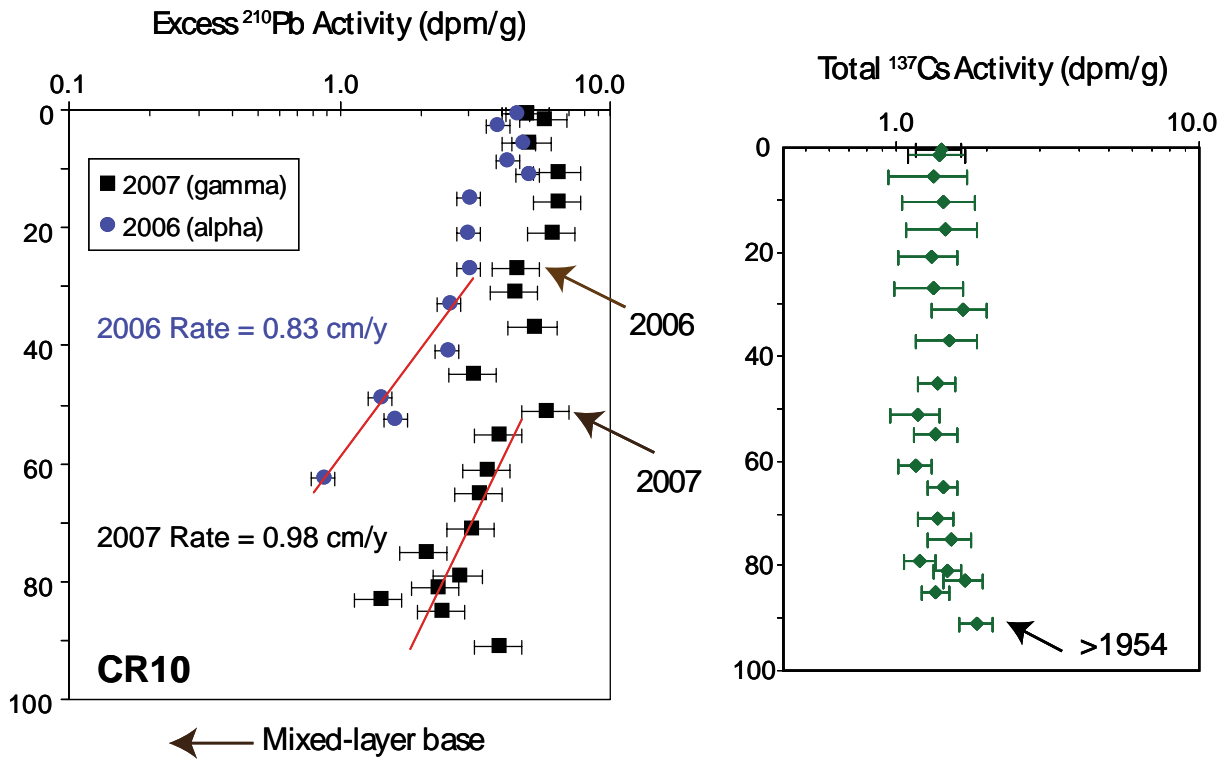


Figure 15. ^{210}Pb and ^{137}Cs profiles for CR10. Note the increase in mixed layer between the 2006 and 2007 ^{210}Pb profiles. ^{137}Cs penetrates to the base of the 2007 core, which is consistent with the observed accumulation rate and mixed-layer thickness.

6.3.5 Summary

Short-term rates for the 4 cores collected in 2007, based on ^7Be dating, range from 1.39-3.04 cm/y. Longer-term accumulation rates at CR9 and CR12 (determined via ^{210}Pb and confirmed with ^{137}Cs) are 0.45 and 0.27 cm/y, respectively. While the short- and long-term rates differ by an order of magnitude, this is typical of many fluvial systems. Based on these data, the mass of sediment deposited on the Corsica River bottom for annual and decadal time scales is $7.69\text{-}10.12 \times 10^3$ and 1.01×10^3 t/y, respectively. Future work should focus better constraining the other terms in the sediment budget, so our results can be placed in a broader context. Based on radioisotope ratios, the source of sediment can be ascribed. CR9 is the depocenter of fluvial material, CR11 is heavily influenced by shoreline sources, and CR12 is likely composed of a combination of Chester River and shoreline sediment. The dynamics at CR10 are difficult to ascertain due to its location in a sheltered environment. The potential small-scale spatial and interannual variability of the sediment dynamics in this system remain to be examined, as well as possible evidence upstream of the increased sedimentation observed at CR9.

6.3.6 2007 Sedimentation References

- Aller, R.C., and J.K. Cochran.** 1976. $^{234}\text{Th}/^{238}\text{U}$ disequilibrium in near-shore sediment: particle reworking and diagenetic time scales. *Earth Planet. Sci. Lett.* 29 37-50.
- Feng, H., J.K. Cochran, and D.J. Hirschberg.** 1999. Th-234 and Be-7 as tracers for the transport and dynamics of suspended particles in a partially mixed estuary. *Geochim. Et Cosmochim. Acta* 63 2487-2505.
- Fuller, C.C., A. van Geen, M. Baskaran, and R. Anima.** 1999. Sediment chronology in San Francisco Bay, California, defined by Pb-210, Th-234, Cs-137, and Pu-239, Pu-240. *Mar. Chem.* 64 7-27.
- Lebeau, C.** 2006. Geochronology and characterization of grain size and trace metals in sediment cores collected from the Corsica River, Maryland. REU Report to Maryland Sea Grant. **Dr. Cindy Palinkas**, Advisor.
- McKee, B.A., C.A. Nittrouer, and D.J. DeMaster.** 1983. Concepts of sediment deposition and accumulation applied to the continental shelf near the mouth of the Yangtze River. *Geology* 11 631-633.
- Olsen, C.R., I.L. Larsen, P.D. Lowry, and N.H. Cutshall.** 1986. Geochemistry and deposition of ^7Be in river-estuarine and coastal waters. *J. Geophys. Res.* 91 896-908.
- Palinkas, C.M., and C.A. Nittrouer.** 2007. Modern sediment accumulation on the Po shelf, Adriatic Sea. *Cont. Shelf Res.* 27 489-505.
- Palinkas, C.M., C.A. Nittrouer, R.A. Wheatcroft, and L. Langone.** 2005. The use of ^7Be to identify event and seasonal sedimentation near the Po River delta, Adriatic Sea. *Mar. Geol.* 222-223 95-112.
- Zaborska, A., J. Carroll, C. Papucci, and J. Pempkowiak.** 2007. Intercomparison of alpha and gamma spectrometry techniques used in ^{210}Pb geochronology. *J. Environ. Radio.* 93 38-50.

7.0 Estuarine Community Metabolism at Potomac River Estuary ConMon Sites (Maryland and Virginia - 2007)

Walter R. Boynton and Kathryn V. Wood

7.1	Introduction and Objectives	7-1
7.2	Station Location and Sampling Period	7-2
7.3	Methods	7-5
7.4	Results for Potomac River Estuary: 2007	7-7
7.5	References	7-16

7.1 Introduction and Objectives

Community production and respiration have repeatedly been shown to be responsive to nutrient enrichment in lakes (e.g., Vollenweider 1976 and many others), estuaries and coastal waters (e.g., Boynton et al 1982; Boynton and Kemp 2007). In the case of the Potomac River estuary, nutrient enrichment was cited as one of the reasons for listing this waterway as being impaired and in need of restoration. In many instances measurements of such fundamental features of ecosystem function as production and respiration are too expensive or simply too difficult to undertake. However, in the Potomac River estuary the State of Maryland Department of Natural Resources (DNR) and the Virginia Department of Environmental Quality have established 16 water quality monitors (11 in Maryland and 5 in Virginia waters) making measurements of water quality variables needed to make these estimates. In this chapter we report on the methods and results of community production and respiration computations for many of these sites in the Potomac River estuary.

System metabolism analyses have been completed in the Patuxent River estuary (see Chapter 6 for a summary) and this technique has been gaining much broader application in estuarine and near-coastal areas. Perhaps the best single example of this was reported by Caffrey (2004). Caffrey assembled high frequency DO, temperature and salinity data from 42 sites located within 22 National Estuarine Research Reserves between 1995 and 2000. She computed the same sort of metabolism estimates described here and found the following: 1) highest production and respiration rates occurred in the SE USA during summer periods; 2) temperature and nutrient concentrations were the most important factors explaining variation in rates within sites; 3) freshwater sites were more heterotrophic than more saline sites; 4) nutrient loading rates explained a large fraction of the variance among sites and; 5) metabolic rates from small, shallow, near-shore sites were generally much larger than in adjacent, but larger, deeper off-shore sites. The fact that nutrient loading rates and concentrations were strong predictors of rates is especially relevant to efforts being made in Chesapeake Bay tributaries like the Potomac River estuary and associated tributaries. Finally, Danish investigators have been using this technique in a variety of shallow Danish systems and they have, quite importantly, started to use four different approaches for estimating the metabolic parameters of interest here (Gazeau *et al.* 2005), including the open water DO approach. Significantly, their evaluations suggest that all techniques produce the same estimates with regard to magnitude and direction (production or respiration). A convergence of estimates, using different techniques, suggests a robust set of variables and that is consistent with the needs of a monitoring program.

This effort represents an un-funded activity by the EPC of the Maryland Biomonitoring Program. This exploratory effort is consistent with the process-based approaches we have recommended for many years and this effort is another such example. The algorithm used to compute metabolism was developed by David Jasinski, formerly with the Chesapeake Bay Program. The actual data reduction and computations were completed via volunteer efforts by one of the authors (K.V.Wood). Our goal here is to highlight another useful application of ConMon data to the overall effort to monitor Chesapeake Bay environments for status, trends and eventual restoration. These data manipulations lead to a very high number (potentially every day from April through October) of rate measurements of system production (related to nutrient conditions) and system respiration (related to the bane of hypoxia). Such a large number of observations at a large number of sites is likely unprecedented in estuarine monitoring programs.

7.2 Station Location and Sampling Period

Station location is shown in Figure 7-1 and more specific information is provided in Table 7-1. There were a total of 16 sites equipped with ConMon sensor systems, 5 in Virginia waters and 11 in Maryland waters. We used data from these locations from March (or April) through October 2007. It may be important to note that all Virginia sites were located in small Potomac tributary systems, not actually on the shoreline of the Potomac River estuary proper. In Maryland, 4 (or 5) of the sites were located on the shore of the mainstem Potomac while the remainder were located in tributaries of various sizes. There was no consistent distance between ConMon location in tributaries and the mainstem waters of the Potomac River estuary. We completed metabolism computations for 14 of the 16 Potomac River estuary ConMon sites using 2007 data. A cursory inspection of ConMon data from the Port Tobacco and Blossom Point sites indicated periods of seemingly erratic DO changes (i.e., DO increased during hours of darkness and abrupt changes in DO exceeding any that could be reasonably attributed to biological processes). It may be that a closer inspection of these data would lead to some parsing and then use of the data. However, our efforts were more limited and because of this we simply did not pursue computations involving data from these sites.

Table 7-1. ConMon Station Names, Locations, Orientations and Mean Depth at Maryland and Virginia sites. *Latitude and longitude values are expressed as decimal degrees (Datum NAD 83). NA = Data not available.*

Station Name	State	Latitude	Longitude	Shore/Tributary <i>(NM= Nautical Miles from Mainstem Potomac River)</i>	Station Depth (m)	Depth Location of Sonde (m)
Piscataway	MD	38.7016	-77.0259	0.9 NM	1.0	0.3
Pohick Creek	VA	38.6759	-77.1664	2.1 NM	0.9	NA
Fenwick	MD	38.6699	-77.1151	Mainstem Potomac	0.4	0.3
Mattawoman Creek	MD	38.5593	-77.1887	1.6 NM	1.0	0.3
Potomac Creek	VA	38.3436	-77.3049	1.0 NM	1.0	NA
Pope's Creek	MD	38.3960	-76.9891	Mainstem Potomac	1.7	0.3
Swan Point	MD	38.3054	-76.9239	Mainstem Potomac	0.5	0.3
Monroe Bay	VA	38.2320	-76.9637	0.2 NM	1.6	NA
Wicomico Beach	MD	38.3275	-76.8660	5.4 NM	NA	0.3
Nomini Bay	VA	38.1316	-76.7176	2.5 NM	1.0	NA
Breton Bay	MD	38.2590	-76.6713	2.2 NM	1.5	0.5
Piney Point	MD	38.1378	-76.5058	Mainstem Potomac	0.9	0.5
St. George's Creek	MD	38.1311	-76.4934	2.2 NM	0.9	0.5
West Yeocomico River	VA	38.0288	-76.5518	1.7 NM	1.0	NA



Figure 7-1. General locations and place names of ConMon sites in Maryland and Virginia portions of the Potomac River estuary. See table 7-1 for more specific station locations.

7.3 Methods

7.3.1 Basic concept for computing community production and respiration

The basic concept and method for computing community production and respiration was developed by H.T. Odum and C.M. Hoskin (in the 1959's) and, with numerous modifications, has been used since for measuring these rate processes in streams, rivers, lakes, estuaries and the open ocean. The technique is based on following the oxygen concentration in a body of water for at least a 24 hour period. During hours of daylight, oxygen increases in the water due to the release of O₂ as a by-product of photosynthesis. During hours of darkness, O₂ declines due to O₂ consumption by both primary producers and all other heterotrophs. The rate processes (gross photosynthesis, Pg; nighttime respiration, Rn) are estimated by computing the rate of change in O₂ concentrations during day and night periods. This rate of change is then corrected for O₂ diffusion across the air-water interface and the result is an estimate of Pg and Rn. ConMon data are exactly the type of data needed for these computations in that all the needed variables are measured (dissolved oxygen, temperature and salinity), the measurement frequency is high (15 minute intervals) and the measurement period is for 9 or more months. It is very rare when a rate process can be measured with such temporal intensity.

7.3.2 Description and Operation of Metabolism Macro: Preliminary Program

Based on earlier work by Burger and Hagy (1998) for calculating water column metabolism from near-continuous monitoring data, an automated Excel spreadsheet (Metabolism.xls) was developed by Mr. David Jasinski (Personal Communication). The worksheet was automated using Microsoft's Visual Basic for Applications (VBA) programming language. Briefly, the steps the spreadsheet undertakes are as follows:

1. An excel file, containing the continuous monitoring data configured by the user in a requisite format (Fig.7 -2) is read into the spreadsheet.
2. Dates and times are reformatted into a continuous time variable or serial number.
3. Sunrise and Sunset times for each date are calculated based on the latitude and longitude of the station.
4. Rows are inserted into the dataset to create an observation at sunrise and sunset on each day.
5. Each observation in the dataset is assigned a daypart – Sunrise, Day, Sunset, or Night
6. Each observation is assigned to a “Metabolic Day”. Each metabolic day begins at sunrise on the current day and continues to the observation immediately before sunrise on the following day.
7. For sunrise/sunset observations created in Step 4, values for water temperature, salinity, dissolved oxygen and dissolved oxygen saturation are calculated by taking the mean of the observations immediately before and after sunrise and sunset.

8. The change in DO, time, air/sea exchange and oxygen flux is calculated between each consecutive observation.

9. The minimum and maximum DO values are calculated between sunrise and sunset on each day and these values are labeled “metabolic dawn” and “metabolic dusk”.

10. Sums of the changes in DO, time, air/sea exchange and DO flux (step 8) are calculated for each metabolic day for the periods between sunrise and metabolic dawn, metabolic dawn and metabolic dusk, metabolic dusk and sunset, and sunset and the following sunrise.

11. From these sums, 6 metabolic variables are calculated and these include: rn, rnhourly, pa, pa_star, pg, pg_star.

These variables are defined as follows:

rn = Nighttime (sunset to following sunrise) summed rates of DO flux corrected for air/water diffusion.

rnhourly = rn divided by the number of nighttime hours

pa = The sum (both positive and negative) of oxygen flux (corrected for air-water diffusion) for the dawn, day and dusk periods.

pa_star = summed oxygen flux (corrected for air-water diffusion) for the day period

pg = pa + daytime respiration. Daytime respiration = rnhourly * (number of hours of daytime+dawntime+dusktime).

pg_star = pa_star + daytime respiration as defined above.

Air-water diffusion of oxygen is considered in these computations and the diffusion correction is based on the difference between observed DO percent saturation and 100% saturation multiplied by a constant diffusion coefficient. For these computations a diffusion coefficient of $0.5 \text{ g O}_2\text{m}^{-2} \text{ hr}^{-1}$ was selected as generally representative of conditions frequently encountered in estuarine tributary situations (Caffrey 2004).

One of the primary assumptions of this method is that temporal changes in DO measured by the continuous monitors are due solely to metabolism (i.e., oxygen production from photosynthesis and oxygen loss from respiration) occurring at the station and not due to advection of water masses with different oxygen conditions moving past the instrument. Because Chesapeake Bay is a tidal system, this may not always be the case. Depending on the hydrodynamics of a given station, this assumption may be more or less realistic and may also be variable from date to date. One way of censoring dates where DO is affected by advection is to preview the data graphically prior to metabolism calculations and determine if there is a relationship between salinity and DO. Large changes in salinity suggest moving water masses and therefore, advection. These dates could then be flagged and reviewed before metabolism variables are calculated.

Another way of dealing with advection is to incorporate in the code a method of detecting changes in DO associated with changes in salinity. It might then be possible to apply a site specific correction factor to remove the advection affect on DO. These possibilities could be investigated further in the future. At the present time we examine data from each site graphically and if there are erratic patterns in dissolved oxygen or salinity we do not attempt calculations for that site. In

addition, the algorithm indicates when a site has unusual dissolved oxygen patterns (e.g., increases in dissolved oxygen during hours of darkness) and these computations are excluded.

	A	B	C	D	E	F	G	H	I	J	K
1	Date	Time	WTEMP	SALIN	DOSAT	DO	Lat	Long	timezone	daylightsavings	
2	6/20/1997	11:45:00	25.42	1.1	114.4	9.3	38.49068	-76.6641	-5	1	
3	6/20/1997	12:00:00	25.44	1.1	117.4	9.55	38.49068	-76.6641	-5	1	
4	6/20/1997	12:15:00	25.45	1.1	117.1	9.52	38.49068	-76.6641	-5	1	
5	6/20/1997	12:30:00	25.38	1.1	112.9	9.19	38.49068	-76.6641	-5	1	
6	6/20/1997	12:45:00	25.45	1.1	115.2	9.37	38.49068	-76.6641	-5	1	
7	6/20/1997	13:00:00	26.07	1.1	127	10.21	38.49068	-76.6641	-5	1	
8	6/20/1997	13:15:00	27.02	1	155.3	12.29	38.49068	-76.6641	-5	1	
9	6/20/1997	13:30:00	27.41	1	173.7	13.65	38.49068	-76.6641	-5	1	
10	6/20/1997	13:45:00	27.48	1	177.8	13.95	38.49068	-76.6641	-5	1	
11	6/20/1997	14:00:00	27.62	1	182.6	14.29	38.49068	-76.6641	-5	1	
12	6/20/1997	14:15:00	27.7	0.9	181.5	14.19	38.49068	-76.6641	-5	1	
13	6/20/1997	14:30:00	27.66	0.9	181.4	14.2	38.49068	-76.6641	-5	1	
14	6/20/1997	14:45:00	27.74	0.9	181.1	14.15	38.49068	-76.6641	-5	1	
15	6/20/1997	15:00:00	27.93	0.9	185.5	14.44	38.49068	-76.6641	-5	1	
16	6/20/1997	15:15:00	28.38	0.9	194.7	15.04	38.49068	-76.6641	-5	1	
17	6/20/1997	15:30:00	28.46	0.8	201.9	15.58	38.49068	-76.6641	-5	1	
18	6/20/1997	15:45:00	28.24	0.8	200.8	15.57	38.49068	-76.6641	-5	1	
19	6/20/1997	16:00:00	28.09	0.7	194.7	15.14	38.49068	-76.6641	-5	1	

Figure 7-2. Screen shot showing the requisite input format needed by Metabolism.xls for calculation of metabolism variables.

7.4 Results for Potomac River Estuary: 2007

We have summarized the community production and respiration measurements available for the Potomac River estuary (Figs. 7-2 a-n) for 2007. It is interesting to note that there are a total of about 984,000 observations of dissolved oxygen, temperature and salinity used in developing these results. With very few exceptions these computed rate measurements (Pg^* and R_n) exhibit robust patterns, not something that is often associated with monitoring program data.

There were several distinctive patterns of primary production (Pg^* ; gross primary production) and respiration (R_n ; respiration during hours of darkness) in this data set. First, values tended to be much lower in early spring (Mar-May) and early fall (Oct) than during late spring and summer. Even at the most eutrophic sites (e.g. Piscataway Creek and Fenwick) Pg^* was less than $5 \text{ g O}_2 \text{ m}^{-3} \text{ day}^{-1}$ during early spring and exceeded $15 \text{ g O}_2 \text{ m}^{-3} \text{ day}^{-1}$ during summer. A similar pattern was evident at all 14 sites examined. Second, there was a clear gradient in Pg^* and R_n with highest values in the nutrient-rich upper estuary and lower values associated with these variables in the mid

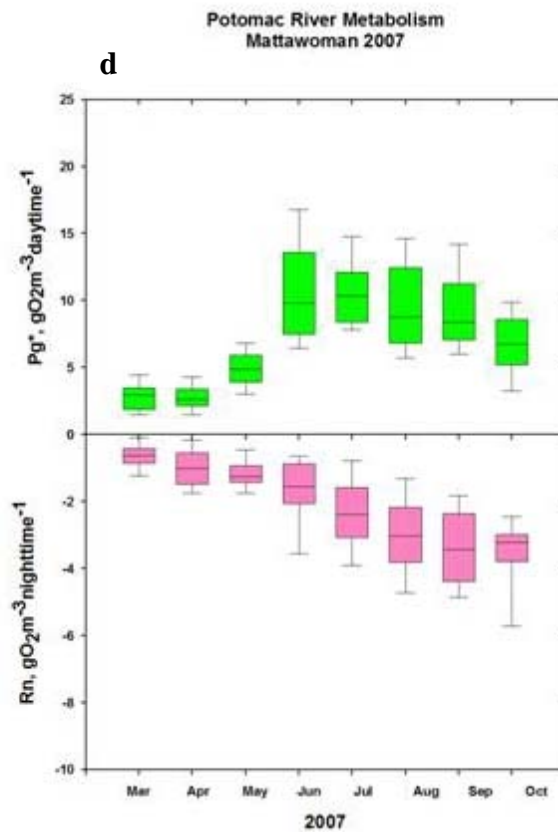
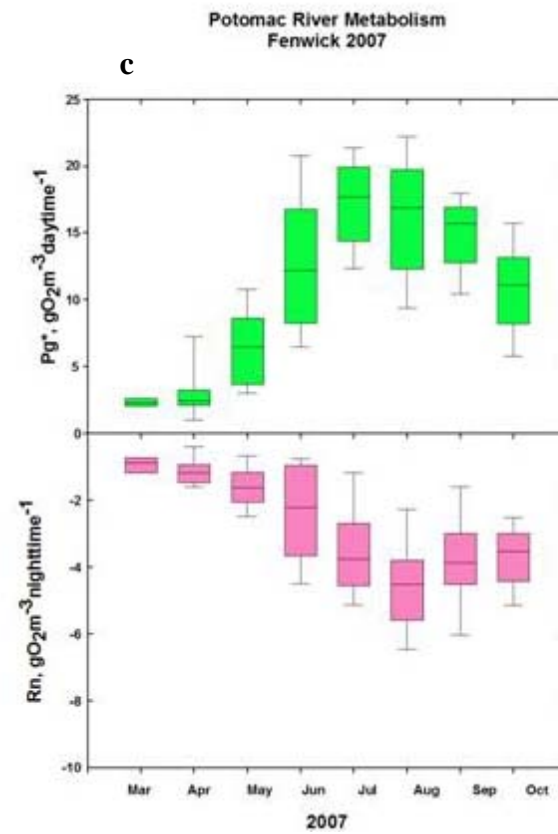
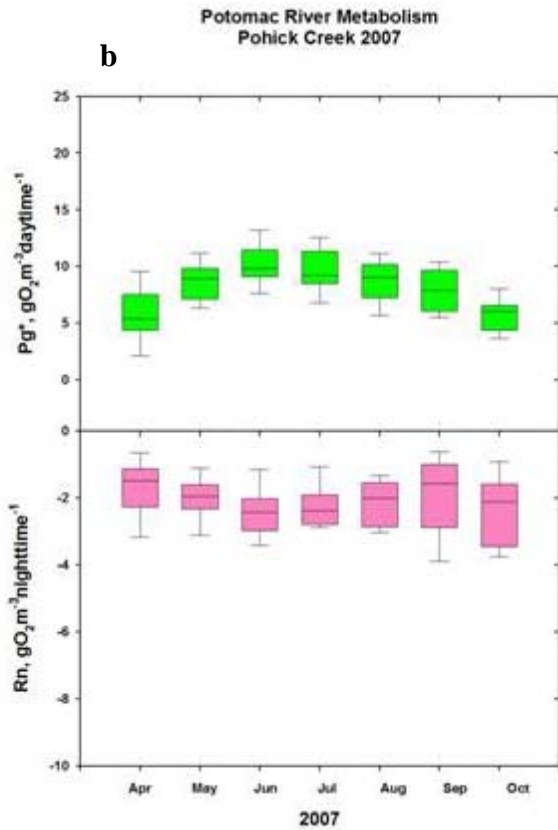
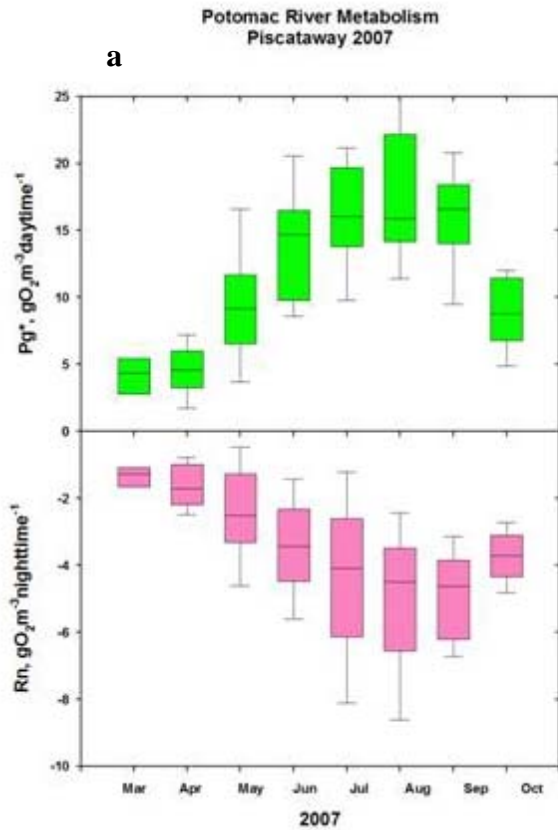
and lower estuary. Only one month exhibited a Pg^* value of $10 \text{ g O}_2 \text{ m}^{-3} \text{ day}^{-1}$ downstream of Monroe Bay adjacent to Colonial Beach, VA (Table 7-2). Third, most of these ConMon sites were actually located in embayments or small to medium sized tributaries of the Potomac rather than on the shoreline of the Potomac River mainstem. However, four sites (Fenwick, Pope's Creek, Swan Point and Piney Point) were located on the mainstem littoral area. A qualitative inspection of rates at adjacent tributary versus mainstem sites does not show any striking differences. We had anticipated that rates of both Pg^* and Rn would have been larger at the tributary sites because of longer water residence times in the creeks (allowing for more algal biomass accumulation) and because of local nutrient additions in addition to those associated with the mainstem Potomac River estuary. However, rates were more similar than different. For example, rates at Piscataway Creek, Pohick Creek and Fenwick (the latter fronting on the Potomac mainstem) were all quite similar and very large.

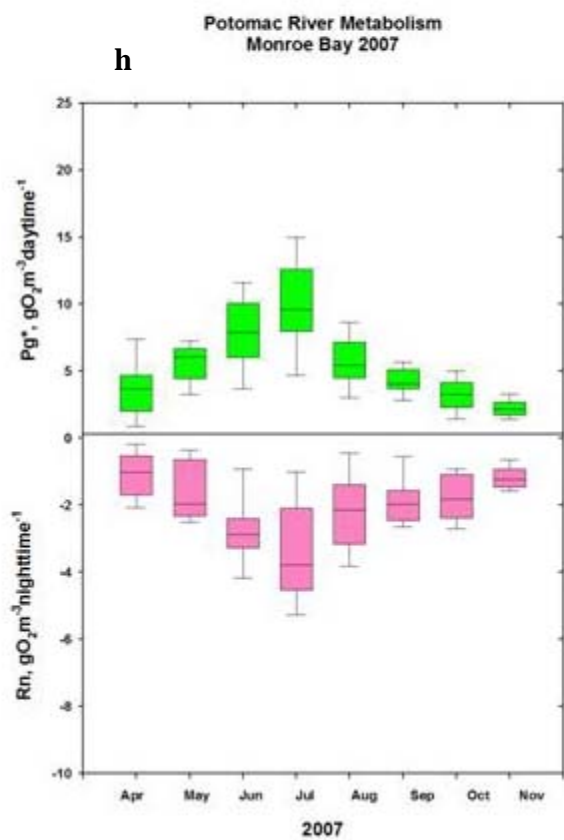
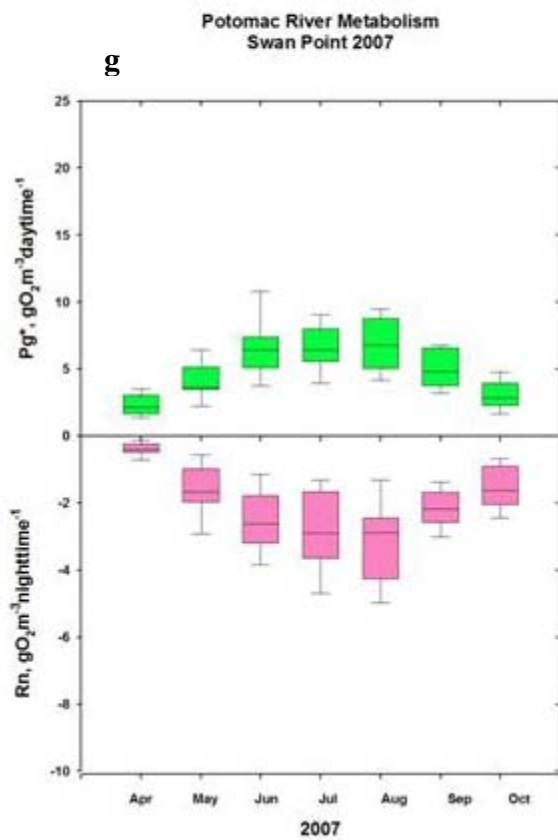
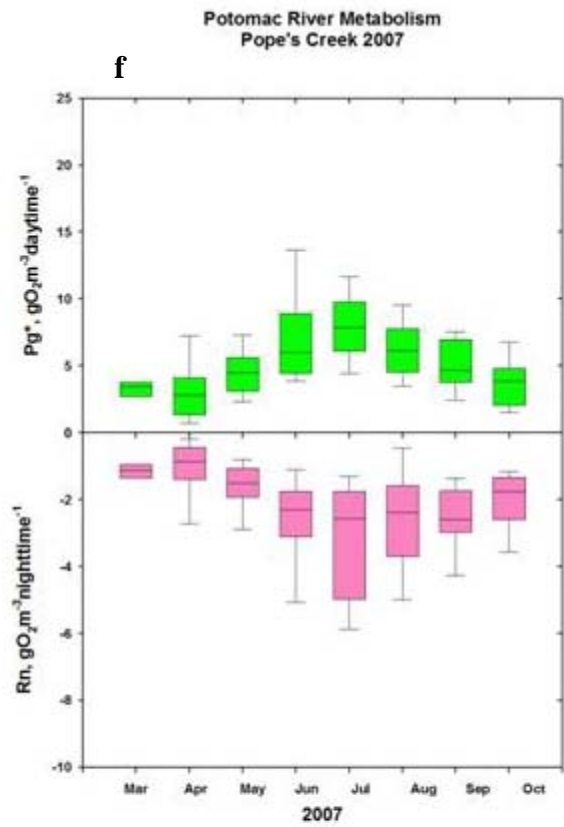
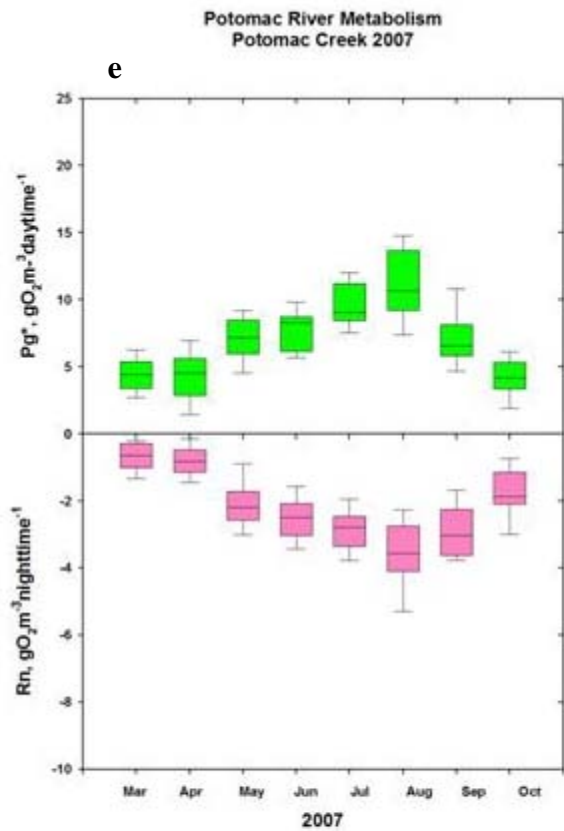
There were two temporal patterns exhibited by both Pg^* and Rn . At 6 of the 14 sites evaluated Pg^* and Rn tracked the pattern of water temperature. Thus, rates were lowest in early spring when water temperature was still low, intermediate in fall when temperatures were intermediate and highest during the period of the summer when temperature was highest (August). The temporal pattern of Pg^* and Rn at the remaining 8 sites tended to exhibit the same pattern as above for low and intermediate rates but peak rates were observed in late spring or early summer (May or June) rather than later in the summer. These different temporal patterns may be a reflection of the degree of eutrophication and thus may serve as another indicator of estuarine condition. We have examined data, from which Pg^* and Rn values were computed, collected at a site in the Patuxent River estuary during the early 1960s, a period prior to extensive and severe eutrophication of this estuary. During the period 1963-1966 Pg^* rates reached maximum values in spring (May) and lower rates during summer and fall. Winter rates were very low. We interpreted this pattern as being associated with the spring freshet when "new" nutrients were delivered to the estuary and were available to support primary production. Summer rates at that time were limited by low additions of nutrients from the drainage basin and probably less nutrient recycling because of more efficient denitrification and nutrient storage in SAV and animal communities. As nutrient loads to the Patuxent increased through the late 1960s, and through the 1970's and 1980's as well, the temporal pattern of Pg^* changed wherein the spring pulse in production was subsumed by rates that continued to increase through the summer until reaching maximum values in August or early September. We have tentatively suggested that this is the eutrophic production pattern. Rates were also very high (compared to the early 1960's rates) so there was a change in both the pattern and magnitude of production. All of the most eutrophic sites on the Potomac exhibited this pattern. Less eutrophic sites exhibited peak rates of Pg^* earlier in the summer or late spring. This pattern of production may result from large nutrient additions during the spring freshet, lower but still enhanced nutrient additions during late spring and early summer and more efficient recycling of nutrients (because of impaired denitrification due to oxygen stress on nitrification) to support summer production. In the current condition of Chesapeake Bay estuaries there is little nutrient buffering from SAV communities, denitrification is severely compromised during the extensive hypoxic period and nutrient storage in longer-lived animals (e.g. large benthic infauna) has also been sharply reduced. Thus, nutrients are more available for re-use in support of elevated rates of production, largely by phytoplanktonic algae. We suggest that if nutrient loads are reduced, the magnitude of Pg^* should also be reduced and the temporal pattern of production should shift from

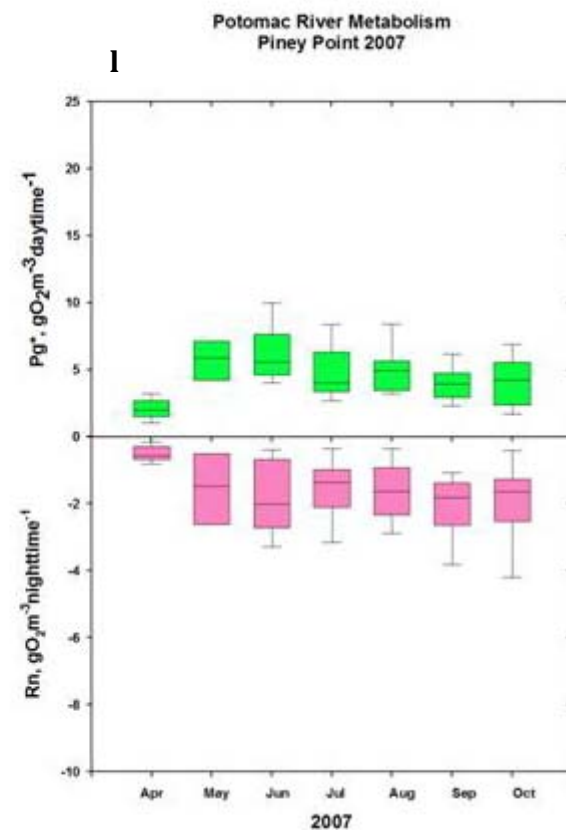
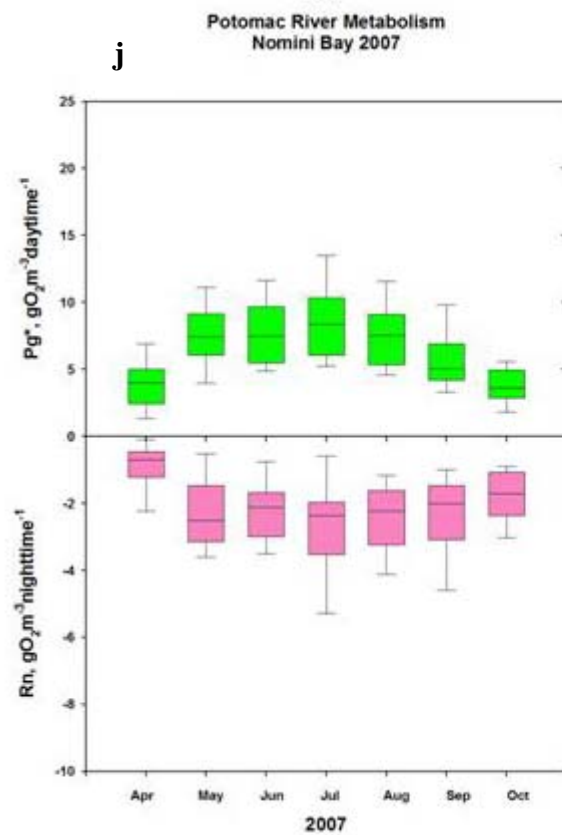
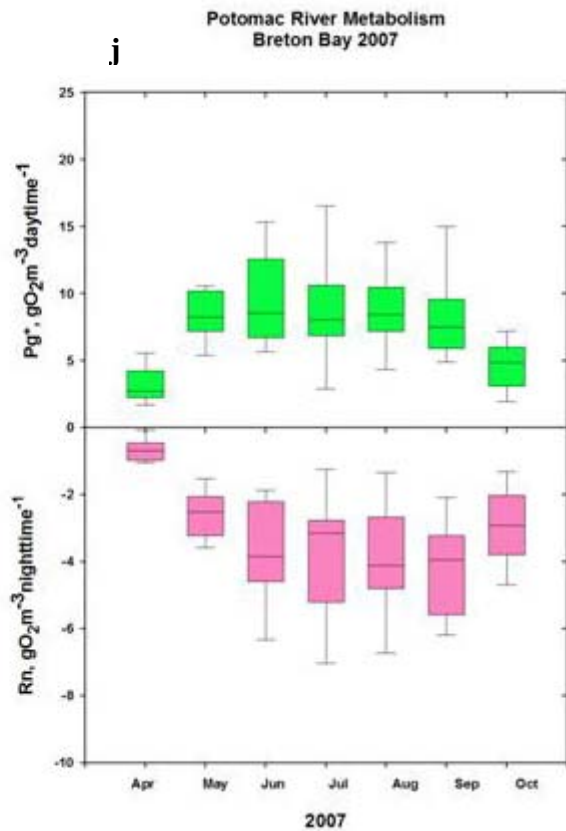
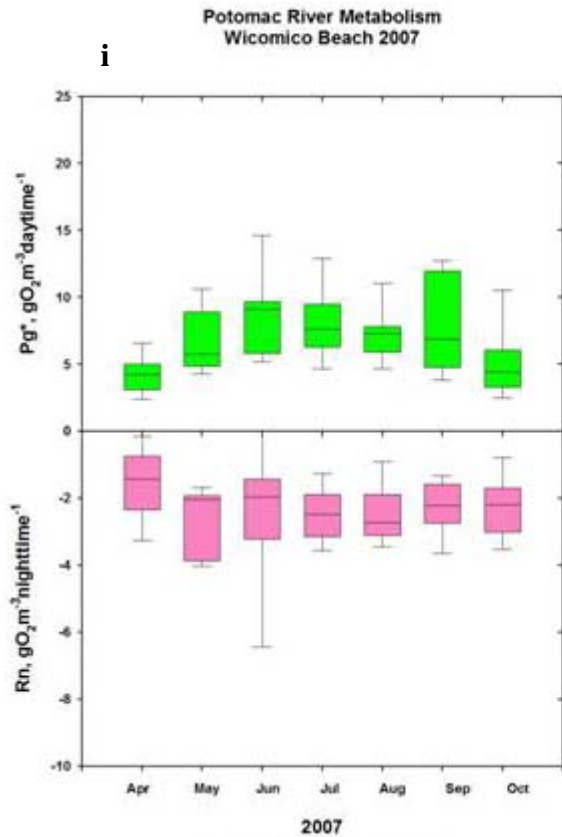
a very high summer peak to a smaller spring peak. Values of Rn should also respond in a similar fashion.

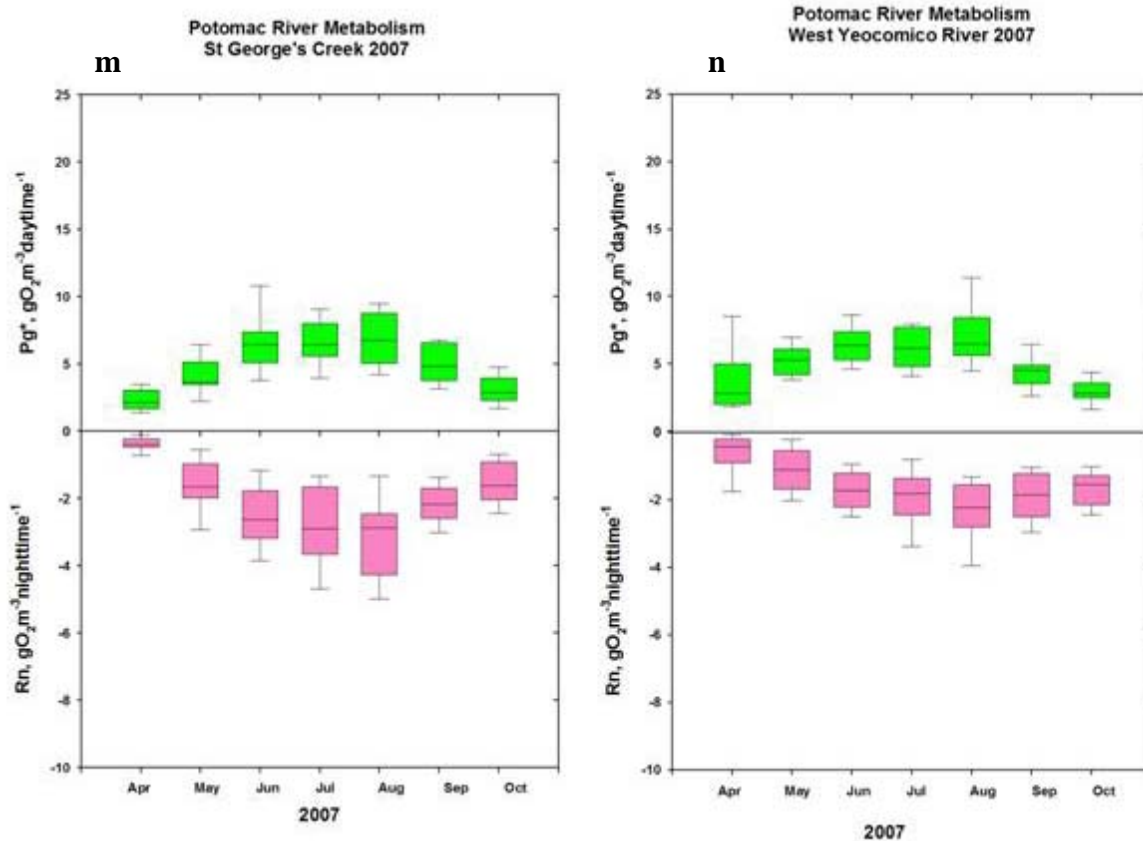
We have started to compile a comparative table of Pg* rates (by month) for several areas of the bay and tributary rivers (Table 7-2). While the list is not currently extensive it does span a range of enrichment conditions. Rates, for example, in the Back River and the dead-end canals of the Maryland Coastal bays were very high, somewhat in excess of the most enriched Potomac River estuary sites. Other sites have more modest rates and virtually all sites have lower rates during early spring and fall. It would be useful to take advantage of the accumulating ConMon database to expand this analysis to additional sites (looking for the “hard to find” minimally impacted sites for bolstering the baseline pattern and magnitude) and to begin to examine individual sites for inter-annual changes in magnitude and pattern. There is also the need to bring some rigorous statistical analyses to these computed rates to determine minimum significant difference in Pg* and Rn values (a power analysis) and further examine the data for significant differences among sites and seasons. We have initiated this process with data collected from the Corsica River estuary but have not had the resources to extend and generalize this analysis.

We have also used Potomac River estuary metabolism data provided in Table 7-2 to construct a time-space contour plot of Pg* rates for the 2007 measurement period (Figure 7-3). These plots are useful for examining time (Apr-Oct) and space (all sites along the Potomac) for distinctive patterns in Pg*. The patterns in this colorful graphic fairly jump out of the page at the viewer. Rates of Pg* were relatively low all along the estuary (and tributary sites) during spring and fall. Highest rates were observed during the summer period and, with one exception, were all located in the upper estuary and tributaries when nutrient loading rates are likely highest. Substantial rates of Pg* were also observed during June-July at three sites that are tributaries of the mesohaline Potomac (Monroe Bay in the vicinity of Colonial beach, Wicomico beach in the middle section of the Wicomico River and Breton Bay). Elevated rates in these tributaries may be supported by nutrient additions both from the mainstem Potomac as well as additions from local sources. This time-space contour plot could be further refined by binning Pg* data into bi-weekly or even weekly means and seeing if that provides any more insights in the temporal domain. If these sites are monitored during 2008 statistical testing could be conducted, as was done with the 2005-2007 Corsica River estuary data, to see if there are differences among years and seasons or months of different years. Finally, it would be useful to examine this huge rate dataset in terms of environmental conditions influencing these rates and this we have not attempted. However, there is a substantial data set available to do this with a range of possibly influential variables available including sunlight (PAR), temperature, water clarity, algal biomass and nutrient concentrations. Since there is a very large range in rates of Pg* this would be a great data set to examine via statistical modeling.









Figures 7-3 (a-n). Monthly box and whisker plots of gross primary production (Pg*) and nighttime respiration at 14 shallow water ($z < 1.6$ m) sites in the Potomac River estuary and tributary rivers. Data were collected at ConMon sites during 2007. The boundary of the box closest to zero indicates the 25th percentile, the line within the box is the median and the boundary of the box farthest from zero indicates the 75th percentile. Whiskers above and below the box indicate the 90th and 10th percentiles. Note that for some sites data began in March 2007 while at most data collection began in April 2007. The X and Y axis scales are the same in all plots to make inter-comparisons easier.

Table 7-2. A summary of average monthly rates of gross primary production (Pg*) at a variety of Chesapeake Bay locations and for all 14 ConMon sites in the Potomac River estuary and tributary rivers. The Potomac River estuary sites are arranged from up-estuary to down-estuary locations. All Potomac data are from 2007. Data from other sites were collected between 1997 and 2006). The number of days included in each monthly mean of Pg* varied between 10 and 30 days. All estimates of Pg* have been rounded to the nearest whole number to facilitate comparisons. Color code: blue = 15 or greater; green = 10 to 14; orange = 5 to 9; black = 5 or less.

Locations	Gross Primary Production (g O ₂ m ⁻³ day ⁻¹)						
	Apr.	May	Jun.	Jul.	Aug.	Sept.	Oct.
Other Maryland Sites							
Back River Site 1			12	17	13	9	
Back River Site 2			13	16	14	10	
Corsica River Sycamore		13	10	14	13	7	5
Coastal Bays Bishopville		15	14	21	16	16	11
Coastal Bays Turville		9	12	15	12	11	6
Patuxent River Littoral		5	8	10	7	5	3
Patuxent River Channel		4	5	9	9	6	3
Coastal Bays Public Landing		3	6	8	8	5	2
Potomac River Sites							
Piscataway Creek	5	9	15	16	16	17	8
Pohick Creek	5	9	10	10	9	8	6
Fenwick	3	6	12	17	17	16	11
Mattawoman Creek	3	5	10	11	9	8	7
Potomac Creek	5	7	8	9	11	6	4
Pope's Creek	3	4	6	7	6	5	4
Swan Point	2	5	6	6	7	5	3
Monroe Bay	6	7	10	5	4	3	3
Wicomico Beach	4	5	9	8	7	6	5
Breton Bay	3	7	8	7	7	7	5
Nomini Bay	4	7	7	8	7	5	4
Piney Point	2	6	6	5	5	4	4
St. George's Creek	2	5	6	6	7	5	3
West Yeocomico River	3	5	6	6	6	5	3

2007 Potomac River ConMon Station Metabolism (g O₂ m⁻³ day⁻¹)

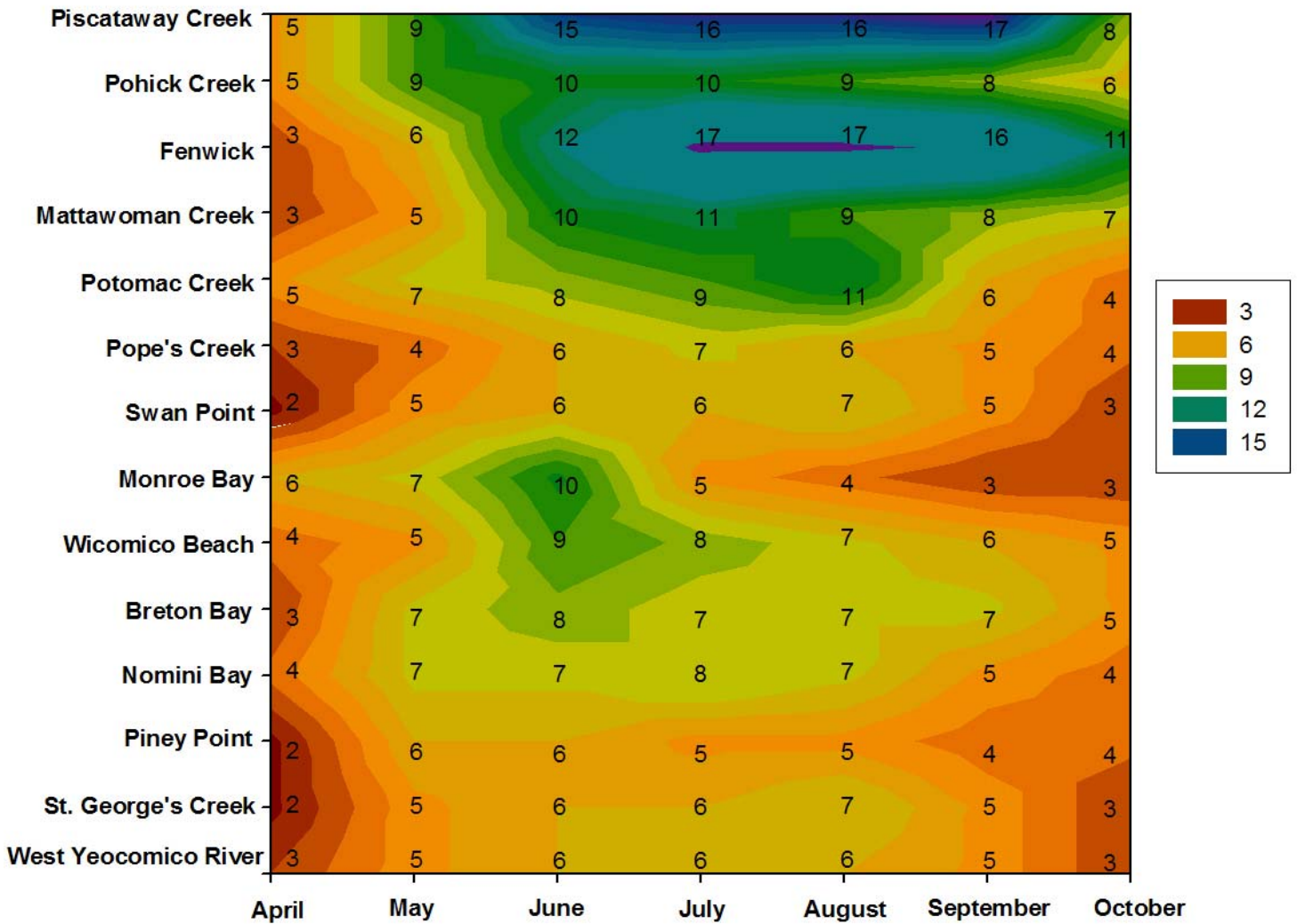


Figure 7-4. A contour plot of average monthly rates of gross primary production (Pg*) at all 14 ConMon sites in the Potomac River estuary and tributary rivers.

7.5 References

- Boynton, W.R. and W.M. Kemp. 1985.** Nutrient regeneration and oxygen consumption by sediments along an estuarine salinity gradient. *Mar. Ecol. Prog. Ser.* 23:45-55.
- Boynton, W.R., Kemp, W.M.,** Nitrogen in Estuaries in Capone, D.G., Bronk, D.A., Mulholland, M.R., Carpenter, E.J., 2007. Nitrogen in the Marine Environment, in press.
- Boynton, W.R., W.M. Kemp and C.W. Keefe.** 1982. A comparative analysis of nutrients and other factors influencing estuarine phytoplankton production, p. 69-90. In: V.S. Kennedy, [Ed.], *Estuarine Comparisons*, Academic Press, NY.
- Burger, N. H. and J. D. Hagy.** 1998. Patuxent River high frequency monitoring, p. 153-183. In: W. R. Boynton and F. M. Rohland (eds.). *Ecosystem Processes Component Interpretive Report No. 15. Ref. No. [UMCES]CBL 98-073a*. Solomons, MD.
- Caffrey, J. 2004.** Factors controlling net ecosystem metabolism in U. S. Estuaries. *Estuaries* 27 (1): 90-101.
- Gazeau, F. et al. 2005.** Net ecosystem metabolism in a micro-tidal estuary (Randers Fjord, Denmark): evaluation of methods. *Mar Ecol Prog Ser* 301: 23-41.
- Sweeney, B. F. 1995.** Community metabolism in the Patuxent River estuary: 1963-1969 and 1992. Masters Thesis. University of Maryland, College Park, MD. 83p.
- Vollenweider, R. A.** 1976. Advances in defining critical loading levels for phosphorus in lake eutrophication. *Mem. Ist. Ital. Idrobiol.* 33: 53-8.

8.0 Estuarine Community Metabolism Web Page Addition

W.R. Boynton and T. A. Wisner

8.1	Introduction and Objectives	8-1
8.2	Community Metabolism: A Central Ecosystem Concept	8-2
8.3	Community Metabolism: A Place on “Eyes on the Bay”?	8-3
8.4	Community Metabolism Web Site: Some Preliminary Designs and Thoughts	8-4
8.5	Figures	8-6
8.6	Where to Go from Here?	8-11

8.1 Introduction and Objectives

The Chesapeake Bay Biomonitoring Program has been active since 1984 and now has a substantial time series of a variety of variables for use in assessing water quality, habitat condition and living resources status and trends. This really is a remarkable assemblage of estuarine data. There has been considerable use of these data in status and trend assessments, in calibration and verification of water quality models, in box models which have been used to infer important rate processes, and as background information needed for designing and implementing experimental studies. Much more is likely to be done with these data sets.

However, much, if not all, of the above uses are technical in nature, some very technical. Thus, non-technical folks (most people living in the Chesapeake watershed) would have little use for all this information. The Maryland Department of Natural Resources, in an effort to make these data sets more available and understandable to the public, launched the “Eyes on the Bay” web page a number of years ago. Similar efforts have been made in this direction with the introduction of “Report Cards” for the Bay and tributary rivers. Again, we would argue that more of this sort of activity would be useful in providing the public with understandable information about Chesapeake Bay and efforts aimed at restoration of the Bay and tributary rivers.

One aspect of the “Eyes on the Bay” web page has been of particular interest to the EPC of the Maryland Biomonitoring Program. Specifically, the ConMon program provides high frequency (data recorded every 15 minutes at fixed locations between April and October) measurements of a suite of water quality variables. Simple plots of these data are instructive (e.g., when DO is less than criteria values, when chlorophyll-a values are above criteria and so forth) and this is currently available on this web page. However, as with many aspects of the monitoring program, additional useful and instructive analyses and/or data presentations could be developed.

It is the objective of this chapter to suggest another use of ConMon data and to suggest a way to add this to the “Eyes on the Bay” web page. Specifically, we suggest that ConMon data be used to compute RATES of community production and respiration and that these values be presented on the web page along with some cartoons of these processes which will make them understandable to a wide audience. This effort of suggesting an outlet for technical data is far removed from our usual activities. We are absolutely not expert in these matters. The thoughts and examples offered here are by way of trying to be responsive to the need for broad public understanding of Bay

conditions and restoration efforts. We realize we may be proposing an activity that is not appropriate and will therefore receive a negative response.

8.2 Community Metabolism: A Central Ecosystem Concept

Community production and respiration have repeatedly been shown to be responsive to nutrient enrichment in lakes, estuaries and coastal waters. In the case many Chesapeake Bay tributaries, nutrient enrichment is cited as a major reason for listing the ecosystem as being impaired and in need of restoration.

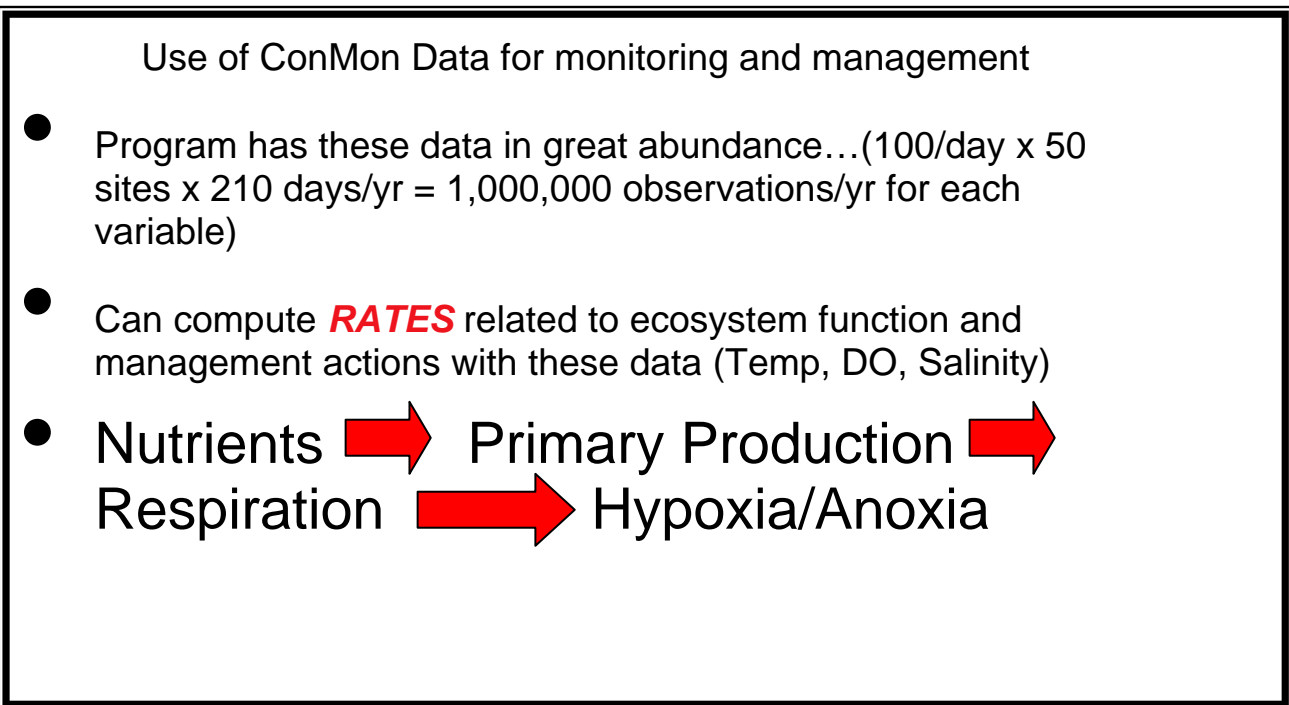


Table 8-1. A simple description of ConMon data and a cause-effect chain relating nutrient inputs to water quality problems (e.g., hypoxia and anoxia).

In many instances measurements of such fundamental features of ecosystem function as community production and respiration are too expensive or simply too difficult to undertake. However, the State of Maryland DNR has established a large number of water-quality monitors making measurements of water quality variables needed to make these estimates. A simple summary of ConMon data collection and how these data can be related to nutrient over-enrichment issues is provided in Table 8-1.

The basic concept and method for computing community production and respiration was developed by H.T. Odum and C.M. Hoskin during the 1950s and, with numerous modifications, has been used since for measuring these rate processes in streams, rivers, lakes, estuaries and the open ocean. The technique is based on following the oxygen concentration in a body of water for at least a 24 hour period. During hours of daylight, oxygen increases in the water due to the release of O₂ as a by-product of photosynthesis. During hours of darkness, O₂ declines due to O₂ consumption by both primary producers (all sorts of plants including phytoplankton, SAV, epiphytes and benthic micro and macroalgae) and all other heterotrophs. The rate processes (gross photosynthesis, P_g*; nighttime respiration, R_n) are estimated by computing the rate of change in O₂ concentrations

during day and night periods. This rate of change is then corrected for O₂ diffusion across the air-water interface and the result is an estimate of P_g* and R_n. ConMon data are exactly the type of data needed for these computations in that all the required variables are measured (dissolved oxygen, temperature and salinity), the measurement frequency is high (15 minute intervals) and the measurement period is for 9 or more months. It is very rare when a rate process can be measured with such temporal intensity.

8.3 Community Metabolism: A Place on “Eyes on the Bay”?

We have found “Eyes on the Bay” to be an especially useful web page. For example, we can quickly access graphical information concerning temporal water quality conditions in littoral areas of the Bay and also assess spatial water quality conditions in many areas of the Bay. As more sites are added and sentinel sites are maintained the data sets become even more valuable. In addition, with a few key strokes we can download numerical data and in this form these data are available for any number of analyses. Thus, our point of departure is to “sing the praises” of this web page.

As with all good things, there may be ways to make it even better. The approach we are suggesting here is basically simple and involves the following steps: 1) ConMon generates a huge number of observations of variables needed to compute rates of community production and respiration; 2) these rates are known to be sensitive to nutrient inputs and in-situ nutrient conditions; 3) high rates of nutrient-induced production leads to high rates of respiration (DO utilization); 4) high rates of respiration can lead to hypoxic and anoxic conditions, one of the primary water quality problems addressed by the Bay Program. Thus, these rate computations provide not just an indication of whether DO is low or high but **WHAT’S MAKING IT LOW OR HIGH and HOW the COMMUNITY RESPONDS TO CHANGES IN RESPONSE TO A VARIETY OF ENVIRONMENTAL VARIABLES, including NUTRIENT INPUTS.** Over time, we can track the system response to management actions (e.g., nutrient load reductions) and this would be a substantial piece of information to present, in an understandable format, to the general public.

The basic data needed for metabolism computations already reside on the “Eyes on the Bay” web page. We suggest that the algorithm used to compute community production and respiration could be added (behind the scenes on the web page) and produce estimates of these variables. At sites where data are recorded in “near-real” time these rates could also be computed on a daily basis. At most ConMon sites this is not the case so rates could be computed when ConMon data are downloaded (~bi-weekly) and after these data are subjected to routine QA/QC review. Thus, in the latter case, rates for several weeks would appear at the same time, lagged from real time by several weeks. As a technical meter we have been doing these computations based on ConMon data collected in the Corsica River estuary (see Chapter 3) and from a variety of sites in the Potomac River estuary (see Chapter 7). We have also made community metabolism estimates based on ConMon and pre-ConMon data collected from other areas of Chesapeake Bay (see Chapter 7 for a summary).

It appears to us that the technical aspects of presenting community metabolism on a web can be reasonably solved. However, making these concepts, which we argue are fundamental, understandable to the general public is a greater challenge. The remainder of this chapter presents some ideas and cartoons suggesting how this might be accomplished.

8.4 Community Metabolism Web Site: Some Preliminary Designs and Thoughts

We have so little experience in web page design, communication with the public via this medium, or other types of technical environmental information sharing/interpretation that we hardly know where to begin. What we have done is to generate a series of cartoon figures of the processes we are trying to interpret for the public. Some of these are very rough sketches and we have included these to show the process we used from the very start. Others are more polished but probably still not ready for prime-time showing. Furthermore, we have included all of these to stimulate thinking about this issue among those reading/reviewing this report and for those active in maintaining and enhancing “Eyes on the Bay”.

The point of departure that we choose to explore was to start with a cartoon of a farm field showing several of the most important ingredients needed for, in this case, corn production (Fig. 8-1). We coupled the cartoon with a graphic showing that corn production increases with fertilization rate, up to a certain point, beyond which no additional corn production is realized. At that point, something other than nutrients is limiting further production. This point of departure also needs to capture the idea that nutrients (N and P in particular) are basically good things....they are the “stuff of life”...without these essential elements all life as we know it is “toast”. So, we wanted to convey the idea that these nutrients are essential but that we currently have a situation in estuaries and coastal waters where we have “too much of a good thing”...a condition we could also call “NUTRIENT OBESITY”. So, the point is made that nutrients are essential (other compounds such as PCBs are truly pollutants), and currently there are too much in the way of nutrients getting to coastal waters.

We constructed (as many have before us) a few cartoons of estuarine production, the aquatic equivalent of the corn production cartoon (Fig. 8-1). Many of the same inputs are required for estuarine production, including nutrients, as for the farm example. However, as nutrient additions increase beyond some point, production (also habitat) starts to degrade and we made this point with a fertilization-estuarine production graphic. So, we tried to build parallels between a well known feature (farming) and a less well known feature (estuarine production) of the coastal zone. Figures 8-1 and 8-2 are the crude sketches that were initially developed. These sketches, and conversation with T. A. Wisner, lead to the development of the next generation of cartoons which are far more polished and, we think, more clearly convey a message. Both Figures 8-3 and 8-4 could be further developed and could also have additional information that could be accessed by clicking on specific areas of the diagram.

An additional way to relate activities on the land with estuarine production was attempted in the top portion of Figure 8-5 where we show a series of boxes, one spilling (influencing) into the next. The idea here is to show a cause-effect chain of events leading to water quality problems...another view of the nutrient obesity issue.

We have yet to develop a cartoon that focuses on defining metabolism in estuarine waters but there are ample opportunities to do this. In fact, some of the eutrophication cartoons currently available could be modified to basically show the production and consumption of oxygen, a key element in metabolism concepts.

We have developed several versions (all rough sketches) of what a community metabolism graphic might look like on a web site (Fig. 8-5 bottom, 8-6 and 8-7). There are several key features that are more or less represented in each of these preliminary cartoons and these include the following:

- The background of the graphic would be color-coded to indicate seasonal ranges of production thought to be healthy, poor and much too high (Fig. 8-5 bottom in color).
- The rates of production would be calculated via an algorithm and shown as daily or weekly averages. Possibly the weekly (or even monthly) averages could be shown as a box and whisker plot (Fig. 8-7, green bars)
- There are data from the Patuxent River estuary collected during the decade of the 1960s prior to the estuary developing signs of moderate to severe eutrophication. We suggest using these data as a “baseline” in these figures as shown in Figures 8-6 and 8-7. The “goal” would be to decrease production from current high levels to the baseline magnitude and pattern.
- We also suggest that ConMon data from past years of monitoring could be developed and thus there is the opportunity to show inter-annual as well as seasonal changes. We indicated a multi-year arrangement in Figure 8-5.
- The most developed graphic for metabolism is shown in Figure 8-7 where we suggest having a multi-click sequence where sunlight. Possibly water temperature and even possibly algal biomass (as chlorophyll-a) be shown through a year (or seasons) and finally the production data shown relative to the baseline data.
- We have also toyed with the idea of having a metabolism thermometer on this page. The thermometer (or some speed gauge) would give the idea that the system is “too hot” when rates are far above the baseline rate. Thus, the gauge would show the difference between what would be a good rate and what is an obese rate. So, the amount of “nutrient dieting” required would be captured. I don’t think we could, at this point, explicitly relate these metabolism rates to needed quantitative nutrient reductions....that would be like having a “real-time” TMDL on a web page....maybe not such a bad idea.

8.5 Figures



Figure 8-1. A preliminary and crude sketch showing several important inputs to large-scale corn production and relating the magnitude of production to fertilization rates. This diagram starts the process of thinking of fertilizers (nutrients) not as a pollutant but as “too much of a good thing”.

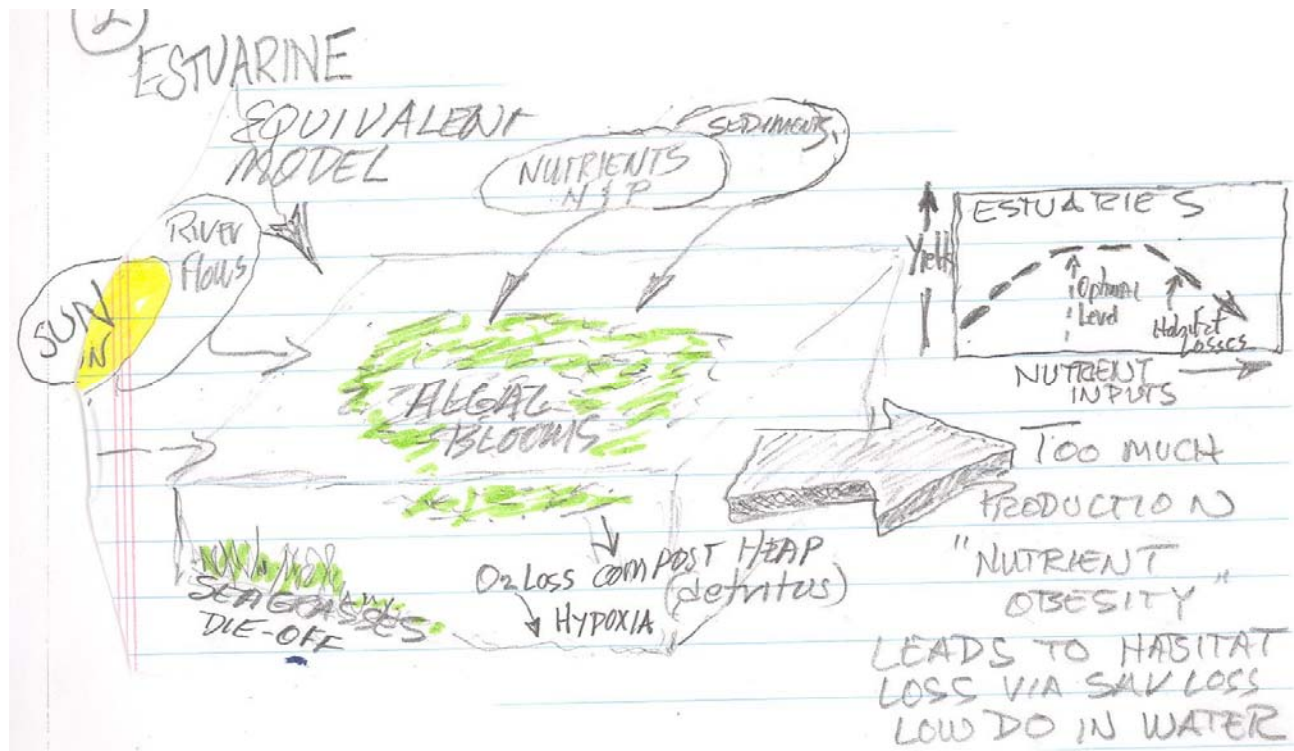


Figure 8-2. A preliminary and crude sketch showing the estuarine equivalent of the farmer’s field. The point here is again that nutrients are “good” when available in the proper amounts but lead to “Nutrient Obesity” and a loss of habitat and production (shown in the graph) when supplied in excessive amounts. We need to be careful here and elsewhere not to blame farmers for all this nutrient obesity problem...other nutrient sources need to be highlighted as well.

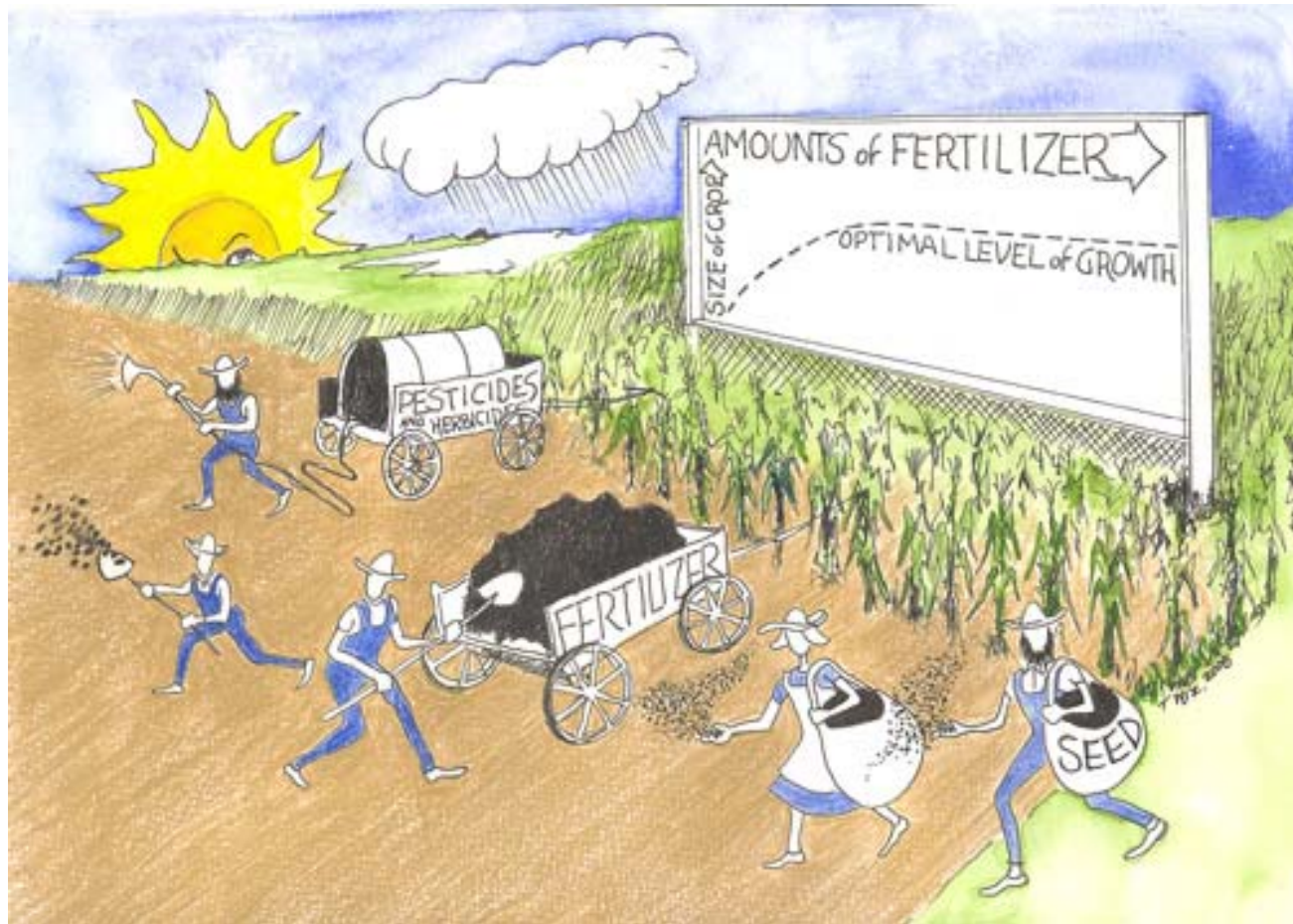


Figure 8-3. A more formal depiction of the processes captured in Fig. 8-1. This cartoon was drawn by Tom Wisner (www.Chestory.org). The emphasis here is again that nutrients in the right proportions aid in the development of good crop production. We may need to have similar diagrams for suburban, urban and forested areas to make the same points., namely that nutrients are essential for life but in excessive amounts lead to serious problems, especially in aquatic ecosystems like Chesapeake Bay.



Figure 8-4. A more formal depiction of the processes captured in Fig. 8-2. This cartoon was drawn by Tom Wisner (www.Chestory.org). In this cartoon there are paired estuaries with the one on the left having adequate fertilization and high levels of production (see inserted graph) and the one on the right subjected to over-fertilization and associated loss of habitat and production (nutrient obesity condition). The emphasis here is again that nutrients in the right proportions aid in the development of good estuarine production. This cartoon may be too busy and would be more effective if drawn as two estuaries, one healthy and one over-fertilized. Something to think about.

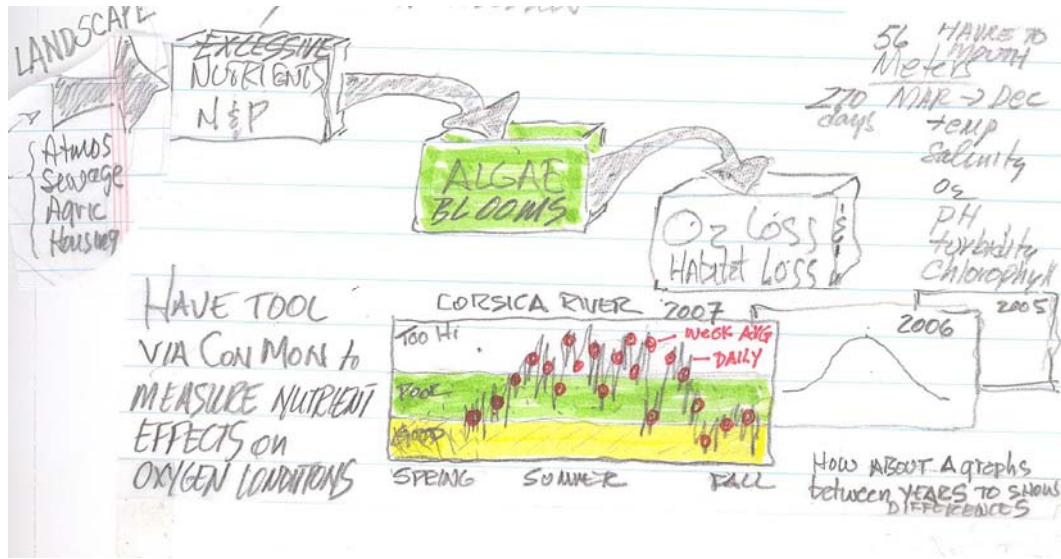


Figure 8-5. Two preliminary and crude sketches of a “cause – effect chain” wherein nutrients from the land eventually cause eutrophic conditions (top sketch) and a first effort at developing a graphic based on ConMon data and resultant metabolism computations. The bottom sketch shows rates of primary production (referred to as Pg^* in Chapters 6 and 7 of this report) for a ConMon site. The rates would be computed in the background of the web page and daily (or weekly) measurements shown against a background indicating rates thought to be good, fair or too high (over fertilized or obese rates). Better cartoons have not yet been developed for these preliminary sketches.

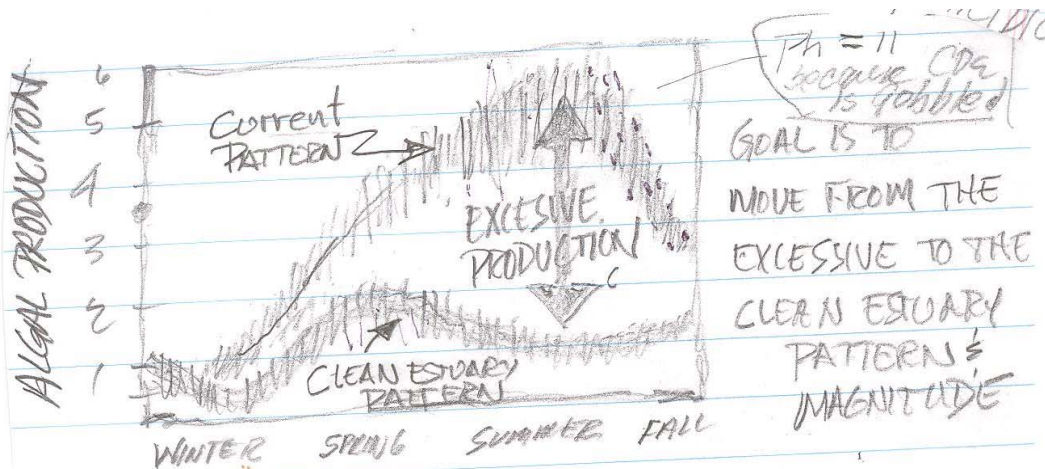


Figure 8-6. A preliminary and crude sketch of the output of metabolism computations based on data from a ConMon site. In this case the “clean estuary” pattern is based on measurements made during the 1960’s in the Patuxent River estuary prior to large increases in nutrient loading rates. In this example we used Pg^* data from the Corsica River estuary. The key points of this diagram are: 1) rates of Pg^* could be taken from “Eyes on the Bay” files and subjected to the metabolism algorithm and the results plotted on the web page graphic, 2) after each week of daily computations, a weekly average could be computed to keep the graphic from becoming too busy, 3) the difference between the clean and obese estuary could be graphed as a reading on a “nutrient obesity” gage or thermometer thus providing the observer with an up to date indication of how much change is needed (thermometer or gage not shown).

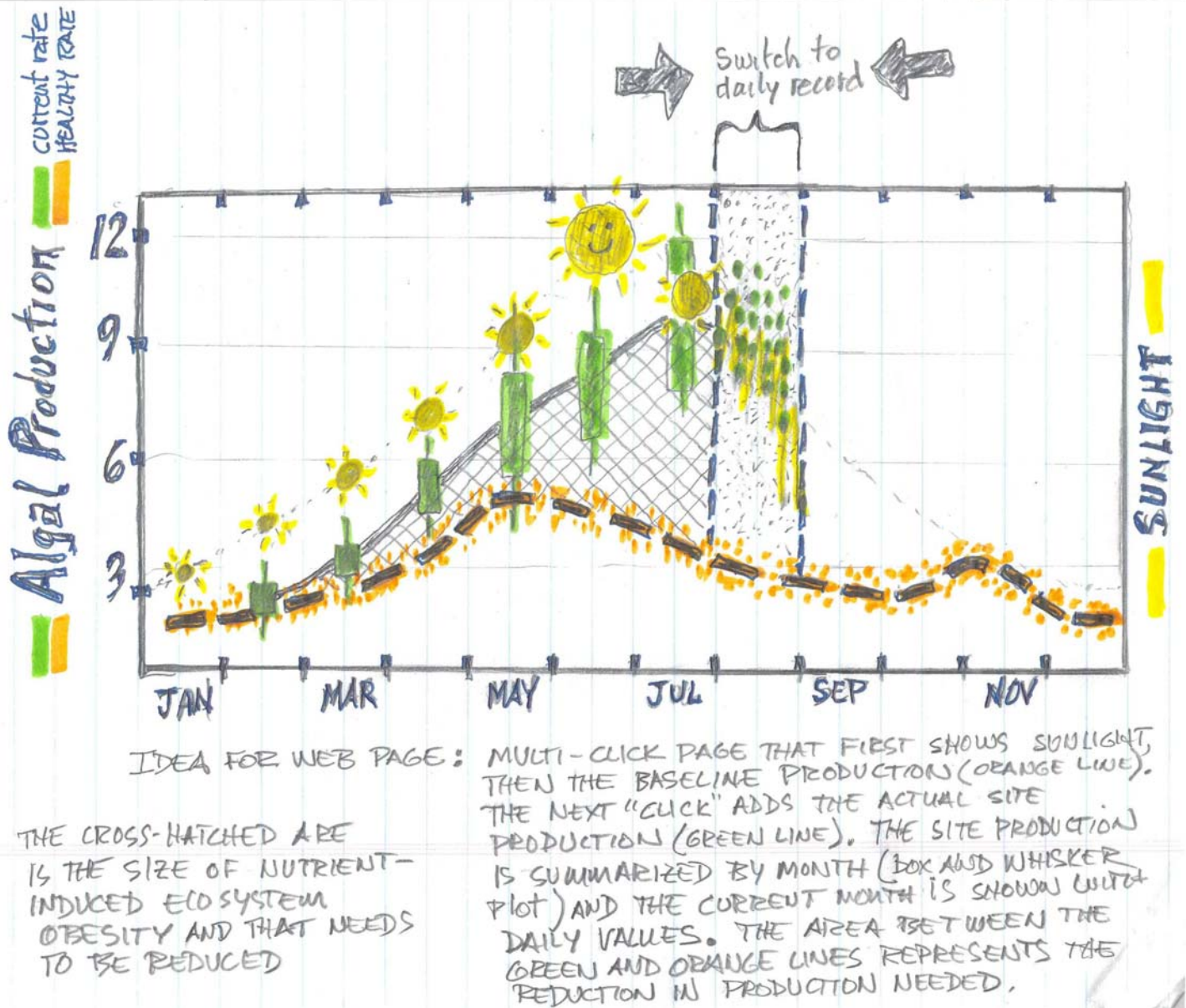


Figure 8-7. A simple “cartoon figure” of what a web page summary of community metabolism might look like. Footnotes on the diagram suggest additional features that could be part of this web page output. It might also be possible to have “click-on” tags on the diagram where the reader can get an explanation of certain events or patterns. It might be useful to initiate this web page using only a few ConMon sites, perhaps one having good water quality (good question where this might be), one with modestly impaired water quality (mesohaline Patuxent, several Potomac River sites) and one with severe problems (many to choose from). Note that we have just shown a graphic for production; similar graphics could readily be developed for respiration.

8.6 Where to Go from Here?

In many ways we don't know what we are doing here. We do, however, believe that making the information collected compelling to the public is a worthwhile goal. So, we have made a stab at this using an outstanding....world-class...data set being developed by the ConMon Program. It would be a remarkable achievement in the monitoring world to have essential rate processes presented in a clear fashion in close to "real-time". We furthermore know that production is a function, sometimes simple and sometimes complex, of nutrient loading rates and this is the item that the Bay Program has focused on reducing. So, why not use a great technology (ConMon) to present these patterns in an exciting and unprecedented fashion.

To move these notions and crude cartoons and associated ideas forward we would need to have some discussions and help from the DNR staff and especially the ConMon and "Eyes on the Bay" team members. There may be far more effective ways of doing what we have suggested or alternative to what we have suggested.

It would seem reasonable to develop this idea with a focus on just one or a few sites having distinctive eutrophication characteristics (e.g., low, medium and high degrees of eutrophication, for example). To consider doing this for all or even most of the ConMon sites seem hopelessly overwhelming at this point. But, a start could lead to some interesting work with good public benefits

Finally, it seems like the "Eyes on the Bay" staff would need some professional code writing assistance to make this project work efficiently. It seems to me that DNR personnel have great skill and experience with web page content. It would seem more desirable to have them working on content and interpretation rather than trying to write efficient code to make a web page work well. This would presumably require more financial support but the investment might well be worth the effort. EPC staff will remain eager to help this process along if DNR wishes to pursue it or some other version of this vision.